LEABHARLANN CHOLÁISTE NA TRÍONÓIDE, BAILE ÁTHA CLIATH | TRINITY COLLEGE LIBRARY DUBLIN
Ollscoil Átha Cliath | The University of Dublin

Terms and Conditions of Use of Digitised Theses from Trinity College Library Dublin

Copyright statement

All material supplied by Trinity College Library is protected by copyright (under the Copyright and Related Rights Act, 2000 as amended) and other relevant Intellectual Property Rights. By accessing and using a Digitised Thesis from Trinity College Library you acknowledge that all Intellectual Property Rights in any Works supplied are the sole and exclusive property of the copyright and/or other IPR holder. Specific copyright holders may not be explicitly identified. Use of materials from other sources within a thesis should not be construed as a claim over them.

A non-exclusive, non-transferable licence is hereby granted to those using or reproducing, in whole or in part, the material for valid purposes, providing the copyright owners are acknowledged using the normal conventions. Where specific permission to use material is required, this is identified and such permission must be sought from the copyright holder or agency cited.

Liability statement

By using a Digitised Thesis, I accept that Trinity College Dublin bears no legal responsibility for the accuracy, legality or comprehensiveness of materials contained within the thesis, and that Trinity College Dublin accepts no liability for indirect, consequential, or incidental, damages or losses arising from use of the thesis for whatever reason. Information located in a thesis may be subject to specific use constraints, details of which may not be explicitly described. It is the responsibility of potential and actual users to be aware of such constraints and to abide by them. By making use of material from a digitised thesis, you accept these copyright and disclaimer provisions. Where it is brought to the attention of Trinity College Library that there may be a breach of copyright or other restraint, it is the policy to withdraw or take down access to a thesis while the issue is being resolved.

Access Agreement

By using a Digitised Thesis from Trinity College Library you are bound by the following Terms & Conditions. Please read them carefully.

I have read and I understand the following statement: All material supplied via a Digitised Thesis from Trinity College Library is protected by copyright and other intellectual property rights, and duplication or sale of all or part of any of a thesis is not permitted, except that material may be duplicated by you for your research use or for educational purposes in electronic or print form providing the copyright owners are acknowledged using the normal conventions. You must obtain permission for any other use. Electronic or print copies may not be offered, whether for sale or otherwise to anyone. This copy has been supplied on the understanding that it is copyright material and that no quotation from the thesis may be published without proper acknowledgement.

IDENTIFICATION OF NOVEL BIOMARKERS IN RECURRENT/CHEMORESISTANT OVARIAN CANCER

A thesis submitted for the Degree of

Doctor of Philosophy

By

Dr Alexandros Laios

MD (Medical Degree)

University of Dublin Trinity College

2009

TRINITY COLLEGE
12 MAY 2012
LIBRARY DUBLIN
9486

DECLARATION

I hereby declare that my thesis is entirely my own work and that it has not been submitted previously for a PhD degree at this or any other university.

I give permission to the librarian of Trinity College to lend or copy this thesis.

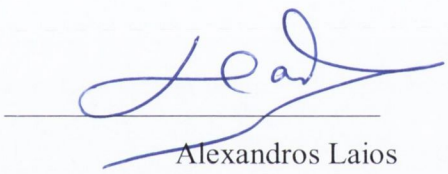

Alexandros Laios

Dedicated to

Mam, Dad, Theodore, Dimitris, Athina, my grandfather and my grandmother-

My Family, my rock.

My Aphrodite, the Goddess of Beauty.

ACKNOWLEDGEMENTS

I would like to thank my supervisor, Prof John O'Leary, for giving me the opportunity to carry out this work and for his continuous support and stimulating advice throughout the study. John is an exceptionally insightful Academic, a sagacious mentor and a very sensitive human being. Working under your guidance has been a privilege but also a pleasurable experience. I have gained a fountain of knowledge, adopted a research lifestyle that I am sure it will be of great help to me in the years to come.

I would like to thank Prof Brian Sheppard for his unwavering support and assistance. I still recall the memories of our first meeting 7 years ago, only a few days after I had arrived in Ireland. Your expert advice throughout this time has been extremely helpful and I will be always grateful to you.

Words are not enough to thank you Sharon. Thank you for answering the millions of questions I have asked over the last four years, for helping me with the lab work, for providing me with invaluable feedback for our posters, publications and meetings. Thank you for reading all my drafts while you were on maternity leave and helping me wrapping up the loose ends. Frankly, this achievement would not have been made possible without your help!

Dr Eamon Mc Guinness deserves a special mention for all the guidance and support he gave me. I know you are delighted with this achievement and yes, I am going to get my membership this coming year, I promise!

I would like to thank Dr Noreen Gleeson and Dr Tom D'Arcy for their continuous support and advice and for giving me the opportunity to return back to the clinical practice.

A special thanks to Dr Richie Flavin, Martina Ring, Dr Bashir and Lynne Kelly for their help, advice, chats and for being good friends.

A special thanks to Dr Lucy Norris, Dr Orla Sheils and Jeanette Brosnan for their help, advice and enthusiasm.

Thanks to Valerie for her continuous support during this time.

Special thanks to all those at the Research Laboratory in the Coombe Women's Hospital; especially Cara Martin and Michael Gallagher. I will see you there in less than a month!

I would like to thank the Royal City of Dublin Hosptal fund for their financial contribution to this project.

I would like to thank Emer Casey's family for being a massive source of inspiration to me.

Thanks to my family for being responsible for who I am today, for being always there at the drop of my hat to offer their love and support whenever I needed it, for putting up with me when the bad days in the lab used to be more than the good ones!

Thanks to Petros and Despoina Florides for being like a family to me in Ireland!

Thanks to all my friends for their understanding and for taking always the pressure away from me with a good laugh!

Thanks to the Mother of Earth for being the source of infinite love and inspiration without even the label or the rights of a "best friend"!

PUBLICATIONS ARISING FROM THESIS

Peer-reviewed Articles

Laios A, O'Toole S, Flavin R, Martin C, Kelly L, Ring M, Finn SP, Barrett C, Loda M, Gleeson N, D'Arcy T, McGuinness E, Sheils O, Sheppard B, O' Leary J. Potential role of miR-9 and miR-223 in recurrent ovarian cancer. Molecular Cancer 2008; 7:35. PMID: 18442408

Laios A, O'Toole SA, Flavin R, Martin C, Ring M, Gleeson N, D'Arcy T, McGuinness EP, Sheils O, Sheppard BL, O' Leary JJ. An integrative model for recurrence in ovarian cancer. Molecular Cancer 2008; 7:8. PMID: 18211683.

Published Abstracts

Laios A, O'Toole SA, Gleeson NC, D'Arcy T, McGuinness EPJ, Ring M, Flavin R, Martin C, O'Brien J, O'Connell D, Sheils O, Cahill D, Gaffney E and O'Leary JJ. Recurrence in Ovarian Cancer; A transcriptomic approach. Laboratory Investigation, 2007 (87) Supplement 1, 204A.

O'Toole SA, Laios A, Sheppard B, Gleeson N, D'Arcy T, McGuinness EPJ, Ring M, Gaffney M, Flavin R, Martin C, O'Brien J, O'Connell D, Sheils O, Cahill D and O'Leary JJ. miRNA Signatures in Primary versus Recurrent Ovarian Cancers. Laboratory Investigation, 2007 (87) Supplement 1, 209A.

Laios A, O'Toole SA, Sheppard BL, Gleeson NC, D'Arcy T, McGuinness EPJ, Ring M, Sheils O and O'Leary JJ. Molecular profiling of primary versus recurrent ovarian serous papillary adenocarcinomas. Laboratory Investigation, 2006, 86, (Suppl 1), pp185A.

Conference Proceedings

A Laios, SA O'Toole, B Png, R Flavin, L Kelly, T D'Arcy, E McGuinness, N Gleeson, B Sheppard, O Sheils, JJ O'Leary. Evaluation of *MMP-9* inhibitor and cisplatin cytotoxicity in chemoresistant ovarian cancer cell line using high content screening (hcs) cell-based assays. JOGS 2008 Annual Meeting, Dublin, November 2008.

Laios A, O'Toole SA, Flavin R, Martin C, Sheppard BL, Gleeson NC, D'Arcy T, McGuinness EPJ, Ring M, Sheils O, O'Leary JJ. An Integrative Transcriptome Map of Recurrence in Ovarian Cancer. PathSoc conference 2008, Oxford, Jan 2008.

Laios A, O'Toole SA, Flavin R, Martin C, Sheppard BL, Gleeson NC, D'Arcy T, McGuinness EPJ, Ring M, Sheils O, O'Leary JJ. Altered Expression of miR-223 and miR-9 in Recurrent Ovarian Cancers may target the FGF Family. PathSoc conference 2008, Oxford, Jan 2008.

Laios A, O'Toole SA, Flavin R, Kelly L, Sheppard B, Martin C, Ring M, D'Arcy T, McGuinness E, Gleeson N, Sheils O, O'Leary JJ. Dysregulation of miR-223 and miR-9 in recurrent ovarian cancer. Annual IACR Meeting, March 2008.

A Laios, SA O'Toole, R Flavin, L Kelly, C Martin, M Ring, T D'Arcy, E McGuinness, N Gleeson, B Sheppard, O Sheils, JJ O'Leary. microRNAs and Recurrent Ovarian Cancer. JOGS 2007 Annual Meeting, Dublin, November 2007.

Laios A, O'Toole SA, Flavin R, Martin C, Sheppard BL, Gleeson NC, D'Arcy T, McGuinness EPJ, Ring M, Sheils O, O'Leary JJ. microRNA signatures in recurrent ovarian cancer. Proceedings of the European Society of Gynaecological Oncology ESGO 15, Berlin, Oct 2007.

Laios A, O'Toole SA, Flavin R, Martin C, Sheppard BL, Gleeson NC, D'Arcy T, McGuinness EPJ, Ring M, Sheils O, O'Leary JJ. microRNA signatures in recurrent ovarian cancer. European Cancer Conference ECCO 14, Barcelona, September 2007.

Laios A, O'Toole SA, Sheppard BL, Gleeson NC, D'Arcy T, McGuinness EPJ, Ring M, Smyth P, Martin C, Sheils O, O'Leary JJ. cDNA and miRNA signatures in recurrent ovarian cancer: evidence of overlap. Annual IACR Meeting, Cork, March 2007.

A Laios, SA O'Toole, B Sheppard, N Gleeson, T D'Arcy, E PJ McGuinness, M Ring, O Sheils and JJ O'Leary. Recurrent ovarian cancer; potential chemoresistant signatures. JOGS 2006 Annual Meeting, Dublin, November 2006 (1st prize).

Laios A, O'Toole SA, Sheppard BL, Gleeson NC, D'Arcy T, Mc Guinness EPJ, Ring M, Sheils O, O'Leary JJ. cDNA signatures in recurrent ovarian cancer. IGOS Meeting, SJH, Dublin, October 2006.

Laios A, O'Toole SA, Sheppard BL, Gleeson NC, D'Arcy T, McGuinness EPJ, Ring M, Sheils O, Smyth P, O'Leary JJ. Recurrent ovarian cancer cDNA signatures. Proceedings of the Centenary Meeting of the Pathological Society of Great Britain and Ireland, Manchester, 2006.

Laios A, O'Toole SA, Sheppard BL, Gleeson NC, D'Arcy T, McGuinness EPJ, Ring M, Sheils O, O'Leary JJ. Signalling pathways implicated in the recurrence of ovarian cancer. Proceedings of the Irish Association for Cancer Research, Galway, 2006.

A Laios, SA O'Toole, B Sheppard, N Gleeson, T D'Arcy, E PJ McGuinness, M Ring, O Sheils and JJ O'Leary. Transcriptome profiling of primary and recurrent ovarian cancers. Proceedings of the Junior Obstetrics and Gynaecology Society, Dublin 2005.

SUMMARY

The aim of this study was to identify novel biomarkers in recurrent/chemoresistant ovarian cancer, yet an incurable disease. Using cDNA microarrays, we identified distinct patterns of gene expression between primary and recurrent ovarian cancers from different patients with the same histology and from same patients with different histology. Selected targets were validated and correlated with microarray results. Signatures from both cohorts were interrogated against each other and also validated against an independent set of serous papillary ovarian adenocarcinomas. Notably, upregulated genes in the recurrent compared to primary tumours in both cohorts, segregated in the same gene families. Our data propose an integrative model for recurrence in ovarian cancer, in which tumour cells during relapse produce adhesion molecules to mediate attachment, cytokines and inflammatory mediators to stimulate survival and a variety of growth factors bound to their cognate receptors to fully proliferate in order to confront and modulate their immediate environment. Some of the mechanisms involved in recurrence could be specific to the drugs used.

Using real-time RT-PCR, we also obtained distinct miRNA expression profiles between primary and recurrent serous papillary ovarian adenocarcinomas in a subset of samples used in our transcriptome approach. Expression levels of top dysregulated miRNA genes, miR-223 and miR-9, were examined using TaqMan PCR in independent cohorts of fresh frozen and formalin fixed paraffin embedded serous ovarian tumours. Concordance was observed on TaqMan analysis for miR-223 and miR-9 between the training cohort and the independent test cohorts. Target prediction analysis for the above miRNAs identified genes previously validated in the transcriptome study. Common biological pathways well characterised in ovarian cancer were shared by miR-9 and miR-223 lists of predicted target genes. This "recurrent metastatic signature" can predict progression free survival in ovarian cancer patients. Components of the miRNA processing machinery, such as Dicer and Drosha are not responsible for miRNA deregulation in recurrent ovarian cancer as deluded by TaqMan and immunohistochemistry.

We carried out TaqMan PCR on 10 gene targets, previously upregulated in recurrent versus primary ovarian cancers in chemoresistant versus chemosensitive ovarian

cancer cell lines. *NRG2* and *MMP9* were consistently upregulated for an average of 3 passages in A2780cis versus A2780 cell lines. We hypothesised that *MMP-9* could be a potential marker of recurrence/chemoresistance. We used a high content screening (HCS) assay to assess cytotoxicity of a highly selective chemical inhibitor of *MMP-9* (*MMP-9*i) alone or in combination with cisplatin in chemoresistant and chemosensitive ovarian cancer cells. Cells were plated in triplicate in 96-well plates overnight and then treated with various concentrations of drugs for 3, 6 and 24 hours. A pre-incubation for 3 hours with *MMP-9*i prior to treatment with cisplatin was also assessed and cytotoxicity was observed at 3 hours and 6 hours. Cells were then stained with three fluorescent dyes to image nucleus, cell permeability and lysosomal mass/pH respectively. The combined treatment of *MMP-9*i and cisplatin enhanced cytotoxicity in cisplatin-resistant cells compared to cisplatin or *MMP-9*i alone. Preincubating cells with *MMP*-9i for 3h at all doses were significantly cytotoxic at 3h but not 6h incubation suggesting, an early apoptotic response. Pre-incubating sensitive ovarian cancer cells with *MMP-9*i resulted to more enhanced cytotoxicity for the 3h incubation compared to the 6h and appeared to be more effective than co-incubation at early time in a concentration dependent way.

Collectively, we propose an integrative transcriptomic and miRNA model for recurrence in ovarian cancer. In addition, we suggest that a highly selective *MMP-9*i may have a role in recurrent/chemoresistant ovarian cancer.

ABBREVIATIONS

AB	Applied Biosystems
AJCC	American Joint Committee on Cancer
ANOVA	Analysis of Variance
C	Cisplatin
Cb	Carboplatin
CCD	Changed couple device
cDNA	Complementary Deoxyribonucleic Acid
CI	Confidence Interval
CL	Chemiluminescence
CLL	Chronic lymphocytic leukaemia
CT	Computed Tomography
Ct	Threshold Cycle
CTR1	Copper transporter-1
DIG	Digoxigenin
DIG-dUTP	Digoxigenin 2'-deoxyuridine 5'-triphosphate
DMSO	Dimethyl Sulfoxide
DNA	Deoxyribonucleic acid
ECM	Extracellular Matrix
EDTA	Ethylenediaminetetra-acetic acid
EMT	Epithelial-to-Mesenchymal Transition
EOC	Epithelial Ovarian Cancer
FBS	Fetal Bovine Serum
FC	Fold Change
FCS	Fetal Calf Serum
FDG	^{18}Fluoro-deoxy-glucose
FDR	False Discovery Rate
FF	Fresh Frozen
FFPE	Formalin Fixed Paraffin Embedded
FIGO	Federation of International Gynaecology and Obstetrics
G	Grade
G1	Gap 1
G2	Gap 2

GF	Growth factor
GOG	Gynaecologic Oncology Group
GS	Growth Signal
GST	Glutathione-S-transferase
H&E	Haematoxylin and Eosin
HCS	High Content Screening
HMM	Hidden Markov Model
HRT	Hormone replacement therapy
IC	Inhibitory Concentration
ID	Identification
IPA	Ingenuity Pathway Analysis
ITH	Intra-tumour heterogeneity
LCM	Laser Capture Microdissection
LMP	Low malignant potential
LN2	Liquid Nitrogen
LOH	Loss of heterozygosity
M	Mitosis
MAGE-ML	MicroArray and Gene Expression Markup Lanquage
MDR	Multidrug Resistance
mg	milligram
ml	millilitre
MMR	Mismatch Repair
mRNA	Messenger Ribonucleic Acid
MT	Microtubule
MTS	3-(4,5-dimethylthiazol-2-yl)-5-(3-carboxymethoxyphenyl)-2-(4-sulfophenyl)-2H-tetrazolium-inner salt
NCI	National Cancer Institute
NCRI	National Cancer Registry
NER	Nucleotide excision repair
ng	Nanogram
nM	Nanomolar
OC	Ovarian Carcinoma
OS	Overall survival

OSC	Ovarian Serous Carcinoma
OSE	Ovarian surface epithelium
P	Primary
PAM	Prediction Analysis of Microarrays
PANTHER	Protein Analysis THrough Evolutionary Relationships
R	Recurrent
PBS	Phosphate Buffer Saline
PCR	Polymerase Chain Reaction
PET	Positron emmision tomography
PFS	Progression free survival
PID	Pelvic inflammatory disease
PMS	Phenazine methosulfate
PPC	Peak Plasma Concentration
RNA	Ribonucleic acid
rRNA	Ribosomal RNA
rpm	Revs per minute
RPMI	Roswell Park Memorial Institute
RQ	Relative Quantitation
RT	Reverse Transcription
RT IVT	Reverse Transcription in Vitro Transcription
RT PCR	Reverse Transcription Polymerase Chain Reaction
S	Synthesis
SEIG	Surface epithelial inclusion glands
siRNA	Silencing RNA
SD	Standard Deviation
S/N	Signal to Noise
TE	Trypsin EDTA
TBS	Tris Buffer Saline
TJ	Tight junction
TMA	Tissue MicroArray
TNM	Tumour, Node, Metastasis
TVS	Transvaginal Ultrasound
UICC	Union Internationale Centre le Cancer
UTR	Untranslated Region

UPGMA	Unweighted Pair Group Method with Arithmetic Mean
US	Ultrasound
WAI	Whole abdominal irradiation
WHO	World Health Organisation
XP	Xeroderma pigmentosum
µl	Microlitre
µm	Micromole

TABLE OF CONTENTS

DECLARATION I

DEDICATED TO II

ACKNOWLEDGEMENTS III

PUBLICATIONS ARISING FROM THESIS V

SUMMARY VIII

ABBREVIATIONS X

1.1 CANCER 2

1.2 CANCER AND THE CELL CYCLE 2

1.3 CARCINOGENESIS 3

1.4 OVARIAN CANCER 8

1.5 EPIDEMIOLOGY 9

1.6 OVARIAN CANCER IN IRELAND 12

1.7 AETIOLOGY AND RISK FACTORS 15

1.8 HISTOLOGICAL CLASSIFICATION OF OVARIAN CANCER 19

1.9 OVARIAN CANCER STAGING 24

1.10 OVARIAN CANCER GRADING 29

1.11 MOLECULAR PATHOGENESIS OF OVARIAN CANCER 30

1.12 EXPERIMENTAL MODELS OF OVARIAN CANCER 38

1.13 DIAGNOSIS 38

1.14 CURRENT MANAGEMENT OF OVARIAN CANCER 44

1.15 GENOMIC APPROACHES IN BIOMARKER DISCOVERY 72

1.16 MICRORNAS (MIRNAS) 80

1.17 HIGH CONTENT SCREENING (HCS) 88

1.18 AIMS OF THE STUDY 91

2.1 INTRODUCTION 93

2.2 FRESH OVARIAN TISSUE ARCHIVE 98

2.3 RNA EXTRACTION FROM FRESH TISSUE 98

2.4 NANO-DROP 1000 SPECTROPHOTOMETER (ND-1000) 102

2.5 MICROARRAYS 105

2.6 RT-IVT LABELING 112

2.7 INGENUITY® PATHWAY ANALYSIS (IPA) 119

2.8 MICRORNA EXPRESSION ANALYSIS USING REAL-TIME PCR (RT-PCR) 119

2.9 LASER CAPTURE MICRODISSECTION (LCM) 136

2.10 TISSUE MICROARRAY (TMA) 140

2.11 CELL CULTURE OF OVARIAN CANCER CELL LINES 141

2.12 CYTOTOXICITY ASSAY 144

2.13 HIGH CONTENT SCREENING (HCS) 145

2.14 PREPARATION OF CELL LINES FOR RNA EXTRACTION 150

3.1 SUMMARY 152

3.2 INTRODUCTION 153

3.3 MATERIALS AND METHODS 154

3.4 RESULTS 165

3.5 DISCUSSION 188

4.1 SUMMARY 197

4.2 INTRODUCTION 198

4.3 MATERIALS AND METHODS 200

4.4 RESULTS 205

4.5 DISCUSSION 230

5.1 SUMMARY 239

5.2 INTRODUCTION 240

5.3 MATERIALS AND METHODS 247

5.4 RESULTS 250

5.5 DISCUSSION 279

6.1 INTRODUCTION 287

6.2 MOLECULAR PROFILING OF RECURRENT VERSUS PRIMARY OVARIAN CANCERS 287

6.3 MIRNA PROFILING OF RECURRENT VERSUS PRIMARY OVARIAN CANCERS 288

6.4 HCS CYTOTOXICITY SCREENING 290

6.5 RECOMMENDATIONS FOR FUTURE RESEARCH 290

6.6 CONCLUSIONS 295

REFERENCES 296

LIST OF FIGURES

Figure 1.1 The Cell Cycle and the Checkpoints 3
Figure 1.2 The hallmarks of Cancer 5
Figure 1.3 Ovarian Cancer 8
Figure 1.4 Global map showing incidence of ovarian cancer 10
Figure 1.5 Age-standardized Incidence and Mortality Rates for Ovarian Cancer 10
Figure 1.6 Age composition of patients at diagnosis (left), death (right) of ovarian cancer 11
Figure 1.7 Comparison of A) new cancer cases and B) death between ovarian and other cancers in Ireland for the years 1994-2005. 13
Figure 1.8 Percentage of invasive cancers in Ireland for two different year groups.. 14
Figure 1.9 Derivation of ovarian neoplasms. 21
Figure 1.10 Representative examples of the major histological subtypes of EOC 24
Figure 1.11 Microscopic view of a poorly differentiated serous papillary cystadenocarcinoma 30
Figure 1.12 Ovarian carcinoma in situ 32
Figure 1.13 Schematic illustration of Type I and Type II ovarian serous carcinoma pathogenesis. 35
Figure 1.14 Activation and functions of *p53*. 36
Figure 1.15 Imaging methods in ovarian cancer 43
Figure 1.16 Management algorithm for patients with ovarian cancer 45
Figure 1.17 Residual disease affects overall survival in patients with stage IIIC ovarian cancer (n=194; log-rank test, P<0.001). 46
Figure 1.18: Milestones in the development of platinum drugs for cancer therapy... 53
Figure 1.19 Some of the possible mechanisms of chemoresistance 61
Figure 1.20: Platinum binds DNA forming platinum-DNA adducts 63
Figure 1.21 Major ongoing strategies to circumvent cisplatin and carboplatin resistance 68
Figure 1.22 Taxol inhibits dissassembly of mitotic spindles and microtubules during the M phase by binding to tubulin heterodimers. 70
Figure 1.23 Search for molecular determinants of ovarian cancer 74
Figure 1.24 Gene expression patterns can be used to classify ovarian carcinomas into clinically relevant subtypes 76
Figure 1.25 Pathways with the highest number of OSE genes 79
Figure 1.26 miRNA function in the regulation of gene expression. 81
Figure 1.27 Schematic representation of miRNA biogenesis. 82
Figure 1.28 Chromosomal alterations at miRNA loci. 84
Figure 1.29: Common miRNA genes are differentially expressed in 6 solid cancers suggesting common altered pathways 85
Figure 1.30 Published data on miRNA expression up to 2006. 85
Figure 1.31 HCS Workstation 89
Figure 2.1 Nandrop ND-1000 Spectrophotometer and main software menu 103
Figure 2.2 Loading of samples on Nanodrop® Spectrophotometer 103
Figure 2.3 The AB 1700 cDNA Array system and microarrays. Micro arrays are sealed in a pre-assembled cartridge and contain oligonucleotides that target transcripts in each gene of the human genome 105
Figure 2.4 RT-IVT DIG-labelling of sample mRNA. 107
Figure 2.5 Chemiluminescent detection of bound DIG-labelled cRNA 108

Figure 2.6 Fluorescence used to image microarray features 109
Figure 2.7 Steps in the management of Microarray Data 110
Figure 2.8 Software workflow; from experimental set-up to secondary analysis.... 111
Figure 2.9 Flowchart of our microarray experiment 112
Figure 2.10 miRNA experimental overview 120
Figure 2.11 Overview of the mirVana™ miRNA Isolation Kit Procedure. 120
Figure 2.12 Overview of the Recoverall™ Total Nucleic Acid Isolation procedure123
Figure 2.13 The Taqman probe. 126
Figure 2.14 The TaqMan® probe binds to the target DNA 127
Figure 2.15 The reporter dye is released 127
Figure 2.16 An example of a graph printout using the TaqMan® probe 128
Figure 2.17 A representative amplification plot including some of the terms frequently used 133
Figure 2.18 Result views for an RQ plate Document 135
Figure 2.19 Schematic diagram of stem-loop RT-PCR 136
Figure 2.20 Laser Capture Microdissection (LCM) 137
Figure 2.21 The Arcturus PixCell II Laser Capture Microdissection system 138
Figure 2.22 Overview of the LCM process 138
Figure 2.23 Tissue MicroArray (TMA). 140
Figure 2.24 HCS Workflow 146
Figure 2.25 Multiparameter Cytotoxicity Assay 148
Figure 2.26 Live cell HCS images 149
Figure 3.1 Continuous integrated workflow 154
Figure 3.2 Flow chart of our study design. 155
Figure 3.3 Quantile Normalisation of Raw Data in cohort 1 166
Figure 3.4 MA plots 167
Figure 3.5 Detection concordance heatmap of the quantile normalized data for A) cohort 1 and B) cohort 2 168
Figure 3.6: Detectable probes with A) p value 0.01 B) FDR 0.1 in primary versus recurrent ovarian cancers in cohort 1 170
Figure 3.7 Volcano plot 171
Figure 3.8 Detectable probes with A) p value 0.05 B) p value 0.01 in primary versus recurrent ovarian cancers in cohort 2 172
Figure 3.9 Volcano plot 173
B 174
Figure 3.10 Hierarchical cluster heatmaps 174
Figure 3.11 Detectable probes with A) p value 0.01 B) FDR 0.25 in primary versus recurrent ovarian cancers in combined cohorts 1&2. 175
Figure 3.12 Example of a hierarchical cluster heatmap 176
Figure 3.13 Gene families involved in the molecular regulation of recurrence in ovarian cancer. 177
Figure 3.14 Example of a biological pathways pie chart 178
Figure 3.15 Example of a biological pathways pie chart 179
Figure 3.16 TaqMan® PCR validation of target genes in both training and test sets. 180
Figure 3.17 TaqMan® PCR validation of microarray experiments in cohort 1 184
Figure 3.18 TaqMan® PCR validation of microarray experiments in cohort 2 185
Figure 3.19 External validation of a subset of upregulated genes in cohort 2 that validated in cohort 1 186

Figure 3.20 Independent TaqMan® PCR validation of a set of selected genes, upregulated in recurrent samples, ... 187
Figure 3.21 An integrative model for recurrence in ovarian cancer..... 194
Figure 4.1 miRNA biogenesis and evolution. 198
Figure 4.2 Flow chart of our study design. 199
Figure 4.3 Relative fold changes are displayed on the y axis and the miRNAs are on the x axis. 207
Figure 4.4 Unsupervised hierarchical cluster heatmap..... 208
Figure 4.5 PAM prediction analysis in primary and recurrent ovarian samples..... 209
Figure 4.6 Esitmated FDRs for given thresholds plotted against the number of genes called significant. 209
Figure 4.7 PAM class prediction analysis and test probabilities..... 210
Figure 4.8 PAM class prediction analysis and test probabilities..... 211
Figure 4.9 TaqMan PCR analysis of top dysregulated miRNAs 213
Figure 4.10 TaqMan analysis of top dysregulated genes in training cohort and FFPE cohort..... 214
Figure 4.11 Common significant biological pathways observed for miR9 and miR223 218
Figure 4.12 Progression free survival curves in FFPE primary ovarian tumours in relation to miR-223 expression levels. 220
Figure 4.13 Overall survival curves in FFPE primary ovarian tumours in relation to miR-223 expression levels. 220
Figure 4.14 Progression free survival curves in FFPE primary ovarian tumours in relation to miR-9 expression levels..... 221
Figure 4.15 Overall survival curves in FFPE primary ovarian tumours in relation to miR-9 expression levels. 221
Figure 4.16 Progression free survival curves in FFPE primary ovarian tumours in relation to miR-93 expression levels..... 222
Figure 4.17 Overall survival curves in FFPE primary ovarian tumours in relation to miR-93 expression levels. 222
Figure 4.18 Progression free survival curves in FF primary ovarian tumours in relation to miR-223 expression levels..... 223
Figure 4.19 Overall survival curves in FF primary ovarian tumours in relation to miR-223 expression levels. 223
Figure 4.20 Progression free survival curves in FF primary ovarian tumours in relation to miR-9 expression levels..... 224
Figure 4.21 Overall survival curves in FF primary ovarian tumours in relation to miR-9 expression levels. 224
Figure 4.22 Progression free survival curves in FF primary ovarian tumours in relation to miR-93 expression levels..... 225
Figure 4.23 Overall survival curves in FF primary ovarian tumours in relation to miR-93 expression levels. 225
Figure 4.24 Expression of eIF6 and Dicer in normal ovarian surface epithelium and ovarian serous adenocarcinoma..... 228
Figure 4.25 Global staining pattern for (e) eIF6 and (f) Dicer in TMA of primary serous papillary ovarian adenocarcinomas..... 229
Figure 4.26 A miRNA model for the molecular pathogenesis of recurrent ovarian cancer. 236
Figure 5.1 Classification of MMPs based on their specificity for ECM components 241

Figure 5.2 Functions of MMPs in cancer progression..... 243
Figure 5.3 (2R)-2-[(4-Biphenylylsulfonyl)amino]-3-phenylpropionic Acid..... 247
Figure 5.4 Heatmap demonstrating two-dimensional hierarchical clustering 252
Figure 5.5 K-means unsupervised clustering of the 8 deregulated genes in A2780 vs A2780 cell lines. 253
Figure 5.6 Scatter plot three dimensional clustering of tested genes based on their fold changes in A2780cis compared to A2780 cell lines. 254
Figure 5.7 Flow chart of our dose and time response experiments..... 255
Figure 5.8(A-E) Simultaneous monitoring of changes in A) cell density B) cell membrane permeability C) lysosomal mass/pH D) nuclear condensation and E) nuclear size following treatment of the A2780cis cells with cisplatin 257
Figure 5.9(A-E) Simultaneous monitoring of changes in cell density, cell membrane permeability, lysosomal mass/pH, nuclear condensation and nuclear size following treatment of the A2780cis cells with *MMP-9*i..... 260
Figure 5.10 Morphology of cisplatin and *MMP-9*i treated cells as demonstrated by HCS image analysis. 261
Figure 5.11(A-J) Effects on cytotoxicity following co-incubation of A2780cis cells with cisplatin and *MMP-9*i for 3h and 6h. 264
Figure 5.12 (A-J) Preincubation of A2780cis cell line with MMP-9i for 3h enhances cytotoxicity. Resistant cell were incubated with MMP-9i for 3h prior to addition of cisplatin and incubation for 3h and 6h.....267
Figure 5.13(A-D) Pre-incubation with *MMP-9*i compared to co-incubation for the A2780cis cell line (3h incubation)..... 269
Figure 5.14(A-H) Pre-incubation with MMP-9i compared to co-incubation for the A2780cis cell line (6h incubation)..... 272
Figure 5.15(A-C) Simultaneous monitoring of changes in A) cell density B) lysosomal mass/pH C) nuclear size following treatment of the A2780cis cells with cisplatin 273
Figure 5.16 Simultaneous monitoring of changes in A)cell density B) nuclear condensation C) cell membrane permeability D) lysosomal mass/pH, following treatment of the A2780 cells with MMP-9i..... 275
Figure 5.18(A-B) Efffect on cell density following co-incubation of A2780 cells with cisplatin and MMP-9i for 3h and 6h. 276
Figure 5.19(A-C) Effects on A) lysosomal mass/pH B) nuclear condensation C) cell membrane permeability following co-incubation of A2780 cells with cisplatin and MMP-9i for 6h. 277
Figure 5.20(A-B) Preincubation of A2780 cell line with *MMP-9*i for 3h followed by treatment with cisplatin and incubation for 3h and 6h..... 278
Figure 5.21. MMPs can be viewed as sophisticated modulators, positive or negative regulators of cancer development and metastatic dissemination..... 281
Figure 5.22 A model of possible implication of MMPIs in the treatment of ovarian cancer. 285
Figure 6.1 Examples of imaging traits in ovarian cancer. 293

LIST OF TABLES

Table 1.1 Summary information, incidence and prevalence in ovarian cancer in Ireland according to NCRI figures 2005. 15
Table 1.2 Summary information on mortality in ovarian cancer according to NCRI figures 2005. 15
Table 1.3 Histological classification of ovarian tumours according to FIGO 22
Table 1.4 Carcinoma of the ovary: FIGO stages and AJCC TNM class 28
Table 1.5 Common precursor lesions and molecular features of Type I and Type II carcinomas. 34
Table 1.6 Table of platinum drugs used in cancer with indications, years of approval from the Food and Drug Administration (FDA) and their dose limiting toxicities). 52
Table 1.7 Cytotoxic agents used in ovarian cancer treatment 71
Table 1.8 DNA microarray studies and their specific aims in ovarian cancer ... 75
Table 1.9 Facts about miRNA profiling in human cancers 86
Table 2.1 Primary Ovarian Specimens 94
Table 2.2 Recurrent Ovarian Specimens 96
Table 2.3 Recommended kits for two-step RT-PCR. 130
Table 2.4 List of reagents used for preparation of RT Master Mix with their volumes 131
Table 2.5 Reaction components for a single RT-PCR 132
Table 2.6 Standard PCR conditions 134
Table 2.7 List of cytotoxic and cytostatic drugs used in our study 144
Table 2.8 Contents of the Cytotoxicity 1 Multiparameter Kit 145
Table 3.1: List of gene targets selected for TaqMan® validation in cohort 1 ... 162
Table 3.2: List of gene targets selected for TaqMan® validation in cohort 2 ... 163
Table 3.3 Nano Drop Analysis of primary (P) and recurrent (R) ovarian cancers 165
Table 3.4 List of selected genes differentially expressed in recurrent versus primary tumours in cohorts 1 and 2 with information about their molecular function, biological processes or pathways involved. Some of these genes have not been previously implicated in ovarian cancer. These genes were chosen to be validated as they might represent markers of recurrence). 181
Table 4.1 List of the miRNA genes differentially expressed between recurrent and primary serous papillary ovarian adenocarcinomas 206
Table 4.2 PAM list of significant miRNA genes for classification prediction in recurrent versus primary tumours. The PAM algorithm was used for gene identification at a threshold of 1.1 (FDR<0.5). 211
Table 4.3 List of important miRNA genes differentially dysregulated in recurrent vs primary ovarian cancers with their predicted gene targets..215
Table 4.4 mRNAs and predicted miRNA targets. 216
Table 4.5 Survival Data and clinicopathological details 219
A Fresh Frozen 219
B Formalin Fixed Paraffin Embedded 219
Table 4.6 One-sided test analysis of two miRNA signatures 226
Table 4.7 Correlation of expression levels of top dysregulated miRNA genes with clinicopathological variables for primary tumours 227
Table 5.1: List of concentrations of Cisplatin and *MMP-9*i; 248

Table 5.2 List of selected genes for TaqMan analysis in the cell lines with their assay ID's. 249
Table 5.3A Nano Drop Analysis 250
Table 5.3B: Nano Drop Analysis 251
Table 5.4 Incubation comparisons between pre-incubation versus co-incubation treatments (3h) with their p values. 268
Table 5.5 Incubation comparisons between pre-incubation vs co-incubation treatments for 6h with their p values. 270

CHAPTER 1

Introduction

1.1 Cancer

Tremendous progress has been made in understanding the pathobiology and molecular biology of cancer in the last 2 decades, yet a cure is hard to achieve. The word cancer refers to about 200 diseases that have a common feature, namely uncontrolled cell growth. Management of these diverse neoplasms is multifaceted and relies on close collaboration among surgeons, radiation and medical oncologists, pathologists and radiologists. Cancer becomes life threatening when tumour cells spread across the body. Identification of high-risk individuals, responders to treatment and early detection of cancer remains the cornerstone of successful treatment. Early detection and advanced treatment have fortunately improved cure rates, however therapy failure is still a major drawback in systemic treatment of cancer patients due to development of intrinsic or acquired resistance during their course of treatment.

1.2 Cancer and the cell cycle

The **cell cycle** is required for cell growth and **cell division** into two daughter cells. Cell division is fundamental to replace cells that are lost by programmed or unprogrammed cell death. A eukaryotic cell cannot divide unless it replicates its genome (DNA) and then separates the duplicated genome. To achieve these tasks cells must perform **DNA synthesis** and **mitosis**. The cell cycle is an ordered set of events. The **G1** phase stands for "GAP-1" and is required for cell growth and preparation of DNA synthesis. The **S**-phase stands for "Synthesis" and replicates the genome. The **G2** phase is "GAP-2" and needed for cell growth and preparation for mitosis. The last phase is **M** and it stands for "Mitosis" in which cells segregate duplicated chromosomes.

The cell cycle proceeds by a defined sequence of events where late events depend upon completion of early events [1]. The aim of the dependency of events is to distribute complete and accurate replicas of the genome to daughter cells. To monitor this dependency, cells are equipped with the **checkpoints** that are set at various stages of the cell cycle [2]. When cells have DNA damage that have to be repaired, cells activate **DNA damage checkpoint** that arrests cell cycle. Upon perturbation of

DNA replication by drugs that interfere with DNA synthesis or obstacles on DNA, cells activate **DNA replication checkpoint** that arrests cell cycle at G2/M transition until DNA replication is complete. There are more checkpoints such as **Spindle checkpoint** and Morphogenesis checkpoint. The spindle checkpoint arrests cell cycle at M phase until all chromosomes are aligned on spindle. This checkpoint is very important for equal distribution of chromosomes. Morphogenesis checkpoint detects abnormality in cytoskeleton and arrests cell cycle at G2/M transition.

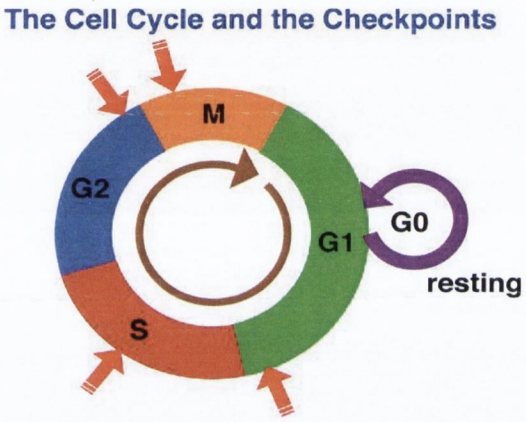

Figure 1.1 The Cell Cycle and the Checkpoints

An abnormality in a cell's regulatory mechanisms results in uncontrolled cell growth and reproduction of the cell eventually forming a new growth, known as tumour or neoplasia. Willis in 1952, defined cancer as "an abnormal mass of tissue, the growth of which exceeds and is uncoordinated with that of the normal tissues and persists in the same excessive manner after cessation of the stimuli which evoked the change".

1.3 Carcinogenesis

Several lines of evidence indicate that carcinogenesis in humans is a multistep process and that these steps reflect genetic alterations that drive the progressive transformation of normal human cells into highly malignant derivatives. Many types of cancers are diagnosed in the human population with an age-dependent incidence implicating rate-limiting events [3]. Pathological analyses of a number of organ sites

reveal lesions that appear to represent the intermediate steps in a process through which cells evolve progressively from normal status via a series of premalignant states into invasive cancers [4] [5]. These observations have been rendered more concrete by a large body of work indicating that the genomes of tumor cells are invariably altered at multiple sites, having suffered disruption through lesions as subtle as point mutations and as obvious as changes in chromosome complement [6].

Cancer cells have defects in regulatory circuits that govern normal cell proliferation and homeostasis [7]. So far, more than 200 disinct types of cancer and subtypes of tumours have been found within specific organs. Six distinct regulatory circuits have been suggested to describe the complexity of cancer. Malignant growth is dictated by: self sufficiency in growth signals, insensitivity to antigrowth signals, evasion of apoptosis, limitless replicative capacity, sustained angiogenesis, tissue invasion and metastasis. These capabilities are acquired during tumour development and are thought to be shared in common by most or all types of human cancers [8].

Self sufficiency in growth signals: Mitogenic growth signals (GS) are required by normal cells in order to move from a quiescent to an active proliferative state. Transmembrane receptors bound to distinctive classes of signalling molecules, such as *growth factors (GF)*, *extracellular matrix components* and *cell-to-cell adhesion molecules*, transmit these signals.

Acquired GS autonomy has been clearly defined by researchers because of the prevalence of dominant oncogenes that have been found to modulate it. The cell surface receptors that transduce growth-stimulatory signals into the cell interior are themselves targets of deregulation during tumorinogenesis. Receptor overexpression may enable the cancer cell to become hyperresponsive to ambient levels of GF that normally would not trigger proliferation. Ligand-independent signalling can also occur through structural alteration of receptors.

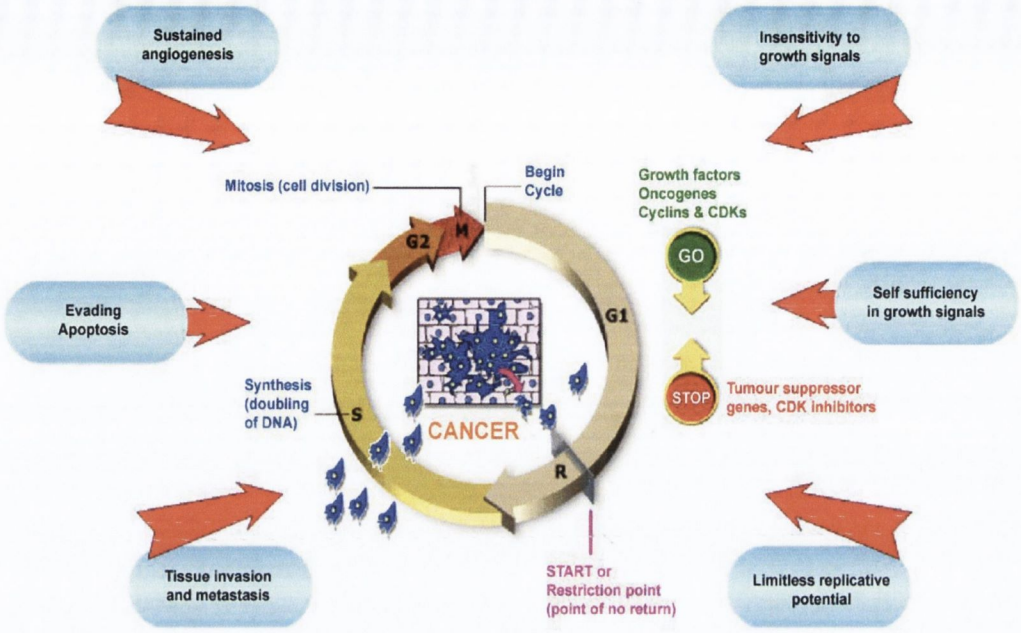

Figure 1.2 The hallmarks of Cancer

The hallmarks are shown in blue shaded ovals. The normal cell cycle is a precisely controlled event and the decision to enter the next phase of cell cycle is made in G1 phase. A balance between the "GO" signals and "STOP" signals determines whether to divide or not. Gene mutations in cancers allow cells to enter a perpetual cell division cycle and achieve the hallmarks (Cell cycle wheel taken from Howard Hughe Medical Institute website. 1996).

Extracellular matrix receptors are also switched by cancer cells to transmit progrowth signals. These heterodimeric cell surface receptors physically link cells to extracellular matrix (ECM) and their successful binding enables signal transduction into the cytoplasm. Failure to maintain the extracellular links can cause cell impairment, induction of apoptosis or even cell cycle arrest [9].

Insensitivity to antigrowth signals: Antiproliferative signals operate in normal cells to maintain tissue homeostasis; these include growth inhibitors received by transmembrane cell surface receptors coupled to their intracellular signalling circuits

and are associated with the cell cycle clock. Cancer cells must evade these antiproliferative signals if they are to prosper. At the molecular level, perhaps all antiproliferative signals are funnelled through the retinoblastoma protein [10].

Evading apoptosis: Acquired resistance towards apoptosis-programmed cell death- is a hallmark of all cancers. The most commonly occurring loss of a proapoptotic regulator through mutation involves the *p53* tumour suppressor gene. Inactivation of the *p53* protein is predominantly seen in > 50% of cancers, including ovarian cancer and results in the removal of a key component of the DNA damage sensor that can induce the apoptosis cascade [11].

Limitless replicative potential: In order for a clone of cells to grow to a size that constitutes a macroscopic tumour, the cell intrinsic program that limits cell multiplication needs to be disrupted. Telomere maintenance at a length above a critical threshold is central to this and this is evident in virtually all types of tumours [12].

Sustained angiogenesis: Growth metastatic potential, particularly of solid tumours, requires vascular support for nutritive supply and oxygen. For a tumour to get larger than $1mm^3$, a process of angiogenesis must occur [13]. The ability to sustain angiogenesis seems to be acquired in a discrete step via an "angiogenic switch". Angiogenesis is subjected to regulatory balance via counterbalanced positive and negative signals [14].

Tissue invasion and metastasis: The migration capacity of cancer cells manifests in two ways. Invasion reflects the ability to become dislodged and travel within the tissue of origin. Metastasis involves travel beyond the tissue of origin. Metastasis represents the most lethal aspect of cancer and is responsible for the majority of deaths among cancer patients. The current view of cancer incorporates a set of overlapping dichotomies: invasion and metastatic spread are both related to cell mobility, which is distinct from cell proliferation, thought to be responsible for tumorigenesis but not for metastatic behaviour. Latest experimental results suggest the possibility that the process of self seeding, a close relative of metastasis may influence important features of cancer [15]. These features include high cell density,

multifocality, amplified growth rate and the capacity to spread as well as reproduce these features in distant organ sites.

While we believe that virtually all cancers must acquire the same six hallmark capabilities, their means of doing so will vary significantly, both mechanistically and chronologically. Thus, the order in which these capabilities are acquired is likely to be quite variable across the spectrum of cancer types and subtypes. Moreover, in some tumors, a particular genetic lesion may confer several capabilities simultaneously, decreasing the number of distinct mutational steps required to complete tumorigenesis. For example, loss of function of the *p53* tumor suppressor can facilitate both angiogenesis and resistance to apoptosis, as well as enabling the characteristic of genomic instability. In other tumours, a capability may only be acquired through the collaboration of two or more distinct genetic changes.

Histopathological studies of different tumour types also suggest that tumours are morphologically heterogeneous. Tumours are variable in several ways. Their features change with organ site and cell origin. Host variables such as age and hormonal status introduce differences; however, tumour heterogeneity reflects also cellular changes within a single neoplasm. Tumours are architecturally complex, differ regionally in vasculature, microenvironments, proliferation behaviour, host infiltrates and connective tissue components, only to mention a few; all that can alter the phenotype of otherwise identical cells. It seems likely that this heterogeneity has an underlying genetic and biological basis and suggests that as tumours develop, they undergo an evolutionary departure from a monoclonal state to a state consisting of multiple sub-clones. Thus, sub-populations of neoplastic cells within a single tumour may be at different stages of development, have different biological characteristics, and different propensities for further neoplastic development. Broadly, this can be referred to as intra-tumour heterogeneity (ITH) [16]. Furthermore, other cellular phenotypes different than those transmittable genetic and epigenetic differences, such as antigen expression, metastatic potential or response to chemotherapy [17] might be also important in terms of biological or clinical significance.

1.4 Ovarian cancer

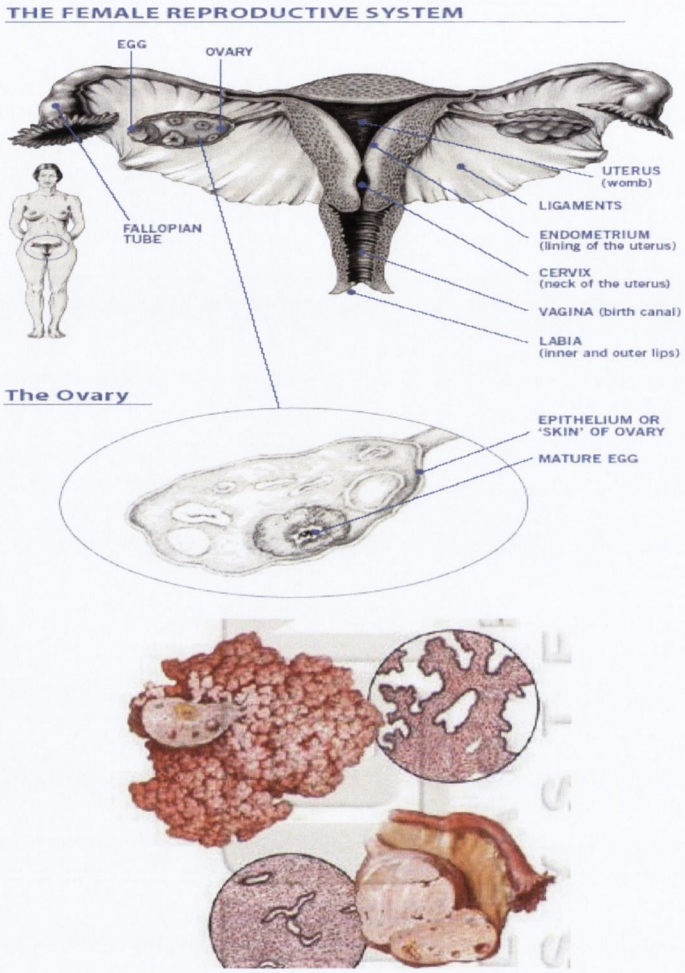

Figure 1.3 Ovarian Cancer

Ovarian cancer represents a major clinical challenge in gynaecologic oncology. Ovarian cancer dissemination differs from the classical metastatic patterns of tumours arising from other organ sites in that ovarian cancer seeds the peritoneal cavity with tumour cell nests that adhere to adjacent organs or float freely and only later lead to ascites formation. As a result ovarian cancer is asymptomatic and most women present with advanced disease often spread as diffuse small-volume deposits. In addition, the vasculature and anatomical position of the ovaries predispose them to

metastasis from the genital and gastrointestinal tract. Tumour metastasis to the peritoneal and/or pleural cavity is evident in two-thirds of cases at diagnosis and relapse is often detected in these anatomic sites.

Marked heterogeneity is a hallmark of the disease, not only in tumour histotype and grade but also in response to treatment and overall prognosis [17].

1.4.1 Recurrent ovarian cancer

It is widely accepted that recurrent tumours represent the "true killers" in cancer patients, because the primary tumours are usually removed by surgery. Cancer mortality and morbidity are related to recurrent and metastatic disease. Identification of molecular targets that are present in recurrent tumours would be important in the development of prognostic tests and novel therapeutic interventions for cancer patients.

1.5 Epidemiology

Ovarian cancer is one of the most common cancers in women and the leading cause of death from gynaecological malignancy in the western world (4% of cases and 4.2% of deaths) [18]. About 205,000 cases of ovarian cancer are diagnosed worldwide each year [19]. Incidence rates are highest in developed countries (Figure 1.4), with rates in these areas exceeding 9 per 100,000, except for Japan (6.4 per 100,000). Incidence in South America (7.7 per 100,000) is relatively high. Incidence rates have been slowly increasing in many Western countries and Japan. For women who immigrate from low-risk countries of origin, such as Asia, to high-risk areas, such as North America, a gradual increase has been observed in the incidence to rates expected for native-born women [20]. The crude incidence in the European Union is 18/100,000 women/year and the mortality is 12/100,000 women/year [21].

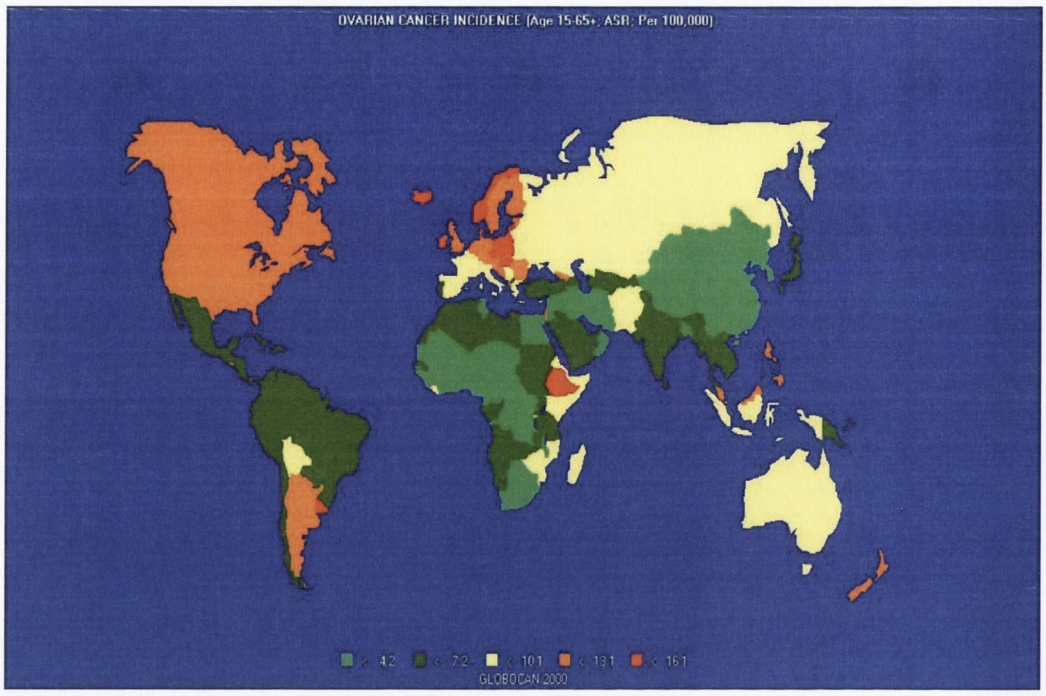

Figure 1.4 Global map showing incidence of ovarian cancer (Statistics obtained from Globocan, 2000).

32% of ovarian cancers present in women aged 50-64 years, with just over 20% presenting in each of the 65-74 and 75 and older age groups (Figure 1.5).

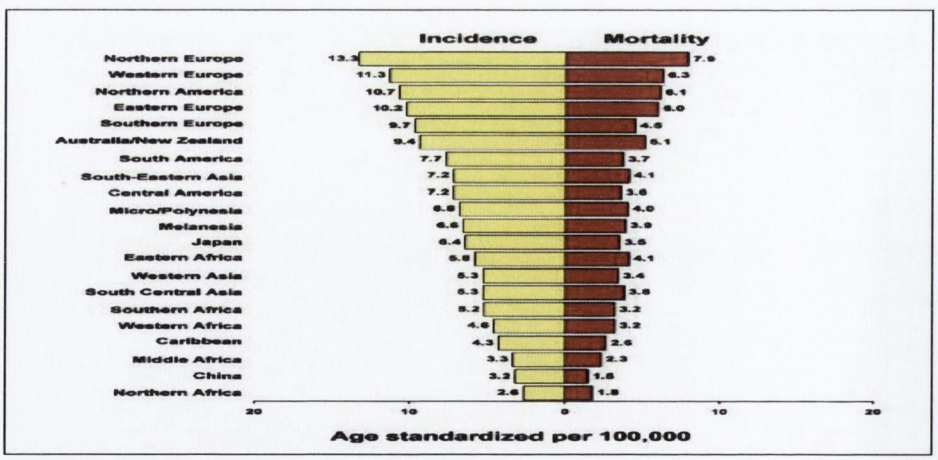

Figure 1.5 Age-standardized Incidence and Mortality Rates for Ovarian Cancer. (Data obtained from Globocan, 2000 are shown per 100,000).

As a result, median age at presentation is 63. The incidence increases with age and peaks in the eight decade. Between the ages of 70 and 74 years the age specific incidence is 57/100,000 women/year [21]. This advanced age at diagnosis contributes to the mortality of the disease. Almost one quarter of cases of ovarian cancer occur in women aged under 50. In terms of deaths, 42% are in women aged under 65, 27% in women aged 64-74 with the remaining 31% in women aged 75 and older (Figure 1.6).

Figure 1.6 Age composition of patients at diagnosis (left), death (right) of ovarian cancer (Data obtained from Globocan, 2000).

However, a consistent determination of an individual's response to treatment and survival cannot be predicted based solely on the above preceding variables [22].

Epithelial ovarian cancer (EOC) is predominantly a disease of peri- and postmenopausal women, with 80% to 90% of ovarian cancers occurring after the age of 40. Premenopausal women usually develop germ cell tumours and have a lower incidence of EOC. 1% of EOC occurs before the age of 20 and two-thirds of ovarian malignancies in these young patients are germ-cell tumours.

Ovarian cancers are mostly sporadic and only 5%-10% are familial. Hereditary ovarian cancers generally occur about 10 years earlier and are associated with a trend towards an earlier age at diagnosis with each successive generation [23], a

phenomenon known as anticipation. While the overall lifetime risk of developing ovarian cancer in industrialized countries is ~2% [19], for women with a family history, the lifetime risk is estimated at 9.4% [24].

1.6 Ovarian cancer in Ireland

According to the National Cancer Registry Ireland (NCRI), ovarian cancer accounts for 3% of female cancer in Ireland with approximately 334 new cases diagnosed every year and 226 deaths from the disease [25]. In Ireland, rates of ovarian cancer are higher than in the rest of the European Union. GLOBOCAN 2000 mortality estimates give some indication of how Ireland compares to its neighbours with respect to ovarian cancer mortality [25]. Ovarian cancer mortality rates in Ireland appear higher than those in UK, Belgium, France, and The Netherlands for reasons that are not clear. In actual fact, Ireland registers highest after Denmark with an incidence rate of 12.8%. One reason may be attributable to a later reduction in parity and the later availability of widespread oral contraceptives in Ireland in the early/mid 1980s compared to its nearest neighbours, since these are the best recognized protective factors with regard to ovarian carcinogenesis [26].

Compared with other cancers, such as breast, lung or colorectal cancers, ovarian cancer is a less common malignancy. A summary of ovarian cancer statistics for Ireland is provided in Figure 1.7 A and B. Nevertheless, because of its detection at an advanced stage and poor prognosis, it remains a difficult medical and scientific challenge. Mortality (per 100,000) has slightly decreased over the last 20 years. This is attributable to an increasing awareness about risk factors and improvement of surgical and chemotherapeutic treatment (Figure 1.8). Unfortunately, due to lack of sensitive screening method for early detection, the overall survival has not changed.
The ovarian cancer mortality rate is predicted to fall from 32.5/100,000 in 2000 to 29/100,000 by 2011/2015 but the numbers of deaths are predicted to increase from 73 to 97 [27].

A

	number of cases						incidence rate*	
	2005			average 1994-2005			1994-2005	
	female	male	both sexes	female	male	both sexes‡	female	male
all cancers	13901	12875	26776	11341	10706	22046	577.9	646.6
all invasive cancers except NMS*	8001	8578	16579	6624	7128	13752	343.1	429.9
non-melanoma skin	2860	3336	6196	2510	2888	5398	123.0	175.3
prostate	–	2407	2407	–	1687	1687	–	102.7
breast	2352	27	2379	1895	14	1910	105.7	0.9
colorectal	936	1248	2184	826	1073	1899	40.5	65.0
lung	750	1092	1842	611	1035	1646	30.3	62.7
unknown site	444	362	806	344	330	674	15.8	20.0
lymphoma	292	350	642	254	294	548	13.2	17.2
melanoma of skin	360	238	598	279	176	454	14.6	10.4
bladder	159	345	504	135	331	466	6.6	20.1
stomach	173	296	469	182	293	475	8.5	17.7
pancreas	200	186	386	181	180	361	8.4	10.9
kidney	154	221	375	111	191	302	5.8	11.7
leukaemia	147	224	371	160	233	393	7.9	13.8
ovary	367	–	367	348	–	348	18.9	–
oesophagus	131	222	353	122	193	316	5.6	11.8
brain and ONS*	138	207	345	127	169	296	6.6	9.8
corpus uteri	297	–	297	243	–	243	13.6	–
cervix uteri	253	–	253	191	–	191	10.5	–

B

	number of deaths						mortality rate*	
	2004			average 1994-2004			1994-2004	
	female	male	both sexes	female	male	both sexes‡	female	male
all cancers	3673	4197	7870	3531	4064	7595	171.7	249.2
lung	624	982	1606	548	963	1511	26.7	58.8
colorectal	400	557	957	404	524	928	18.6	32.2
breast	663	3	666	642	4	646	34.0	0.3
unknown primary site	172	182	354	208	219	427	9.6	13.4
stomach	109	196	305	144	216	360	6.6	13.3
prostate	–	547	547	–	520	520	0.0	32.1
pancreas	194	185	379	182	185	367	8.3	11.4
oesophagus	124	203	327	117	193	310	5.3	11.8
lymphoma	124	131	255	115	133	248	5.6	6.1
ovary	252	–	252	230	–	230	12.0	–
brain and ONS*	105	162	267	94	127	221	5.0	7.6
leukaemia	110	185	295	100	138	238	4.6	8.4
bladder	50	99	149	52	111	163	2.3	6.8
liver	75	97	172	60	82	142	2.8	5.0
kidney	49	131	180	51	95	146	2.5	6.0
mouth and pharynx	43	81	124	37	94	132	1.8	5.9
multiple myeloma	60	77	137	67	79	146	3.1	4.9
other digestive	83	75	158	80	87	167	3.5	5.3

Figure 1.7 Comparison of A) new cancer cases and B) death between ovarian and other cancers in Ireland for the years 1994-2005. Statistics, obtained from the NCRI refer to cases/deaths per 100,000 persons per year and are age-standardised to European standard population.

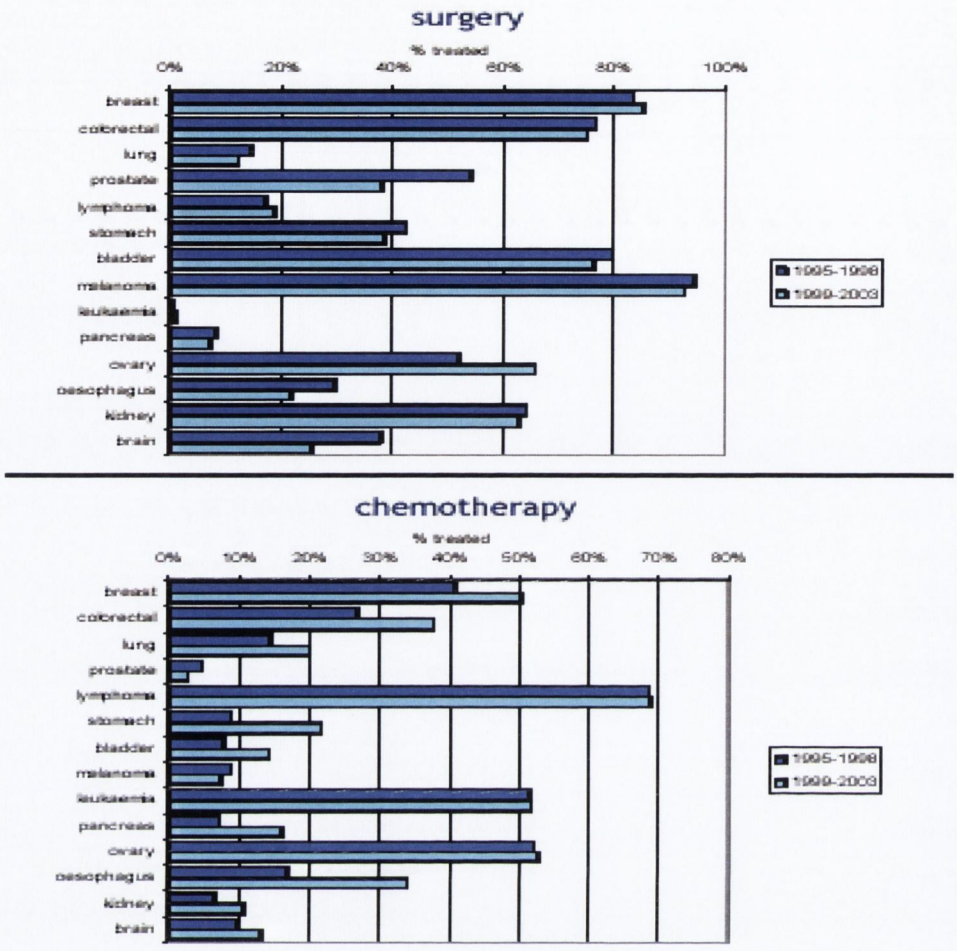

Figure 1.8 Percentage of invasive cancers in Ireland for two different year groups. Note percentage of ovarian cancer cases treated with surgery and systemic chemotherapy has increased up to 20%. Statistics were obtained from NCRI.

A summary of ovarian cancer statistics for Ireland is provided in tables 1.1 and 1.2.

Table 1.1 Summary information, incidence and prevalence in ovarian cancer in Ireland according to NCRI figures 2005.

Rank among the common cancers in women	4th
% of all new cancer cases	5.4%
Average number of new cases per annum	334
Average age at diagnosis with ovarian cancer	62
Chance of developing ovarian cancer	
• by age 65	1.0%
• by age 75	1.5%
Estimated number of women alive in 2001 following a diagnosis of ovarian cancer	2800
Estimated number of cases that will be diagnosed in 2006	403

Table 1.2 Summary information on mortality in ovarian cancer according to NCRI figures 2005.

Rank among the common cancers in women	4th
Average number of deaths per annum	225
% of all cancer deaths due to ovarian cancer	6.5%
Average age at death from ovarian cancer	68
% women with ovarian cancer who die from the disease within 5 years of diagnosis	54%
% of person-years of life-lost due to ovarian cancer	7.3%
Average number of years of life-lost for a woman dying from ovarian cancer	17

1.7 Aetiology and Risk Factors

The aetiology of ovarian cancer is multifactorial and many genetic, hormone and environmental factors are directly or indirectly involved. For the last few decades, two major theories, the *incessant ovulation* [28] and *the gonadotropin hypotheses* [29], have been proposed to explain epidemiological data [30].

Consistent epidemiological and pathophysiologic data indicate that the risk of EOC increases with the number of ovulatory events; in other words, the more frequent a

woman ovulates, during her reproductive life, the higher is her risk for epithelial ovarian cancer in the future. The incessant ovulation hypothesis postulates that the repetitive wounding and recurring cell proliferation in postovulatory repair of the ovarian surface epithelium results in mutations accumulating in the epithelial cells and ultimately tumour formation. This straightforward and conceptually obvious explanation easily gained acceptance. Support for this concept was also provided by laboratory experiments demonstrating spontaneous transformation of rat ovarian surface epithelial cells following prolonged subculturing [31] [32], in which the passaging of the cells in culture mimics repeated injury and proliferative repair of ovarian surface epithelium implied by incessant ovulation. Recent experimental evidence supports the idea that higher ovulatory activity is associated with more inclusion cysts and other changes in the ovarian surface, such as invaginations. It has been suggested that these inclusion cysts are a fertile environment for ovarian cancer development [33] [34]. In support of the "incessant ovulation" hypothesis, an early age at menarche and a late stage at menopause increase the risk of EOC.

The gonadotropin theory postulates that the surges of pituitary gonadotropins that initiate each ovulation and persist in high levels for years following menopause also stimulate the ovarian surface epithelial cells and increase cancer risk. Abundant epidemiological data and animal models exist to support this idea [29]. For example, a late age at menopause delays the risk in post-menopausal women and possibly decreases risk. Inflammation of the ovarian epithelium was also suggested as a mechanism by which gonadotropin stimulation and ovulation contribute to ovarian cancer risk [35], since inflammation is a well-known factor contributing to cancer [36]. Inflammation can also provide an explanation for the increased risk associated with talc and asbestos exposure, endometriosis, pelvic inflammatory disease (PID), and mumps viral infection, possibly by increasing mutations in epithelial cells [35].

Although molecular mechanistic studies provide further support for incessant ovulation, gonadotropin stimulation and inflammation hypotheses, all the theories concerning the aetiology of ovulation-associated ovarian cancer are not mutually exclusive. Additional hypotheses concerning steroid hormones and the retrograde transport of carcinogens through fallopian tubes [30] may also contribute to ovarian cancer risk. Another hypothesis that can explain the reproductive risk factors in

ovarian cancer, proposes a pregnancy-dependent clearance of transformed malignant cells from the ovaries [37].

Pregnancy leads to anovulation and suppresses secretion of pituitary gonadotrophins and in line with the above hypotheses, is expected to reduce the risk of EOC. The protective effect of full-term pregnancies on EOC risk has been well documented [38].

Lactation suppresses the secretion of pituitary gonadotropins and leads to anovulation, especially in the initial months after delivery and in this respect, it protects against EOC [38].

Oral contraceptive pills (OCPs) have been linked with increased risks for some cancers (breast and cervix) and with protective effects for others (ovarian, endometrial, and colorectal) [39]. Combined oral contraceptives containing both oestrogens and progestins, suppress mid-cycle gonadotrophin surge and inhibit ovulation. In ovarian cancer epidemiology there is strong evidence that OCP use truly reduces ovarian cancer risk [40]. OCP use seems to protect against all histological types of EOC with the possible exception of mucinous tumours [41]. The overall protection for ever users is 30%. Reduced risks are present across all strata of parity and age at diagnosis, with a stronger protection observed among nulliparous women [42]. The protection increases with duration of OCP [42] use with a 50% decline in risk after 5 years on the pill [43]. The reduced risk persists for at least 10 years after cessation of use.

The question of whether hormone replacement therapy (HRT) alters the risk of epithelial ovarian cancer remains unanswered. Theoretically, if the "gonadotrophin" hypothesis applies to EOC, a reduced risk is expected, although post-menopausal HRT does not decrease the secretion of pituitary gonadotrophins to pre-menopausal levels. If an association exists, its relative magnitude is probably small. Neverthless, it is equally important to establish protective or adverse effects of HRT.

After correcting for the effect of voluntary nulliparity, studies have found that infertility adds to EOC risk in nulliparous women. The association between fertility drugs and EOC risk is not necessarily causal as women with refractory infertility are mostly exposed to prolonged treatment with fertility drugs [44]. Tubal ligation and hysterectomy are associated with a 67% risk reduction for EOC, the mechanism being rather speculative. This protective effect appears to last for at least 20 to 25 years after surgery [45].

In a recent pooled analysis of 12 cohort studies, height was associated with an increased ovarian cancer risk, especially in premenopausal women. Body mass index was not associated with ovarian cancer risk in postmenopausal women but was positively associated with risk in premenopausal women [46].

Additional variables associated with ovarian cancer with various degrees of correlation include radiation exposure and psychotropic medication [47]. No statistically significant relations were found for consumption of specific dairy foods, galactose, caffeine or vitamin D and ovarian cancer risk dietary factors [48]. Smoking, caffeine and alcohol intake are all potentially modifiable factors that have an unclear association with ovarian cancer risk. Alcohol is not associated with ovarian cancer risk. Cigarette smoking may only increase the risk for mucinous ovarian tumours. High caffeine intake decreases ovarian cancer risk, particularly in women not using hormones [49].

A prior history of PID [50], polycystic ovary syndrome [51] and endometriosis have been associated with an increased risk for ovarian cancer, the latter especially for endometrioid and clear cell histologies [52].

1.7.1 Family History as a Risk Factor

The most significant risk factor for ovarian cancer is a family history of the disease. This risk depends on the number of affected first- and second- degree relatives, as well as their age at diagnosis with ovarian or breast cancer. The majority of hereditary ovarian cancers appears to be due to mutations in the *BRCA1* and *BRCA2*

genes [53]. *BRCA1/2* both encode for tumour suppressors involved in repairing double-stranded DNA breaks and maintaining genomic stability [54]. Women carriers of *BRCA1* or *BRCA2* mutations are at higher risk, with average cumulative risks by age 70 of ~40% and 10% respectively. At least two thirds of cancers are linked to *BRCA1* mutations on chromosome 17q and up to one third associated with *BRCA2* mutations, located on chromosome 13q [55]. Cells that are defective for *BRCA1* and *BRCA2* are hypersensitive to agents that cross link DNA strands or that produce breaks in double-stranded DNA, such as cisplatin.

Germline *BRCA1* and *BRCA2* mutations are present in 10%-15% of all EOCs [56]. Less commonly, EOCs contain somatic mutations in these genes [57], however ovarian cancers with germline *BRCA1/2* mutations are indistinguishable from their sporadic counterparts [58]. The risk of developing cancer is not identical for all carriers of *BRCA1* and *BRCA2* mutations. Risk can be influenced by allelic heterogeneity, modifier genes, and environmental and hormonal cofactors. It is also widely accepted that the risk of ovarian cancer among carriers of *BRCA1* mutations (about 40%) exceeds that for carriers of *BRCA2* mutations (about 20%).

On the other hand, there are those individuals who have ovarian cancer as part of the hereditary non-polyposis colorectal cancer syndrome or Lynch II syndrome due to mutations in DNA mismatch repair genes [59]. This syndrome combines familial colon cancer with an increased risk of ovarian and endometrial cancer, as well as other malignancies of the GI or GU system.

1.8 Histological classification of ovarian cancer

The histology of ovarian tumours exhibits a wide variety of histological features due to their diverse morphology and plethora of cell types. The task forces of the International Federation of Gynecology and Obstetrics (FIGO) endorse the histological typing of ovarian tumours as presented by the World Health Organisation (WHO) [60], based on histogenetic principles which categorize ovarian tumours with regard to their derivation from coelomic surface epithelial cells, germ cells and mesenchyme.

Over 90% of cases arise from the surface epithelium. EOC are grouped according to resemblance to Müllerian epithelium in the female genital tract. They exhibit Mullerian-type cells, including serous, mucinous, endometrioid, and clear cell, reflecting a common pathway in embryological development (Figure 1.9).

According to FIGO, it is recommended that all ovarian epithelial tumors be classified histologically as follows: serous tumors, mucinous tumors, endometrioid tumors, clear cell tumors, Brenner tumors, undifferentiated tumors (too poorly differentiated to be placed in any other group), mixed epithelial tumors (composed of 2 or more of the 5 major cell types of common epithelial tumors, which are usually specified), and intraperitoneal cancer (the ovaries appear to be incidentally involved and not the primary origin, which should be classified as extraovarian peritoneal cancer) (Table 1.3).

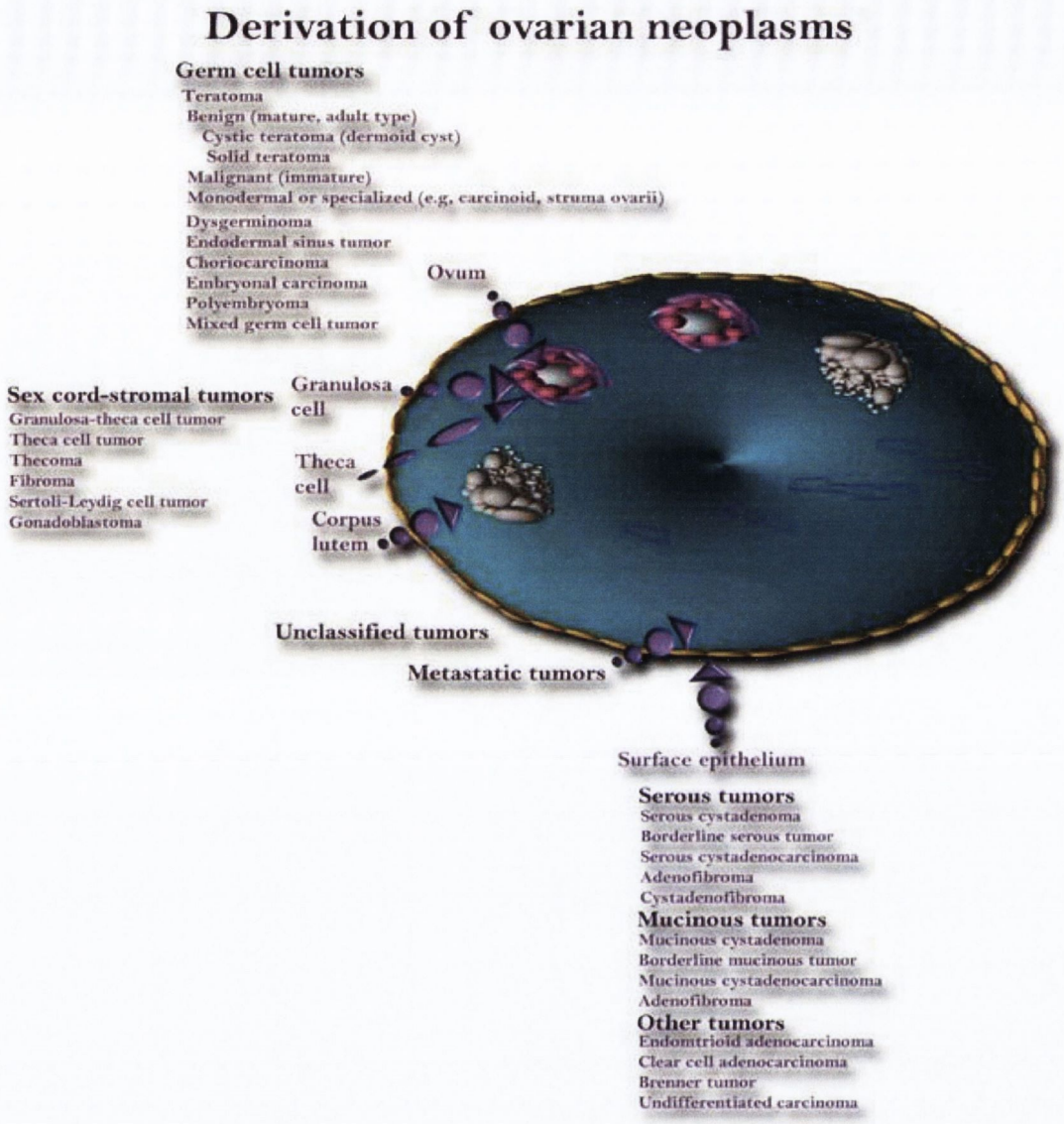

Figure 1.9 Derivation of ovarian neoplasms. Epithelial cancers develop in the cells on the surface of the ovary. Stromal cell tumours develop in the deeper supportive tissue of the ovary. Germ cell tumours develop in an egg cell produced in the ovary. They most typically occur in girls and young women.

Table 1.3 Histological classification of ovarian tumours according to FIGO

- **Serous tumours**

-Benign serous cystadenomas

-Of borderline malignancy: serous cystadenomas with proliferating activity of the epithelial cells and nuclear abnormalities, but with no infiltrative destructive growth (carcinomas of low malignant potential)

-Serous cystadenocarcinomas

- **Mucinous tumours**

-Benign mucinous cystadenomas

-Of borderline malignancy: serous cystadenomas with proliferating activity of the epithelial cells and nuclear abnormalities, but with no infiltrative destructive growth (carcinomas of low malignant potential)

-Mucinous cystadenocarcinomas

- **Endometrioid tumours**

-Benign endometrioid cystadenomas

-Endometrioid tumours with proliferating activity of the epithelial cells and nuclear abnormalities, but with no infiltrative destructive growth (carcinomas of low malignant potential)

-Endometrioid adenocarcinomas

- **Clear cell tumours**

-Benign clear cell tumours

-Clear cell tumours with proliferating activity of the epithelial cells and nuclear abnormalities, but with no infiltrative destructive growth (low potential malignancy)

-Clear cell cystadenocarcinomas

- **Brenner tumours**

-Benign Brenner

-Borderline malignancy

-Malignant

- **Transitional cell tumours**

- **Undifferentiated carcinomas**

A malignant tumour of epithelial structure that is too poorly differentiated to be placed in any other group.

- **Mixed epithelial tumours**

These tumours are composed of two or more of the five major cell types of common epithelial tumours (types should be specified).

Cases with intraperitoneal carcinoma in which the ovaries appear to be incidentally involved and not the primary origin should be labelled as extra-ovarian peritoneal carcinoma.

Malignant serous adenocarcinomas (resembling the fallopian tube) are the commonest, accounting for 40%-50% of malignant neoplasms [61] and predominate in postmenopausal women [62], almost always present as advanced disease. They tend to be high grade and are most often seen in *BRCA* mutation carriers [56]. Endometrioid carcinomas (resembling endometrium) comprise about 10-20% of EOC and are typically spread beyond the ovary at the time of diagnosis. These cancers are sometimes associated with endometriosis. Clear cell (resembling the endometrial glands in pregnancy) are relatively uncommon, occurring most often in women in their 40s. Approximately 50% of women with clear cell tumours have associated endometriosis. Although 33% of clear cell tumours are diagnosed at stage I, they tend to behave aggressively. Mucinous tumours (resembling endocervix) are less frequent, each accounting for less than 10% of all EOC, more likely to be found in younger women. 80% are benign and develop in one ovary. They tend not to secrete CA-125 (Figure1.10). The histological similarity of ovarian epithelial tumors to epithelia in other portions of the female genital tract is not surprising, given that all of these epithelia, as well as the cells lining the peritoneal cavity, are thought to be derived from a common embryological precursor, the coelomic mesothelium.

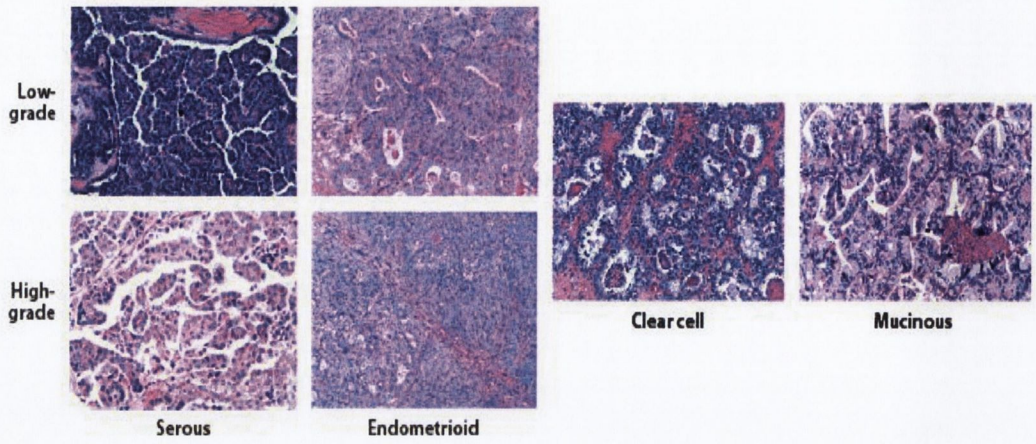

Figure 1.10 Representative examples of the major histological subtypes of EOC.

The frequency of histological types differs dramatically between those diagnosed in low-stage, where the majority are clear cell, endometrioid and mucinous carcinoma [63]. Although premenopausal women develop more germ cell tumors with a lower incidence of epithelial tumors [64], cancer of the latter cell type predominates in postmenopausal women who suffer from ovarian cancer. However, as not all postmenopausal women will develop ovarian cancer, other factors, including genetic predisposition or environment-related epigenetic influences, could increase the risk for ovarian tumors.

1.9 Ovarian Cancer Staging

Once diagnosis of cancer is made, it is important that the stage of cancer be assessed. Cancer staging systems describe how far cancer has spread anatomically and attempt to put patients with similar prognosis and treatment in the same staging group. The concept of stage is applicable to almost all cancers except for most forms of leukemia. Cancer staging can be divided into a clinical stage and a pathological stage.

Because they use different information, clinical stage and pathological stage are often different. Pathological staging is usually considered the "better" or "truer" stage because it allows direct examination of the tumor and its spread, contrasted with clinical staging which is limited by the fact that the information is obtained by

making indirect observations of a tumor which is still in the body. However, clinical staging and pathological staging should complement each other.

Although correct staging is difficult to achieve, it is critical because treatment is directly related to disease stage, hence it may lead to improper treatment with an adverse effect on patient survival.

The concept of a classification system that would encompass all aspects of cancer in terms of primary tumour (T), regional lymph nodes (N) and distant metastasis (M) was first introduced by the Union Internationale Centre de Cancer (UICC) in 1958 for worldwide use. In this respect, solid tumours are defined in terms of a more detailed staging system called the "TNM" system.

The TNM system is one of the most commonly used staging systems. This system has been accepted by the UICC and the American Joint Committee on Cancer (AJCC). Most medical facilities use the TNM system as their main method for cancer reporting.

The TNM system is based on the extent of the primary tumor **(T)**, the extent of spread to the lymph nodes **(N)**, and the presence of metastasis **(M)**. Each of these is categorized separately and classified with a number to give the total stage. While definitions of T, N and M are specific to each cancer, a physician generally needs to look at three things:

T: Tumor

T Classifies the extent of the primary tumour, and is normally given as T1 through T4. T1 represents a tumor that has just started to invade the local tissues. T4 on the other hand represents a large primary tumor that has probably invaded other organs by direct extension, and which is usually inoperable.

N: Lymph Nodes

N classifies the number of regional lymph node involvement. It is important to understand that only the lymph nodes draining the area of the primary tumor are considered in this classification. Involvement of distant lymph nodes is considered to

be metastatic disease. The definition of just which lymph nodes are regional depends on the type of cancer. N0 means no lymph node involvement while N1 means regional lymph node metastases. In general more extensive involvement means some combination of more nodes involved, greater enlargement of the involved nodes, and more distant (but still regional) node involvement.

M: Metastasis

M classifies according to the presence (or absence) of cancer that has spread into other organs or parts of the body. It is either M0 if there are no metastases or M1 if there are metastases.

The TNM staging system allows a health professional to recommend the most effective treatment options and discuss the prognosis based on the type of tumour, the stage of the cancer, the age and overall health condition.

Gynaecologists have a long and proud tradition of using various updated staging systems for female cancers, dating back to the staging system for cervical cancer, first published in 1920. In 1954, the FIGO Committee was set up, which had as its aim, the extension of the general technique of classification of cancer at all sites by anatomical extent of the disease using the TNM system. The FIGO system of classification, now the most commonly used staging system, was originally based on clinical examination, essentially of the anatomical extent of disease. Over the years, with the exception of cervical cancer, it has moved from a clinical basis to one of a surgical pathological nature and was finally modified in 1988.

AJCC TNM and FIGO staging classification (Rio de Janeiro 1988)

The primary tumor (T) is staged in the following way with the AJCC classification first and the FIGO stage in parentheses (Summarised in Table1.4):

- TX. Primary tumor cannot be assessed.
- T0. No primary tumor is seen.
- T1 (Stage I). Ovarian cancer (carcinoma) is limited to one or both ovaries.

- T1a (Stage IA). Tumor is limited to one ovary. The ovarian capsule is intact and there is no tumor on the surface of the ovary. There are no cancer cells in the body fluid (peritoneal fluid) around the ovary.
- T1b (Stage IB). Tumor is limited to both ovaries. The ovarian capsule is intact and there is no tumor on the surface of the ovaries. There are no cancer cells in the body fluid (peritoneal fluid) around the ovaries.
- T1c (Stage IC). Tumor is limited to one or both ovaries and the ovarian capsule is ruptured or there is tumor on the surface of the ovaries or there are cancer cells in the body fluid (peritoneal fluid) around the ovaries.
- T2 (Stage II). Tumor involves one or both ovaries and extends into the pelvis or has implanted into the uterus.
- T2a (Stage IIA). Tumor has extended or implanted into the uterus or fallopian tube but there are no cancer cells in the body fluid (peritoneal fluid) around the ovaries.
- T2b (Stage IIB). Tumor has extended or implanted into other pelvic tissues but there are no cancer cells in the body fluid (peritoneal fluid) around the ovaries.
- T2c (Stage IIC). Tumor has extended or implanted into other pelvic tissues (T2a or T2b) AND there are cancer cells in the body fluid (peritoneal fluid) around the ovaries.
- T3 (Stage III). Tumor involves one or both ovaries and there are cancer cells outside the pelvis (peritoneal metastasis).
- T3a (Stage IIIA). Cancer cells are identified microscopically outside the pelvis (peritoneal metastasis) or on abdominal peritoneal surfaces.
- T3b (Stage IIIB). Tumor involves one or both ovaries and implants on abdominal peritoneal surfaces measure 2 cm or less in size.
- T3c (Stage IIIC) and Any T, N1M0 (Stage IIIC). Tumor implants on abdominal peritoneal surfaces measure 2 cm in size and cancer involves regional lymph nodes.
- Any T, any N, M1 (Stage IV).

Table 1.4 Carcinoma of the ovary: FIGO stages and AJCC TNM class

Stages and classes of ovarian cancer	
FIGO stage	**TNM class**
Stage I	T1N0M0
Stage IA	T1aN0M0
Stage IB	T1bN0M0
Stage IC	T1cN0M0
Stage II	T2N0M0
Stage IIA	T2aN0M0
Stage IIB	T2bN0M0
Stage IIC	T2cN0M0
Stage III	T3N0M0
Stage IIIA	T3aN0M0
Stage IIIB	T3bN0M0
Stage IIIC	T3cN0M0
	Any T, N1, M0
Stage IV	Any T, any N, M1

1.10 Ovarian cancer grading

Tumor grade is a system used to classify cancer cells in terms of how abnormal they look under a microscope and how quickly the tumor is likely to grow and spread. This can refer to the appearance of the cells or to the percentage that appear to be dividing. The higher the grade, the more aggressive and fast growing the cancer. Tumors are typically classified from least to most aggressive as grade I through IV.

Histological grade, also called differentiation, refers to how much the tumor cells resemble normal cells of the same tissue type. The more undifferentiated a cell is, the less "normal" it looks under the microscope. The grade is much more important for some cancer types than for others. In some cancers, grade can impact on treatment decisions.

Historically, the most commonly used grading systems have been those proposed by FIGO, WHO, and the Gynecologic Oncology Group (GOG). The FIGO system uses three grades based on architectural criteria, i.e., the proportion of glandular or papillary structures relative to areas of solid tumor growth. Grades 1, 2, and 3 correspond to <5%, 5–50%, and >50% solid growth, respectively (well-differentiated, moderately differentiated, or poorly differentiated). The WHO system incorporates both architectural and cytological features, but these are not assigned based on quantitative criteria; as a consequence, this system can be considered rather subjective. In the GOG system, the grading method varies depending on the histological type of the tumor.

Grade is related to prognosis in ovarian cancer, with patients with low-grade cancers doing better. Grade information is factored into treatment decisions for women with stage I disease.

- Well-differentiated cancers have very clear boundaries and cells look relatively normal. They usually do not grow or spread rapidly.
- Poorly differentiated cancers have less clearly defined boundaries and cells look very abnormal (Figure 1.11). They often grow and spread rapidly.

A unique feature of ovarian cancer is the subdivision of "low malignant potential" (LMP) or borderline tumours, which form one end of the pathologic grade (grade 0). As a result, the different histological subtypes are further classified as benign, borderline (low grade) and malignant (high-grade) to reflect their behaviour.

Ovarian tumors are evaluated in the following grades:

- GX: Grade cannot be assessed
- GB: Borderline cancer (malignant)
- G1: Well-differentiated cancer
- G2: Moderately differentiated cancer
- G3: Poorly differentiated or undifferentiated cancer

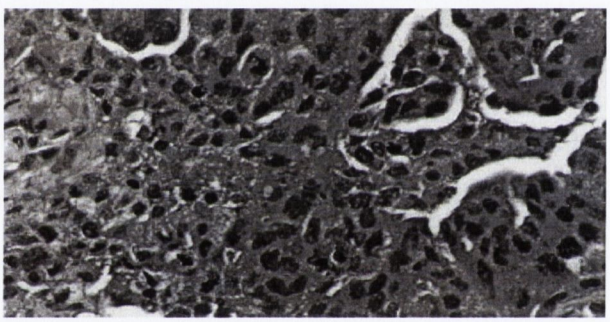

Figure 1.11 Microscopic view of a poorly differentiated serous papillary cystadenocarcinoma

1.11 Molecular Pathogenesis of Ovarian Cancer

Sharp changes in the incidence of ovarian cancer most probably reflect its multifactorial causation. The development of ovarian cancer is a multi-step phenomenon involving genetic events that result in key abnormalities of cell cycle regulation, growth factor activity and intercellular adhesion mechanisms [65].

1.11.1 Origin of ovarian cancer based on morphologic and molecular data

The precise origin of EOC still remains unknown. From a pathological perspective, the origin of EOC remains multifactorial. Historically, the ovarian surface epithelium

(OSE) is accepted to be a distinct cell population that embodies both mesothelial and epithelial characteristics and from which Mullerian inclusions can be derived [66]. However, this belief has recently been called into question for the high grade serous subtype [67] and there is growing evidence implicating the distal fallopian tube as a potential site of origin [68].

One of the major stumbling blocks has been the characterization of a mutually agreed upon precursor lesion or the identification of intermediate or precursor lesions. For example, it is still controversial whether OSE or fallopian tubes display precursor lesions.

Two types of ovarian surface epithelial lesions have been described as possible precursors of these carcinomas: lesions that appear *in situ* in surface epithelium or surface epithelial inclusion glands (SEIG); and pre-existing benign epithelial ovarian tumors and endometriosis [62].

Accumulating evidence indicates that high-grade serous and possibly endometrial carcinomas most probably arise from SEIG with *p53* mutations and dysfunction of *BRCA1/2* in a stepwise fashion while low-grade serous carcinomas arise from adenoma-borderline tumour-carcinomas via activation of the *RAS-RAF* pathway secondary to mutations to *kRAS* and *BRAF*.

1.11.2 Surface epithelium and surface epithelial inclusion glands

Despite the widespread acceptance of the origin of surface epithelial cancers from the ovarian surface epithelium and its inclusion glands, only rarely have putative precursor lesions been described at these sites. Two types of lesions have been suggested as possible precursors: proliferative–metaplastic changes and cytologic atypia. Ovaries have been examined for such lesions in four settings: (1) prophylactic oophorectomy specimens from patients with a strong family history of ovarian cancer or breast cancer or both, or with known *BRCA1* or *BRCA2* gene mutations; (2) uninvolved ovaries contralateral to ovarian carcinomas or benign or borderline epithelial tumors or a combination of these tumors; (3) surface epithelium and epithelial inclusion glands adjacent to invasive ovarian carcinomas; (4) ovaries

removed after positive or suspicious cul-de-sac aspirates performed to screen for ovarian cancer.

Only rare examples of lesions showing significant epithelial atypia (severe dysplasia or carcinoma *in situ*) of the ovary have been reported [69, 70]. These lesions are characterized by stratification of cells lining the ovarian surface or epithelial inclusion glands with loss of nuclear polarity and marked nuclear pleomorphism, hyperchromasia and chromatin clumping. Figure 1.12 displays an ovarian carcinoma in situ with thickened epithelium and stratified cells showing loss of nuclear polarity and marked nuclear pleomorphism, hyperchromasia and chromatin clumping.

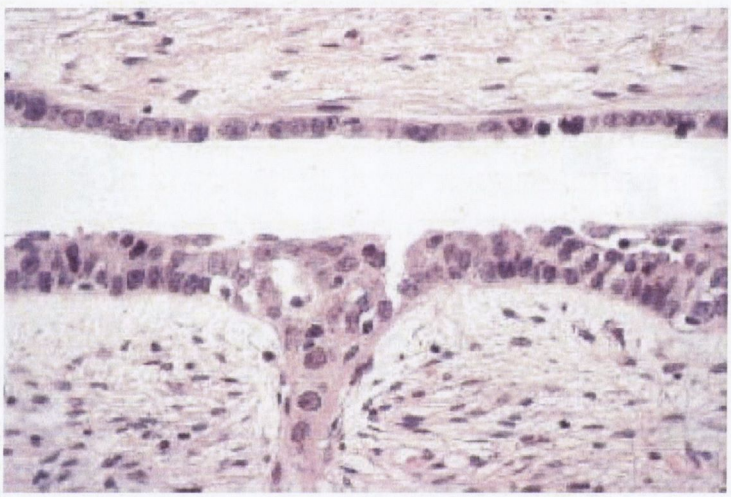

Figure 1.12 Ovarian carcinoma in situ.

Early studies had suggested that proliferative or metaplastic changes of the ovarian surface epithelium such as papillae, epithelial stratification, tufting and metaplasia are precursors of ovarian carcinoma [71]. Similar findings have been reported to be increased in frequency in only one more recent large series of prophylactic oophorectomy specimens from women with a strong family history of ovarian cancer [72].

1.11.3 Fallopian tube as the primary site of origin of epithelial ovarian carcinoma

Studies including careful sampling of the fallopian tubes have reported examples of tubal carcinoma-*in situ* or severe atypia or small tubal carcinomas, especially in

women with *BRCA1* mutations [73]. These findings have led to the speculation that 'ovarian' carcinomas in women with *BRCA1* mutations may originate from undetected exfoliated tubal carcinomas so that ovarian and fallopian tube carcinomas in women with *BRCA* mutations should be termed "female adnexal carcinoma" [74]. A recent study validates the fimbria as the site of origin of many serous carcinomas [75] and distal fallopian tube has been suggested as a precursor of serous pelvic carcinoma. It is also well known that in women with *BRCA* mutations, the risk for developing ovarian-type cancer after prophylactic oophorectomy, although reduced, is not entirely eliminated. In fact, the risk of these patients developing primary peritoneal carcinoma after prophylactic oophorectomy, is 4.3% over a median follow-up period of 3 years [76]. These peritoneal carcinomas are histologically identical to high-grade ovarian serous carcinoma.

1.11.4 Proposed classification of EOC

Because serous carcinomas constitute the majority of ovarian carcinomas, most published studies of generic ovarian cancer, unless otherwise indicated, likely include mainly serous carcinomas. It has been suggested that EOC can be divided in two broad categories, designated Type I and Type II tumors, based on their pattern of tumor progression and molecular genetic changes. In this model, Type I and Type II refer to tumorigenic pathways and are not specific histopathologic terms (Table 1.5).

The division of Type I and Type II serous carcinomas is illustrated in Figure 1.13. Type I tumors include low-grade serous carcinomas, low-grade endometrioid carcinomas, mucinous carcinomas, and a subset of clear cell carcinomas, which develop in a stepwise fashion from well recognized precursors, in most cases borderline tumors. The borderline tumors, in turn, appear to develop from the OSE or inclusion cysts in the case of serous and mucinous tumors and from endometriosis in the case of endometrioid and clear cell tumors. For these tumors, the stepwise progression of borderline tumor to carcinoma resembles the well-characterized adenoma-carcinoma sequence in colorectal carcinoma.

Table 1.5 Common precursor lesions and molecular features of Type I and Type II carcinomas.

Type I tumours	Common precursors	Most frequent mutations	Chromosomal instability
Low grade serous	Serous borderline	*kRAS, BRAF*	Low
Low grade endometrioid	Endometriosis	*PTEN, CTNNB1*	Low
Clear cell	Endometriosis	*PIK3CA*	Low
Mucinous	Mucinous borderline	*kRAS*	Low
Type II tumours			
High grade serous	Not recognized	*p53*	High
High grade endometrioid	Not recognized	*p53*	High
Undifferentiated	Not recognized	?	?

Most Type I tumors are slow growing, as they are generally large and are often confined to the ovary at diagnosis. In contrast, Type II tumors are high grade and have almost always spread beyond the ovaries at presentation. Type II carcinomas include high-grade serous carcinomas, high-grade endometrioid carcinomas, undifferentiated carcinomas, probably some clear cell carcinomas, and malignant mixed mesodermal tumors (carcinosarcomas). Type II carcinomas presumably evolve rapidly, disseminate early in their clinical course and are highly aggressive not only because of the malignant nature of the cancer cells, but also because the anatomic locations in which they arise (i.e., ovary, or perhaps fallopian tube) provide immediate access to adjacent pelvic organs and the peritoneal cavity. In contrast to Type I tumors, Type II tumors are rarely associated with morphologically recognizable precursor lesions.

Chromosomal instability levels, as reflected by genome-wide changes in DNA copy number, are much higher in Type II tumors than in Type I tumors. Type I tumors often harbor somatic mutations of genes encoding protein kinases, including *kRAS*,

BRAF, *PIK3CA*, and *ERRB2*, as well as other signaling molecules including *CTNNB1* and *PTEN*. In contrast, Type II tumors generally lack these mutations but are characterized by a high frequency of *p53* mutations, which are rare in Type I tumors (Figure 1.13).

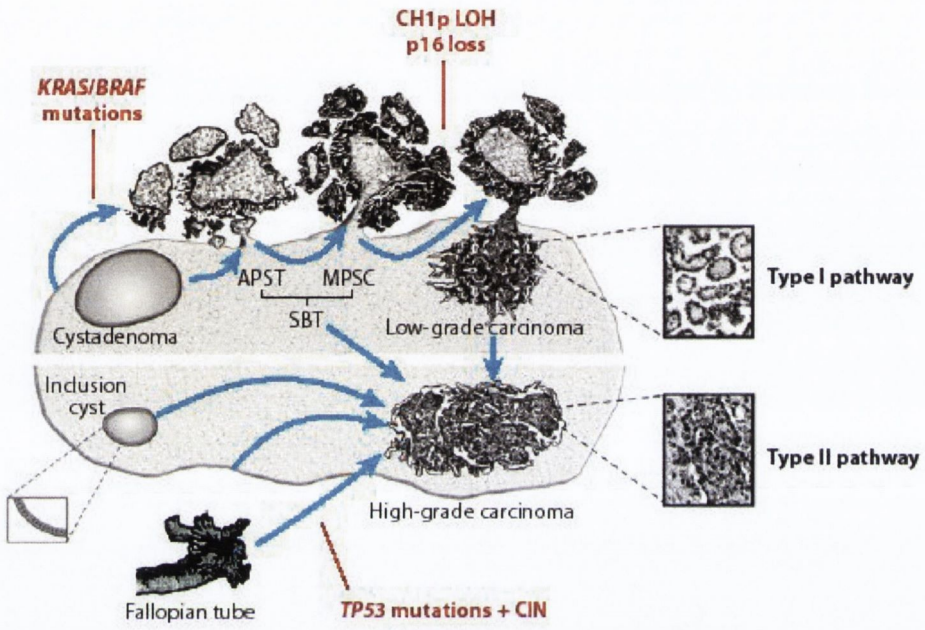

Figure 1.13 Schematic illustration of Type I and Type II ovarian serous carcinoma pathogenesis.

(Development of ovarian high-grade and low-grade serous carcinomas involves two distinct pathways. Low-grade (Type I) carcinomas arise from serous borderline tumors, which in turn develop from serous cystadenomas. This stepwise tumor progression in the low-grade pathway contrasts with the rapid progression pathway of high-grade (Type II) carcinomas, for which precursor lesions are not well recognized. High-grade carcinomas may arise from ovarian surface inclusions, peritoneal mesothelium, or the distal portion (fimbriae) of the fallopian tube. These carcinomas disseminate to pelvic and peritoneal organs early in their progression. Abbreviations: APST, atypical proliferative serous tumor; CIN, chromosomal instability; LOH, loss of heterozygosity; MPSC, micropapillary serous carcinoma (modified with permission from [77]).

Certain molecules (e.g, Ets transcription factors) are expressed at all anatomic sites in ovarian carcinoma, others (e.g, cadherins, integrins and growth factors) are differentially expressed along tumour progression and would obviously have different prognostic values depending on the organs sampled [78].

1.11.5 *p53* mutations

In mammalian cells, *p53* represents a multi-leveled protection against oncogenic mutations. The *p53* gene and its protein have become the center of intensive study ever since it became clear that almost all cancers contain mutations in this gene. It contains 393 amino acids and is divided into four domains. In tumours, *p53* is often functionally inactivated even though the *p53* gene remains intact.

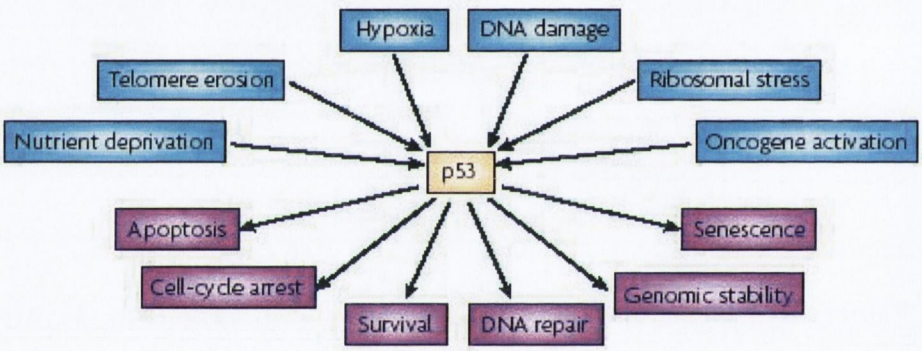

Figure 1.14 Activation and functions of *p53*. *p53* has a key role in integrating the cellular responses (pink boxes) to different types of stress (blue boxes). Activation of *p53* can result in a number of cellular responses, and it is possible that different responses are induced by different stress signals. There is evidence that *p53* can play a part in determining which response is induced through differential activation of target-gene expression. The role of *p53* in tumour suppression, development and ageing is likely to depend on which cellular response is activated and on the context in which the activation occurs.)

p53 is a transcription activator that signals for the upregulation of genes involved in cell cycle arrest and apoptosis [79] and plays a pivotal role in the maintainance and regulation of normal cellular functions. *p53* is activated by cellular stress, such as DNA damage. *p53* induces cell cycle arrest to repair DNA damage. If this fails, *p53* induces apoptosis (Figure 1.14). If *p53* is mutated, as found in many human cancers,

the cell cycle proceeds unregulated, cell growth proliferates, apoptosis pathways are not induced and proliferating cells transform into cancer [80]. On the other hand, if *p53* levels are too high, then phenotypes associated with senescence occur [81]. Thus, *p53* is highly regulated by numerous posttranslational modifications and via interactions with other proteins to regulate its activity [82]. Loss of heterozygocity (LOH) on chromosome 17q13.1 is a common event in high-grade serous carcinomas [83]. The more diligently *p53* mutations are sought, the higher the frequency.

1.11.6 Molecular Genetic Data for high-grade serous carcinomas

It has been well established that *p53* mutations are frequent in both hereditary and sporadic high-grade serous carcinoma [84]. The pattern of K-ras and *p53* mutations appears to distinguish LMP tumors from invasive carcinomas. [85]. It has also been demonstrated that loss of *BRCA1* or *BRCA2* function by a variety of mechanisms is present in the majority of both sporadic and hereditary high-grade serous and endometrioid carcinomas [86]. Laboratory based evidence suggests that mutation of *p53* is an early event in the development of ovarian carcinoma and is present prior to stromal invasion [87]. Additionally, microarray analysis between early and late-stage tumours observed differences at the genomic level providing support for a progression model for ovarian cancer development [88], distinct molecular events during oncogenesis [89] and natural history, including response to chemotherapy [90].

These data demonstrating increasing atypia and common and accumulating genetic alterations in SEIG, ovarian 'carcinoma *in situ*', microcarcinomas and typical high-grade serous carcinoma suggest that high-grade serous and perhaps endometrioid ovarian adenocarcinomas arise from these structures. Additionally, the data from a small number of cases indicates that *p53* mutation occurs in preinvasive epithelium with loss of *BRCA1* or *BRCA2* function in the majority of tumors, findings compatible with the high degree of genetic instability of these tumours.

1.11.7 Growth promoting signals

High-grade serous carcinomas are characterized by a high proliferation rate. The median Ki-67 labelling index (a measure of tumour cell proliferation) is approximately 2.5 times higher than clear or endometrioid carcinomas. Serous carcinomas are characterized by disturbed expression of proteins that are involved in the signaling network of cell cycle regulation [91]. A critical switch in cell cycle progression is the G1-S checkpoint which is restrained by the tumour suppressor gene retinoblastoma 1 (*RB1*). Active *RB1* sequesters the *E2F* family of transcription factors.

1.12 Experimental models of ovarian cancer

The lack of ovarian cancer-prone mammals has hampered the ability to experimentally determine whether and how changes in the surface epithelium occur and if they are an aspect of ovarian oncogenesis. Recently, significant progress has been made in genetic modeling of EOC in immunocompetent mice [92]. In one model, an avian retroviral gene delivery technique was employed to introduce multiple genetic lesions in mouse ovarian cells engineered to produce the avian virus receptor, TVA. Combinations of c-*myc*, *kRas,* and *Akt* oncogenes introduced into primary mouse ovarian cells from *p53*-deficient mice were able to induce phenotypic changes in mouse ovarian surface epithelial cells in culture and form ovarian carcinomas in vivo. Additionally, a transgenic mouse model of EOC expressing the simian virus 40 DNA under the control of an ovarian epithelial cell specific gene promoter has recently been developed [93]. Female transgenic mice in this model develop bilateral ovarian adenocarcinomas accompanied by ascites and peritoneal implants.

1.13 Diagnosis

1.13.1 Clinical presentation

Symptoms. The symptoms of ovarian cancer are fairly nonspecific and often occur when the disease is already spread throughout the abdominal cavity. Abdominal discomfort or vague pain, abdominal fullness, bowel habit changes, early satiety,

dyspepsia, and bloating are frequent presenting symptoms [94]. Occasionally, patients may present with bowel obstruction due to intra-abdominal masses infiltrating the bowel or shortness of breath due to pleural effusion. Early-stage disease is usually asymptomatic, and the diagnosis is often incidental, although such patients may occasionally present with dyspareunia or pelvic pain due to ovarian torsion.

Signs. The presence of a pelvic mass at physical examination is the most important sign of ovarian cancer. Irregularity, solid features, and nodularity are the most important characteristics that suggest ovarian cancer. In advanced stages, abdominal distension due to ascites and abdominal masses (the omentum can be palpated when infiltrated by tumor) can also be felt. In stage IV disease, a pleural effusion can be detected. If nodal metastases are present, inguinal, supraclavicular, and axillary nodes may be enlarged at palpation. Rarely, paraneoplastic syndromes may be present, including cerebellar degeneration. Superficial thrombophlebitis, dermatomyositis, and polyarthritis have also been observed. Venous thromboembolism occurs in a significant proportion of ovarian cancer patients and adversely impacts survival, particularly among cases with local or regional stage cancer [95]. The typical routes of metastases for ovarian carcinoma are intraperitoneal and retroperitoneal. Of these metastases, the majority are intraperitoneal. Of the retroperitoneal spread, lymphatics associated with the ovarian vessels drain into the left renal vein and the inferior vena cava, while lymphatics associated with the broad ligament drain into the external and internal iliac veins, the obturator vein, and the round ligament to the inguinal lymphatics [96].

Ultrasonography or abdominal-pelvic computed tomography (CT) is often performed to aid in the evaluation of a pelvic mass. Features highly suggestive of ovarian cancer include the presence of a complex ovarian mass, with both solid and cystic components, sometimes with internal echoes and/or septations. The presence of ascites or evidence of an omental cake or peritoneal metastases, in the presence of an ovarian mass, is suggestive of advanced ovarian cancer. Other imaging techniques, such as magnetic resonance imaging or positron emission tomography, may provide additional information but are not routinely necessary in preoperative evaluation.

1.13.2 Prognostic factors

Several factors are recognized prognostic of clinical outcomes (response to therapy and overall survival) in patients with EOC. FIGO stage and residual disease after primary surgical cytoreduction, ie debulking status are the most consistently reported [97, 98], with tumour stage being the most important prognostic factor. Studies have shown that patients treated by a gynaecologic oncologist are more likely to undergo a complete surgical staging or have optimal cytoreductive surgery [99]. According to GOG, age at diagnosis (younger than 69 year), performance status, tumour histology (grade, non clear cell histology) and residual tumour volume reflecting success of primary surgery, are independent predictors of overall survival (OS) [100]. However they are considered to give little information about the biological variables responsible for stage progression and outcome. Several studies, however, have shown that tumor ploidy status is of prognostic significance in both early and advanced stage disease [101].

The relationship between age at diagnosis of ovarian cancer and prognosis has been historically evaluated. In general, younger patients have a higher frequency of borderline and well-differentiated invasive EOC. Patients younger than 30 years who present with early-stage disease are more likely to be optimally cytoreduced when compared with those older than 40 years. Data also suggest that older women are at increased risk of recurrence and death. Poorer prognosis in elderly patients can also be explained by differences in immune response and comorbidities. Hesitation to treat older patients aggressively needs be also considered and this reluctance potentially might contribute to the linear relationship between age and progression [102].

1.13.3 Screening for ovarian cancer

CA-125, a high molecular weight glycoprotein, is the product of the human mucin 16 gene and is expressed by both mullerian and coelomic epithelium [103]. After its initial discovery in the early 1980 [104], the serum CA-125 level has been widely used as a marker for a possible epithelial ovarian cancer in the primary assessment of a pelvic mass. The serum level of the CA-125 antigen has been documented as a useful marker for evaluating the status of disease in individual patients with EOC

[105]. A rising antigen level, confirmed on repeat laboratory testing, provides very strong evidence for progression of the disease process. Conversely, a declining value is a reliable indicator of a biological response to a particular therapeutic program.

Increases of CA-125 above the normal range have been shown to herald radiographic progression and recent studies have been shown rises above the normal range to be predictive of disease progression [106, 107]. CA-125 is even an independent predictor of progression free survival (PFS) and OS in ovarian cancer patients with surgically defined status at second look laparotomy [108].

However, the sensitivity and specificity in both pre and post menopausal women are still low [109]. In this setting, false-positive results may derive secondary to several conditions, especially those associated with peritoneal inflammation, such as endometriosis, adenomyosis, PID, menstruation, uterine fibroids, or benign cysts [110]. Malignancies other than ovarian cancer such as endometrial, lung, breast, pancreas and colon can also increase CA-125 levels, but the most marked elevations (>1500 U/mL) are generally seen with ovarian cancer. Due to these limitations, it has been proven insufficient for population-based screening.

1.13.3.1 Clinical applications of CA-125

The primary use of CA-125 measurement is to monitor the disease status of patients with ovarian cancer such as detecting recurrence or assessing response during chemotherapy. Rising values of serum CA-125 correlate with disease progression in approximately 90% of cases. Persistent elevation of CA-125 correlates with residual disease at second-look surgery in 95% of the cases. Also in patients who are in complete remission, an elevation of CA-125 may preceed any other evidence of recurrence. Serum CA-125 levels are also included in the American College of Obstetricians and Gynecologists and Society of Gynecologic Oncologists guidelines for referring patients to a gynecologic oncologist.

CA-125 has also a role in distinguishing malignant from benign pelvic masses. Transvaginal Scan (TVS) and power Doppler can often determine whether a pelvic mass is likely to contain cancer, but an elevated CA-125 is associated with a malignant pelvic mass in 94% of cases. Jacobs *et al.* developed a risk of malignancy

index incorporating CA-125, sonography and menopausal status that can estimate the malignant potential of a pelvic mass with high sensitivity and even higher specificity [111].

CA-125 half life correlates with the survival of ovarian cancer patients [112]. Following complete resection, CA-125 normalizes in 2 weeks; a rapid and complete response to chemotherapy will shorten the apparent half life of CA-125. In this respect, CA-125 can be an estimate of prognosis.

1.13.4 Identification of novel biomarkers

In an attempt to improve CA-125 measurement for the detection of epithelial ovarian cancers, especially at an early stage, several novel tumour markers have been evaluated in patients with ovarian cancer. Examples include lysophosphatidic acid, (found to be elevated in serum and ascitic fluid) [113], mesothelin [114], HE4 [115], osteopontin [113], angiogenic factors [116] and different kallikreins [117] [118]. Although their sensitivities and specificities for predicting ovarian cancer were no better than those of CA-125 alone, the combination of multiple markers is promising [119].

1.13.5 Imaging in ovarian cancer

Non-invasive imaging is extensively used in the investigation of patients with malignancy including ovarian cancer (Figure 1.15). A range of diverse but often distinctive imaging traits are exhibited using ultrasound (US), CT, magnetic resonance imaging (MRI) and positron emmision tomography (PET), many of which currently are of unknown significance, but which probably reflect the underlying biochemical and physiological interplay between cancer cells, stroma and blood vessels.

The mainstay of ovarian imaging is gray scale TVS. TVS augmented by 3D Colour Doppler mapping of vessel distribution improves detection of malignancies compared to grey scale imaging [8]. Vascular indices such as vascularization index or flow index may be associated with tumour angiogenesis [9].

CT can provide staging information for preoperative planning and determination of surgical resectability, can assess tumor response to chemotherapy, and can detect persistent or recurrent disease after primary treatment in patients with epithelial ovarian cancer [120]. Its major limitation is the low sensitivity for small tumor implants, especially on the small bowel or mesentery.

^{18}Fluoro-deoxy-glucose (FDG)-PET scanning uses the fact that malignant cells have an increased glucose metabolism; therefore, a higher uptake of FDG occurs in malignant cells than it does in normal tissue.

CT and FDG-PET may detect metastatic disease [13]. Combined PET/CT is a new imaging technology where the patient undergoes PET and CT in one session and the functional and anatomical images are fused. Recently, FDG-PET/CT has been increasingly used and appears to have a high diagnostic value in differentiating between malignant and benign tumors [121]. MRI has a very high sensitivity in detecting ovarian cancer and can also identify common benign tumours [122].

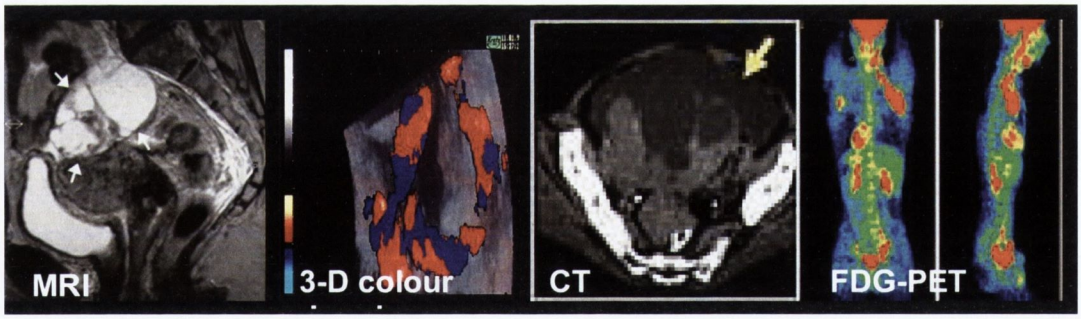

Figure 1.15 Imaging methods in ovarian cancer

1.13.6 Screening programs

Clinical algorithms for the triage of patients with a pelvic mass to tertiary centers are lacking. Historically, the tumour marker CA-125, pelvic ultrasound and bimanual pelvic examinations have been used as screening tools for ovarian cancer detection in asymptomatic pre- or postmenopausal women. Of those, CA-125 has proven the most useful [123].

Early-stage ovarian cancer is associated with an excellent prognosis after optimal therapy. Thus, detection of early-stage disease is a key goal in reducing mortality due to this disease. Unfortunately, no screening program for ovarian cancer tested thus far has been shown to achieve this purpose. Several large prospective studies attempted to identify the best strategy for detecting early-stage disease and therefore reducing mortality by using either CA-125 [124] or ultrasonography [125] as the primary screening test. A low positive predictive value was observed obviously due to the commonality of benign pelvic lesions, even in postmenopausal women. High specificity is vital in screening strategies for ovarian cancer because a positive test result generally requires definitive surgical assessment. Given the relatively low prevalence of ovarian cancer, a test with 99% specificity would result in 10 surgical procedures for every ovarian cancer detected [126]. Combination test strategies only slightly improved the predictive value of CA-125 [127].

Finding an effective strategy to screen for ovarian cancer is a high priority in the cancer research community. Current approaches being studied include high-throughput techniques using microarray technology and proteomic screening to identify panels of novel markers that may be altered early in the disease [128].

1.14 Current management of ovarian cancer

The first step in the management of patients with epithelial ovarian cancer is an accurate diagnosis and thorough staging, with optimal surgical cytoreduction of metastatic disease, also referred to as debulking surgery (Figure 1.16). Postoperative platinum-based and taxane chemotherapy is then administered to patients with a significant risk of recurrence [97, 129].

Despite improved outcomes for many ovarian cancer patients over the past decade, the long term survival has not been yet uniformly improved. For this reason, identification of prognostic factors predictive of clinical outcome in patients with

ovarian cancer may facilitate the design of more targeted, tailored therapeutic regimens in the future.

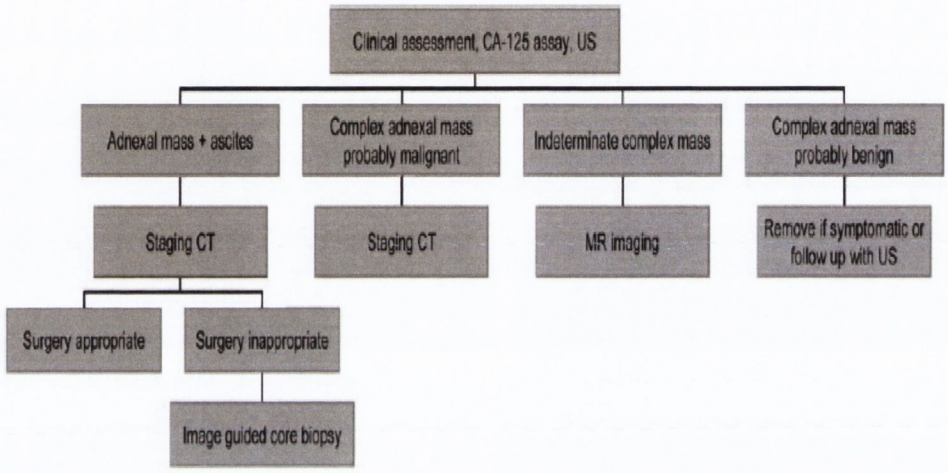

Figure 1.16 Management algorithm for patients with ovarian cancer

Three reasons are responsible for unfavourable prognosis in ovarian cancer.

- Lack of robust and minimally invasive methods for early detection
- Asymptomatic nature of the disease in its early onset
- Development of recurrence/ resistance to chemotherapy which makes response to first-line treatment largely unpredictable

1.14.1 Surgery

In patients with disease apparently confined to the pelvis, thorough staging is essential to define the correct extent of the disease at time of diagnosis [130]. Considering the possible routes of spread, other than the debulking of all visible tumor, peritoneal washing, peritoneal biopsies representative of the entire abdominal cavity, and a retroperitoneal assessment that involves both the pelvic and para-aortic area are performed. Sites of unsuspected disease are most likely to be pelvic peritoneum, ascites fluid, other pelvic tissue, para-aortic nodes, and diaphragm.

Inadequate surgical staging can lead to understaging and subsequently inadequate postoperative treatment, which can ultimately worsen patients' prognosis. Adequate staging presents as perhaps the best treatment option in patients with presumed early-stage disease [131].

Cytoreductive surgery is the cornerstone of the initial treatment of patients with advanced ovarian cancer. The amount of residual disease after primary surgery is generally considered the most important modifiable prognostic factor that influences survival of patients with advanced disease. Nearly all retrospective and prospective studies have confirmed that the extent of cytoreductive surgery and the amount of residual disease after primary surgery are the most important factors that influence the survival of patients with advanced ovarian cancer [132] (Figure 1.17).

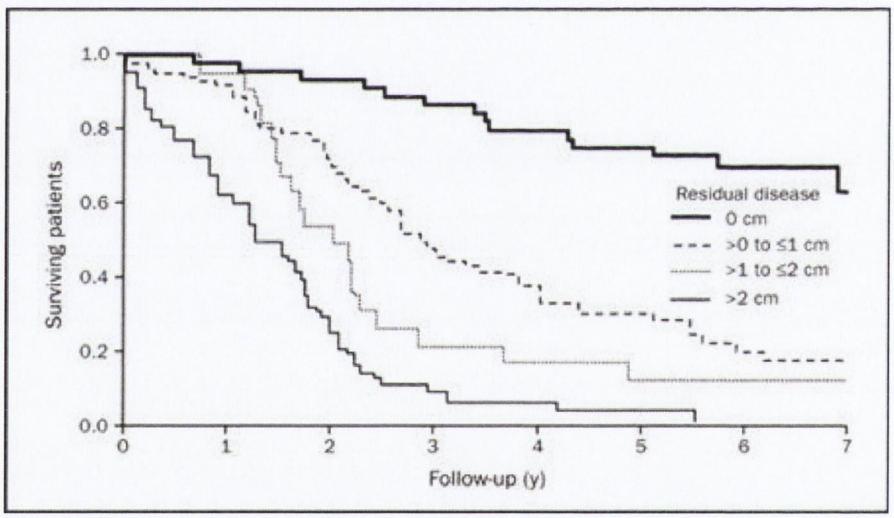

Figure 1.17 Residual disease affects overall survival in patients with stage IIIC ovarian cancer (n=194; log-rank test, P<0.001).

The tendency of ovarian cancer to remain clinically confined in the peritoneal cavity also reflects the ability to achieve optimal cytoreduction in 60% of women with advanced EOC. Optimal cytoreduction for advanced ovarian cancer is defined as removal of all disease 1 cm or larger in diameter. Tumours amenable to cytoreduction are rather characterized by superficial implants without distant metastatic or parenchymal disease, are usually well differentiated without deep-tissue

invasion or dense adhesions and this contributes to an improvement in long-term outcomes. This unusual biology has prompted evaluation of various intraperitoneal treatment modalities, including cytotoxic chemotherapy, radioisotopes or monoclonal antibodies.

The quoted sites of disease most frequently precluding optimal cytoreduction are the diaphragm, bowel and portal triad. Studies consistently show that gynecologic oncologists are more likely than general surgeons to perform optimal surgery for ovarian cancer [133]. As a result, the National Institutes of Health, American College of Obstetricians and Gynecologists, and Society of Gynecologic Oncologists all recommend that women with ovarian cancer be referred to a gynecologic oncologist for their initial surgery [99].

An often-stated justification against aggressive surgical resection arises from the hypothesis that the initial extent of advanced disease correlates with the aggressiveness of the underlying tumor biology and that this will ultimately dictate outcome, independent of the amount of residual disease at the end of the surgical procedure [134]. In view of this, several radical surgical procedures, including intestinal resection, splenectomy, diaphragmatic resection and hepatic resection have been described as treatments of advanced ovarian cancer with acceptable morbidity, in the context of primary or secondary debulking.

1.14.1.1 Interval Debulking

Interval debulking surgery is defined as an operation performed after a course of induction (or neoadjuvant) chemotherapy, usually 2 or 3 cycles of chemotherapy. The primary aim of this procedure, which is the same as for upfront surgery, is to reduce the volume of residual disease and hence improve the likelihood of complete response to chemotherapy. Many clinicians and medical centers have already started this alternative treatment strategy [135], usually reserved for patients with a high risk of major perioperative morbidity at initial diagnosis, even though the precise role of neoadjuvant chemotherapy in the management of advanced-stage EOC has not yet been established. The absolute indications for neoadjuvant chemotherapy appear to be Stage IV disease (excluding pleural fluid) or metastases of more than 1cm at sites where resection is impossible [136]. This type of operation can be performed even

after a suboptimal primary attempt of debulking, followed by 2 to 3 courses of platinum-based chemotherapy and it is shown to improve survival [137].

1.14.1.2 Can we predict surgical "resectability"?

A critical and challenging point in defining patients who might benefit either from an upfront radical surgical or an interval debulking approach is the development of models that allow physicians to have clear and reliable selection criteria for identifying patients who are not candidates for primary cytoreduction. Numerous studies have tried to develop a model to predict which patients are more likely to be able to undergo optimal debulking using features that can predict surgical outcome, such as disease extent on imaging, amount of ascites, serum marker CA-125, or gene expression [138-140]. The prediction rate in these studies ranges widely, from 70% to 90%, indicating that it is unclear whether these results are patient or center dependent.

1.14.1.3 Second-look surgery and Secondary Debulking

Nowadays, second-look operation is not routinely used because of the lack of adequate data showing a clear survival benefit for patients undergoing this surgical procedure, and it should be reserved to patients enrolled in clinical research protocols or to selected cases [141]. In general, for advanced disease, even if the second-look laparotomy is negative, one-half will develop a recurrence. The role of the second-look laparotomy as a secondary debulking procedure has been suggested by some but appears to be beneficial in only a small subset of patients-less than 10%. It is therefore performed in US and some European centers and is not a common practice in Ireland, which makes availability of "recurrent" samples limited and extremely valuable. [142]. Although primary cytoreduction is universally considered the cornerstone of initial management for patients with advanced disease, the role of secondary cytoreductive surgery at the time of second-look operation is still debated. Several factors correlate with good prognosis after secondary cytoreductive surgery: longer disease-free interval, number of tumor nodules at time of recurrence, smaller residual tumor at primary surgery, good response to first-line platinum chemotherapy, and smaller size of maximum tumor at recurrence. In an attempt to identify ideal candidates for secondary surgery, Onda *et al.* suggested that patients

with recurrent ovarian cancer should be considered ideal for secondary surgery when they have 3 or all of the following 4 factors at recurrence: (1) disease-free interval longer than 12 months, (2) no liver metastasis, (3) a solitary tumor, and (4) tumor size smaller than 6 cm. Exclusion criteria included (1) age of 75 years or older at recurrence, (2) bad performance status and (3) progressive disease during presurgical chemotherapy, if undertaken. A complete secondary surgical cytoreduction was achievable in most of these selected patients and was associated with a significant survival benefit [143]. Elevated CA-125 values at the time of second-look operation are strong predictors of persistent disease, while normal antigen levels can be associated with both negative and positive second-look findings [144].

1.14.1.4 Fertility-Sparing Surgery

Two groups of young patients with epithelial cancer may be considered for a conservative surgical approach: (1) young women with borderline ovarian tumors - often diagnosed incidentally after oophorectomy or cystectomy- since the rate of recurrence after a conservative treatment is very low (3%-6%) suggesting that eventual restaging after an incomplete primary staging is not required. (2) young women with invasive ovarian cancer macroscopically confined to one ovary, who desire further childbearing. These patients undergo a unilateral salpingo-oophorectomy with comprehensive staging. Again, the recurrence rate and the overall survival rate have been reported to be similar among patients with ovarian cancer who were treated conservatively and those who underwent more aggressive surgical procedures [145]. Pregnancies after fertility-sparing procedures have also been reported.

1.14.2 Radiation

The use of whole abdominal irradiation (WAI) as consolidation therapy would appear to be a logical strategy given its ability to sterilize small tumour volumes. Despite the clinically proven efficacy of WAI, the use of radiotherapy in ovarian cancer has profoundly decreased mainly due to high treatment-related toxicity. Postoperative radiotherapy as a consolidation treatment with or without prior chemotherapy has been investigated on numerous occasions, though initially with inconsistent and often disappointing results [146]. In addition to inappropriate patient selection, another

possible explanation for the treatment failure observed in these trials was the high-degree of toxicity resulting in delayed or incomplete radiotherapy.

1.14.3 Chemotherapy

Ovarian cancer is a chemosensitive disease and combination chemotherapy can result in complete remission in approximately 75% of patients. Clinicians generally treat ovarian carcinomas as a single entity despite pathological classification. The decision to give chemotherapy is generally based on stage and grade. Oncologists have noted that the dismal response rate of clear cell and mucinous carcinomas to chemotherapy (15%) contrasts sharply with that of high-grade serous carcinomas (80%) [147] [148]. With the exception of clear cell carcinoma, histology has not been a factor used to determine chemotherapy management.

1.14.3.1 Early-Stage Disease

The role of chemotherapy for patients with stage I and II ovarian cancer was studied by the GOG in 1980. Current recommendations are for no postoperative treatment of patients with early-stage (stage IA and IB) ovarian cancer with well- or moderately well-differentiated tumors. Postoperative treatment with either paclitaxel plus carboplatin is recommended for patients with early-stage disease with poor prognostic features, such as stage IC with tumor on the ovarian surface, ruptured capsule, ascites or positive peritoneal washings, clear cell histology regardless of stage and all patients with stage II disease).

1.14.3.2 Evolution of Chemotherapy for Advanced-Stage Ovarian Cancer

From the 1960s to the present, primary chemotherapy for advanced ovarian cancer has evolved from single alkylating agents to cisplatin and cisplatin-based combinations, followed by incorporation of paclitaxel and substitution of carboplatin for cisplatin [149]. Currently, platinum drugs are the most active agents in epithelial ovarian cancer [150] (Table 1.6). Several platinum analogues have entered the clinic in the past 30 years and since the turn of the new millennium, this strategy seems to finally be proving successful (Figure 1.18). Oxaliplatin, originally described in the late 1970s, has a spectrum of activity and mechanisms of action and resistance that

appear to be different from those of other platinum-containing compounds, notably cisplatin. In contrast to cisplatin and carboplatin, the accumulation of oxaliplatin seems to be less dependent on the copper transporter *CTR1* [151]. Mismatch repair (MMR) recognition proteins do not recognize oxaliplatin-induced DNA adducts [152] Despite these advances, most patients with stage III and IV ovarian cancer are not cured of their disease.

Melphalan, chlorambucil, or cyclophosphamide as single agents in advanced ovarian cancer produced response rates of 35-65% [153]. In the 1970s, combination chemotherapy resulted in improved response rates and survival times compared with single-agent therapy. A few years later, the first study to show improved survival with combination chemotherapy was published. The combination of altretamine (hexamethylmelamine), cyclophosphamide, methotrexate, and fluorouracil was compared with melphalan, with overall response rates of 75% vs 54% and a longer median survival (29 vs 17 months) for the combination [154]. In 1982, Decker *et al.* reported 2-year survival rates of 52% and 19% with cyclophosphamide plus cisplatinum vs cyclophosphamide alone [155].

In 1986, GOG reported a study of doxorubicin plus cyclophosphamide vs cyclophosphamide, doxorubicin and cisplatin with median survival times of 7.7 vs 13.1 months and an overall survival time of 9.7 vs 15.7 months [156].

Table 1.6 Table of platinum drugs used in cancer with indications, years of approval from the Food and Drug Administration (FDA) and their dose limiting toxicities).

Indication	Approval year or approval/ development status	Dose-limiting toxicities
Cisplatin (IV injection)		
Metastatic testicular cancer	1978	Nephrotoxicity
Metastatic ovarian cancer	1978	Neurotoxicity, ototoxicity
Transitional bladder cancer	1993	Nausea and vomiting
Carboplatin (IV injection)		
Ovarian cancer (palliative after previous chemotherapy)	1989	Myelosuppression (thrombocytopenia and neutropenia)
Ovarian cancer, first line	1991	Nausea and vomiting (but less than with cisplatin)
Oxaliplatin (IV injection)		
Accelerated approval, metastatic colorectal cancer (second line with 5FU with LV)	2002	Neurotoxicity (sensory peripheral neuropathy)
Colorectal cancer (previously untreated or adjuvant treatment with 5FU with LV)	2004	Nausea and vomiting
Satraplatin		
Hormone-refractory prostate cancer	Under consideration for approval by the FDA	Myelosuppression (thrombocytopenia and neutropenia)
Picoplatin		
Small-cell lung cancer	Phase III trial about to begin	Myelosuppression (thrombocytopenia and neutropenia)

These studies and a Netherlands Cancer Institute study established the routine addition of cisplatin to combination chemotherapy for advanced ovarian cancer [157]. With the widespread adoption of adjuvant platinum-based combination chemotherapy for advanced-stage disease, the relapse-free interval after completion of that therapy (or the platinum-free interval) has been recognized as a predictor of the likelihood of subsequent response to chemotherapy. Patients with a relapse-free interval of more than 6 months (platinum sensitive) had a higher probability of responding to platinum again and to other chemotherapeutics. Platinum-resistant disease included disease that relapsed within 6 months of adjuvant therapy or disease that progressed while the patient was taking platinum in the salvage setting.

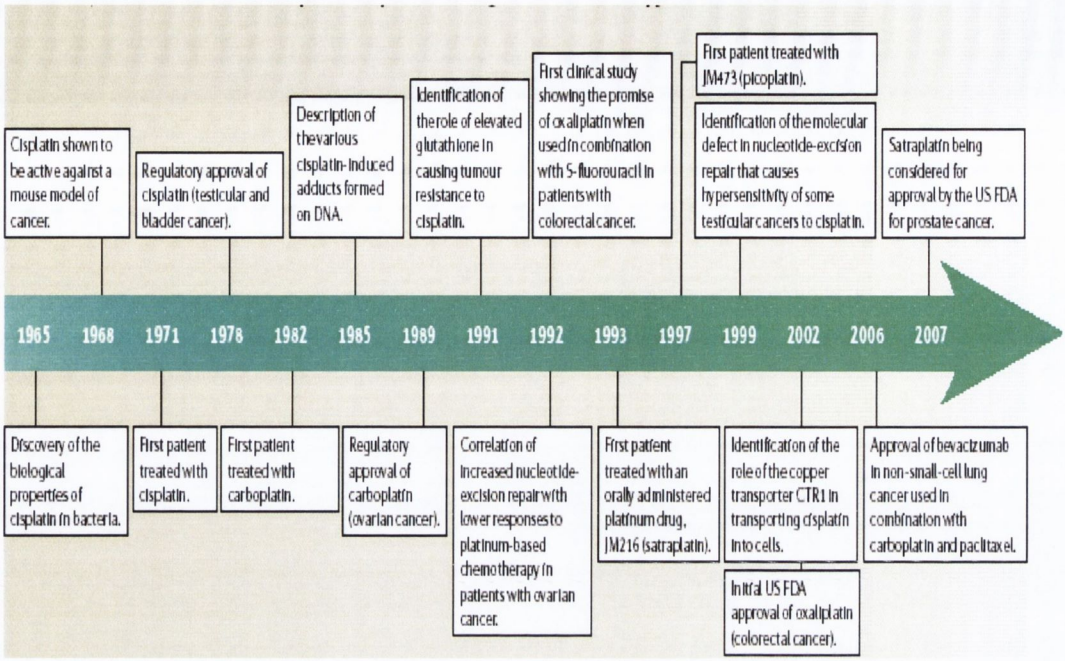

Figure 1.18: Milestones in the development of platinum drugs for cancer therapy

In 1989, paclitaxel was first reported as an active agent in ovarian cancer with a response rate of 24% in platinum-resistant disease [158]. In 1996, McGuire *et al.* [129] reported the results of GOG 111, which studied cyclophosphamide and cisplatin compared with paclitaxel and cisplatin in patients with stages III and IV ovarian cancer. That study found response rates of 60% vs 73%, progression-free survival times of 13 vs 18 months, and median survival times of 24 vs 38 months, all favoring the paclitaxel and cisplatin combination. A European-Canadian trial published in 2000, confirmed the superiority of paclitaxel plus cisplatin over cyclophosphamide and cisplatin [159].

Carboplatin has then substituted cisplatin in combination with paclitaxel with similar efficacy but reduced toxicity [160], possibly because carboplatin administration before paclitaxel has not been shown to interfere with clearance of paclitaxel. In patients with advanced ovarian cancer, a chemotherapy regimen consisting of carboplatin plus paclitaxel results in fewer gastrointestinal and metabolic toxic effects, is easier to administer, and is not inferior, when compared with cisplatin plus paclitaxel [161]. Thus, 3-hour paclitaxel with carboplatin became the standard first-line chemotherapy for epithelial ovarian cancer.

GOG 182–ICON-5 was a 5-arm phase 3 trial of intravenous paclitaxel and carboplatin vs that same doublet plus a third agent, gemcitabine, liposomal doxorubicin, or topotecan, in patients with advanced stage ovarian or primary peritoneal cancer. No evidence was available to indicate that adding a third cytotoxic agent prolonged progression-free survival [162].

1.14.3.3 Intraperitoneal Chemotherapy

Because advanced ovarian cancer is often limited to the peritoneal cavity, intraperitoneal as opposed to systemic administration of chemotherapy was proposed as a strategy to increase drug concentrations in the abdominal cavity. While studies with intraperitoneal cisplatin have documented a modest improvement in median survival [163] [164], this was at the expense of toxicity and overall treatment complexity [165]. On the basis of these findings, the National Cancer Institute (NCI) issued a clinical advisory that recommended a regimen containing intraperitoneal cisplatin and a taxane given intravenously or intravenously and intraperitoneally for women with optimally debulked stage III ovarian cancer [166]. The optimal dose and schedule of intraperitoneal chemotherapy are under investigation. Unfortunately, no intraperitoneal regimen has been compared with what many consider the current standard, intravenous carboplatin and paclitaxel [167].

1.14.3.4 Maintenance Therapy.

Maintenance (or consolidation) therapy for patients in complete remission, represents another area of controversy in ovarian cancer management. Treatment with topotecan [168], interferon alfa [169] and vaccines targeting CA-125 [170] did not improve survival after chemotherapy. A randomized trial of 12 vs 3 months of maintenance paclitaxel after complete response to initial therapy improved progression-free survival but not overall survival [168]. A prospective randomized trial of whole abdominal radiation therapy after induction therapy did not improve survival [171]. Cure *et al.* found no improvement in overall survival with high-dose chemotherapy and stem cell support compared with 3 cycles of conventional dose carboplatin and cyclophosphamide after response to primary therapy for advanced disease [172].

Intraperitoneal radioactive ^{32}P vs observation in patients with stage III disease after negative second-look laparotomy did not decrease the risk of relapse or improve survival [173].

1.14.3.5 Neoadjuvant Therapy

Neoadjuvant therapy is a strong consideration for those individuals who are deemed to be poor surgical candidates at the time of initial diagnosis. In addition, for patients diagnosed with stage IV disease, especially those with a high burden of metastatic disease, treatment can begin with chemotherapy and response to chemotherapy can dictate subsequent decisions about aggressive surgical debulking. No published randomized trials have evaluated neoadjuvant chemotherapy, but one trial is in progress [174].

1.14.3.6 Chemotherapy for recurrent disease

The management of patients with recurrent ovarian cancer remains an area of active investigation. Salvage chemotherapy is important in ovarian cancer because many patients respond to several salvage regimens. Because of the high response rate of ovarian cancer, even after relapse, it is probably better to consider 10-year survival as the ideal endpoint [175].

Unfortunately, most women with advanced-stage ovarian cancer will experience disease relapse after primary chemotherapy and will develop symptomatic recurrent disease. Median survival after recurrence is 2 years [176]. Since cure is not essentially feasible, the primary goal of therapy is management of symptoms [177]. However, palliation in recurrent ovarian cancer has not been adequately studied due to difficulty evaluating quality of life and symptom control. Data from platinum compounds provide the best evidence that the "platinum-free interval" following platinum based treatment is a strong predictor of response to chemotherapy for recurrent disease [178]. Surprisingly, in a trial of second-and third-line paclitaxel treatment, other factors such as serous histology, tumour burden (as assessed by size of the largest lesion and number of disease sites) and normal baseline haemoglobin were found to be significant predictors of response [179]. While it is reasonable to accept why smaller tumours should be more responsive and that patients with only

one or two sites of disease should benefit from therapy, it is somewhat surprising that serous histology represents the most favorable in response to subsequent chemotherapy in relapsed ovarian cancer [180].

Patients have been categorized as having platinum-sensitive disease if their disease-free interval is >6 months. Following administration of single regimen carboplatin in the above patients, combination chemotherapy with carboplatin and paclitaxel has provided higher response rate than that achievable with single agents [177]. At present, a phase III randomized trial is being conducted by GOG, comparing paclitaxel plus carboplatin versus gemcitabine plus carboplatin, both regimens being currently acceptable treatment options for patients with platinum-sensitive recurrent ovarian cancer.

For patients with platinum-resistant disease, the selection of several agents have shown some activity, including topotecan [181], liposomal doxorubicin [182], taxanes [183], gemcitabine [184], oral etoposide [185], altretamine (hexamethylmelamine) [186] and ifosfamide [187]. The selection of which individual agent to use has been primarily based on toxicity considerations. These agents usually have response rates of approximately 5-20%, possibly because they ignore certain aspects of tumour biology. With these rather low response rates, patients frequently have to make a decision about either continuing chemotherapy or receiving supportive care only. Assessment of chemotherapy sensitivity and resistance assays in the front-line setting identified no assays for which the evidence base was sufficient to support their use in oncology practice outside a clinical trial setting [188].

1.14.3.7 Individualized Therapy

An ultimate goal in cancer therapy is to devise individually tailored treatment that targets growth-promoting pathways and circumvents drug resistance. Exploration of alternative treatment options represents a real challenge and growing evidence suggests that uncommon histologies are not generally platinum responsive [189]. As a global strategy for second- or third-line treatment does not exist, initial efforts have been made to evaluate chemosensitivity assays for patients with recurrent disease [190]. Also, models have been proposed for prospective validation of treatment

selection criteria [191], hopefully to be applied to future randomized trials of assay-directed therapy. Identification of new biomarkers to be included in clinical trials is urgently needed.

1.14.3.8 New therapeutic strategies

Unfortunately, in women with advanced disease, cells initially sensitive to chemotherapy can later regrow and this reflects unacceptably low median overall survival (24-60 months). Apart from the manipulation of doses, schedules, mode of delivery and combination of existing drugs, the development of new therapeutic approaches represents a challenging priority. Numerous strategies are being pursued. One is to use current high-throughput genomic studies to analyze thousands of genes in the tumors of women with chemosensitive vs chemoresistant disease [192]. The goal of this approach is to be able to predict, at the outset, which women will benefit significantly from standard chemotherapy approaches vs those who should be treated with alternative approaches.

Technologic advances that allow us to examine the molecular machinery driving cancer cells have helped to identify numerous mediators within ovarian cancer cells that can be targeted with new molecular strategies. Examples include agents that block stimulatory growth factor receptors at the cell surface, small molecule inhibitors of signal transduction pathways, approaches that harness specific elements of the immune system that ovarian cancers have successfully suppressed, gene and viral therapy strategies, and antiangiogenesis strategies, covering all aspects of cancer hallmarks.

1.14.3.9 Novel cytotoxics

Epothilones are natural bacterial microtubule stabilizing agents that act similar to taxanes, inducing microtubule bundling, formation of multi-polar spindles and mitotic arrest [193]. One of their potential advantages is that their cytotoxicity in vitro is minimally reduced by p-glycoprotein overexpression, a well known factor involved in multi-drug resistance [194].

Yondelis, also known as trabectedin, is a marine-derived compound which selectively binds to the minor groove of DNA and by inhibiting transcription in a promoter- and gene-dependent fashion, it induces apoptosis and cell cycle arrest [195]. Trabectedin was found to be active in both platinum-sensitive and platinum-resistant ovarian cancer patients [196] and is currently being evaluated in relapsed advanced ovarian cancer.

Telcyta is a glutathione pro-drug activated by glutathione-S-transferase (GST), releasing electrophilic fragments capable of inducing apoptosis. It is expected to overcome chemoresistance to alkylating and platinum agents, associated with GST overexpression [197].

1.14.3.10 Molecularly targeted agents

As the various cellular processes involved in tumorigenesis are progressively uncovered, a wide array of molecular targets have been developed to target processes such as angiogenesis, signal transduction, cell cycle regulation, metastasis, apoptosis and protein translation. Given the biological heterogeneity of ovarian cancer and the absence of a specific mutation as responsible for initiation or progression of disease, combining molecular targeted agents with cytotoxic regimens appear to be the more attractive strategy [198].

Inhibitors of the erbB family of receptor tyrosine kinases have been studied in ovarian cancer. This receptor family and their ligands promote tumorigenesis through a variety of stimulatory and cell survival pathways. *ErbB1* or epidermal growth factor (*EGFR*) is overexpressed in 40-70% of ovarian cancer cases and is associated with poor prognosis. Inhibitors of *EGFR* signaling include small molecules such as gefitinib and monoclonal antibodies, such as cetuximab. Trastuzumab (Herceptin) is a humanized monoclonal antibody against *HER-2/erbB-2*. Small molecule inhibitors of the epidermal growth factor receptor (*EGFR, erbB1*) have shown minimal activity in women with recurrent ovarian or peritoneal cancer [199]. Humanized monoclonal antibodies against *EGFR* are currently being tested either alone or in combination with chemotherapy in ovarian cancer. Lapatinib is a potent dual inhibitor of *EGFR* and *HER-2/erbB2*. It is hypothesized that a dual inhibitor of these important

pathways should have significant therapeutic advantages over single receptor inhibitors.

Angiogenesis, which is controlled by a range of pro-angiogenic factors, plays a central role in the physiological function of the healthy ovary. It could therefore be anticipated that the abnormal angiogenesis that characterises malignancy would be especially relevant in ovarian cancer disease [200]. The driving factor behind angiogenesis in ovarian cancer is *VEGF*. Previous work in our lab suggest *VEGF* acts as a prognostic marker in ovarian cancer with an association with *CD31*, suggesting it plays a role in angiogenesis.and chemoresistance [201].

Several agents have been developed to inhibit *VEGF* or its receptors (*VEGFR* and *VEGFR2*). Bevacizumab is a recombinant humanized monoclonal antibody against *VEGF*, which has shown activity in ovarian cancer [202]. Several case series and Phase II studies indicate that in ovarian cancer bevacizumab is active as a single agent or in combination with other drugs. Currently, ongoing Phase III trials are testing bevacizumab in front-line adjuvant therapy with carboplatin and paclitaxel [203].

Numerous other biologic therapies are being pursued in ovarian cancer [204], including new strategies that target unique receptors that are overexpressed in ovarian cancer [205], members of the PI3K/AKT/mTOR pathway [206], metalloproteinases [207], immunotherapies focusing on varied modes of anti-tumor vaccine development, (dendritic cell vaccines, adoptive T-cell transfer, immune modulatory therapy), thus subverting natural tolerance mechanisms or boosting effector mechanisms, use of cytokines and/or chemotherapy with immune therapy [208].

CA-125 has been used as a response criterion of molecular targeted agents with controversial results [209].

1.14.3.11 Chemoresistance and survival outcomes in ovarian cancer patients

Tumour resistance to chemotherapy is a well-known clinical phenomenon, considered to represent a complex pleiotropic response [210]. Although extrapolation to the *in vivo* situation is linked with certain limitations, *in vitro* systems can also

reflect fundamental mechanisms of acquired resistance under simplified but standardized experimental conditions [211]. Nevertheless, cell line studies verify the Goldie-Coldman hypothesis, according to which chemoresistance is believed to result from a clonal selection process driven by the acquisition of drug resistance mutations; only those cells that survive a drug-induced insult will regrow.

When investigating primary tumours, parameters introducing variations are clonal heterogeneity of the tumour cells, variable genetic backgrounds of donors, contamination with other cells and cross-talk with other non tumour structures. Thus, in primary tumours only a small percentage of the cells are likely to possess a chemoresistant phenotype.

In vitro chemoresistance and biomarker profiles are unique for histologic subtypes of EOC [212]. For example, endometrioid tumours are less frequently resistant to cisplatin when compared to papillary serous tumours. Mucinous tumours have the highest percentage of cisplatin resistance and surprisingly clear cell and undifferentiated carcinomas slower rates of paclitaxel resistance. These findings support the idea that histologic subtype may be a more significant factor than grade in determining chemoresponsiveness [213].

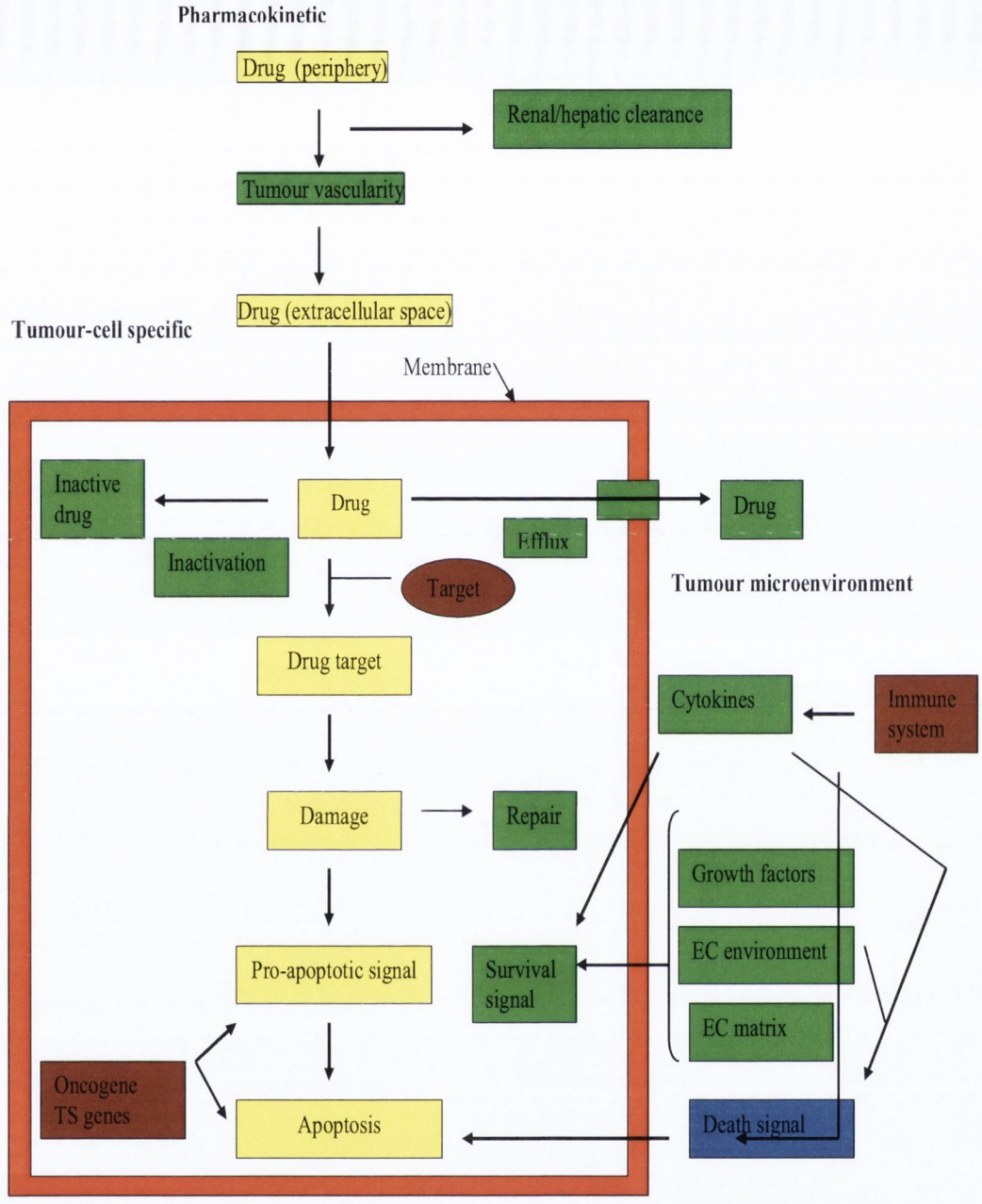

Figure 1.19 Some of the possible mechanisms of chemoresistance. These may be due to pharmacokinetics, the tumour microenvironment or may be cancer-cell-specific. These influence the response to chemotherapy by principally affecting intracellular active drug concentrations, drug-target interactions, target-mediated cell damage, damage-induced apoptotic signalling or the apoptotic effector machinery.

EOC is considered to be a chemoresponsive neoplasm, with initial response rates to systemic therapy exceeding 80% when integrated with primary cytoreductive

surgery. While advances in treatment strategies have improved the median overall survival for optimal debulked patients to 66.5 months, the majority of patients will relapse and eventually develop chemotherapy-resistant disease [214]. The treatment course for advanced ovarian cancer is marked both by chemotherapy sensitivity at the outset and by eventual death from resistant disease in patients who relapse. Aggressive surgical debulking and platinum plus taxane therapy have improved median survival from 1 year in 1975 to approximately 5 years in 2005, but the long-term cure rate remains in the 20% to 30% range [215]. Approximately 50% of patients will enter a pathological first complete clinical remission, yet 90% of suboptimally debulked patients and 70% of optimally debulked patients relapse in 18 to 24 months. Subsequent and repeated chemotherapy responses are often seen with ever shortening intervals until broad chemotherapy resistance develops.

As a result, there is increasing evidence in evaluating consolidation strategies following primary therapy as a means to further increase survival outcomes [216]

Resistance to chemotherapy is a major barrier to effective treatment for many cancer types and possible mechanisms are displayed in Figure 1.19. Resistance mechanisms may either act directly against a drug (e.g. limiting intracellular drug accumulation, increasing drug detoxification via glutathione conjugation [217], or failing to convert drug precursors into their active form), mediated by members of the ATP binding cassette transporter superfamily [218] or act by compensating for drug-induced effects (e.g. altering amounts or activities of drug targets, activating analogous pathways not targeted by drugs, or increasing DNA repair and antiapoptotic signalling) [219]. Where multiple drugs are used to treat a tumor, multidrug resistance (MDR) may arise – sometimes by activation of a single gene [220]. To develop effective treatment strategies for the clinic, it is necessary to understand mechanisms of chemoresistance.

1.14.3.12 Cisplatin resistance

There is overwhelming evidence to support the view that the major mechanism of action of cisplatin is that it becomes activated intracellularly by the aquation of one of the two chloride 'leaving' groups, and subsequently covalently binds to DNA, forming DNA adducts. This activates various signal-transduction pathways involved

in DNA-damage recognition and repair, cell-cycle arrest and finally programmed cell death/apoptosis [221]. Interestingly, in ovarian cancer cell lines, DNA damage induces different modes of cell death. Depending on the severity of DNA damage, cells might die by apoptosis or necrosis. Functional *p53* and caspase-2 are required for the apoptotis response, however in their absence, cells might undergo mitotic catastrophe, followed by necrosis-like lysis [222].

Platinum enters the cell using a copper transporter. Once inside the cell, the chlorine groups of cisplatin are exchanged for water (aqua) species, which are more chemically reactive. The intracellular target for cisplatin is DNA, where a variety of platinum adducts are formed, some on the same strand of DNA (intrastrand adducts) and others between strands (interstrand adducts). Of the 4 bases, guanine is the preferred site for binding and the most common adduct involves linkages on 2 adjacent guanines on the same strand of DNA. It remains uncertain which of the various types of adduct is the most important in terms of producing antitumour effects (Figure 1.20).

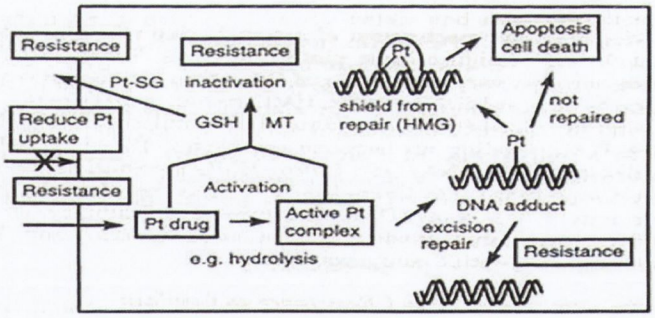

Figure 1.20: Platinum binds DNA forming platinum-DNA adducts, which impede replication and transcription processes that require DNA strand separation to different extents. They can also cause arrest at the G2 phase.

Compared with cisplatin, carboplatin is essentially devoid of nephrotoxicity, and is less toxic to the gastrointestinal tract and less neurotoxic; by contrast, myelosuppression, is dose-limiting for carboplatin. Interestingly, adducts formed by carboplatin on DNA are essentially the same as those formed by cisplatin, but 20–40 fold higher concentrations of carboplatin are required, and the rate of adduct formation is around 10-fold slower [223].

Resistance to cisplatin has been studied extensively using tumour cells repeatedly exposed to the drug *in vitro*. In these cell models, resistance is generally due to a combination of mechanisms, some resulting in reduced damage to DNA and others following DNA damage. Resistance due to inadequate binding to DNA has been shown to be caused by reduced drug uptake (influx rather than efflux) and inactivation by thiol-containing species such as glutathione and metallothioneins. Resistance occurring post-DNA binding may be due to changes in DNA repair pathways [an increase in nucleotide excision repair (NER) or a loss of DNA MMR]. Conversely, the hypersensitivity of some cell lines to cisplatin has been shown to be due to defective NER, through loss or reduced expression of NER proteins such as XPG and XPA. Resistance may also be mediated through alterations in proteins involved in programmed cell death (apoptosis) such as *p53* and the *BCL2* family. A basic understanding of cisplatin resistance pathways has made a major impact in the development of new multinuclear platinum analogues capable of circumventing resistance, such as the trinuclear platinum BBR3464, which has markedly different DNA binding properties compared with cisplatin [224].

Resistance through insufficient DNA binding. Cisplatin is highly polar and enters cells relatively slowly in comparison to other classes of small-molecule cancer drugs. The uptake of cisplatin is influenced by factors such as sodium and potassium ion concentrations, pH, and the presence of reducing agents; and a role for transporters or gated channels has been postulated in addition to passive diffusion [225]. In the past few years, the major plasma-membrane transporter involved in copper homeostasis, copper transporter-1 (*CTR1*), has also been shown to have a substantial role in cisplatin influx [226]. Loss of *CTR1* results in less platinum entering cells and a 2–3-fold increase in drug resistance [151]. Both copper and cisplatin (at clinically relevant concentrations) cause a rapid downregulation of *CTR1* expression in human ovarian cancer cell lines [227].

Platinum might enter cells using either transporters, (a significant one being the *CTR1*) or by passive diffusion. Loss of *CTR1* results in less platinum entering cells and consequently drug resistance. Once inside cells, cisplatin is activated by the addition of water molecules to form a chemically reactive aqua species. This is facilitated by the relatively low chloride concentrations that are found within cells. In

the cytoplasm, the activated aqua species preferentially reacts with species containing high sulphur levels by virtue of their containing many cysteine or methionine amino acids. These species include the tripeptide glutathione or metallothioneins. In some platinum-resistant cancer cells, glutathione and metallothionein levels are relatively high, so activated platinum is effectively 'mopped up' in the cytoplasm before DNA binding can occur, thereby causing resistance. Finally, active export of platinum from the cells through the copper exporters ATP7A and ATP7B as well as through the glutathione S-conjugate export GS-X pump (also known as MRP2 or ABCC2) can contribute to platinum drug resistance.

The MDR phenotype is traditionally attributed to the activity to ATP-binding cassette (ABC) transporters such as P-glycoprotein. Recent research suggests evolution of the MDR phenotype is a dynamic, multigenic process in the genomes of cancer cells involving a network of genes associated with the extracellular matrix, previously implicated in tumour invasion and cell proliferation [220].

In recent years, efflux proteins that are involved in copper transport, the ATPases ATP7A and ATP7B have been shown to modulate cisplatin export [228]. For example, human ovarian carcinoma cells that were transfected with ATP7A showed a small increase in ATP7A expression, enough to cause resistance to cisplatin and carboplatin owing to increased sequestration of platinum into the vesicular fraction [229].

An extensive body of evidence implicates increased levels of cytoplasmic thiol-containing species as causative of resistance to cisplatin or carboplatin. These species, such as the glutathione and metallothioneins, are rich in the sulphur-containing amino acids cysteine and methionine, and lead to detoxification because platinum binds avidly to sulphur [230], but they are not significant predictors of survival [231]. For example, early studies using a panel of eight human ovarian carcinoma cell lines showed a significant correlation between sensitivity to cisplatin and carboplatin, and levels of the sulphur-containing tripeptide, glutathione [232]. The conjugation of cisplatin with glutathione is catalysed by glutathione S-transferase (GST), which makes the compound more anionic and more readily exported from cells [233] . A study of two ovarian cancer cell lines that were derived from the same patient before and after the onset of drug resistance showed 2.9-fold

higher levels of GST in the cells derived from the drug-resistant tumour [234]. Most translational studies support a role for the glutathione metabolic pathway in acquired and inherited drug resistance to the platinum drugs, as well as to other DNA-damaging drugs such as the alkylating agents [235]. Increased levels of thiol-containing proteins, the metallothioneins (MTs), have also been associated with tumour resistance to cisplatin in human ovarian cancer cells [236].

Resistance mediated after DNA binding. After platinum–DNA adducts have been formed, cellular survival (and therefore tumour drug resistance) can occur either by DNA repair or removal of these adducts, or by tolerance mechanisms as well indicated by the hypersensitivity of testicular cancer to cisplatin, resulting from DNA-repair deficiency [237]. By contrast, many cisplatin-resistant cell lines that are derived from various tumour types have been shown to have increased DNA-repair capacity in comparison to sensitive counterparts [238]. Of the four major DNA-repair pathways, nucleotide-excision repair (NER), base-excision repair (BER), MMR and double-strand-break repair, NER is the major pathway known to remove cisplatin lesions from DNA. Particular attention, in both cell lines and clinical biopsy specimens, has focused on the NER endonuclease protein ERCC1 (excision repair cross-complementing-1) and resistance to platinum drugs. ERCC1 forms a heterodimer with *XPF* (xeroderma pigmentosum (*XP*), complementation group F) and acts to make a 5′ incision into the DNA strand, relative to the site of platinated DNA. For example, increased NER in cisplatin-resistant ovarian cancer cells was associated with increased expression of ERCC1 and *XPF* (predominantly ERCC1) [239]. A clinical translational study links overexpression of the NER DNA-repair pathway gene *ERCC1* to poor response to platinum-based chemotherapy in patients with ovarian cancer [240].

Increased tolerance to platinum-induced DNA damage can also occur through loss of function of the MMR pathway. Research demonstrates a correlation between failure of the DNA mismatch repair proteins to recognize the platinum adduct and low-level resistance, suggesting a role for the DNA mismatch repair system in generating signals that contribute to the generation of apoptotic activity [241].

During MMR, cisplatin-induced DNA adducts are recognized by the MMR proteins MSH2, MSH3 and MSH6. It is postulated that cells then undergo several

unsuccessful repair cycles, finally triggering an apoptotic response. Loss of MMR with respect to cisplatin–DNA adducts therefore results in reduced apoptosis and, consequently, drug resistance. The clinical relevance of the loss of MMR to platinum-drug-containing chemotherapy resistance in patients with ovarian cancer, is rather controversial; some data indicate a possible role in acquired drug resistance [242], whereas other data show no correlation with intrinsic resistance [243]. Another tolerance mechanism involves enhanced replicative bypass, via DNA polymerases; polymerase has been shown to have a role in acquired resistance to cisplatin and carboplatin [244]. Finally, resistance might occur to platinum, and other cancer drugs, through decreased expression or loss of apoptotic signalling pathways as mediated through various proteins such as *p53*, anti-apoptotic and pro-apoptotic members of the *BCL2* family, and *JNK* [245].

Overall, knowledge of how ovarian tumours are, or become, resistant to cisplatin or carboplatin has largely arisen from studies that have been carried out in cell lines in vitro with numerous mechanisms shown to be involved.

1.14.3.13 Proposed strategies to circumvent platinum-drug resistance in cancer patients

Resistance can be tackled by increasing the levels of platinum reaching tumours (for example, liposomal platinum products) thereby resulting in greater killing; combining existing platinum drugs with molecularly targeted drugs (for example, bevacizumab); using novel platinum drugs such as oxaliplatin that are capable of circumventing cisplatin-mediated resistance mechanisms; and using other drugs either alone (for example, TLK286) or in combination (for example, decitabine), which exploit particular cisplatin-mediated resistance mechanisms (Figure 1.21).

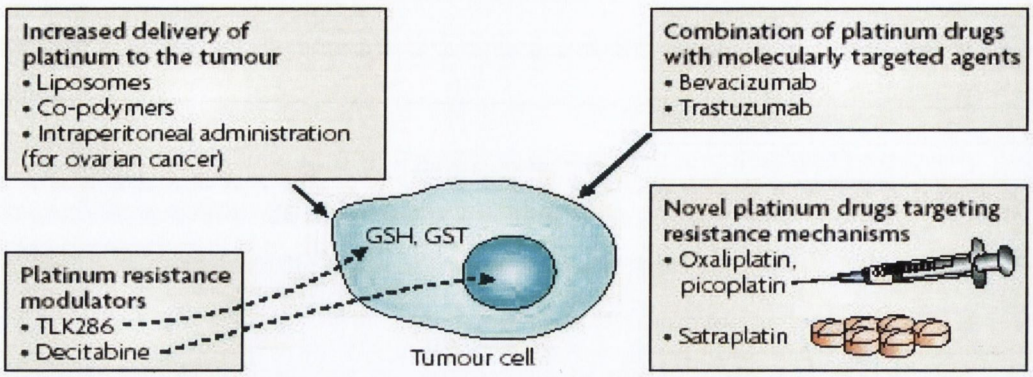

Figure 1.21 Major ongoing strategies to circumvent cisplatin and carboplatin resistance (Adapted from [221]).

1.14.3.14 Improved delivery of platinum to tumours

The strategy of using delivery vehicles to selectively transport more of a tumour-killing agent to tumours is attractive, and has now been clinically validated with doxorubicin [246] and paclitaxel [247]. Unsurprisingly, a liposomal preparation of cisplatin, SPI-77, has been tested clinically in lung cancer with minimal toxicity but only modest antitumour activity in comparison to cisplatin [248].

A second strategy links a platinum-based drug to a water-soluble, biocompatible co-polymer, such as hydroxypropylmethacrylamide, in order to exploit the enhanced permeability and retention effect of macromolecules in tumours. As with the liposome approach, clinical studies have progressed from using a cisplatin-like platin (AP5280) [249] to ongoing trials with the derivative A*P5*346 that possessed superior antitumour activity to oxaliplatin in a xenograft model of human ovarian carcinoma. A*P5*346 delivered more platinum to the tumour than oxaliplatin and with a higher release rate at a lower PH [250]. As the extracellular pH of solid tumours has been shown to often be more acidic than normal tissues, this might also explain, in part, the increased tumour delivery of this agent.

Finally, in particular situations, such as in patients with ovarian cancer, localised platinum-drug administration through intraperitoneal injection might be applied. In support of this strategy, a recent randomized trial in over than 400 ovarian cancer

patients indicated a significant improvement in tumour response rates through intraperitoneal administration of platinum-based chemotherapy [165].

Platinum-resistance modulation. The glutathione-mediated detoxification pathway is an important determinant of platinum-drug sensitivity and resistance and the use of glutathione modulation using agents such as buthionine sulfoximine in patients with heavily pretreated, drug-resistant ovarian cancer has been assessed in phase I clinical trials [251].

Another approach exploits loss of the DNA-MMR pathway through hypermethylation of the MLH1 gene, which has been shown to lead to resistance to cisplatin and carboplatin, and predicts for poor survival of patients with ovarian cancer [242]. This has led to the concept of using the DNA demethylating agent decitabine in combination with cisplatin or carboplatin to reverse this resistance mechanism. Pre-clinical studies have used platinum drug-resistant human ovarian or colon carcinoma cells that are MMR deficient owing to MLH1 hypermethylation. Nude mice with xenografts of these cells were treated with decitabine in combination with either cisplatin or carboplatin, which decreased tumour growth further than is seen with either platinum drug alone, thus demonstrating proof of principle for the combination therapy of a demethylating agent and a platin [252].

1.14.3.15 Taxane resistance

Taxanes are microtubule-stabilizing drugs that have been extensively used as effective chemotherapeutic agents in the treatment of solid tumours, such as ovarian, lung and breast cancer. However, taxane resistance limits clinical utility to approximately 50% of patients with breast or ovarian cancer.

Paclitaxel, a prototype taxane, a potent drug of natural origin isolated from the bark of the pacific yew, Taxus brevifolia, acts by stabilizing microtubule (MT) polymers- inhibiting MT depolymerization and changing MT dynamics- leading to mitotic arrest and apoptosis [253]. It also induces post-translational modifications of tubulin, such as detyrosination or acetylation that accumulate in these stable microtubules. Detyrosination exposes Glu residues at the carboxy terminus of a-tubulin, which can be detected using antibodies and therefore used as a marker of microtubule stability

[254]. Taxol-treated cells are unable to proceed normally through the cell cycle and arrested in the G2/M phase [255]. As paclitaxel primarily targets polymerized microtubules, an increased in the proportion of unstable microtubules induces paclitaxel resistance (Figure 1.22) [256].

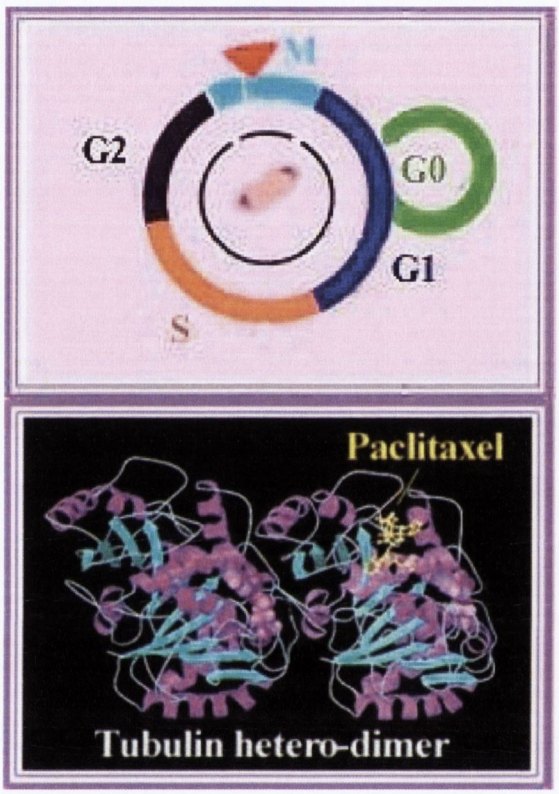

Figure 1.22 Taxol inhibits dissassembly of mitotic spindles and microtubules during the M phase by binding to tubulin heterodimers. The mitotic block further increases polymerization of microtubules and formation of microtubular bundles, which block entry at the S phase.

General mechanisms of drug resistance can apply to taxanes, including overexpression of the ABC/MDR transporter family of proteins [257], delayed G2/M transition [258], defective mitotic checkpoints [259] and alterations in apoptosis regulation [260]. More specifically, alterations of microtubules, such as those caused by b-tubulin mutations [261] induce severe taxane resistance [262]. Alternatively, factors that increase the ratio of unstable to stable microtubules induce profound taxane resistance, probably by mutations in nonpaclitaxel binding sites or alterations in tubulin isoforms [263]. ECM proteins appear to modulate microtubule stability and alter paclitaxel sensitivity in ovarian cancer [264]. In support of this, integrin-

mediated adhesion of cells to fibronectin induces microtubule stabilization [265], suggesting that ECM and paclitaxel might have additive effects on microtubules.

The functional status of *p53* can regulate the sensitivity of cancer cells to chemotherapeutic drugs [266]. *p53* regulates the sensitivity of antimicrotubule drugs, such as taxanes and Vinca alkaloids, by controlling the expression of proteins that affect the dynamic equilibrium of microtubule assembly [267].

In pathological specimens, morphological changes typical of paclitaxel-induced cytotoxicity include cytoplasmic vacuolation and multinucleation [268].

A list of cytotoxic agents routinely used in the clinical setting of ovarian cancer treatment is summarised in Table 1.7 and illustrates the diversity of molecular targets, schedule dependence and potential for interaction with platinum.

Table 1.7 Cytotoxic agents used in ovarian cancer treatment

Abbreviations: GSH, glutathione; MDR, multidrug-resistant glycoprotein; MRP, membrane-associated resistance protein.

Agent	**Target**	**Mechanism**	**Schedule**	**Resistance**	**Interaction with platinum**
Platinum	↑↓ DNA	DNAadduct formation	Independent	↑GSH, ↑damage	N/A
Paclitaxel	β-tubulin	↑tubulin aggregation	Dependent (toxicity)	↑MDR-MRP, Tubulin mutations	↑ Heme toxicity, ↑ neuropathy
Topotecan	RNA reductase, DNA incorporation	↑DNAsynthesis, ↓nucleotide synthesis	Dependent (efficacy)	↓ Topo-1	↑ Heme toxicity
Liposomal Doxorubicin	Topo-1	DNA synthesis	Prolonged clearance	↑ MDR-MRP	↑ Heme toxicity

1.15 Genomic approaches in Biomarker Discovery

Molecular research studies may improve the management of ovarian cancer patients. The finding that no single gene marker can reliably predict response to therapy and outcome and advances in genomics and proteomics have generated many candidate markers with potential clinical value [269]. Gene expression profiling by micro arrays or real-time reverse transcription polymerase chain reaction (RT-PCR) can be useful in the classification or prognosis of various types of cancer, including ovarian cancer [270]. With the advent of microRNA (miRNA) expression profiles, significant efforts have been made to correlate miRNA expressions with tumour prognosis.

1.15.1 Complementary DNA (cDNA) Micro arrays

DNA micro arrays were originally developed in the Brown laboratory at Stanford University. This technology enables investigators to measure the expression of tens of thousands of genes in a biological specimen in parallel [271]. This represents a significant advantage over the previously available techniques for measuring gene expression, ie, Northern Blot and RT-PCR, where only a few genes could be studied. This is made possible in one hybridisation experiment because of two basic principles of nucleic-acid hybridisation: DNA and RNA will specifically bind to their complementary sequence and this binding happens in proportion to the abundance of a sequence in a mixture.

The resultant expression signatures can also give valuable information on key pathways involved in carcinogenesis and tumour behaviour. It also allows identification of genes within each pathway that show altered expression within a tumour, thereby gaining insight into the origin of pathway deregulation and possibly tumour pathogenesis.

DNA micro arrays, also called "gene chips", fundamentally consist of DNA attached to a surface in an ordered, predetermined fashion at extremely high density. The most commonly used micro arrays are "spotted" micro arrays" [271] in which the array probes are manufactured separately from the arrays and consist of cDNA and either PCR products or oligonucleotides. Using a robotic system, microscopic quantities of any designed probe are typically spotted onto the arrays. Probes can be quality

controlled prior to spotting making it easier to determine if probes have been correctly synthesized prior to running an experiment [272].

Prior to the development of genome-wide expression analysis technology, efforts to delineate the molecular underpinnings of ovarian cancer relied on single-gene strategies [273]. In those studies *p53* tumour suppressor gene was the single molecular marker more consistently shown to be associated with ovarian cancers that present with metastatic disease [274]. Mutation of *p53* is the most common genetic alteration in ovarian cancer, occurring in at least 70% of advanced stage cases [275]. However, neither *p53* mutational status nor other single gene alterations have proven strong predictors of outcome. Studies on the role of single molecular markers have shown ovarian carcinogenesis to be a complex process, multifactorial in nature and associated with genetic abnormalities in multiple gene families. This "gene by gene" analysis, while helpful, has not been able to provide a global mechanistic basis for the clinicopathologic characteristics of these tumours, nor determine the biological relationship among these different tumours.

1.15.2 Transcription profiling in ovarian cancer

Microarray technology (Figure 1.23) has permitted analysis and simultaneous monitoring of expression levels of thousands of genes within a cell. The gene expression pattern can be correlated with many clinically relevant characteristics of an individual tumour [276]. Therefore, it can be used to characterize the biological relationships among histological subtypes of ovarian cancer and identify genes whose altered gene expression is important in the development of ovarian cancer. Further, it has the potential to identify activated pathways and key genes which can be targeted for the effective prevention and treatment of the disease.

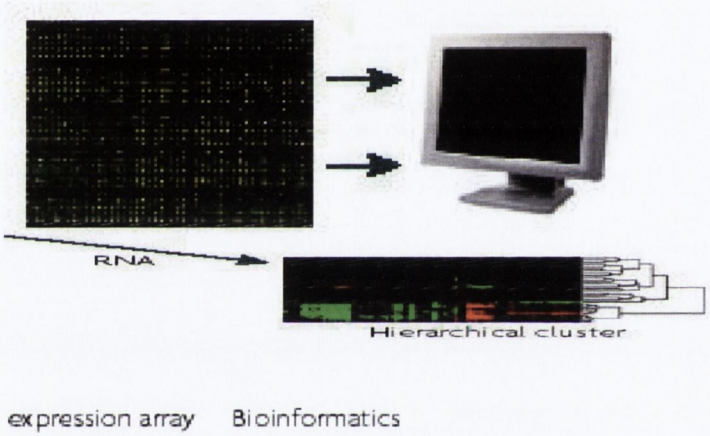

Figure 1.23 Search for molecular determinants of ovarian cancer. RNA is hybridized to microchips containing probes representing the entire pattern of expressed human genes. The complex patterns obtained from these microchip experiments require a sophisticated bioinformatics analysis to reveal those signatures associated with recurrent ovarian cancer.

As with many cancers of epithelial origin, it is important to establish an appropriate control for evaluating differential gene expression between "normal" and cancer. Expression profiling studies of ovarian cancer have relied on a variety of sources of "normal" cells for comparison with tumours, including whole ovary samples, OSE exposed to short-term culture and immortalised OSE cell lines [277]. As a result the selection of a normal control to compare to EOC samples can strongly influence the genes that are identified as differentially expressed. In fact, the majority of genes found in each molecular gene signature comparing "normal" to ovarian tumour are

unique to that comparison pair as deluded by low Pearson correlation between any "two" normal groups.

In addition, these studies have allowed the identification of thousands of additional differentially expressed genes, for which there is little structural or functional information. Clustering of genes with known and unknown functions provides insights into signaling pathways that are essential for development of human cancers.

Several studies using DNA microarrays to determine gene expression profiles in ovarian cancer cell lines or ovarian carcinomas have been reported (Table 1.8).

Table 1.8 DNA microarray studies and their specific aims in ovarian cancer

Aim of microarray study	Material	Number of studies
Diagnostic markers & carcinogenesis	Normal epithelial tissue or cell lines vs. cancer cell lines or carcinomas	30
Carcinogenesis	Carcinomas	9
Molecular determinants of classic clinicopathological factors (stage, grade, histiotype, (sub)optimal cytoreduction, response to chemotherapy)	Carcinomas	20
Acquired drug-resistance	Cancer cell line/tumor resistance model	15
Drug action & response to chemotherapy	Cancer cell lines or xenografts	12
Effect of overexpression of a particular gene on gene expression & drug-response & metastasis	Cancer cell lines	5
Methylation alterations, genes, or profile associated with (progression-free) survival & response to chemotherapy	Carcinomas	10

Most studies have tried to identify diagnostic markers by comparing ovarian cancers or cancer cell lines with normal ovarian epithelium. Cell line models were also used to identify genes related to drug resistance [278] [279]. Microarray technology also allowed for the identification and subclassification of tumors based on their distinct molecular signatures, also addressing the molecular differences of tumors of varying grades [280] [281].

Gene expression profiling has been used to characterize the histotypes and the unique clinical phenotypes displayed by ovarian cancer (Figure 1.24). Comparisons of gene expression profiles from tumours with similar histotypes across different organs have also been performed to allow understanding of the similarities and differences of the transformation processes that produce these tumours. It is well recognized that tumours of similar histology are found in the ovary and in the endometrium [282]. Expression profiling on EOC of varying histologies has also afforded the elucidation of genes which contribute to the biological and clinical features seen in the four major histological types of ovarian carcinoma [283].

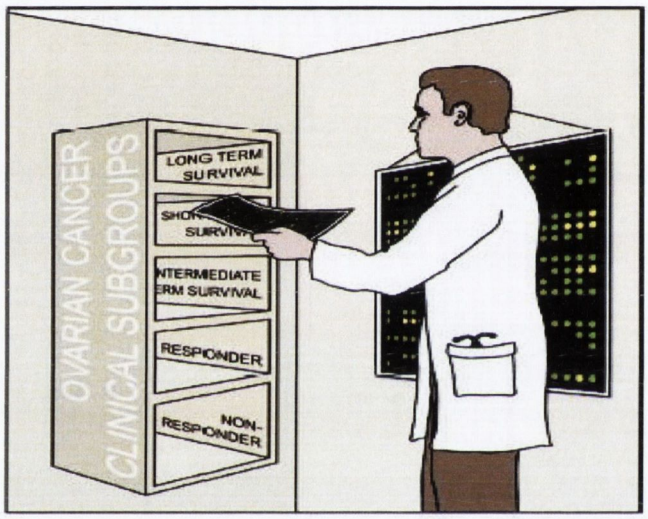

Figure 1.24 Gene expression patterns can be used to classify ovarian carcinomas into clinically relevant subtypes

Gene expression profiling has been also used to address the molecular differences of tumours of varying grades. LMP and grade 1 serous tumours share a similar molecular fingerprint and may lie on the same developmental continuum, whereas low and high- grade tumours develop along two different pathways [91].

Other studies have looked at prognostic and/or predictive genes and gene profiles for predicting individual disease outcome in advanced ovarian cancer and response to chemotherapy [284] [285-288]. Ovarian cancer cell line models were mostly used to identify genes related to drug resistance. Spentzos *et al.* [284] used 34 tumour samples to identify a 115-gene profile. When applied to a validation set of 34 samples, the profile distinguished patients with a favorable overall survival.

Interestingly, that prognostic 115-gene profile for overall survival, showed no gene overlap with another 93-gene profile associated with predicting response to chemotherapy. Berchunk *et al.* [289] by using classification tree models, identified 26 genes that reflected short-term versus long-term survival from 54 advanced stage ovarian cancer patients. These genes held their prognostic value in the set of independent tumours profiled by Spentzos *et al.,* [284, 290].

Alternatively, microarray technology discovered gene signatures that can predict early response in ovarian cancer after chemotherapy [192]. In this way, they attempted to predict which women were at risk for early (<21 months) versus late (>21 months) relapse. By profiling 79 advanced stage, high-grade tumours, a 14-gene profile was predictive for early recurrence.

In addition to these prognostic studies, others attempted to identify a profile predictive of response to platinum-based therapy. Spentzos *et al.* [290] discovered a 93-gene profile predictive of pathological complete response to chemotherapy by profiling tumours from patients undergine second-look surgery. The same profile could distinguish patients with favourable versus unfavourable profile in a validation set. Combination of micro arrays and RT-PCR was used to classify ovarian tumours according to their response to platinum-based therapy based on a 9-gene profile [291]. Using RT-PCR, this profile predicted platinum resistance in an independent validation set of 72 patients. In contrast to the Spentzos study, clinical response was assessed not according to pathological but WHO criteria. Obviously, the differences in definition of response to chemotherapy could be the reason for the low number of genes shared between the two studies. A predictive model for response to platinum-based therapy on a training set of advanced serous ovarian cancers showed an accuracy of 78%.

In parallel, expression signatures defining the status of oncogenic clinical pathways were evaluated. Integration of chemotherapy response signatures with signatures of oncogenic pathway deregulation can be used to identify new therapeutic strategies [270]. In patients with platinum resistance disease the authors identified expression signatures consistent with activation of Src, β-catenin and Rb/E2F signaling pathways [292]. Several genes reported are known to affect the malignant phenotype (such as those encoding heat shock protein 27, BAX, PDGFR, lysophospholipase II,

fibronectin, etc) [293-296] yielding mechanistic insights into ovarian carcinogenesis and chemoresistance.

Clinical evidence of prognostic microarray studies shows that they never progressed beyond the level of a small retrospective study [297]. Reasons to explain the limited overlap between the prognostic profiles in ovarian cancer microarray studies include a) overfitting, that is, finding a discriminatory pattern by chance, when large numbers of potential predictors are used to discriminate among a small number of outcome events [298] b) different types of microarray platforms using different types of probes and c) low signal-to-noise ratio. Intensities observed from microarray experiments are composed of signal (gene expression level) and experimental noise [299]. Potential experimental sources of error include dye, print-tip or array effects. As such, cross-validation of genome-wide microarray results, using additional methods, such as real-time quantitative RT-PCR remain critical steps. Moreover, independent test set analysis not used for determining pre-processing parameters, model building or model selection can be used to estimate the true performance of models [300]. This is further strengthened by a recent review, which indicated a biased estimation of the accuracy as the most common flaw in recently published microarray studies focusing on cancer related outcomes [301]. Predicting response to chemotherapy appears even more challenging than predicting disease stage [302].

However, microarray analyses, providing lists of significant genes with p-values, are insufficient to understand the aetiology or molecular regulation of ovarian cancer. Full functional annotation and knowledge of the relative distribution of the gene product and its interaction with other genes has to be further ensured, by placing these genes in gene regulatory networks to reveal whether molecular pathways are deregulated. It is equally important to elucidate which molecular pathways contribute to the development and clinical outcome of ovarian cancer.

1.15.3 Gene expression profiles of ovarian surface epithelial cells in vivo.

As discussed earlier, EOC is thought to arise from the OSE and that constant rounds of proliferation and repair following ovulation contribute to neoplastic

transformation. A recent study highlighted on genes and pathways which are involved in the normal functions of the ovarian epithelium, in particular hormone responsive genes, central to functions such as proliferation and apoptosis [303]. This approach can also lead to a better understanding of the aberrations leading to a malignant transformation (Figure 1.25).

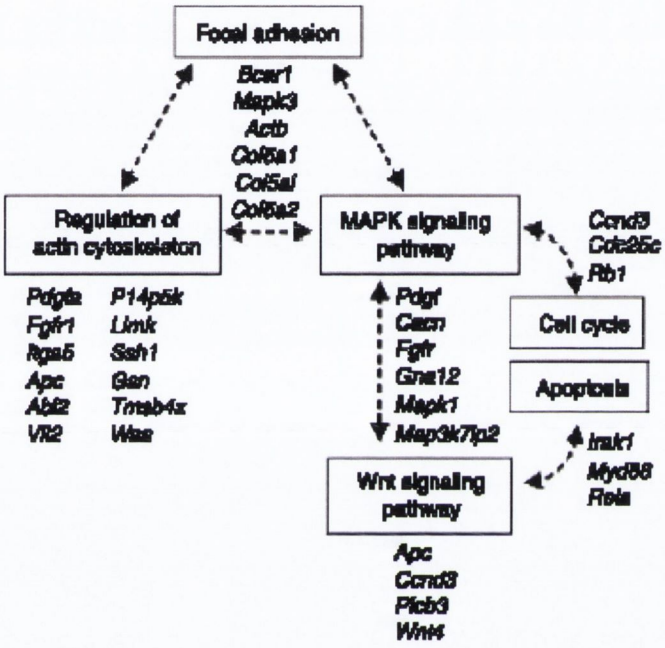

Figure 1.25 Pathways with the highest number of OSE genes include actin cytoskeleton, focal adhesion, cell cycle, apoptosis, MAPK signaling and Wnt Signaling pathways irrespective of estrous developmental stage (Adapted from Gava N 2008, J of Mol Endocrinology). A subset of these genes overlap with gene upregulated in our cohorts of primary versus recurrent ovarian cancers as discussed later.

1.15.4 Validation of microarray experiments

Quantifying gene expression levels has become a staple of most molecular biological laboratories. By measuring the amount of cellular RNA, one is able to determine to what extent that particular gene is being expressed. For many genes, the expression levels may change dramatically from gene to gene, cell to cell or during various

experimental conditions. Quantitative gene expression studies include most commonly a validation of the extent of transcription of a gene.

3 methods of microarray validation have been reported so far:

a) Validation of the level of expression by RT-PCR has the advantage of unparalleled sensitivity, although it does not generate the throughput achieved by cDNA micro arrays. It is ideal in situations where one wants to profile up to several hundreds of genes (given that PCR instruments are equipped with 96 or 384 well plate configuration. Another such application is miRNA.

b) Validation by application of selected targets in another set of samples.

c) Run of the samples on another array platform: to examine platform differences. An ANOVA test is usually performed looking for differential effect of response by platform.

1.16 microRNAs (miRNAs)

Regulation of gene expression is a complex process requiring the co-ordinated interaction of proteins and nucleic acids and de-regulated gene expression is one of the key hallmarks of cancer (Figure 1.26). miRNAs are small non-coding RNAs of 19-24 nucleotides in length that negatively regulate gene expression. Discovered just over a decade ago, they are thought to regulate up to 30% of human genome. Each miRNA is supposed to target several hundreds of transcripts, making miRNAs one of the biggest family of gene regulators [304]. They are commonly clustered and located in the introns of protein coding genes [305].

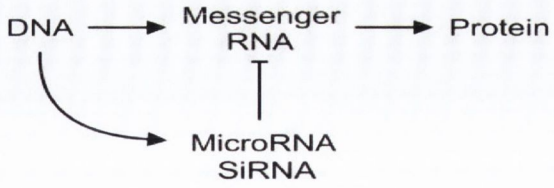

Figure 1.26 miRNA function in the regulation of gene expression. miRNAs are non-coding small RNA molecules that represent a new class of regulators of gene expression. miRNAs negatively regulate gene expression by obstructing the translation of messenger RNAs into protein, in a manner analogous to short interfering RNAs (siRNAs). The fundamental role of the RNAi machinery in modulating the flow of genetic information through posttranscriptional gene silencing was highlighted by the joint award of the 2006 Nobel Prize in Medicine and Physiology.

miRNAs act at the translational stage to orchestrate profound changes in gene expression. In this way they impact fundamental cellular processes such as differentiation, proliferation and survival and provide new insights in cancer research [306] [307].

Hundreds of miRNAs have now been identified in humans and an overwhelming body of evidence now implicates miRNAs in the process of carcinogenesis.

1.16.1 miRNA nomenclature

miRNA terminology can be confusing and international guidelines have been put forward for their annotation [308]. A "miR" prefix is typically used to denote miRNAs and a prefix to identify the species of origin, for example "hsa" to represent *Homo Sapiens*. The only exception to this rule is the let-7 family of miRNAs which have retained their originally described "let" prefix (e.g. has-let-7a). A unique identifying number is also given for each miRNA, sequentially assigned; genes coding for miRNAs are similarly named: miRNA paralogs differ by only one or two nucleotides and are given lettered suffixes (e.g. has-miR-27a and has-miR-27b, which differ at only one base) [309].

1.16.2 miRNA history

miRNAs were discovered in 1993 during ground breaking research in the laboratories of Victor Ambros and Gary Ruvkun. They found that the lin-4 gene, known to be crucial for temporal regulation of developmental changes in *C. elegans*, does not encode a protein, but instead gives rise to a small 22 nucleotide RNA molecule. Gene expression was regulated through translational repression of the miRNA of the lin-14 gene, via antisense complementarity to its 3' untranslated region (UTR) [310]. Later in 2000, the let-7a family of miRNAs was discovered and subsequently, hundreds of miRNAs have been identified and registered in the online database that compiles the miRNA sequences (miRBase).

1.16.3 miRNA biology and mechanism of action

miRNAs are produced in a complicated series of steps that begin in the cell nucleus (Figure 1.27).

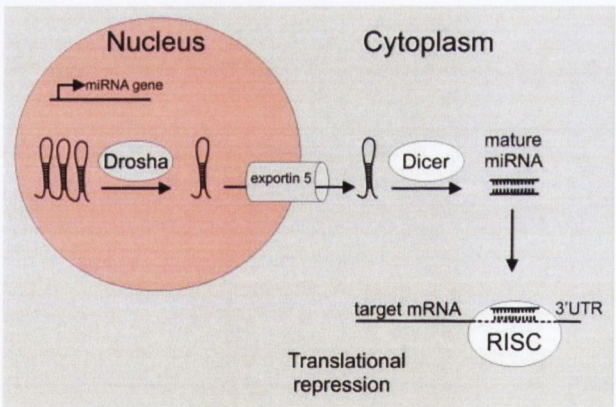

Figure 1.27 Schematic representation of miRNA biogenesis.

miRNA genes are transcribed into long transcripts called primary miRNAs (Pri-miRNA) containing multiple stem-loop/hairpin structures. Pri-miRNAs undergo cleavage by the endonuclease enzyme Drosha to form approximately 70 nucleotide precursor miRNAs (Pre-miRNA). Pre-miRNAs are actively exported to the cytoplasm by the nucleocytoplasmic transport factor Exportin 5, and there undergo further processing to give rise to mature single stranded miRNAs of about 20–25 nucleotides in length. Mature miRNAs are assembled onto the RNA-induced silencing complex (RISC) in association with other co-factors, and interact with

complementary sites in the 3′UTR of target messenger RNA (mRNA)s to negatively regulate gene expression through inhibition of translation. Perfect base pairing between the RISC-bound miRNA and the target mRNA results in cleavage and degradation of the latter, whereas imperfect complementarity generally leads to translational repression of the target [311]. RISC recruits a multiprotein complex containing the anti-association factor eIF6. Depletion of eiF6 in human cells abrogates miRNA-mediated regulation of target protein and mRNA levels [312].

1.16.4 miRNA regulation

miRNA expression can be regulated at multiple steps during RNA biogenesis, although it remains to be determined which step is controlled and how this control is achieved. Transcriptional regulation appears to be the major control mechanism, although some miRNAs seem to be controlled at the post-transcriptional level. Expression profiling studies indicate that most miRNAa are under the control of developmental or tissue-specific signaling, or both [313, 314].

Common causes of abnormal miRNA expression include:

- Location of miRNAs at cancer association genomic regions
- Epigenetic regulation of miRNA expression
- Abnormalities in miRNA processing genes and proteins.

1.16.5 miRNAs and cancer

The first evidence linking miRNAs to human cancers came from findings in chronic lymphocytic leukaemia (CLL). Deletions at chromosome 13q14 are common in CLL and occur in 50% of the patients. Two miRNAs, miR-15 and miR-16 were found to be encoded in this region and shown to be downregulated in the majority of cases with CLL [315].

Futher evidence linking miRNAs and cancer formation was the observation that over 50% of miRNA genes are located within regions showing LOH, amplification, viral integration sites and other cancer associated genomic regions [316].

How does deregulated miRNA expression contribute to cancer formation? If miRNAs function as negative regulators of gene expression, then over-expression of

oncogenic miRNAs can contribute to tumorigenesis by affecting pathways promoting the acquisition of the hallmarks of cancer. Equally, reduced expression of tumour suppressive miRNAs can have similar effects. One example of an oncogenic miRNA is miR-21. miR-21 forms part of a 22 gene miRNA signature in human solid cancers and its overexpression has been shown to lead to caspase activation and increased apoptotic cell death [317]. miR-21 regulates expression of the PTEN tumour suppressor gene in human hepatocellular cancer [318]. Thus it represents an oncogenic miRNA or "oncomir". In contrast, miR-15 and miR-16, through targeting BCL2 and freeing the apoptotic pathway, represent tumour suppressor genes [319]. miRNAs located in genomic regions amplified in cancers (such as the miR-17-92 cluster) function as oncogenes, whereas portions of miRNAs located in portions of chromosomes deleted in cancers (such as the miR-15a-miR-16-1 cluster) function as tumour suppressors (Figure 1.28).

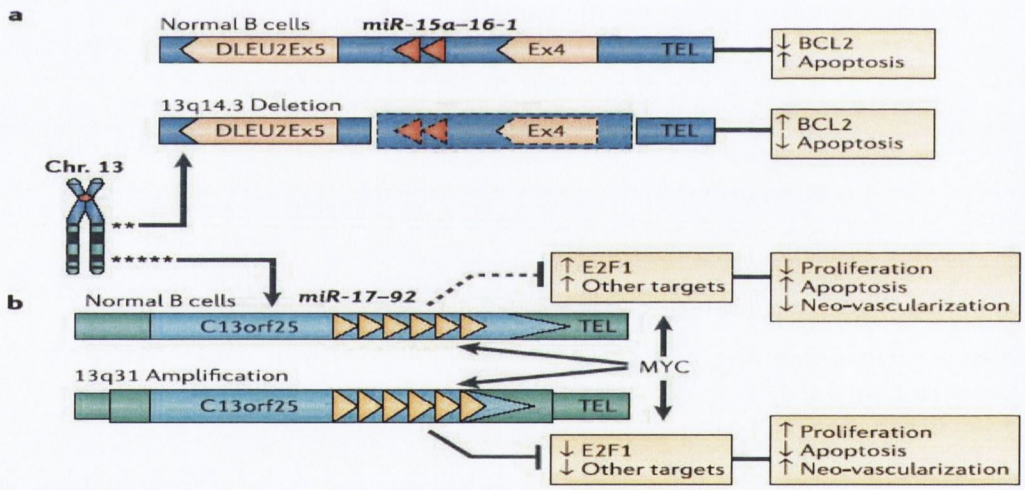

Figure 1.28 Chromosomal alterations at miRNA loci. OncomiRNAs and tumour suppressor genes may represent two different views of the same gene.

A common signature for distinct types of solid carcinomas indicates that specific miRNAs are involved in common molecular pathways [317] (Figure 1.29) .

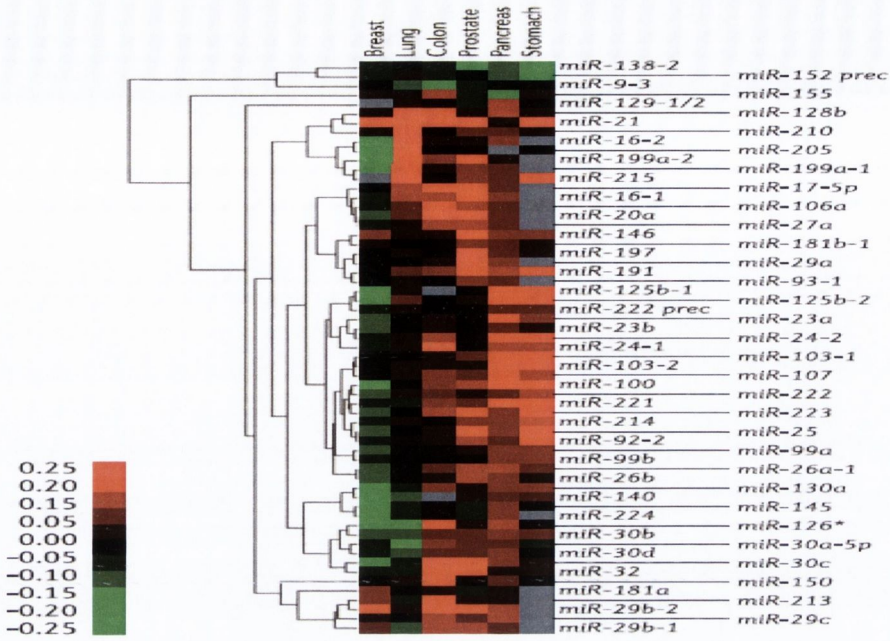

Figure 1.29: Common miRNA genes are differentially expressed in 6 solid cancers suggesting common altered pathways (Adapted with permission from Volivia *et al.*, 2007) [317].

1.16.6 Clinical applications of miRNAs

The discovery of miRNAs and their role in tumorigenesis opened up opportunities for translational bridging of this latest research into clinical gain (Figure 1.30). Foremost amongst these is the ability of miRNAs to allow diagnosis and prognostication, even better than mRNA profiling. miRNA based approaches can also be adapted for therapeutic applications with use of synthetically designed miRNAs to specifically silence genes in vivo.

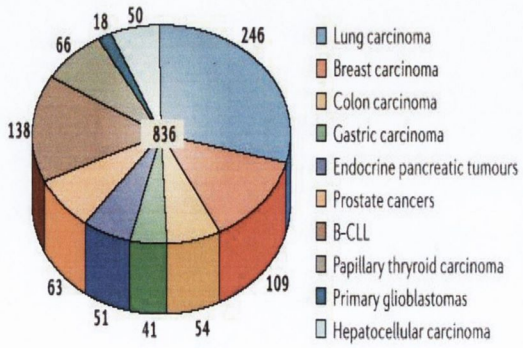

Figure 1.30 Published data on miRNA expression up to 2006.

Table 1.9 summarises the facts about miRNA profiling in human cancers.

Table 1.9 Facts about miRNA profiling in human cancers

Cancer type*	MiRNA profiling data	Significance
Chronic lymphocytic leukaemia	A unique signature of 13 genes associated with prognostic factors (ZAP70 and IgVH mutation status) and progression (time from diagnosis to therapy)	MiRNAs as diagnostic markers (the identification of two categories of patients)
Lung adenocarcinoma	Molecular signatures that differ with tumour histology; miRNA profiles correlated with survival (*miR-155* and *let-7*)	MiRNAs as prognostic and diagnostic markers
Breast carcinoma	MiRNA expression correlates with specific pathological features	MiRNAs as prognostic markers
Endocrine pancreatic tumours	A signature that distinguishes endocrine from acinar tumours; the overexpression of *miR-21* is strongly associated with both a high Ki67 proliferation index and the presence of liver metastases	MiRNAs as diagnostic and prognostic markers
Hepatocellular carcinoma	MiRNA expression correlated with differentiation	MiRNAs as prognostic markers
Papillary thyroid carcinoma	MiRNA upregulation (for example, *miR-221* and *miR-222*) in tumoral cells and normal cells adjacent to tumours, but not in normal thyroids without cancers	MiRNAs probably involved in cancer initiation
Glioblastoma	A specific signature compared with normal tissues	MiRNAs as diagnostic markers
Human cancers	MiRNA-expression profiles accurately classify cancers; an miRNA classifier classes poorly differentiated samples better than a messenger RNA classifier	MiRNAs as diagnostic markers
Human solid cancers	Common signature for distinct types of solid carcinomas	Specific miRNAs are involved in common molecular pathways

1.16.7 miRNAs as a diagnostic tool

Several aspects of miRNAs make them useful for clinical diagnostics. One possible application is in establishing a diagnosis of cancer and a number of studies have shown that miRNA expression patterns can accurately differentiate tumour tissue from benign disease [320]. miRNA profiling can also determine the tissue of origin of tumour [321-324]. miRNA expression signatures are also helpful in distinguishing different classes of tumours [325] or identifying the tissue of interest in poorly differentiated tumours with non-diagnostic morphological appearances [326].

1.16.8 miRNAs in prognostication

Perhaps more importantly than simply classifying tumours, miRNA expression patterns can also predict the clinical behaviour of certain tumours. High miR-155 and

low let-7a-2 expression levels correlate with poor survival in lung cancer [327]. In colorectal cancer, miR-200 has been associated with overall survival (OS) after surgery [328]. Apparently, miRNA based profiling has clear advantages over conventional mRNA based methods. miRNAs are long lived and stable in vivo and can be efficiently extracted from conventional formalin fixed paraffin embedded tissue, whereas mRNAs are subject to significant degradation [329, 330]. The fewer relative numbers of miRNAs (hundreds only) compared to mRNAs (tens of thousands) also makes analyses easier and more applicable to clinical practice.

1.16.9 miRNAs as therapeutic targets

Although at present there are no reports of miRNAs being trialled in human cancer therapy, theoretical evidence for implication of deregulated miRNAs in novel treatments has emerged. Oncogenic miRNAs can be targeted for downregulation by use of anti-sense miRNA oligonucleotides to their precursor or mature forms and tumour suppressive miRNAs may be directly upregulated for an anticancer effect. For example, in breast cancer, miR-21 can inhibit proliferation [331] whereas reduced invasion and migration is induced by miR-125 [332]. Recent work also demonstrates that miRNA directed therapy may be useful in combination with conventional chemotherapy [318]. Significant advances in the more established area of RNA interference and the similarities between RNAi and miRNAs can make possible the delivery of stable and non-toxic levels in into target cells. Intravenous administration of chemically engineered oligonucleotides, termed "antagomirs" in mice resulted in powerful silencing of endogenous miRNAs in a variety of organ systems [304]

miRNA genes are scattered in all chromosomes in humans except for the X chromosome. This observation may be more helpful in elucidating the complexity of female cancers. Approximately 50% of known miRNAs are found in clusters 1, 3 and 26. The miRNAs in a given cluster are often related to each other, suggesting that the gene cluster is a result of gene duplication. Unrelated miRNAs are also included. A plausible possibility is that the clustered miRNAs target the same gene or different genes in the same pathway.

1.16.10 miRNA quantification

A range of techniques are available for miRNA quantification, including northern blotting, dot blotting, RNase protection assay, primer extraction analysis and quantitative PCR. New easy quantification methods, such as cDNA cloning, micro arrays and bead based flow cytometry, have enabled for large-scale expression profiling of miRNAs [305]. Although microarray is a powerful method for high-throughput analysis, the small size of miRNAs poses a challenge because it is difficult to create a single hybridization condition for all miRNAs on a chip.

RT-PCR is the most sensitive method but would be very laborious in high through-put analysis if the number of miRNAs exceeds 300. A recent study showed that RT primers containing a stem-loop structure enhances the specificity for mature miRNAs [333]. Stem-loop RT-PCR involves a 2-step approach; step 1 involves annealing of stem-loop RT primers in a RT reaction followed by a RT-PCR.

1.16.11 Evidence of coupling of expression between mRNA and miRNAs

Both miRNAs and mRNA genes are encoded in DNA. Both classes of primary transcript are formed by RNA polymerase II [334]. Both types of RNA are extensively processed post-transcriptionally [335]. In model systems, miRNAs and mRNAs have been shown to interact directly, forming a regulatory circuit [312].

1.17 High content screening (HCS)

Understanding cellular biology in a physiologically relevant setting has tremendously increased the need to capture specific cellular events in a spatial-temporal fashion for target discovery/validation and drug identification and subsequent development.

Over the last few years, High Content Screening (HCS) has firmly established itself as a high-throughput fully automated technology for the analysis of microscopy-based cellular assays (Figure 1.31). It applies sophisticated image processing algorithms to analyze cell images generated by automated fluorescence microscopy.

This technology opens up a wide range of cell biological parameters for high-throughput analysis, essentially allowing measurememement of changes in object localisation, intensity, texture or shape, thereby enabling the analysis of cellular events. HCS has been rapidly adopted by the drug discovery industry and has quickly established itself as a core technology for secondary compound screening.

Figure 1.31 HCS Workstation

Historically, the number of primary publications on HCS has been low. Earlier literature was mainly restricted to reviews of the technology and its potential [336] [337]. Current high content analysis hardware and software tools are robust for custom development of specific algorithms. Limitations in reagents for live imaging of post translational modifications, which are the key events that control intracellular signaling mechanisms in cellular growth and homeostasis has primarily divided high content screens into two subtypes, namely fixed cell assays and live cell assays.

Cells fixation has been the one of the key means to analyze various events as endpoint readouts at a given time in space. Although live cell imaging has taken precedence over fixed cell imaging, fixed cell imaging still remains the single choice to monitor critical early events such as phosphorylation. Events in fixed cell assays can be captured using specific antibodies or dyes that can be excited to emit fluorescence at specific wavelengths. The major drawback with fixed cell assays is

the additional steps in preparation of the cells for analysis. For this reason, it may not be a preferred method for most high throughput primary screens.

The use of fluorescent antibody-based detection or immunofluorescence staining allows the monitoring of specific protein targets. For these types of assays, cells are routinely fixed which essentially freezes the cellular phenotype at a given time point. Although surface staining does not require additional steps, imaging of intracellular changes in fixed cell assay of various proteins requires additional manipulations like permeabilization to allow the entry of antibodies into the cell and bind to specific targets. Monitoring post-translational events, such as phosphorylation on critical residues of target proteins, can be achieved using specific antibodies that recognize site-specific phosphorylation. A critical parameter that is essential to high throughput high content data acquisition via immunofluorescence requires defining cells in the acquisition field. This is accomplished by the use of nuclear dyes such as Hoechst 33258 or 33342 or ethidium bromide for fixed cell assays.

Visualization of specific compartments can be performed using compartment specific fluorescent dyes. These can be used to monitor protein trafficking or assess changes in organelles. Such dyes can target specific organelles such as the nucleus, mitochondria, and lysosomes and can emit in specific color ranges such as green, red and blue. Hence, they can be used in various combinations with immunofluorescence assays in a manner that will allow monitoring changes with respect to the redistribution of the target.

1.17.1 Cytotoxicity screening

Multiparametric analysis of compound cytotoxicity at the level of individual cells using cellular imaging-based approaches such as HCS have played key roles in the detection of toxicity and classification of cytotoxic compounds. Historically, cellular toxicity screening has relied on the use of single-parameter readouts for toxicity markers such as cell proliferation, mitochondrial activity or membrane permeability. However, parallel analysis of multiple markers for cytotoxicity allows early reversible and late irreversible effects to be distinguished and in this way, it provides a more thorough interpretation of compound-induced toxicity [338].

HCS-based cytotoxicity assays analyze the effects of compounds on a number of parameters such as nuclear size, mitochondrial membrane potential, membrane permeability, lysosomal mass and cell count, offering increased specificity and selectivity for toxic events.

1.18 Aims of study

Our hypothesis is that:

- A distinct transcriptome and miRNA profile exists between primary and recurrent ovarian cancers

- Alterations in transcriptome and miRNA profiles may ultimately define the development of recurrence/chemoresistance

- Targeting potential biomarkers of recurrence/chemoresistance will have important therapeutic potential in the treatment of ovarian cancer

Based on the above combined approach, our aim is:

- To identify novel biomarkers, which govern the recurrence and resistance to chemotherapy in ovarian cancer

- To investigate the cytotoxicity effect of targeting potential biomarkers, using multiparametric cytotoxicity assays

CHAPTER 2

Material and Methods

2.1 Introduction

This chapter is a comprehensive account of all methodologies employed in this thesis, accompanied by background information on some of the newer and more complex techniques, several of those being used in a number of chapters. Where this occurs, the full description of the technique is restricted to this chapter, with specifics appearing in their relevant chapters only.

A list of all the samples (primary and recurrent ovarian cancers) used in this study with their clinicopathological details are displayed in Table 2.1 and 2.2.
The specimens are divided into 4 groups according to what study they were used for. Transcriptome specimens were fresh frozen (FF) and used in chapter 3. miRNA specimens were fresh frozen and used for miRNA analysis in chapter 4. Samples in bold were used as the training set. Dicer/Drosha specimens were fresh frozen and used for TaqMan analysis in chapter 4, samples in bold here represent the additional histologies which will be referred to in chapter 4. miRNA FFPE were formalin fixed paraffin embedded samples used for miRNA analysis in chapter 4.

Table 2.1 Primary Ovarian Specimens

Sample	Age	Transcriptome	miRNA fresh	Dicer/Drosha	miRNA FFPE	Histology	Stage	Grade
P1	64	X		x		Serous papillary adenocarcinoma	3C	3
P2	48	X	x	x		Serous papillary adenocarcinoma	3C	3
P3	59	X		x		Serous papillary adenocarcinoma	3C	3
P4	58	X	x	x		Serous papillary adenocarcinoma	3C	3
P5	84	X	x	x		Serous papillary adenocarcinoma	3C	3
P6	43	X		x		Small cell carcinoma	3C	3
P7	39	X		x		Serous papillary adenocarcinoma	4	2
P8	74	X		x		Mixed mullerian	3C	2
P9	74	X		x		Serous papillary adenocarcinoma	4	3
P10	61	X		x		Serous papillary adenocarcinoma	3C	3
P11	74	X	x			Serous papillary adenocarcinoma	3C	3
P12	60	X	x	x		Serous papillary adenocarcinoma	3C	3
P13	44	X	x	x		Serous papillary adenocarcinoma	3A	3
P14	64	X	x			Serous papillary adenocarcinoma	3C	3
P15	74	X	x	x		Serous papillary adenocarcinoma	3C	3
P16	68	X	x	x		Serous papillary adenocarcinoma	3C	3
P17	54	X	x	x		Serous papillary adenocarcinoma	3C	3

P18	42	X	x			Serous papillary adenocarcinoma	3B	3
P19	58			x		Serous papillary adenocarcinoma	4	2
P20	86		x		X	Serous papillary adenocarcinoma	3C	3
P21	59		x			Serous papillary adenocarcinoma	3C	3
P22	63		x			Serous papillary adenocarcinoma	3C	2
P24	66				X	Serous papillary adenocarcinoma	2	3
P25	71				X	Serous papillary adenocarcinoma	1C	3
P26	63				X	Serous papillary adenocarcinoma	2C	3
P27	59				X	Serous papillary adenocarcinoma	3C	2
P28	55				X	Serous papillary adenocarcinoma	4	2
P29	56				X	Serous papillary adenocarcinoma	3C	3
P30	45				X	Serous papillary adenocarcinoma	3C	2
P31	59				X	Serous papillary adenocarcinoma	3C	3
P32	40				X	Serous papillary adenocarcinoma	3C	3
P33	47				X	Serous papillary adenocarcinoma	4	3
P34	85				X	Serous papillary adenocarcinoma	1A	3
P35	59				X	Serous papillary adenocarcinoma	3C	3
P36	59				X	Serous papillary adenocarcinoma	3C	3

Table 2.2 Recurrent Ovarian Specimens

Sample	Age	Transcriptome	miRNA fresh	Dicer/Drosha	miRNA FFPE	Histology	Stage	Grade
R1	68	X	**x**	x	X	Serous papillary adenocarcinoma	Recurrent	3
R2	45	X	**x**	x		Serous papillary adenocarcinoma	Recurrent	2
R3	43	X	x		X	Serous papillary adenocarcinoma	Recurrent	3
R4	47	X	**x**	x		Serous papillary adenocarcinoma	Recurrent	2
R5	59	X		x		Serous papillary adenocarcinoma	Recurrent	3
R6	43	X		**x**		Small cell carcinoma	Recurrent	3
R7	43	X	x	x		Serous papillary adenocarcinoma	Recurrent	2
R8	74	X	x	**x**		Mixed mullerian	Recurrent	3
R9	59	X		x		Serous papillary adenocarcinoma	Recurrent	3
R10	45	X	x	x		Serous papillary adenocarcinoma	Recurrent	3
R11	67	X	x	x	X	Serous papillary adenocarcinoma	Recurrent	3
R12	40	X	x	**x**	X	Clear cell adenocarcinoma	Recurrent	1
R13	53	X		**x**		Yolk Sac	Recurrent	D
R14	71			**x**		Adenocarcinoma and clear	Recurrent	2-3
R15	53				X	Serous papillary adenocarcinoma	Recurrent	1-2
R16	71				X	Clear cell adenocarcinoma	Recurrent	3
R17	66				X	Serous papillary adenocarcinoma	Recurrent	2

R18	44		x			Serous papillary adenocarcinoma	Recurrent	2
R19	62				X	Serous papillary adenocarcinoma	Recurrent	2

D: Differentiated

2.2 Fresh ovarian tissue archive

All surgically removed ovarian tissue with appropriate informed consent was considered for tissue banking. Fresh tissue was taken directly from theatre to pathology laboratory. On receipt, a pathologist was available to dissect the specimen and harvest the tissue for banking, in order to ensure no compromise of the diagnostic potential of the specimen.

A piece of normal or tumour/diseased tumour was taken in all cases when appropriate. A new scalpel blade was used for each sample. The amount of tissue harvested, depended on the size of the specimen or tumour. Tissue was transferred to sterile Eppendorf tubes and labelled with specimen number and date. Additional data sheet with all patient clinical information was completed. Tissue was immersed in liquid nitrogen for 1 min prior to their storage in a dedicated section of the freezer at -80°C.

For a minority of known tumours, tissue fragments were placed in Eppendorf tubes containing RNA later® (Ambion, Huntington, UK), a proprietary stabilizing solution used for storing RNA without degradation, to be used within 4 weeks at 2-8°C or for archival storage at -20°C or -80°C.

2.3 RNA extraction from fresh tissue

The extraction of pure, intact RNA is very important in a variety of molecular biological techniques and is also essential for gene expression analysis. The RNeasy® mini kit (Qiagen Ltd, West Sussex, UK) was used to obtain larger quantities of RNA, when required. The RNA produced is completely free of both DNA and protein.

RNeasy® Mini Kit

RNeasy Mini Spin Column
Collection tubes (1.5ml)
Collection tubes (2ml)
Buffer RLT
Buffer RW1
Buffer RPE

RNase-free water (tube and bottle)
Buffer RDD
RNase-free DNase

2.3.1 Preparing solutions

The volume needed for RLT buffer was prepared with β-mercaptoethanol in the hood (β-mercaptoethanol is toxic and an aliquot lasts for 6 weeks). 50ml falcon tube was wrapped in tin foil as the buffer is light sensitive. 10µl β-mercaptoethanol was added per 1 ml RLT buffer.

70% ethanol was made up and then filtered through 20µm membrane with syringe into a clean sterile universal.

DNAse I was prepared in stock solution before using the RNAse-free DNAse set for the first time. Solid DNAse I (1500 Kunitz units) was dissolved in 550µl of the RNAse-free water provided by securing that no DNAse I was lost when opening the vial and then mixed gently by inverting the tube. DNAse was not vortexed as it is extremely sensitive to physical denaturation. For long-term storage of DNAse I, the stock solution was removed from the glass vial, divided it into single-use aliquots and stored at -20°C for up to 9 months. Thawed aliquots can be used at 2-8°C for up to 6 weeks. Aliquots were not refreezed after thawing. DNase was prepared in RDD buffer and kept in the fridge at 4°C until needed; 10µl DNase was then added to 70µl buffer RDD.

4 volumes of 96%-100% ethanol were added to RPE to create a working solution.

Diethylene Pyrocarbonate (DEPC) water was prepared as follows:
500ml bottles were filled with distilled water and autoclaved.
500ul of DEPC was added to each 500ml bottle, incubated at room temperature for 1-2 h and reautoclaved.

Liquid Nitrogen (LN2) container was cleaned out with DEPC water, dried out in the oven and and kept in the fridge to cool before use.

Tissue was transferred directly from the freezer to the plate and cut with sterile blade to a maximum amount of 30mg. It was then immersed in LN2. The LN2 may be allowed to evaporate but the tissue should not be allowed to thaw. It was then thoroughly homogenised by grinding and the resultant powder or tiny fragments transferred directly to an RNA free Eppendorf tube.

2.3.2 Sample preparation

2.3.2.1 Preparation of fresh tissue for RNA extraction

A max of 30µg can be processed with RNeasy® mini columns. For ovarian tissue the binding capacity of the column (100µg) and the lysing capacity of buffer RLT never exceeded this amount. The tissue was not allowed to thaw during weighing or prior to disruption in buffer RLT.

Prior to extraction using the RNeasy® mini kit, fresh tissue was homogenised with a mortar and pestle as described below.

The banked frozen tissue was removed from the -80°C freezer and placed on dry ice during the extraction process

The mortar and pestle was autoclaved, treated with an RNAse inhibitor (RNA Zap®) and washed with DEPC water prior to homogenisation. DEPC inactivates ribonucleases by covalent modification. It was then placed in an ice box with tin foil and precooled with LN2.

2.3.2.2 RNeasy mini kit

Qiagen Shredder system QIA shredders® are a commercially available spin column based shearing system, used for further homogenization of tissue initially homogenised by mortar and pestle or for cultured cells as a primary form of homogenization. It allows for up to 100µg of RNA (that equals to more than 200 bases to bind to RNeasy silica membrane.

2.3.3 Protocol for on column DNA digestion

Although the RNeasy silica membrane technology efficiently removes most of the DNA without DNAse treatment, further DNA removal might be necessary for certain RNA applications that are sensitive to very small amounts of RNA (eg, TaqMan RT-PCR analysis with a low-abundant target) and cDNA micro arrays.

2.3.3.1 Overview of RNA extraction

- One shredder column (purple) and one mini-column (pink) were placed in eppendorf spare collection tubes.
- Fresh tissue was ground into the mortar with LN2 to a fine powder.
- The mortar was taken into the hood and using a new pestle, 600µl of RLT buffer was added. Grinding was continued until the powder was liquidified again (Disruption).
- Lysate was pipetted onto the purple shredder column in a 2 ml collection tube and centrifuged lysate at max speed for 5 min to homogenize (Homogenization). The supernatant was pipetted into a new 2ml collection tube and the pellet was discarded.
- 600µl (1:1) of 70% ethanol was added to the cleared lysate and mixed well by pipetting without centrifugation. (Adjusting binding conditions).
- Up to 700µl of the sample (including any precipitate) was applied to an RNeasy mini column placed in a 2ml collection tube and centrifuged for 15 sec at 10,000 rpm. Flow through was then discarded and tube was changed (washes).
- 350µl of buffer RW1 was pipetted into the RNeasy mini column and centrifuged for 15 sec at 10,000 to wash. The flow through was then discarded.
- 10µl DNase I was added to 70µl buffer RDD and the DNase incubation mix (80µl) was directly pipetted onto the RNeasy silica- gel membrane and place on the benchtop for 15 min at 20-30°C.
- 350µl of buffer RW1 was pipetted into the RNeasy mini column and centrifuge for 15sec at 10,000rpm to wash. The flow through and collection tube were then discarded.
- Using a new collection tube, 500µl RPE buffer was pipetted onto the column and centrifuged for 15 sec at 10,000rpm to wash. The flow through was discarded and collection tube was reused.

- Another 500µl RPE buffer was pipetted onto the column and centrifuged for 2 min at 10,000rpm to dry the RNeasy silica-gel membrane. The flow through and collection tube were then discarded.
- The RNeasy column was transferred to a new 2ml collection tube and centrifuged at full speed for 1 min.
- The RNeasy column was transferred to a new 1.5 ml collection tube. 30-50µl RNAse-free water was directly pipetted onto the RNeasy silica-gel membrane and centrifuged for 1 min at 10,000rpm to elute (Elution).

If the expected RNA yield was >30µg, the elution step was repeated with the same second volume of RNAse free water in the same collection tube. Column was discarded and RNA concentration was determined by measuring the absorbance at 260nm (A260) in a spectrophotometer.

Purified RNA was stored at -80°C in RNAse-free water.

2.4 Nano-Drop 1000 Spectrophotometer (ND-1000)

RNA concentration and quality was measured using the NanoDrop® (Figure 2.1). The NanoDrop® is a full spectrum (220-750nm) spectrophotometer that measures 1µl sample with high accuracy and reproducibility. It utilizes a patented sample retention technology that employs surface tension alone to hold the sample in place and eliminates the need for cuvettes and capillaries which decreases the measurement cycle time. In addition, ND-1000 is capable of measuring highly concentrated samples without dilution (50X increased concentration than the samples measured by a standard cuvette spectrophotometer).

To measure nucleic acid samples, the "nucleic acid"application module was selected and then "RNA sample" was clicked.

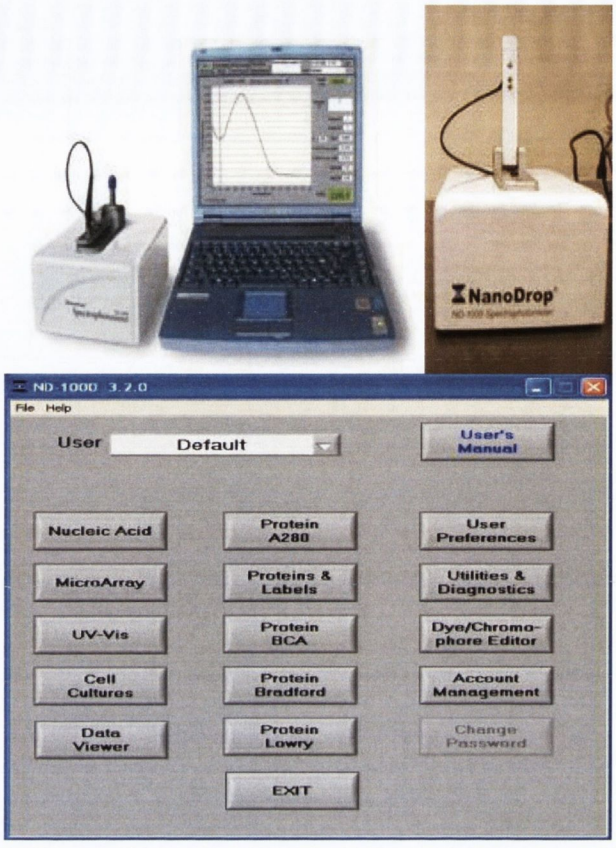

Figure 2.1 Nandrop ND-1000 Spectrophotometer and main software menu

2.4.1 Loading of samples (RNA and water blanks)

With the sampling arm open, the sample/blank was pipetted onto the lower measurement pedestal. Sampling arm was closed and measurement was initiated using the operating software on the PC. The sample arm slightly compresses the droplet and a sample column is automatically drawn (Figure 2.2). Surface tension alone holds the sample in place. The spectral measurement is then made and quantification is made based on the tightly controlled path length of 1mm.

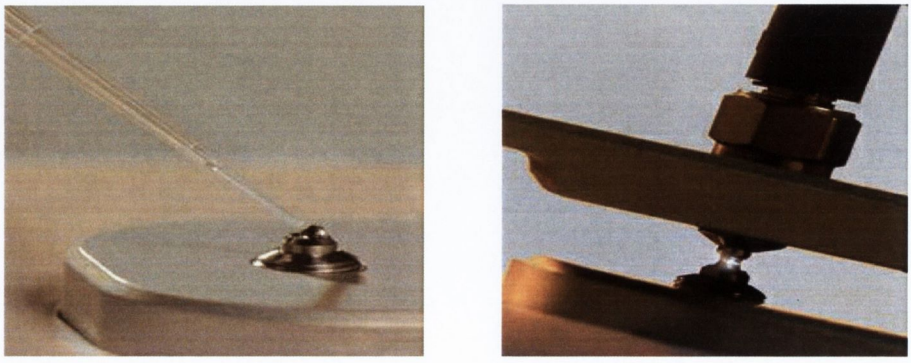

Figure 2.2 Loading of samples on Nanodrop® Spectrophotometer

When measurement was complete, the sampling arm was opened and was wiped from both the upper and lower pedestals using a soft laboratory wipe to prevent sample carryover.

2.4.2 Blank measurement

The measurement pedestal surfaces were cleaned, 1µl water sample was loaded onto the lower measurement pedestal and `OK` button was clicked. Then a message "*Initializing Spectrometer-please wait*" appeared. When this message disappears, the instrument will be ready for use.

Before making a sample measurement, a blank must be measured and stored. After making an initial blank measurement, a straight line will appear on the screen; subsequent blanks will clear any sample spectrum.

A blank sample was loaded and the `Blank` button was clicked.

The blanking buffer was wiped from both pedestals using a laboratory wipe.

An aliquot of the blanking solution was analysed as if it were a sample by using the `Measure` button. The result should be a spectrum with a flat baseline. Sample measurement was initiated after wiping the blank from both measurement pedestal surfaces.

2.4.3 Sample measurement

Following blank measurement, the sample was loaded exactly as described above in 2.5.2. 1µl samples were loaded to ensure accurate results when measuring aqueous RNA samples.

2.4.4 Interpretation of the results

A260/280 Ratio of sample absorbance at 260 and 280 nm. The ratio of absorbance at 260 and 280nm provides an estimate of the purity of RNA with respect to contaminants that absorb in the UV spectrum. A ratio of ~2.0 is generally accepted as "pure" for RNA. If the ratio is appreciably lower in either case, it may indicate the presence of protein, phenol or other contaminants that absorb strongly at or near 280 nm. The A260/280 ratio is considerably influenced by pH; lower pH results in a lower ratio and reduced sensitivity to protein contamination.

A260/230 Ratio of sample absorbance at 260 and 230 nm. This is a secondary measure of nucleic acid purity, being usually higher than the respective 260/280 values for "pure" nucleic acids. It is usually in a range of 1.8-2.2; if lower, it may indicate co-purified contamination.

Concentration (ng/µl) Sample concentration in ng/µl based on absorbance at 260nm minus the absorbance at 340 nm (i.e. normalized at 340 nm) and the selected analysis constant.

2.5 Microarrays

The development of microarray technology has been phenomenal in the past few years; it has revolutionized the approach to biological research. Instead of working on a gene-by-gene basis, scientists can now study tens of thousands of genes at once. The Applied Biosystems (AB) Expression Array System, integrated with AB Sequence Detection System (SDS)-based products for gene expression analysis and the Celera Discovery System online platform, is based on a microarray that represents the whole human genome (Figure 2.3).

Figure 2.3 The AB 1700 cDNA Array system and microarrays. Micro arrays are sealed in a pre-assembled cartridge and contain oligonucleotides that target transcripts in each gene of the human genome.

The AB Expression Array System is based on highly sensitive, chemiluminescent technology for gene expression detection and incorporates DNA probes that are each approximately 60 base pairs long. Chemiluminescent detection uses an enzymatic initiated chemical reaction to generate light without the need for a laser. The

combination of chemiluminescence and long oligonucleotides provides higher sensitivity and specificity compared with other commercially available microarray products that incorporate shorter oligonucleotide lengths or use fluorescence detection methods. The long oligonucleotides enable tighter binding to the target, which leads to the detection of more genes with greater selectivity and specificity. All probes, prior to microarray manufacture undergo analysis by mass spectrometry for quality control. As a result, customers should be able to detect more genes using less biological sample, which should be a significant advantage for researchers working with small, difficult-to-obtain or expensive samples, such as samples often required for cancer research.

In oligonucleotide arrays, the probes are short sequences (small DNA fragments) designed to match part of the sequence of known or predicted open reading frames. Oligonucleotide arrays are produced by printing short oligonucleotide sequences designed to represent a single gene or family of gene splice-variants by synthesizing this sequence directly onto the array surface.

The Applied Biosystems Expression Array System includes, on a single microarray, probes to detect an annotated and fully curated set of more than 30,000 human genes. In particular, these "oligonucleotide" arrays contain 32,878 oligonucleotide probes (60 base pairs long) and target a complete annotated and fully curated set of 29,098 human genes from the public and Celera databases Applied Biosystems employed its sophisticated bioinformatics pipeline to design oligonucleotide probes (synthetic DNA) based on these well-defined genes for use on the microarray.

In addition to the microarray, the system comprises the 1700 Chemiluminescent Microarray Analyzer, software, and reagents. The Analyzer can image arrays in chemiluminescence and then measure the gene expression even at very low levels and in fluorescence to locate auto-grid features. The 1700 is also equipped with a high resolution, large format CCD camera, back illuminated that has very low read noise. This feature, coupled with low background noise from chemiluminescence is responsible for the very high sensitivity. To facilitate analysis of results, the system is supplied with an industry standard database, continuously updated that includes gene acronyms, gene names, cross references for gene identification, gene ontologies and protein characterization data from the Panther™ Protein Classification System.

2.5.1 Digoxigenin (DIG) Labeling Kits

Excellent results can be achieved from as little as 500ng of starting total RNA by using the AB Chemiluminescent reverse transcription-in vitro transcription (RT-IVT) Labelling Kit. The chemistry of the RT-IVT kit, based on a linear amplification procedure, increases the yield of cRNA from cDNA by >1,000 fold. A genetically modified Reverse Transcriptase with no RNase H activity incorporates deoxynucleotides and digoxigenin-dUTP (DIG-dUTP) in the synthesis of single-stranded cDNA from sample RNA and RT Labelling Control RNA (Figure 2.4). Multiple transcription rounds result in the production of DIG-labelled cRNA, which can then specifically hybridize to the AB microarray.

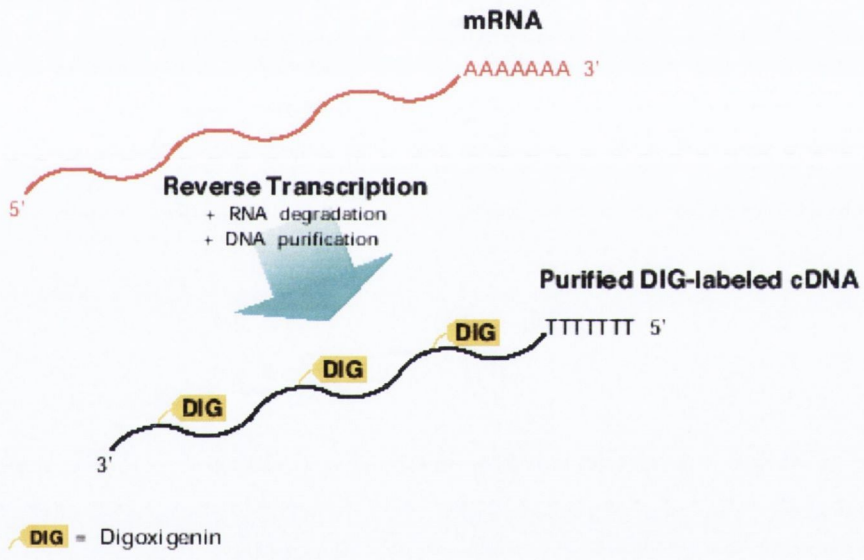

Figure 2.4 RT-IVT DIG-labelling of sample mRNA. The RT labeling process begins with reverse transcription of poly(A) mRNA, a component of total RNA, using an oligo (dT) primer. Transcription of the mRNA into cDNA incorporates a nucleotide modified with DIG-dUTP. Extraneous mRNA is then removed from the mixture. After purification, the DIG-labeled cDNA is ready for hybridization to Applied Biosystems microarrays.

2.5.2 Chemiluminescence Detection kit

When unbound materials have been washed from the microarray, The AB Chemiluminescent Detection kit is used to visualize features that have digoxigenin-labelled cDNA or cRNA bound to the oligonucleotide probes by incubating the microarray with an anti-digoxigenin alkaline phosphatase conjugate. Alkaline phosphatase hydrolyses the chemiluminescent substrate and emits light at a wavelength of ~458nm. The signal intensity is proportional to the mRNA level expressed in the cells (Figure 2.5).

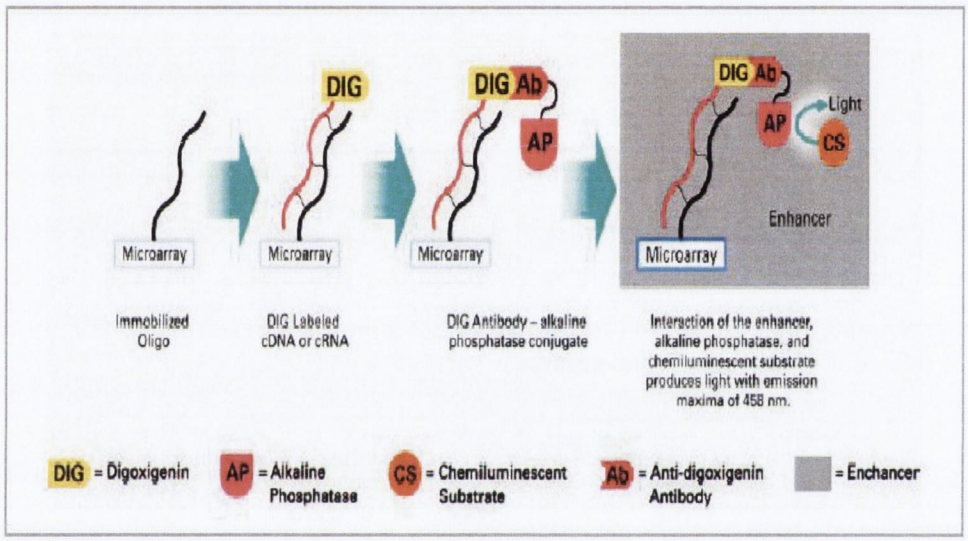

Figure 2.5 Chemiluminescent detection of bound DIG-labelled cRNA. The addition of substrate and a chemiluminescence enhancer initiates the chemiluminescent reaction. The presence of enhancer further strengthens the chemiluminescent signal.

During microarray manufacture, in addition to the unique probe (60-mer), an internal control probe (a 24-mer oligo) is co-spotted on the microarray. At the hybridization step, this complementary oligo is included with the hybridization mixture. It is referred to as an internal control target that is pre-labeled with a fluorescent dye (LIZ® dye). The fluorescent signal, which has a close spatial correlation with the chemiluminescent signal, locates all features on the microarray, even in the absence of gene expression signal products (chemiluminescent signal) (Figure 2.6). As a result, the internal control probes monitor microarray manufacturing quality, providing normalization of feature-to-feature and array-to-array variations. Also,

spot-finding and autogridding of the array is enabled by fluorescent internal-control probes.

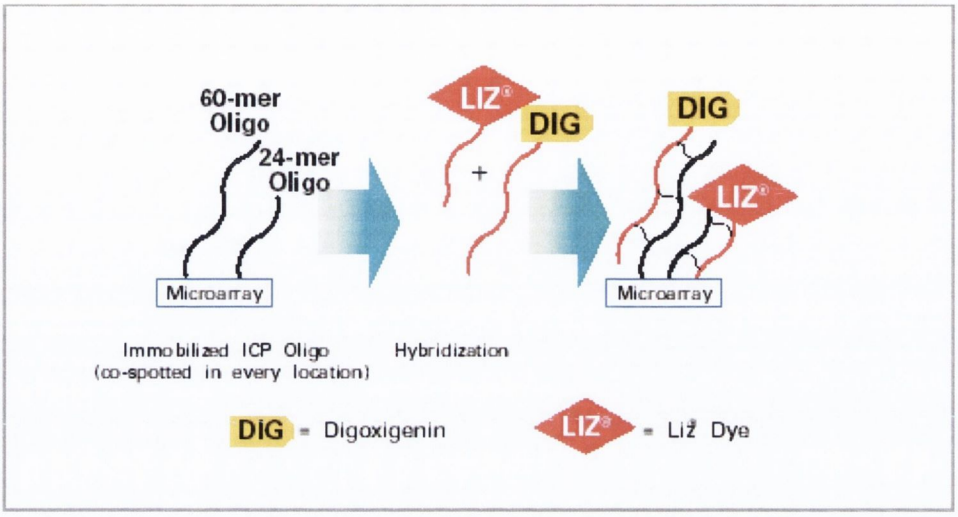

Figure 2.6 Fluorescence used to image microarray features

2.5.3 Multiple Microarray Images

The AB Chemiluminescent Analyzer incorporates a CCD camera capable of detecting chemiluminescent and fluorescent signals when the microarray is moved into the optical path of the analyzer. When the microarray is loaded into the 1700 analyzer, the temperature is raised to 35°C in order for the enzymatic reaction to reach a steady state. Multiple images are then taken in both short (5 seconds) and long (25 seconds) read times to bring the microarray into focus and to measure, in turn, the fluorescent and chemiluminescent signals. The total time required to image a microarray, including the pre-incubation and focus steps, is approximately 12 minutes. Light production on the microarray reaches a steady state within the first five minutes, while the microarray is being focused and brought up to 35°C. The chemiluminescent reaction emits light at a steady state for at least 60 minutes thereafter. System software can then relate the resultant intensities to gene expression, accurate feature registration and data quality control.

Hybridization conditions, such as sample mixing and washing stringency are monitored by use of chemiluminescent and fluorescent fiducials to ensure signal uniformity. Labeling kit controls are also included with both the AB Chemiluminescent RT Labeling Kit and the RT-IVT Labeling Kit. These are

synthetic bacterial control genes (*Dap, Lys, Phe, BioB, BioC,* and *BioD*) that provide quality information on RT and RT-IVT Kit enzyme activity and DIG-label incorporation efficiency for each experiment. Labelled oligonucleotides are also included with hybridisation controls in the AB Chemiluminescent Detection Kit, being complementary to those deposited on the microarray during manufacture.

2.5.4 Microarray Data Management

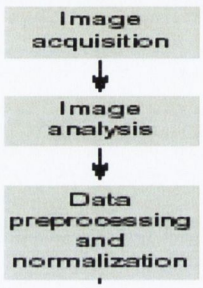

Figure 2.7 Steps in the management of Microarray Data

Image analysis

Following image acquisition, computational image analysis involves inspection of the gridding result and application of an appropriate segmentation-differentiation of the pixels within a spot-containing region into foreground (true signal) and background-algorithm and all quality measures to aid decision of spot quality. Substracting the averaged background pixel intensities from the averaged pixel foreground intensities, gives the average spot intensity.

Data preprocessing and normalization

The data extracted from image analysis need to be pre-processed to exclude poor-quality spots and normalized to remove as any systematic errors as possible before downstream analysis. In this respect, noise, which is of no biological significance and can arise from sample preparation, labelling, hybridization or scanning must be minimised to ensure the accuracy of downstream data analyses. Various forms of global normalization have been applied to micro arrays in recent studies, most commonly Median, Quantile and Trimmed Mean. We applied the quantile method to our microarray study, in order to make the distribution of each array in our set of

arrays the same. This method implies that each array can be given the same distribution by taking the mean quantile and substituting it as the value of the data item in the original set. Spots with intensity lower than the background plus at least 2 SD are excluded. Intensity ratios are also log-transformed so that up or down regulated values are of the same scale and comparable.

The 1700 Gene Expression Microarray System uses an Oracle® object relational database to manage the multitude of data content types and values that are associated with each of the millions of experimental data points produced over the course of a microarray gene expression project. This third-party software covers all main analysis steps through the experimental set-up and management, microarray imaging, algorithm data management, primary analysis, and final output of the microarray data to secondary analysis (Figure 2.8).

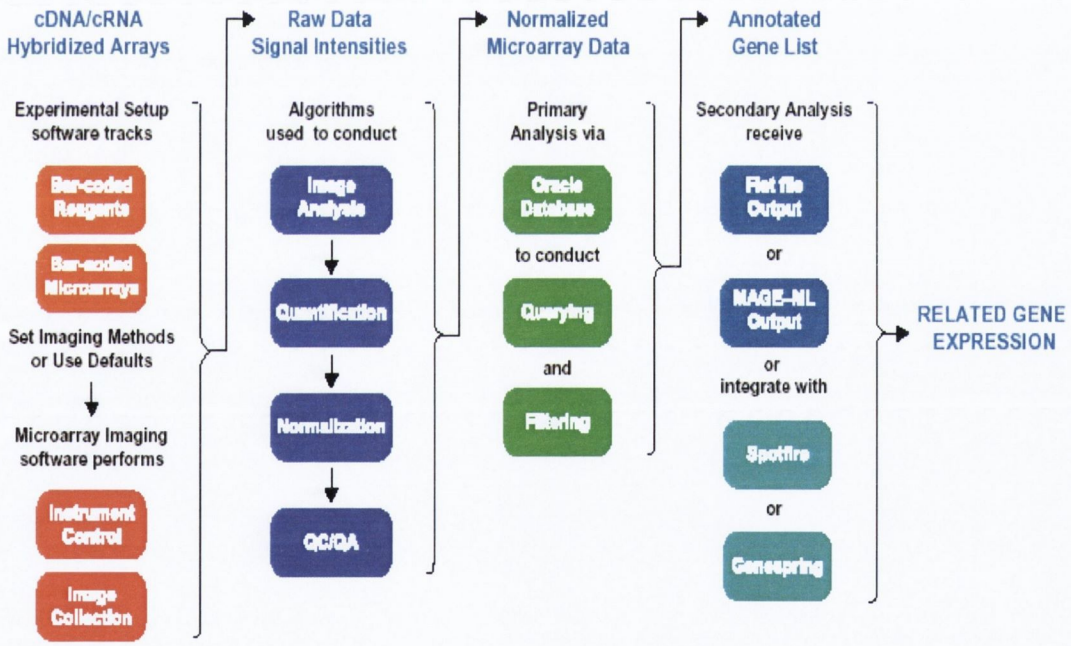

Figure 2.8 Software workflow; from experimental set-up to secondary analysis.

A flowchart of our microarray experiment is illustrated in figure 2.9.

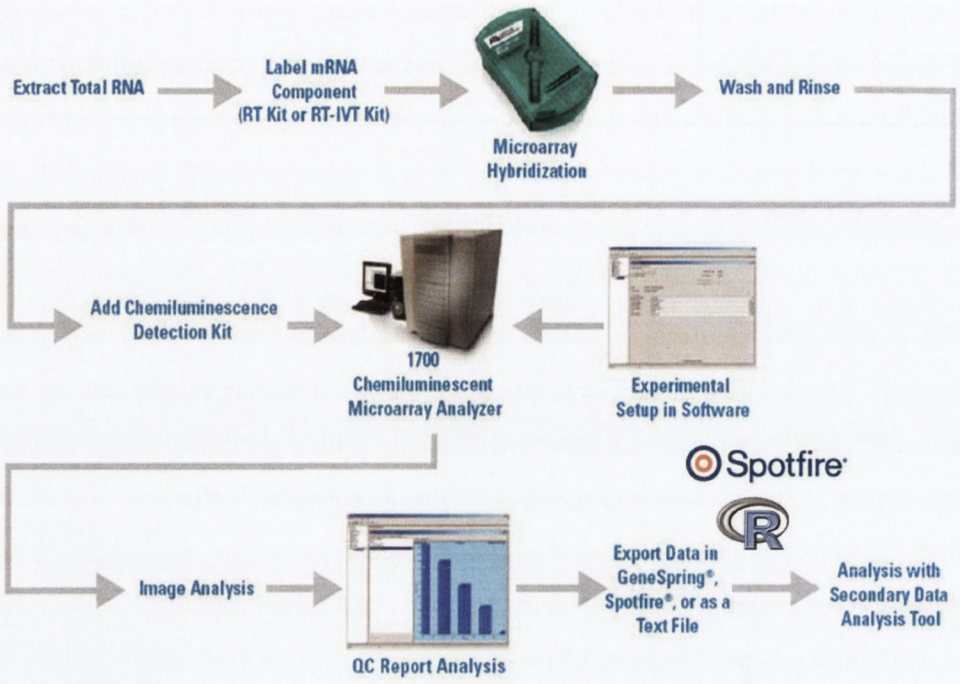

Figure 2.9 Flowchart of our microarray experiment: Gene expression analysis was performed using the chemiluminescence based Applied Biosystems 1700 array system. Bioinformatics was performed using Spotfire and R.

2.6 RT-IVT labeling

2.6.1 RT labeling

Performing Reverse Transcription and second strand synthesis

Sample and reagents were thawed on ice: 9µl of RNA sample (made up by mixing 2µg total RNA and nuclease free water), 4µl Control RNA and 2µl T7-Oligo (dT) primer (for a total volume of 15µl per tube. They were mixed by vortexing and then tubes were briefly centrifuged.

The RNA and primer mixture was heated and cooled in a thermal cycler (70°C for 5min, 4°C hold). After the run, the tube was placed on ice.

The following components were added to the reaction tube on ice and mixed thoroughly by pipetting: 2µl 10X 1st Strand Buffer Mix and 3µl RT Enzyme Mix.

RT (1st strand cDNA synthesis) was performed in a thermal cycler: 25°C for 10min, 42°C for 2h, 70°C for 15min and 4°C hold. After the run, the tube was placed on ice

and the following components were added to the cDNA mixture: 30µl 5X 2nd Strand Buffer Mix, 5µl Strand Enzyme Mix and 95µl nuclease-free water (for a total volume 150µl, including 20µl of the cDNA mixture).

Second strand synthesis was performed in a thermal cycler: 16°C for 2h, 70°C for 15min and 4°C hold.

Purifying cDNA

In a 1.5ml nuclease-free microcentrifuge tube, the following reagents were combined: 150µl DNA Binding Buffer and 150µl 2nd strand synthesis reaction mix.

A nano DNA purification column was inserted into a 2.0-ml receptacle tube. The reaction-DNA Binding Buffer mixture (300µl) was transferred to the column and centrifuged at 10,000rpm for 1h.

The column was removed from the tube, the liquid was discarded and the column was reinserted into the tube.

300µl of DNA Wash Buffer was added to the column and centrifuged at 10,000rpm for 1min.

The column was removed from the tube, the liquid was discarded and the column was then reinserted into the tube.

300µl of DNA Wash Buffer was added to the column and centrifuged at 10,000rpm for 1 min.

The column was then removed from the tube, the liquid was discarded and then the column was reinserted into the tube.

The column and tube were centrifuged at 13,000rpm for 1min.

The column was transferred to a new 1.5-ml elution tube.

30µl of DNA Elution Buffer was pipetted onto the fiber matrix at the bottom of the column and incubated the column at room temperature for 1 min.

The column and tube were centrifuged at 13,000rpm for 1min for an elution volume of 10µl.

Elution step was repeated twice for a final elution volume of 20µl and the column was discarded.

2.6.2 IVT labeling

The volume of cDNA output required was calculated based on the amount of RNA input:

Amount of RNA input	Volume of cDNA output required
≤2μg	24μl (volume of cDNA+ nuclease free water)

The following IVT components were added to the 24μl cDNA output at RT: 8μl 5X IVT Buffer Mix, 4μl DIG-UTP and 4μl IVT Enzyme Mix, for a total of 40μl.

IVT was performed in the thermal cycler: 37°C for 9h followed by a 4°C hold. After the run the tubes were placed on ice.

Purifying cDNA

In a new 1.5ml nuclease-free microcentrifuge tube, the following components were combined and then vortexed briefly to mix: 20μl nuclease-free water and 40μl IVT reaction.

200μl RNA Binding Buffer and 140μl 100% ethanol were added and mixed by pipetting.

An RNA purification column was inserted into a 2ml receptacle tube.The IVT reaction-RNA and Binding Buffer-ethanol mixture (400μl) was added to the column and centrifuged at 10,000rpm for 1min.

The column was removed from the tube, the flow through was discarded and the column was then reinserted into the tube.

500μl of RNA Wash Buffer was added to the column and centrifuged at 10,000rpm for 1min. The flow through was then discarded.

500μl of RNA Wash Buffer was added to the column and centrifuged at 10,000rpm for 1min. The flow through was then discarded.

The column and tube were then centrifuged at 13,000 x g for 1 minute.

Eluting the cRNA

The column was transferred to a new 1.5 ml elution tube. 50μl of RNA Elution Buffer was pipetted onto the fiber matrix at the bottom of the column.

The column was incubated at room temperature for 1 minute.

The column and tube were centrifuged at 10,000rpm for 1 minute for an elution volume of 50μl.

50μl of cRNA Elution Buffer was pipetted onto the fiber matrix at the bottom of the column and incubated at room temperature for 2min.

The column and tube were centrifuged at 10,000rpm for 1min for a final elution volume of 100µl.

Labeled cRNA was stored on ice and quantity was assessed using UV spectroscopy. cRNA can be stored at -20°C for up to months or -80°C for long term storage.

2.6.3 Chemiluminescence detection

Before starting, the hybridization oven was powered on and the temperature was set to 55°C, as it takes up to 3h to equilibrate to this temperature.

Pre-hybridization

Once the oven temperature was verified at 55°C, microarrays were equilibrated to room temerature.

Pre-hybridization mixture was prepared in a nuclease-free tube and vortexed to mix: 150µl nuclease-free water, 330µl Hybridization Buffer, 100µl Hybridization Denaturant and 420µl Blocking Reagent.

It was then transferred (1ml) into each microarray cartridge: after removing the foil wrapping from a cartridge it was pipetted into the port with tip at a 90° angle. The port surface was dried with lint-free tissue and the port was sealed with the plug. The plug was turned 90° to secure it. The arrays were tilted several times to wet evenly.

All cartridges were rocked in a vertical orientation on the rocking platform shaker for 5 min.

All cartridges were incubated in a 55°C oven at 100 rpm for 1h.

Fragmenting cRNA

The following components were combined in a 0.2 ml Microamp® reaction tube on ice and mixed by pipetting: 10µl cRNA Fragmentation Buffer and 90µl of DIG-labelled cRNA and nuclease-free water. Reagents were allowed to equilibrate at room temperature for 1h before use.

The tubes were heated in a thermal cycler at 60°C for 30 min.

50µl of cRNA Fragmentation Stop Buffer was added, mixed by pipetting and placed on ice.

Hybridization

For each microarray:

A hybridization mixture in a nuclease-free microcentrifuge tube was prepared: 100µl nuclease free water, 170µl Hybridization Buffer, 30µl Hybridization controls, 50µl Hybridization Denaturant and 150µl fragmented cRNA targets.

The hybridization mixture was vortexed and centrifuged briefly.

The hybridization mixture was quickly transferred into each microarray cartridge, drying the port with lint-free tissue prior to sealing.

The cartridge was returned to the oven and incubated at 55°C at 100 rpm for 16h.

Hybridization washes

600µl hybridization wash buffer 1 was added to a clean wash tray.

Microarrays were removed from their cartridges; liquid was decanted and submerged in wash buffer. They were then agitated on the rocking platform shaker for 5min (tilt angle 10°C, tilt speed 30 tilts back and forth per min)

600µl hybridization wash buffer 2 was added to a clean wash tray. Microarrays were transferred to a new tray, draining them in the process. It was then agitated on the rocking platform shaker for 5 min.

The buffer was discarded from the wash tray.

400µl chemiluminescence rinse (CL) rinse buffer was added to the wash tray ensuring that all microarrays were submerged in buffer.

It was then agitated on the rocking platform shaker for 5 min.

The wash tray was removed from the rocking platform shaker. Microarrays may be left in CL rinse buffer at room temperature for up to 1h.

Antibody binding

The following components were combined for the CL blocking buffer/antibody mixture in a nuclease free tube and mixed by inversion without vortexing: 2.8ml nuclease free water, 200µl Chemiluminescence Rinse Buffer Concentrate, 1ml Blocking Reagent and 15µl Anti-Digoxigenin-AP.

Each microarray was removed from the wash tray, gently shaken and tapped, then placed vertically on the rocking platform shaker.

4µl CL blocking blocking buffer/ antibody mixture was immediately to the microarray.

The arrays were covered with the wash tray cover and agitated on the rocking platform shaker for 20 min at room temperature.

Antibody washes

500µl CL Rinse Buffer was added to a clean wash tray.

CL blocking buffer/ antibody mixture was decanted, the microarray was shaken and tapped gently and then placed in the wash tray.

The wash tray was covered and agitated on the rocking platform shaker for 10 min.

The buffer was drained from the wash tray.

500µl CL Rinse Buffer was added to the wash tray and agitated on the rocking platform shaker for 10 min.

The buffer was then discarded from the wash tray.

500µl CL Rinse Buffer was added to the wash tray and agitated to the rocking platform shaker for 10 min.

The wash trays were removed from the rocking platform shaker. Microarrays may be left in the CL Rinse Buffer at room temperature for up to 3h.

Chemiluminescent reaction

This step needs to be performed quickly as it is time-dependent. Only one microarray was used at a time:

100µl CL Enhancing Rinse Buffer was placed in a 4X5 inch tray.

One microarray was removed from the wash tray, CL Rinse Buffer was decanted, then gently shaked and tapped, then placed in the CL Enhancing Rinse Buffer.

It was then agitated on the rocking platform shaker for 10 min.

The microarray was removed from the small tray, decant CL Enhancing Rinse Buffer was decanted, the microarray was gently shaken and tapped, then placed vertically on the rocking platform shaker.

4µl of Chemiluminescence Enhancing Solution was quickly added to the microarray and agitated on the rocking platform shaker for 20 min.

100µl CL Enhancing Rinse Buffer was added in a second small tray.

The Enhancing solution was decanted from the microarray.

The microarray was gently shaken and tapped, then placed in the second small tray and agitated on the rocking platform shaker for 5 min.

The microarray was removed from the small tray, the CL Enhancing Rinse Buffer was decanted, the microarray was then gently shaken and tapped.

The bottom of the microarray was wiped with lint-free tissue and 3.5 µl of Chemiluminescence Substrate was added to it.

We then proceeded immediately with performing CL detection on the AB 1700 Chemiluminescent Analyser.

2.6.4 Starting cDNA micro arrays

After entering username and password, the 1700 gene expression window was clicked, a new username and password was entered and then:> AB Navigator >Expression Array System Software and New Microarray was double clicked.

The following information was entered for each array:

Barcode/ID (*ie,HB00056)*

Lot number

Microarray type*: human*

Security group: *AB*

Chemistry method: *RT-IVT*

Sample name (*ie, primary vs recurrent*)

2.6.4.1 Reading the 1700 Microarray Data

The Analyzer was powered on at least 10min before getting started with reading data. The Expression Array System Software was activated as per above >AB1700 >Data Collection and OK clicked when temperature was set to 35°C and camera temperature to -49°C.

Bar code was entered as per above (ie, HB00056) and tab was pressed; all details appeared on the screen including the cartridges settings and then start button was clicked.

2.6.4.2 R script Analysis

A dataset was created in AB1700 and all the arrays analysis data were added. Clicking on filter gene features allowed the transfer of necessary data. Data were exported as ASCII Wide format. The following features were needed: Probe ID, Gene ID, Signal, S/N and flags.

The columns read across the top in the order mentioned above with signal, s/n and flags for each sample. The new file was saved in a new folder as a text tab delimited file (working file).

A design file was created and placed in the same folder so that only the two files were in this folder.

A design file has 3 columns, sample name, assay name and group; sample name must be the same as what is in the working file and assay name can also be the same e.g if working file says Signal_untreated then the sample name in the design file is untreated. (it is very important to be named exactly as in the working file).

The sample names were put in the same order as the working file.

The group column allows you to specify what you want to compare e.g primary vs recurrent etc, so each sample was labelled as primary or recurrent. The design file was saved as a text tab delimited file.

After opening R:

The folder was selected, specified where to go to file and directory was changed.

The following commands were entered:

library(Biobase) return

library(1700) return

eset<-1700("workingfile.txt","design.txt","group")return e.g.

eset<-1700("ovary.txt","designovary.txt","group") no spaces

This order puts the results in the same folder.

2.7 Ingenuity® Pathway Analysis (IPA)

Ingenuity® Pathways Analysis (IPA) was additional used to quickly analyze our expermental data. Using Ingenuity's® extensive library of well-characterized signaling and metabolic pathways as a starting point, we attempted to build our own dynamic pathway model or key interactive pathways representing the key genes identified in our work. The IPA explores beyond the constraints of "canonical" pathways with a range of interactive tools for modeling upstream and downstream relationships among identified genes, thus bridging novel discovery and known biology. In this respect, it was also used to validate our experimental assumptions.

2.8 MicroRNA Expression Analysis using Real-Time PCR (RT-PCR)

Several methods have been used to study miRNA expression levels: microarray analysis, real-time PCR, Northern blots, in situ hybridization (ISH), etc. Of those, RT-PCR is the most sensitive and accurate method (Figure 2.10).

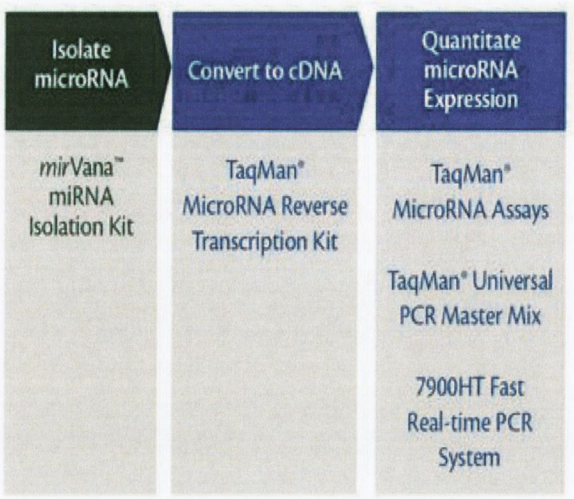

Figure 2.10 miRNA experimental overview

2.8.1 miRNA extraction from fresh tissues

Isolation of miRNA begins when total RNA that includes the small RNA fraction is isolated from the samples of interest. RNA was extracted from fresh tissues using the Ambion mirVana™ miRNA isolation kit (Ambion, Austin, TX) (Figure 2.11). The kit uses a fast and efficient glass fiber filter based procedure to isolate total RNA ranging in size from kilobases down to 10-mers. It also includes a procedure to enrich the population of RNAs that are 200 bases and smaller, which enhances the sensitivity of small RNA detection by solution hybridization and Northern blot analysis.

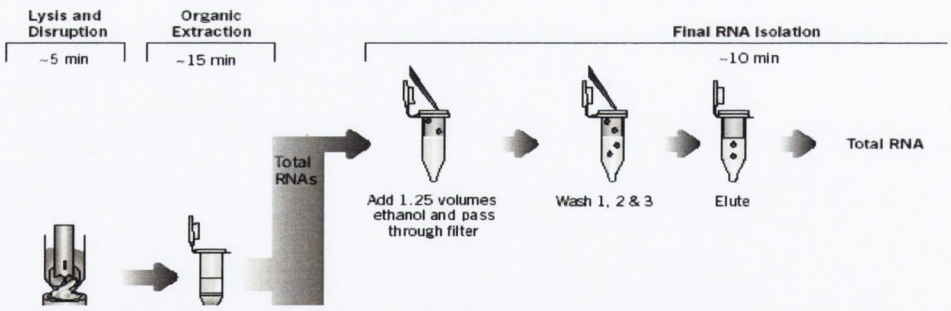

Figure 2.11 Overview of the mirVana™ miRNA Isolation Kit Procedure. The first step involves disruption of the sample in a denaturing lysis buffer. Next, the sample is subjected to Acid-Phenol:Chloroform extraction which removes most of the other cellular components, leaving a semi-pure RNA sample.Different protocols are then used for final RNA purification. To isolate RNA for miRNA expression profiling, the procedure for total RNA isolation was followed.

2.8.2 Overview of the mirVana™ miRNA Isolation Kit Procedure

The Wash solutions were prepared first by adding and mixing 21ml of 100% ethanol to the bottle labeled miRNA Wash Solution 1 and 40ml of 100% ethanol to the bottle labeled Wash Solution 2/3.

Fresh sample removed from the -80°C freezer was prepared as described in section 2.3.2.1, starting with 30mg tissue, then processed immediately and ground to powder using a mortar and pestle.

Sample disruption

300µl Lysis/Binding Solution (10 volumes per tissue mass) was added. Tissue cells lysed immediately upon exposure. The mixture was then transferred to a tube and vortexed to completely lyse the cells and to obtain a homogenous lysate.

Organic extraction

30µl of miRNA Homogenate Additive (1:10 volume) was added to the tissue lysate and mixed well by inverting the tube several times. The mixture was left on ice for 10min.

300µl of Acid-Phenol: Chloroform (1:1 volume) was added and vortexed for 30-60 sec to mix, followed by centrifugation for 5 min at maximum speed at room temperature to separate the aqueous and organic phases. The interphase was ensured to be compact or else the centrifugation was repeated. The aqueous (upper) phase was then removed, the volume was noted and transferred to a fresh tube.

Total RNA isolation procedure

375µl of RT 100% ethanol was added to the aqueous phase (1.25 volumes).

A Filter Cartridge was placed into the collection tube and up to 700µl of the lysate/ethanol mixture was pipetted onto it. If the sample was larger, the mixture was applied in successive applications to the same filter.

The mixture was centrifuged for 15 sec at 10,000 rpm to pass the mixture through the filter. The flow through was discarded and centrifugation was repeated until the whole mixture is through the filter. The collection tube was reused for the subsequent washing steps.

700µl Wash Solution 1 was applied to the Filter Cartridge and centrifuged for 10 sec, the flow through was then discarded from the collection tube and the Filter Cartridge was replaced into the same collection tube.

500µl Wash Solution 2/3 was applied through the Filter Cartridge as per previous step.

The above step was repeated with a second 500µl aliquot of Wash Solution 2/3.

The flow through was discarded and the asssembly was spun for 1 min to remove residual fluid.

The Filter Cartridge was transferred to a fresh collection tube and 100µl of pre-heated (95°C) nuclease-free water was applied to the center of the filter, followed by spinning for 30 sec at maximum speed to recover the RNA. The eluate was collected and stored it at -20°C or below.

2.8.3 miRNA extraction from formalin fixed paraffin embedded (FFPE) tissues

This was performed using the Recoverall™ Total Nucleic Acid (NA) Isolation Kit (Ambion, Austin, TX). The kit is designed to extract NA, including miRNAs from archived FFPE tissue. Up to 20µm sections or up to 35 mg of unsectioned core samples can be processed per reaction. Although degree of the RNA fragmentation in FFPE tissues cannot be reversed, the protein digestion conditions of the Recoverall™ kit are designed to release a maximum amount of RNA fragments of all sizes, including miRNA, in a relatively short amount of time. The recovered miRNAs are then suitable for downstream applications such as microarray analyses, qRT-PCR and mutation screening.

2.8.3.1 Overview of miRNA isolation using the Recoverall™ Total Nucleic acid Isolation Kit (Figure 2.12)

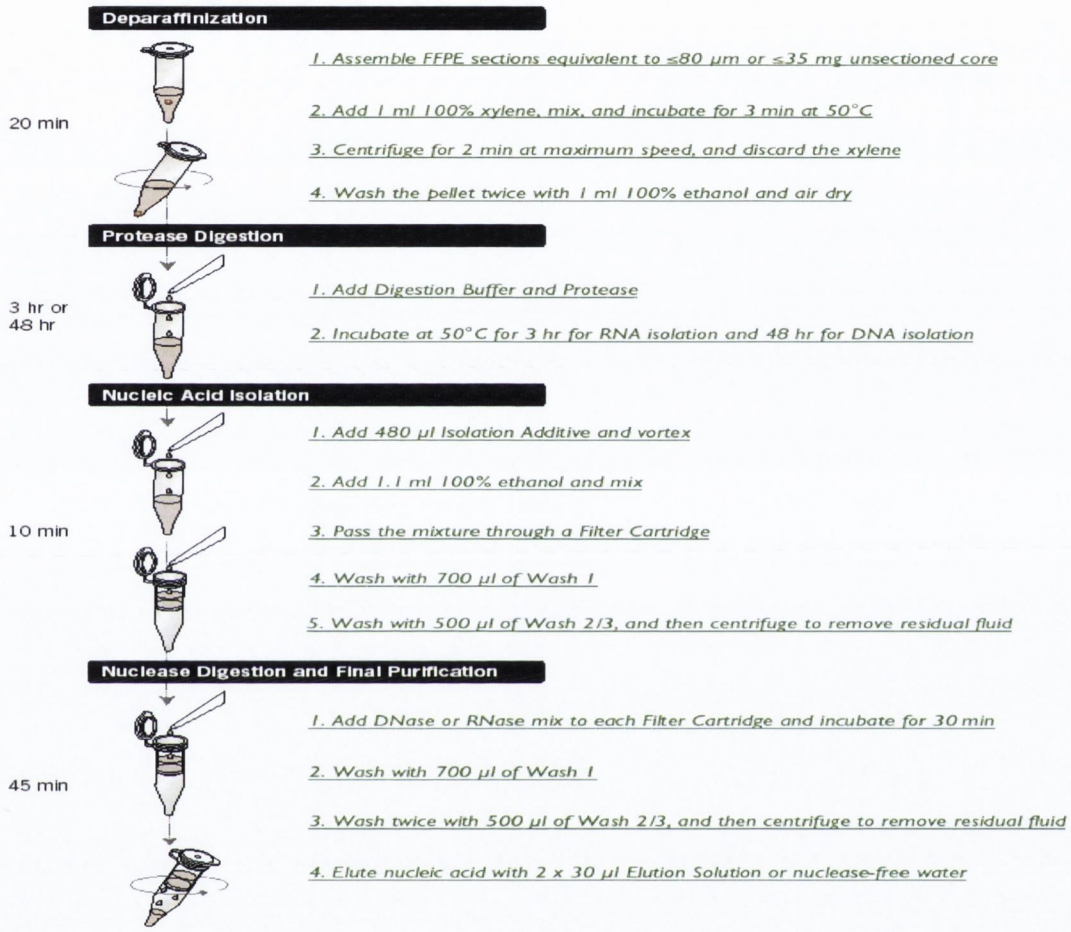

Figure 2.12 Overview of the Recoverall™ Total Nucleic Acid Isolation procedure

20µm sections from FFPE tissue blocks (4slices) were cut using a microtome.

Deparrafinization

1 ml of 100% xylene was added to the sample, removing the paraffin from the sections.

The sample was vortexed briefly to mix and then heated at 50°C for 3 min to melt the paraffin.

The sample was centrifuged for 4 min at room temperature and maximum speed to ensure a tight pellet.

The xylene was then removed and discarded without disturbing the pellet.

1ml of 100% ethanol was added to the sample and vortexed to mixing and removing xylene from the sample and accelerating drying of the tissue. The sample was then centrifuged for 2 min at room temperature and maximum speed to pellet the tissue.

The above wash was repeated for a second time with 1ml of 100% ethanol and briefly centrifuged to remove any residual ethanol in the bottom of the tube without disturbing the pellet which was then dried for 15 min.

Protease digestion

400µl Digestion Buffer and 4µl of protease were added to each sample and the tube was swirled gently to immerse the tissue.

The sample was incubated in a heat block for 3h at 50°C.

RNA isolation

480µl Isolation Additive was added to each sample and vortexed to mix. The solution usually appears cloudy white and cloudy after mixing.

1.1ml of 100% ethanol was added to each sample by pipetting two aliquots of 550µl to accommodate adjustable pipettors. Each sample was mixed by pipetting up and down to make the solution clear.

A filter cartridge was placed in one of the collection tubes supplied and 700µl of the sample/ethanol mixture was pipetted onto it.

The mixture was centrifuged at 10,000rpm for 60 sec to pass the filter, the flow through was then discarded and the filter cartridge was reinserted to the same collection tube. The above step(s) were repeated until all the sample mixture passed through the filter.

700µl of Wash 1 was added to the filter cartridge, followed by centrifugation for 30 sec at 10,000rpm to pass the mixture through the filter. The flow through was then discarded and the filter cartridge was reinserted to the same collection tube.

500µl of Wash 2/3 was added to the filter cartridge, followed by centrifugation for 30 sec at 10,000rpm to pass the mixture through the filter. The flow through was then discarded and the filter cartridge was reinserted to the same collection tube.

The assembly was spun for an additional 30 sec to remove residual fluid from the filter.

Nuclease Digestion and final nucleic acid purification

The following solutions were combined to make the DNA mix (or a mastermix in case of one or more samples):

Amount (per reaction)	Component
6 µl	10X DNase Buffer
4 µl	DNase
50 µl	Nuclease-free Water

60µl of the DNase mix was added to the center of the filter cartridge and the tube was incubated for 30 min at room temperature.

700µl of Wash 1 was added to the filter cartridge and incubated for 30-60 sec at room temperature, followed by centrifugation for 30 sec at 10,000rpm. The flow through was then discarded and the filter cartridge was reinserted to the collection tube.

500µl of Wash 2/3 was added to the filter cartridge and centrifuged for 30 sec at 10,000rpm. The flow through was then discarded and the filter cartridge was reinserted to the collection tube.

The above step was repeated to wash a second time with 500µl of Wash 2/3. The assembly was centrifuged for 1 min at 10,000rpm to remove residual fluid from the filter.

The filter cartridge was transferred to a fresh collection tube. 30µl of elution solution, pre-heated in a water bath to 95°C, was applied to the center of the filter. The sample was allowed to sit at room temperature for 1 min and then centrifuged for 1 min at maximum speed to pass the mixture through the filter.

The above step was repeated with a second 30µl aliquot of eluant, using the same collection tube. The volume of the collected eluate was determined. The eluate was stored at -20°C.

2.8.4 TaqMan® PCR

The advent of PCR by Kary B. Mullis in the mid-1980s revolutionized molecular biology as we know it. PCR is a fairly standard procedure now, and its use is extremely wide-ranging. At its most basic application, PCR can amplify a small amount of template DNA (or RNA) into large quantities in a few hours.

TaqMan® PCR exploits the 5' nuclease activity of *Taq* DNA polymerase (of the species *Thermus aquaticus*, a thermophile whose polymerase is able to withstand extremely high temperatures to cleave a TaqMan probe during a PCR. The temperature is then alternated between hot and cold to denature and reanneal the DNA, with the polymerase adding new complementary strands each time. In addition to the basic use of PCR, specially designed primers can be made to ligate two different pieces of DNA together or add a restriction site, in addition to many other creative uses.

How TaqMan® works:

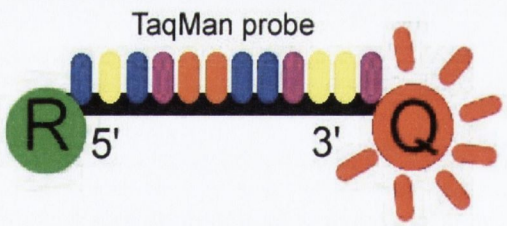

Figure 2.13 The Taqman probe. The red circle represents the quenching dye that disrupts the observable signal from the reporter dye (green circle) when it is within a short distance.

The probe consists of two types of fluorophores; while the probe is attached or unattached to the template DNA and intact (before the polymerase acts), the **quencher (Q)** fluorophore (usually a long-wavelength colored dye, such as red) reduces the fluorescence from the **reporter (R)** fluorophore (usually a short-wavelength colored dye, such as green). It does this by the use of Fluorescence (or Förster) Resonance Energy Transfer, which is the inhibition of one dye caused by another without emission of a proton. The reporter dye is found on the 5' end of the probe and the quencher at the 3' end (Figure 2.13).

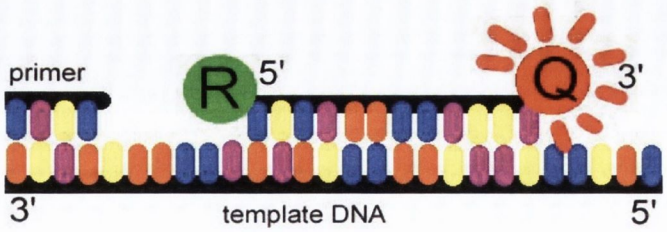

Figure 2.14 The TaqMan® probe binds to the target DNA, and the primer binds as well. Because the primer is bound, *Taq* polymerase can now create a complementary strand.

Once the TaqMan® probe has bound to its specific piece of the template DNA after denaturation (high temperature) and the reaction cools, the primers anneal to the DNA (Figure 2.14). *Taq* polymerase then adds nucleotides and removes the Taqman® probe from the template DNA. This separates the quencher from the reporter, and allows the reporter to give off its energy (Figure 2.15). This is then quantified using a computer. The more times the denaturing and annealing takes place, the more opportunities there are for the Taqman® probe to bind and, in turn, the more emitted light is detected.

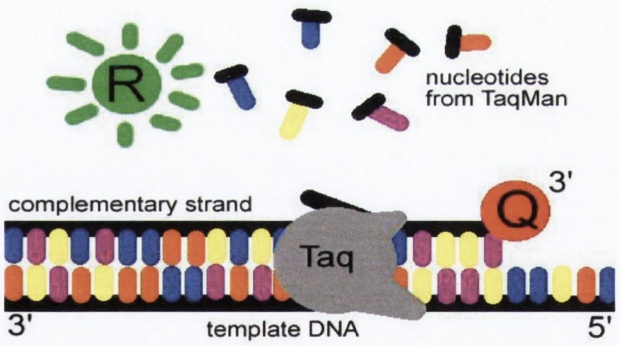

Figure 2.15 The reporter dye is released from the extending double-stranded DNA created by the Taq polymerase. Away from the quenching dye, the light emitted from the reporter dye in an excited state can now be observed.

The TaqMan® PCR based system was selected for mRNA quantitation. It requires very small amounts of target RNA (only a few ng).

Quantification

The light emitted from the dye in the excited state is received by a computer and shown on a graph display, such as this, showing PCR cycles on the X-axis and a logarithmic indication of intensity on the Y-axis (figure 2.16).

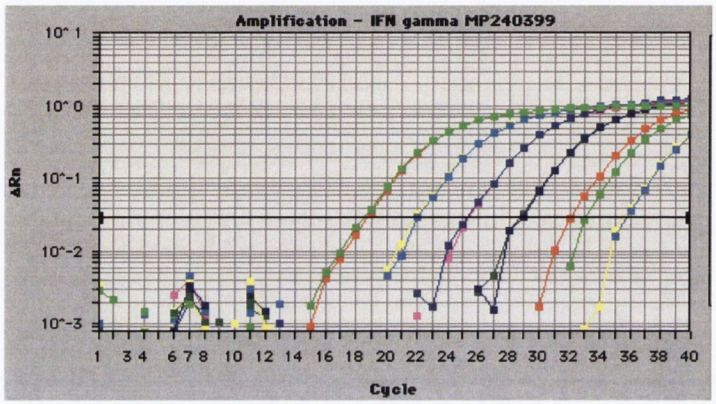

Figure 2.16 An example of a graph printout using the TaqMan® probe displaying various amplification plots.

2.8.5 Real-time quantitative TaqMan® RT-PCR

Real-time PCR allows the scientist to actually view the increase in the amount of nucleic acid as it is amplified (ie, in real time).

It is the most sensitive technique for mRNA detection and quantitation currently available. Data is collected through the PCR process rather than at the end of the PCR. This completely revolutionizes the way one approaches PCR-based quantitation of RNA because reactions are characterised by the point in time during cycle when amplification of a target is first detected, rather than the amount of target accumulated after a fixed number of cycles. The higher the starting copy number of the RNA target, the sooner a significant increase is observed.

RT-PCR has become the preferred method for validating results obtained from array analyses used to evaluate gene expression changes on a global scale.

RT-PCR can be one-step or two-step in nature. In the initial cycles, there is a little change in fluorescence signal. This defines the baseline for the amplification plot. An increase in fluorescence above the baseline indicates the detection of the target. A fixed fluorescence threshold can be set above the baseline. The parameter threshold

cycle (Ct) is defined as the fractional cycle number at which fluorescence passes the fixed threshold.

For relative quantitation, quantity is expressed relative to some basis sample, such as the calibrator. For all experimental samples, target quantity is determined from the standard curve and divided by the target quantity of the calibrator. Thus, the calibrator becomes the 1X sample and all other quantities are expressed as an n-fold difference relative to the calibrator.

For quantitation normalized to an endogenous control, standard curves are prepared for both the target and the endogenous reference. Then the target amount is divided by the endogenous reference amount to obtain a normalized target value. For the quantitation of gene expression, various endogenous controls have been used such as, β-actin, GAPDH, or ribosomal RNA (rRNA).

Several methods have been developed over the years to present relative gene expression. The efficiency correction method calculates the relative expression ratio from the real-time PCR efficiencies and the Ct. RT-PCR data have been analysed using the sigmoidal curve method that fit the experimental data to an empirical equation and results in the prediction of PCR efficiency [339]. The commonest method of presenting RT-PCR data is the comparative Ct method (also known as the 2 to the power-Delta Delta CT method ($2^{-\Delta\Delta Ct}$)) [340] and has been widely used by scientists [341].The comparative Ct method makes several assumptions, including that the efficiency of the PCR is close to 1 and the PCR efficiency of the target gene is similar to the internal control gene [340].

The final form of the $2^{-\Delta\Delta Ct}$ as has been previously reported in Applied Biosystems User Bulletin No 2 is:

Fold change $=2^{-\Delta\Delta Ct}$

This form of equation may be used to compare the gene expression in two different samples (sample A and sample B); each sample is related to an internal control gene. Sample A may be a primary diseased sample and sample B the normal state or a recurrent diseased sample. Expanding the above equation to its full form:

$2^{-\Delta\Delta Ct}$ = [(Ct gene of interest –Ct internal control) sample A – (Ct gene of interest –Ct internal control) sample B)].

In this way our data are interpreted as "the expression of the gene of interest relative to the internal control in the primary diseased sample compared with the recurrent control".

2.8.5.1 Two-step PCR

Two-step PCR is performed in two separate reactions; total RNA is reverse transcribed into cDNA, which is then amplified by PCR. This method is useful for detecting multiple transcripts from a single cDNA template or for storing cDNA aliquots for later use. In our study a large number of gene targets were amplified including the endogenous cnotrol. Table 2.3 lists the recommended kits for two-step RT-PCR.

Table 2.3 Recommended kits for two-step RT-PCR.

Chemistry	Step	Reagent
TaqMan kit	RT	High Capacity cDNA Archive Kit
TaqMan reagent	PCR	TaqMan Universal PCR Master Mix

2.8.5.2 cDNA synthesis

The High Capacity cDNA Archive Kit (AB, USA) was used to convert total RNA to single stranded cDNA. This kit uses the random primer scheme for initiating cDNA synthesis. Random primers ensure first strand synthesis occurs efficiently with all species of RNA molecules present including mRNA and rRNA. cDNA is preferred as it is considered less susceptible to degradation than RNA and more stable for long term archiving.

cDNA reaction preparation

A Reverse transcription (RT) Master Mix was prepared using the following reagents: 10X Reverse Transcription Buffer, 25X dNTPs, 10X random primers, MultiScribe ™ Reverse Transcriptase and Nuclease-free water.

The volume of components needed to prepare the cDNA archive plate was calculated, using table 2.4 below:

Table 2.4 List of reagents used for preparation of RT Master Mix with their volumes

Component	Volume (µL) / Reaction
10X Reverse Transcription Buffer	10
25X dNTPs	4
10X random primers	10
MultiScribe™ Reverse Transcriptase, 50 U/µL	5
Nuclease-free H_2O	21
Total per Reaction	50

50µl 2X RT Master Mix was used for each reaction. An equal volume of RNA sample (2µg RNA brought up to 50µl with Rnase free water) was added per reaction.
50µl of 2X RT Master Mix was pipetted into a PCR tube.
50µl of RNA sample was pipetted into the PCR tube and mixed by repeated pipetting up and down three times.
The tube was placed on ice and loaded to the PCR Thermal Cycler (Thermo Hybaid) using the following conditions: 25°C for 10 min, 37°C for 2 hours (Program 20 REV in the thermal cycler). The reaction volume was set to 100µl.
The cDNA was stored at -20°C until further use.

2.8.5.3 TaqMan® Gene Expression Assays

TaqMan® Gene Expression Assays consist of a 20X mix of unlabeled PCR primers and TaqMan® MGB probe (FAM™ dye-labeled). These assays are designed for the detection and quantitation of specific human genetic sequences in RNA samples converted to cDNA. Gene expression quantitation is performed as the second step in a two-step RT-PCR protocol on the 7000 AB PRISM® Sequence Detection System Instrument.

2.8.5.4 PCR amplification

The second step in the two-step RT-PCR procedure is amplifying the cDNA. TaqMan® Universal Master Mix reagents provide a PCR mix to be used with appropriately designed primers and probes to detect cDNA sequences.

Preparing the PCR Master Mix

Table 2.5 below refers to the preparation of the reaction components for a single 10µl reaction (96-well plate). Components were prepared in separate wells (singleplex assay). Also an endogenous control of choice 18S (Ribosomal RNA control reagent, VIC probe, Part no: 4308329 Applied Biosystems) was run in separate wells as this does not require any validation experiments.

Table 2.5 Reaction components for a single RT-PCR

10µl reaction with their volumes A) Gene Expression Assay® B) Endogenous control

A

Reaction component	**Volume/Well (10µl volume reaction)**
TaqMan® Universal PCR Master Mix, No AmpErase® UNG	5
20X Assays-on-Demand™ Gene Expression Assay Mix	0.5
Rnase-free-water	3.5
cDNA	1
Total	10

B

Reaction component for 18S	**Volume/Well (10µl volume reaction)**
TaqMan® Universal PCR Master Mix	5
Forward primer	0.28
Reverse primer	0.28
TaqMan probe	0.2
cDNA sample	1
Nuclease free water	3.44
Total	10

The reaction plates were labelled ensuring that an endogenous control was included on each plate.

9µl of the appropriate PCR master mix and 1µl of cDNA for each sample were pipetted into each well of the plate. Samples were vortexed before use.

The same tip was used to load the Master Mix onto the well and different tips to load our samples onto each well. Notes of any bubbles in the wells were taken and separate tips were used to remove them, if possible.

After finishing loading, a cover was added and the tips were held without touching the cover. The plate was vortexed briefly to spin down wells and eliminate bubbles. The reaction plates were kept on ice until ready to load into the 7000 system.

Creating a Relative quantitation (RQ) Plate Document

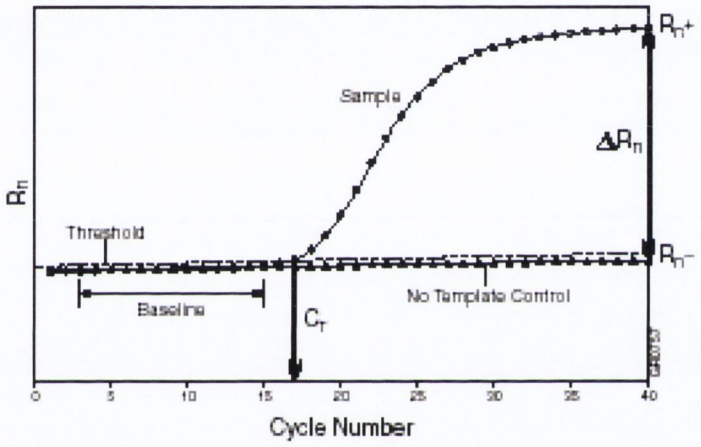

Figure 2.17 A representative amplification plot including some of the terms frequently used.

An RQ plate document is an SDS document that stores data collected from an RQ run for a single plate; it also stores info about the run, including sample names and detectors.

A new plate document was created by:

Selecting Start> Programs> ABI Prism 7000>ABI Prism 7000 SDS Software.

Selecting file>New. In the drop-down list, RT plate was selected and the default settings were accepted, eg 96-well Clear and Blank document. By clicking ok, the software opened a new RQ Plate document.

The detectors for the plate were specified by selecting Tools> Detector Manager. New detectors were created if no detectors were listed in Detector Manager dialog

box. Appropriate detectors were selected. The detectors were then added to the plate document by clicking "Add to Plate document" and then click Done.

After selecting View>Well Inspector, the wells on the plate were labeled by highlighting the replicate wells for our samples. The sample name was entered in the well inspector.

In the well Inspector, the detectors were selected and the detector tasks were assigned (FAM or VIC) for each sample. After closing the well inspector the information was verified on each well in the set up tab. This sample information was saved as a template document to set up further plate documents.

The instrument tab was selected. The standard PCR conditions for the PCR step of the two-step RT-PCR method (RT step completed) are displayed by default as shown in the following table (Table 2.6). The sample volume was set to 10μl.

Table 2.6 Standard PCR conditions

	Initial step	PCR(each of 40 cycles)	
PCR step	AmpErase® UNG Activation	Melt	Anneal/Extend
	HOLD	CYCLE	
	2min at 50°C	15sec at 95°C	1min at 60°C

A name for the RQ plate document was entered and the file was saved.

The plate was loaded into the instrument with well A1 at the upper left-hand corner and the run was initiated by clicking Start.

During the run, the instrument recorded the fluorescent emissions resulting from cleavage of TaqMan probes in the presence of the target and reference sequences. All data generated were saved to the RQ plate document.

Analyzing and viewing RQ Plate Data

By selecting Analysis>Analyze, the SDS software automatically transformed the raw fluorescent data to establish a comparative relationship of the changes between the reference dye and the reporter dyes. Based on that comparison, the software

generated 4 different result views: Plate, spectra, Component and Amplification Plot (Figure 2.18).

In the Results tab, the results of the run were viewed and the parameters were changed if necessary. For example, options were provided for omitting samples or manually setting the baseline and threshold. If any parameters were changed, the data was reanalyzed. The Results tab has four secondary tabs, each of which is described below.

Plate Tab

Displays the results data of each well, including the:

- Sample name and detector task and color for each well
- Calculated R_n value

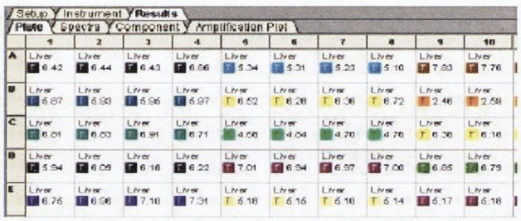

Spectra Tab

Displays the fluorescence spectra of selected wells.

- The Cycles slider allows you to see the spectra for each cycle by dragging it with the pointer.
- The Cycle # text box shows the current position of the slider.

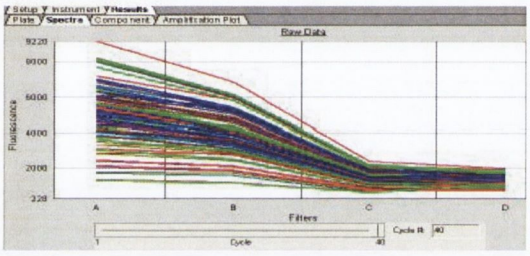

Component Tab

Displays the complete spectral contribution of each dye in a selected well over the duration of the PCR run. Only the first selected well is shown at one time.

Note: If you are using TaqMan® products, three components (ROX® dye, reporter dye, and TAMRA™ quencher) are displayed in the Component tab. If you are using TaqMan® MGB products, only two components (ROX and reporter dyes) are displayed, as shown in the figure on the right.

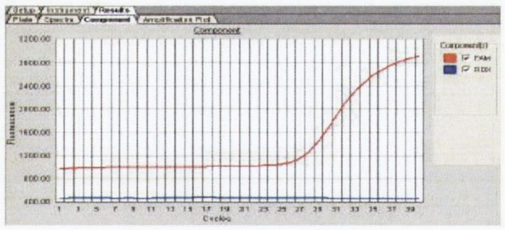

Amplification Plot Tab

Displays a plot of R_n as a function of cycle number for the selected detector and well(s).

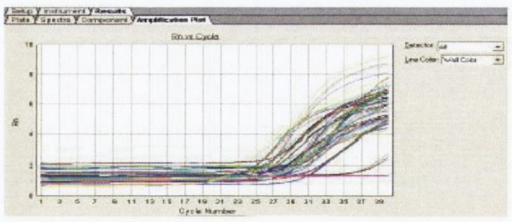

Figure 2.18 Result views for an RQ plate Document

The amplification plot or Rn vs Cycle (Log) displayed Rn dye fluorescence as a function of cycle number. This plot can be used to identify and examine irregular amplification and manually set the threshold and baseline parameters for the run.

Exporting RQ Plate Documents

By selecting File> Export the data type were selected to export. Enter a file name for the export file was entered and saved.

2.8.6 Early Access Human miRNA Panel

The AB TaqMan® miRNA assays (Foster City, CA, USA) are designed to detect and quantify mature miRNAs using a looped-primer real-time PCR. The human early access panel used in this study contained 180 individual assays covering many of the identified human miRNAs. Quantification was carried out using a two-step RT-PCR process; step 1 involves annealing of stem-loop RT primers in a RT reaction followed by a RT-PCR (Figure 2.19).

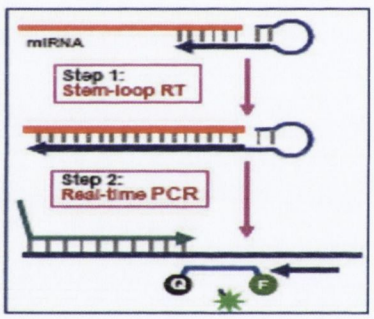

Figure 2.19 Schematic diagram of stem-loop RT-PCR

Step 1: Stem-loop RT primers anneal to miRNA targets and extend in the presence of reverse transcriptase.
Step 2: microRNA-specific TaqMan® PCR primers and probes are used to amplify cDNA.

2.8.6.1 Reverse Transcription

Reverse transcription was performed as per section 2.8.5 above.

2.9 Laser Capture Microdissection (LCM)

LCM enables the dramatic increase of sensitivity and accuracy of molecular assays by starting with samples of homogeneous cell types and multi-cellular structures

isolated from whole tissue or cytology samples. This unique approach to microdissection, developed in 1996 at the National Institutes of Health ensures that biological molecules such as RNA and DNA, remain undamaged during the microdissection process.

LCM has enormous flexibility with respect to tissue and cell fixation preparations. LCM effectively extracts cells from both paraffin-embedded and frozen tissue sections prepared using a wide variety of different dyes, slide surfaces, and protocols (Figure 2.20).

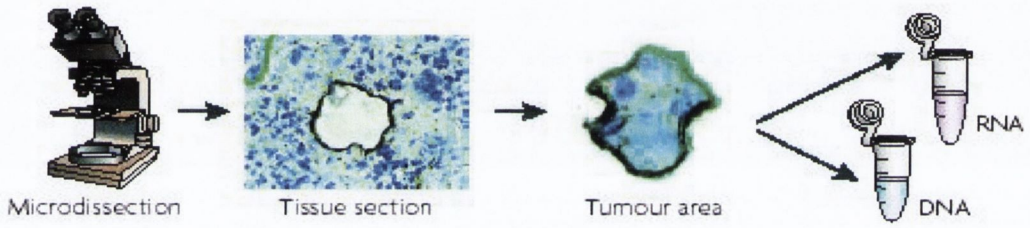

Figure 2.20 Laser Capture Microdissection (LCM) To avoid contamination with normal or stromal tissue present in tumours, areas containing tumour cells are laser-microdissected and the DNA or RNA from these areas are isolated according to different protocols.

LCM utilizes a low-power infrared laser to melt a special thermoplastic film over the cell(s) of interest, especially developed CapSure Macro Caps that are coated with this thermoplastic film are placed on the tissue section or cytology sample. The PixCell™ LCM instrument (Figure 2.21) is then used to direct the laser through the cap to melt the film onto the cells of interest. It can transfer cells from paraffin-embedded frozen tissue samples, stained and immunolabelled slides. A single cell or large groups of cells can be located. LCM preserves the exact morphologies of both the captured cells as well as the surrounding tissue. When the cap is lifted, the selected cells remain attached and are captured for further analysis. The entire process is documented and images can be stored in the archiving workstation.

LCM was employed in six of the recurrent FFPE tumour samples to yield sufficient homogenous populations of malignant epithelilal cells. 8μm sections were cut from each block, dewaxed and stained with haemotoxylin and eosin (H&E). Malignant

epithelial cells from the tumour papillae in each case were laser capture microdissected, using the PixCell 11™ System (Arcturus Engineering Inc., CA, USA) for subsequent expression analysis.

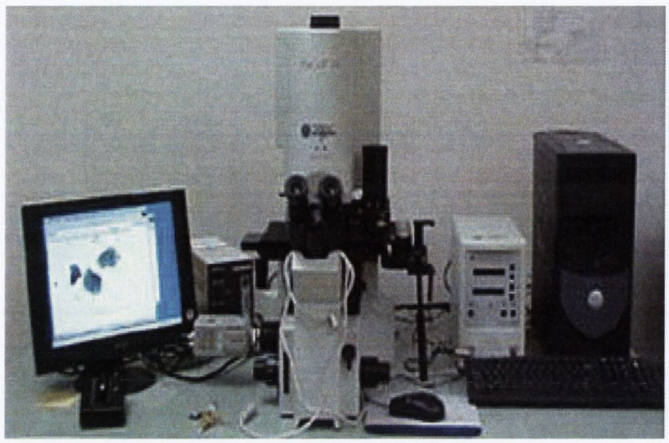

Figure 2.21 The Arcturus PixCell II Laser Capture Microdissection system

2.9.1 LCM procedure

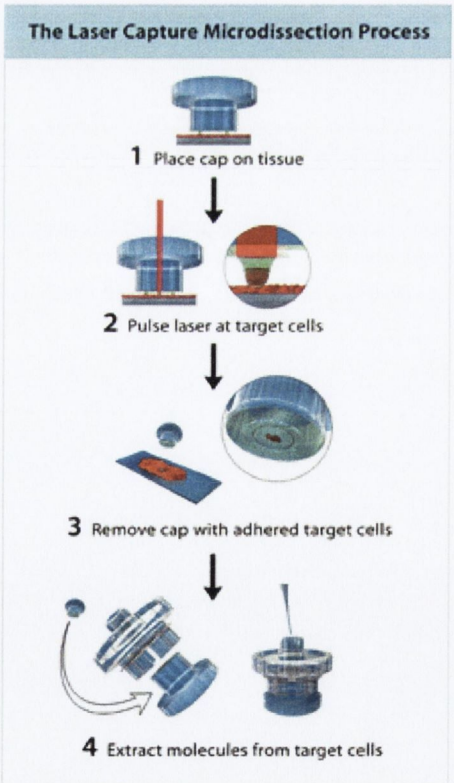

Figure 2.22 Overview of the LCM process

After turning on power switches for PixCell II, Controller and Video Monitor (Figure 2.22), the laser was enabled via the keyswitch located on front of Controller.

The cassette module was removed from the PixCell platform. The flanges of the cassette module were pressed down and the end locking pins were pressed in to hold the place down in the loading position.

A CapSure® cartridge, which holds four film carriers slided into the cassette module until it hit a stop.

The flanges of the loaded cassette were pressed down, the locking pins were retracted to gently raise the cassette to its loaded position.

The joystick was moved to the vertical position to centre the translation stage on the optical axis ensuring proper registration of the sample slide relative to the capture area. This also maximises the transfer area available for microdissection.

The vacuum chuck was turned off via the switch and was covered by the slide placed on the translation stage. It was further manually positioned to locate the transfer area in the centre of the field of view. The vacuum chuck was then turned on and the illumination and focus control was adjusted.

The CapSure Placement Arm was rotated over the tissue sample.The visualizer was inserted by pressing the silver plunger button located above the joystick.

In order to perform LCM, the tab located below the plunger button was pressed to retract the visualizer and the microscope light source was re-adjusted.

The CapSure® cassette module was slided to a detent position making sure there was a CapSure at the load line.

The placement arm was rotated to the CapSure pick-up position. The placement arm was vertically raised to remove the CapSure® from the cassette module, then rotated to transfer position over the slide and released. In this way the CapSure® automatically lowered onto the slide to ensure that the placement arm would seat the CapSure® properly on the sample.

When the laser was enabled, an aiming beam was visible on the monitor.

A laser spot size was selected with the "Spot Size Adjust" and the joystick was used to aim the laser beam on the capture region.

Cells were captured according to a standard protocol as follows: Laser spot size=30 μm, pulse power=40mW, pulse width= 1.5ms, threshold voltage=285mV. The total number of pulses in each case was approximately 700. Laser power and duration determine the size of the LCM Transfer. Optimum transfers usually occur when the

melted plastic after firing the laser is similar in size to the target beam.This yielded a tissue volume in the range of 10^{-7} to 10^{-6} um^3 (representing 5000 cells).

The laser was fired by pressing the "fire" button and an audible beep was noticed.

The activated portion of the transfer film was visible as a ring of film fused to the tissue. The joystick was moved to other areas in the tissue to capture other cells of interest.

The captured tissue was then removed by lifting the placement arm in a smooth but swift motion.

Following microdissection the Capsures™ were placed in sterile Eppendorf tubes

2.10 Tissue Microarray (TMA)

A paraffin tissue microarray (TMA) of 56 primary EOC and 15 recurrent OC was constructed, composed of tumors arrayed in quadruplicates. Samples were age-matched to 40 normal ovaries containing normal ovarian surface epithelium (NOSE). FFPE blocks were selected that contained over 90% tumour. Slides of archival material were reviewed to determine suitable areas for the TMA construction. 4 representative areas were selected and verified by a secondpathologist (CV) for core biopsy.

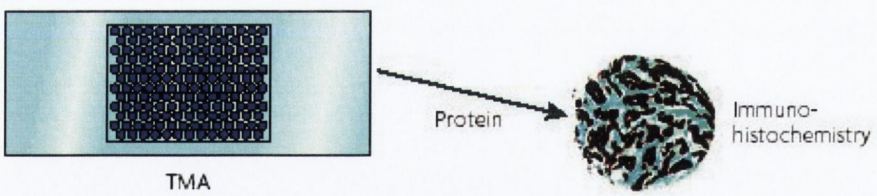

Figure 2.23 Tissue MicroArray (TMA). Validation of candidate genes can be rapidly performed on TMAs containing up to hundreds of tumour samples from an independent cohort of cancer patients with known clinical status.

2.10.1 Immunohistochemistry (IHC) of eIF6 and Dicer (miRNA process machinery proteins) on TMAs

4μm sections of the ovarian serous carcinoma (OSC) tissue array were cut and mounted on glass slides. For antigen unmasking, deparaffinized sections were boiled

(eIF6) or microwaved (Dicer) in citrate buffer [10mmol/L sodium citrate buffer (pH 6.0)] before incubation with primary antibodies. eIF6 (BD Biosciences, Belgium) and Dicer (Abcam, UK) protein levels were examined using mouse monoclonal antibodies at dilutions of 1:200 and 1:50 respectively. Antibody staining was done using the Biogenex Super Sensitive™ Link-Label IHC Detection system.

Intensity of eIF6 and Dicer immunoreactivity was recorded in the neoplastic glands for every specimen. The intensity of staining was graded on a scale from 0 to 3. "0" reflected a lack of immunoreactivity, "1" reflected weak immunoreactivity, "2" reflected moderate immunoreactivity and "3" reflected strong homogenous nucleocytoplasmic (eIF6) or cytoplasmic (Dicer) staining. "0" and "1" were the most common pattern of staining in NOSE. Scores from all cores were averaged. Two pathologists (RF, CB) scored the stained slides.

2.11 Cell culture of ovarian cancer cell lines

Cell lines

Human ovarian epithelial carcinoma cell lines A2780 and A2780cis (the cisplatin resistant counterpart), were purchased from the European Collection of Cell Cultures (ECACC, Salisbury, UK).

Formulation of Cell Culture media and other solutions

Culture media: The base medium for the above cell lines was RPMI 1640 (Gibco). To make the complete growth medium, the following components were added to the base medium: fetal bovine serum FBS (SIGMA) to a concentration of 10%, 1% L-glutamine (Gibco), 1% penicillin/streptomycin (Gibco) (100units/ml). Media was stored at 4°C.

Trypsin- EDTA 0.25% (Gibco): 5ml aliquots were made and stored at -20°C.

Freezing solution: Dimethyl sulfoxide (DMSO) (Gibco). Stored at -20°C.

2.11.1 Resuscitation of frozen cells from stocks

All surfaces were wiped with 70% alcohol. Everything going in the laminar flow cabinet was spayed with alcohol. Aliquots for all purchased media were made and dated.

Cell culture media was prewarmed for 30 minutes at 37°C. A T25 culture flask (Corning), with bottom surface areas of 25cm², was brought to the laminar flow cabinet and the caps were loosened. 5ml cell culture media was added to the T25 flasks.

One cryovial of cells (1 ml in each) was removed from LN2 and brought to the, at room temperature. A tissue soaked in 70% alcohol was held around the cap of the frozen ampoule and the cap was turned a quarter to release any residual LN2, then it was re-tightened. The ampule was quickly transferred to a 37°C waterbath, but not totally immersed, until one or two small ice crystals, if any, remained (usually 1-2 min). Rapid thawing was ensured to minimize any damage to the cell membranes.

The ampule was wiped with a tissue soaked in 70% alcohol prior to opening.

The whole content of the ampoule was pipetted into the T25 flask, containing 5ml pre-warmed medium that has been already supplemented with the appropriate constituents. Before incubation, the cells were quickly checked for any obvious defects by using an inverted microscope.

The flask was then laid flat and incubated at 37°C in a humidified atmosphere containing and 5% CO_2 as recommended on the data sheet, overnight.

The cells were checked the following day; some cells were expected to adhere to the media surface but also some dead ones floating around, particularly for the A2780 cis cell line. The media was changed to remove the nonadherent cells.

2.11.2 Subculture of adherent cell lines (A2780 and A2780cis)

Adherent cell lines will grow *in vitro* until they covered the surface area available or the medium is depleted of nutrients. At this point, the cell lines were sub-cultured to prevent the culture dying. To subculture cells, cells are required to be brought into suspension. Proteases such as trypsin, are used to release cells from the flask.

Following overnight incubation, cultures were viewed using an inverted microscope to assess the degree of confluence and confirm the absence of contaminants.

The media was changed usually every second day by tilting the flask and removing the spent medium with a sterile stripette from the corner.

The cells were harvested in the log phase of growth as close to 80-90% confluency as possible. At 80% confluence, as specified on the cell line data sheet, the spent culture medium was carefully removed and monolayer of cell was washed twice with 2 ml PBS (volume equivalent to half the volume of culture medium).

2ml of 0.25% Trypsin/EDTA (Gibco) solution was added ensuring that all cells were covered.

Flasks were incubated for 5-7min at 37°C or until the cells started detaching from the flask. The cells were examined using an inverted microscope to ensure all cells were detached and floating. The sides of the flasks were gently tapped to release any remaining attached cells. Cells that were difficult to detach were incubated at 37°C to facilitate dispersal.

The cells were resuspended in the same volume of fresh medium to inactivate the trypsin and centrifuged on 1200rpm for 5-10min to pellet the cells. The supernatant was carefully removed and resuspended in 1ml of fresh medium. At that stage, a cell count was performed using a trypan blue stain, a haemocytometer and an inverted microscope to count the cells. The required number of cells was transferred to a new labeled flask containing pre-warmed medium and incubated as appropriate for the cell line.

2.11.3 Cryopreservation

After cell pellets were obtained by centrifugation, cells were resuspended slowly in 1ml of DMSO in cryovials (1 ml in each cryovial).

The vials were placed on ice for 10 minutes, then at -20°C for 1h and overnight at -80°C. They were then transferred to a LN_2 storage tank for long-term storage.

2.11.4 Cell counting with Trypan blue to assess cell viability

Cells were reconstituted in 1ml of media.

1ml of trypan blue was filter sterilized into a clean sterile container (in the fume hood).

The haemocytometer was cleaned with alcohol and sterile gauze and then a cover slip was attached to the counting area (square area).

10µl of cell suspension was added to 90µl of sterilized Trypan blue and mixed gently by pipetting up and down.

10µl of the resulting solution were added to the edge of the coverslip allowing it to diffuse into the counting area.

The haemocytometer area is divided into 4 areas and a central area was divided into 16 to make counting easier.

Viable cells were those which had excluded Trypan blue only. Clumped cells were counted as one. Each of the four quadrants was counted separately, then the cell counts were averaged.

The cell count obtained, was the average count $x10^4$. We next allowed for the dilution factor, ie multiplied by 10. This would give us the final cell count per ml since the cells were reconstituted in 1ml.

2.12 Cytotoxicity Assay

The cytotoxicity of the following compounds shown in Table 2.7 was tested.

Table 2.7 List of cytotoxic and cytostatic drugs used in our study

Drug	Manufacturer	PPC(μg/ml)	IC50(nM)
Cisplatin(cytotoxic)	Sigma-Aldrich	2.5	
MMP-9/MMP-2 inhibitor 1 (cytostatic)	Calbiochem		240

The toxic effect of *MMP-9*i (cytostatic) and cisplatin (cytotoxic) alone or/and *MMP-9*i+cisplatin in combination was determined using the multiparameter cytotoxicity 1 Kit by Thermo Fisher®.

A pre-incubation for 3 hours with *MMP-9*i prior to treatment with cisplatin for 3 and 6 hours was also assessed. Cells were plated ($8X10^3$) in triplicate in 96-well plates overnight and then treated with titrated concentrations of drugs for 3, 6 and 24 hours. Only the inner 60 wells of 96-well plates were used due to evaporation-related edge effects in the outside wells. Prior to staining, cells were washed with PBS, then 65ul of a fluophore mixture containing Hoechst 33342, lysosomal mass/pH indicator and cell membrane permeability dye were made up in 10% supplemented RPMI media. Cells were incubated with 50ul of the fluophore mixture for 40min under tissue culture conditions to enable measurement of cytotoxicity indicators (Table 2.8). Cells were washed twice with 100ul of PBS and 200ul of wash buffer was added in each well.

To get reliable information six fields per well were imaged and analysed at 10x magnification using the HCS tool. This instrument enables fully automated monitoring of fluorescence intensity at three wavelengths. Fluorescence was monitored kinetically for the three dyes for 3h with a single cell count made at the

end of the assay. The relative fluorescent intensity was used to quantify the cytotoxicity indicators. The channels for detecting emission of dyes were set to auto-exposure so that the exposure time was automatically determined based on the cellular fluorescence of untreated (negative control) cells and then set constant for the whole plate. The High Content Screening (HCS) assay was conducted immediately after addition of drugs to cells with the exception of cases in which a preincubation of cells with *MMP-9*i was required.

2.12.1 Cytotoxicity 1 Multiparameter Kit

Reagents

Table 2.8 Contents of the Cytotoxicity 1 Multiparameter Kit

Dyes	Location
Hoechst 33342	Nucleus
Lysosomal mass indicator	Cytoplasm
Membrane permeability dye	Cytosol

A commercial kit, the Cytotoxicity 1 Multiparameter Kit (Thermoscience) is an in vitro assay tool, used to monitor the toxic effects induced by cytotoxic drugs on live cells. It allows users to rapidly acquire information on the changes in the following cellular properties: (1) nuclear morphology/size, (2) cell membrane permeability, (3) lysosomal mass/pH and (4) cell density (number of cells per field). Therefore it can also be used as a cell health assay. It does not require cell lysis, purification, or filtration steps, thus saving time and labor.

2.13 High Content Screening (HCS)

The HCS is a fully automated system that can provide quantitative and qualitative information at the sub-cellular level. It involves fluorescent cell-based assays and carries the ability to use a wide variety of fluorescent indicators. In this respect it allows for live cell imaging and observation of cellular or subcellular morphological and structural changes (Figure 2.24).

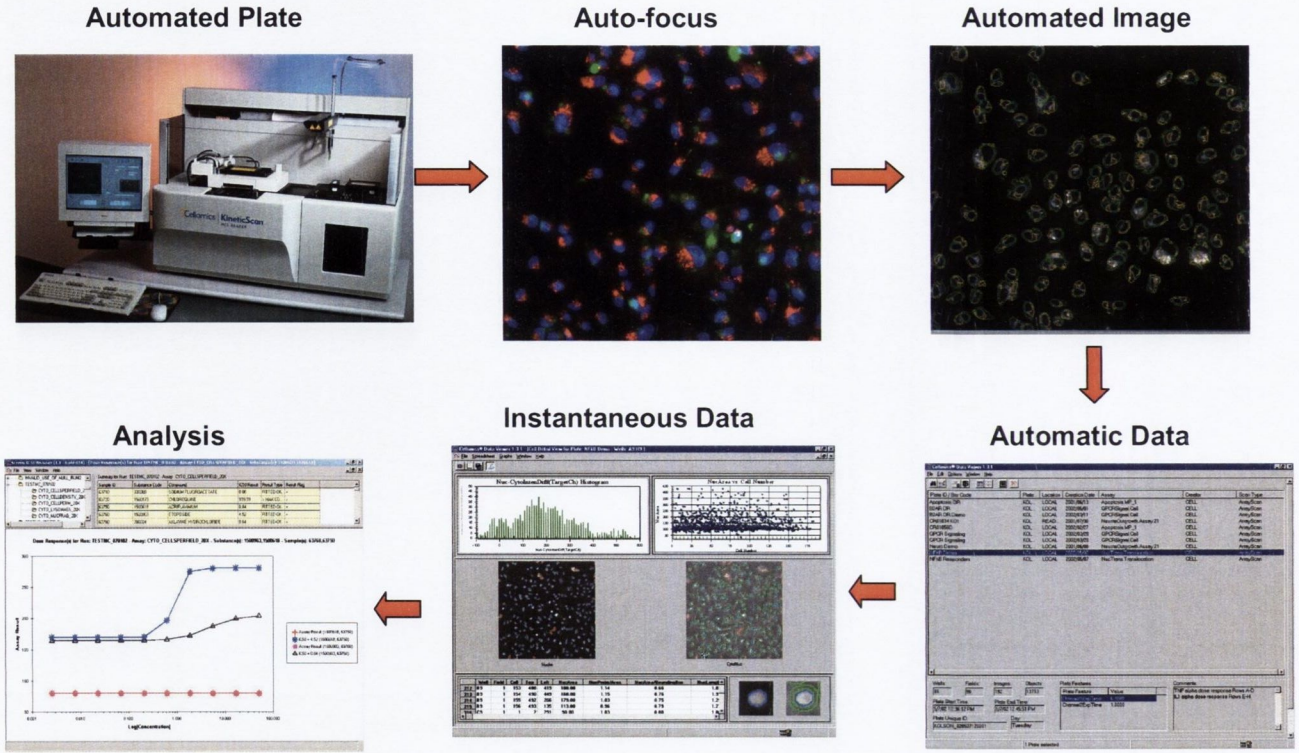

Figure 2.24 HCS Workflow

The cytotoxicity assay was performed using the HCS in a 96-well format on a well-by-well and cell-by-cell basis. After labeling, cells are fixed with formaldehyde and scanned and analyzed with the ArrayScan HCS Reader and the Multiparameter Cytotoxicity 1 BioApplication software.

2.13.1 Image acquisition and analysis

This system automatically aquires images from cells seeded into multiwell plates. It has the capability of simultaneously acquiring digital images from several fluorescent channels, all of which have excitation and emission characteristics that roughly correspond to different stains used.

Image analysis utilizes dedicated algorithms designed to identify and distinguish between whole cells and/or subcellular structures. The HCS system permits compartmentalisation or segmentation using the multi coloured channel cellular imaging, thus allowing for the monitoring of biological processes within defined regions of cells (Figure 2.25). Once cells or objects are segmented, the information from these defined regions can be extracted and exported to an excel file. The large amount of data obtained ensures robustness of the assay.

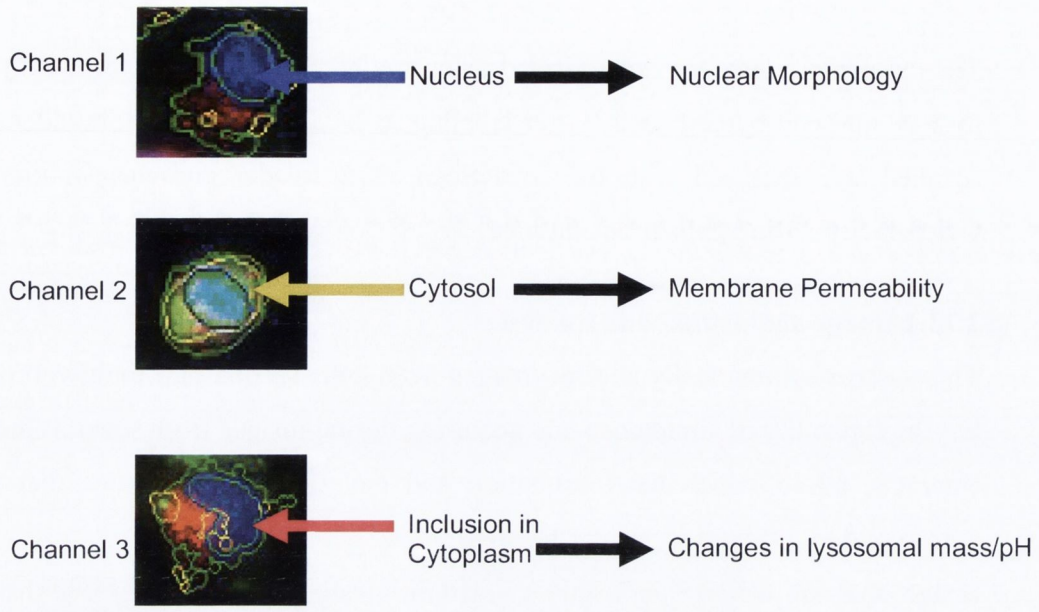

Figure 2.25 Multiparameter Cytotoxicity Assay. The nucleus (Hoechst dye, blue) is gated (highlighted) in channel 1. Channel 2 (green) is used to measure cell membrane permeability. Any inclusions within a defined radius from the nucleus were gated for measurement of the lysosomal pH in channel 3 (red). Values of the size of the nucleus are usually in pixel numbers, while the permeability and lysosomal pH are quantified as the average intensity of pixels within the gated area.

Depending on the type of toxic insult, cells often undergo either necrosis or apoptosis, accompanied by changes in nuclear size or morphology. The assay uses the nuclear stain (Hoechst 33342), that labels DNA and emits a blue fluorescence, to identify individual nuclei (and hence the cell) and measures nuclear changes that result from toxic insults.

The cell membrane maintains cellular homeostasis, providing a specialized environment different from its extracellular surroundings, and providing a mechanism for the controlled exchange of its nutrients with its surroundings. Certain toxins can affect cell membrane integrity leading to the cell becoming permeable, eventually causing cell death. Healthy cells are nearly impermeable to the indicator dye used in this assay; however, after compromising the cell membrane's permeability, the dye stains the nucleus with a green fluorescence.

Physiologically healthy cells have intracellular organelles with characteristic properties, including lysosomes and endosomes that maintain specific internal acidic pH ranges for cells to function normally. Toxins can interfere with cell functionality by affecting the pH of these organelles or by causing a change in lysosome number. The dye used in the assay to determine changes to lysosomal physiology is a weak base that accumulates in acidic organelles such as lysosomes and endosomes. A decrease in pH caused by the cytotoxicity of a compound directly correlates to the amount of accumulated dye and thus to the fluorescence (red) intensity. Conversely, an increase in pH results in a decrease in staining intensity. On exposure to toxic compounds, cells can respond by exhibiting changes in nuclear size and shape, increased cell membrane permeability and increases in the pH (Figure 2.26).

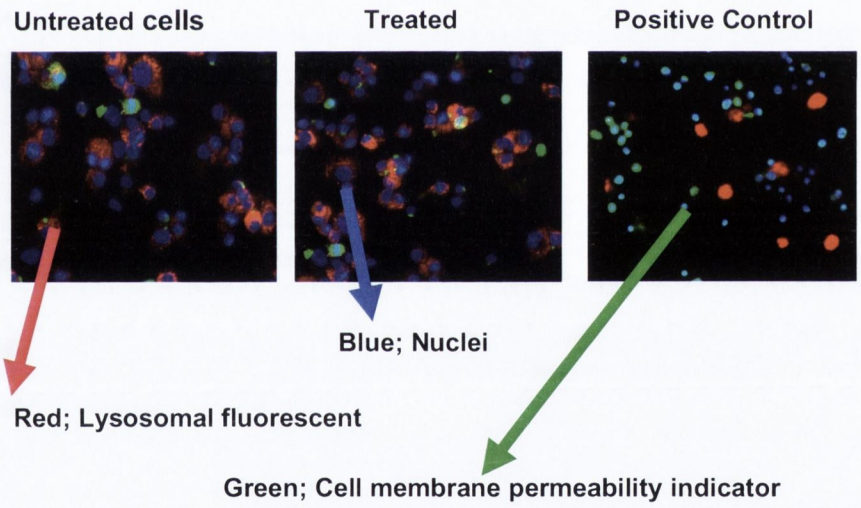

Figure 2.26 Live cell HCS images showing the fluorescence dye response for a) lysosomal mass/pH (red) b) nuclear size and intensity (blue) c) cell membrane permeability (green) for cells 1) untreated 2) treated with cytotoxic drug c) treated with positive (vehicle) control. Increases in green intensity are indicative of increased permeability, while increases in red indicate an increased lysosmal mass or decreased lysosomal pH.

2.14 Preparation of cell lines for RNA extraction

Following trypsinization of cultured cells, 1-5 x 10^6 cells were centrifuged for 12 minutes at 1200rpm and supernatant was removed. The number of cells was then determined. The cell pellet was then loosened thoroughly by gently flicking the tube and disrupted by adding 350µl Buffer RLT. RNA extraction was then carried out as per tissue protocol.

CHAPTER THREE

An integrative model for recurrence in ovarian cancer

3.1 Summary

Background: Ovarian cancer is a devastating disease partly because conventional chemotherapy ignores aspects of tumour biology. Recurrence represents the "true killer" among ovarian cancer patients and identification of novel molecular markers present in recurrent tumours is urgently required. We carried out gene expression profiling between primary and recurrent ovarian cancers and identified potential biomarkers of recurrence.

Results: Using cDNA microarrays, we identified distinct patterns of gene expression between primary and recurrent ovarian cancers from different patients with the same histology and from the same patients with different histology. Selected targets were validated and correlated with microarray results. Signatures from both cohorts were also validated against an independent set of serous papillary ovarian adenocarcinomas. Notably, upregulated genes in the recurrent compared to primary tumours in both cohorts, segregated in the same gene families.

Conclusions: Collectively, our data propose an integrative model for recurrence in ovarian cancer, in which tumour cells during relapse produce adhesion molecules to mediate attachment, cytokines and inflammatory mediators to stimulate survival and a variety of growth factors bound to their cognate receptors to fully proliferate in order to confront and modulate their immediate environment. Some of the mechanisms involved in recurrence could be specific to the drugs used.

3.2 Introduction

3.2.1 AB Microarray Platform

Throughout the course of the study the Expression Array system from Applied Biosystems was used, which has 31,077 probes and targets a complete annotated and fully curated set of 27,868 human genes from the public and Celera databases. 21% of the genes have been curated only by Celerea genomics and the other 79% are based on public-domain reference sequence (Ref Seq), Gen Bank mRNAs and MGC (Mammalian Gene Collection) transcripts. The system combines chemiluminescent detection with improved probe design, providing an average sensitivity of 0.5 copies per cell as opposed to 1-3 copies per cell afforded by most fluorescent platforms. In a fluorescent reaction, the light used to excite the fluorescent probes can overlap with their emission spectra. However, a chemiluminescent reaction produces light only when a label binds to a substrate, rather than relying on light to excite the bound label, thus eliminating the problem. The probes are 60 pairs long and are designed to report an activity level from alternatively spliced transcripts of a gene. Another advantage is AB offers custom probes for subsequent real-time PCR analysis for validation work (Figure 3.1).

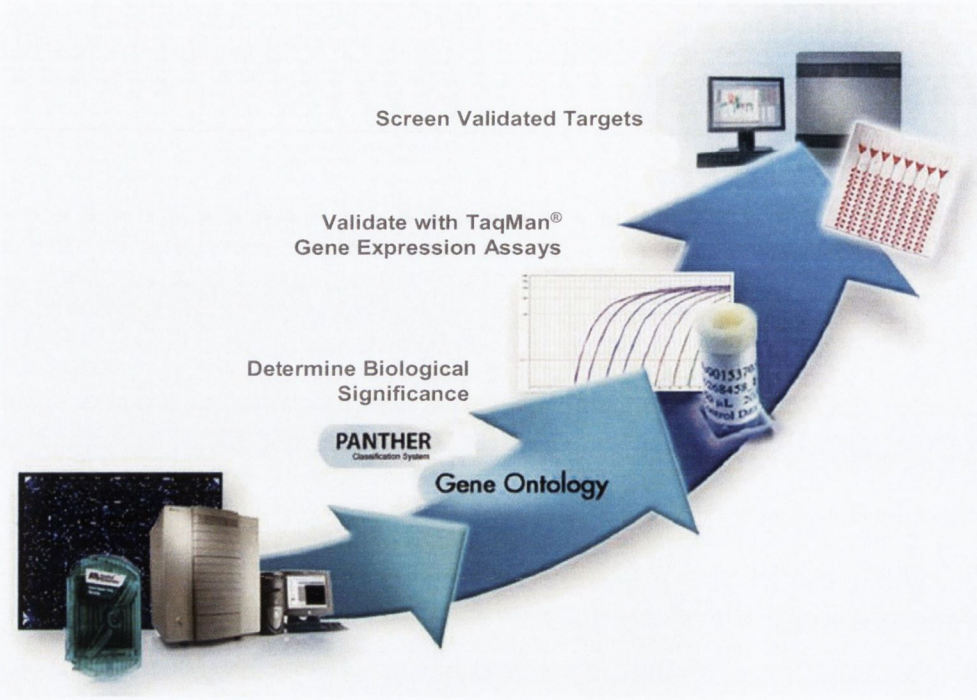

Figure 3.1 Continuous integrated workflow of microarray data with Panther online tool for gene ontology and TaqMan® Assay system streamlines gene expression research. "Follow on" experiments from microarrays were achieved by linking to qRT-PCR TaqMan® probe based assays that enable microarray data validation.

3.2.2 Aim of the study

While numerous studies have characterized primary ovarian cancers, less information is available regarding expression patterns of recurrent ovarian cancers. The aim of this study was to determine whether primary and recurrent ovarian tumors could be distinguished based on their gene expression profiles, by using gene expression arrays and to identify potential biomarkers of recurrence.

3.3 Materials and Methods

2 cohorts were used in this study: In the first one, we selected a homogeneous series of primary and recurrent serous papillary adenocarcinomas from different patients (Between patient cohort). The second cohort consisted of 3 paired ovarian cancers (primary and recurrent samples coming from the same patient) but of different histology (Within patient cohort). Selected genes identified from microarray experiments were validated for both cohorts and a subset of these genes (n=12) were

validated in an independent set (test set) of 13 serous papillary adenocarcinomas using TaqMan® PCR. A flow chart of our study is shown in Figure 3.2.

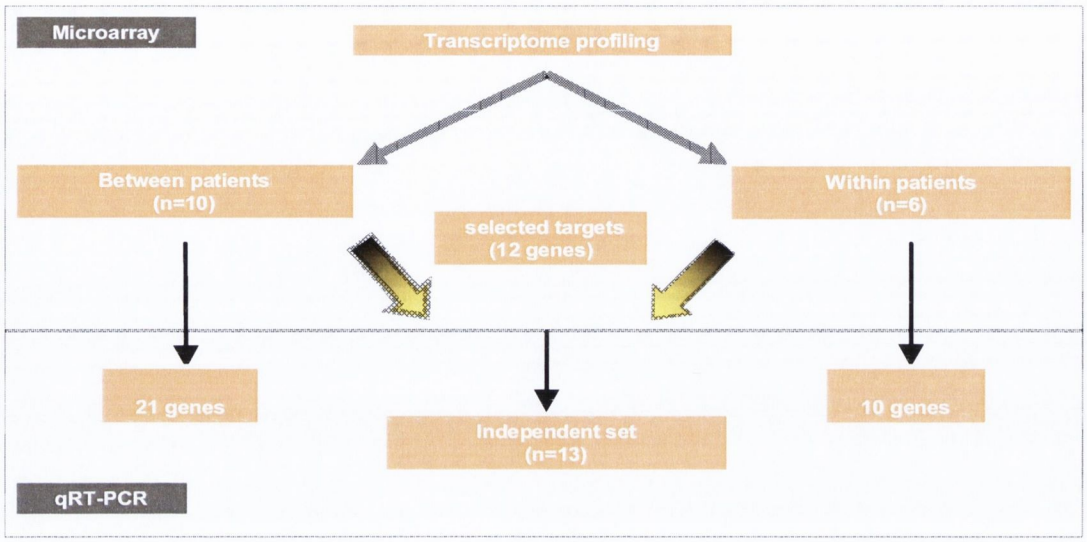

Figure 3.2 Flow chart of our study design.

3.3.1 Patients and tissue samples (see Table 2.2 Materials and Methods)

The study consisted of 2 cohorts: cohort 1 comprised 5 primary serous papillary adenocarcinomas (P1-P5), grade 3, FIGO stage III and 5 recurrent serous papillary adenocarcinomas (R1-R5) of the same grade. The mean age in years for patients in the primary and the recurrent group in cohort 1 was 62.6 (range 48-84) and 52.4 (range 43-68). The recurrent group consisted of patients for which primary surgery was performed prior to the commencement of the study. In cohort 2, 3 paired ovarian cancers were used (primary and recurrent coming from the same patient), but of different histology, namely small cell carcinoma of hypercalcemic type (P6, R6), papillary serous (P7, R7) and mixed mullerian (P8, R8) carcinomas. The mean age in years for patients in cohort 2 was 52 (range 39-74) for the primary and 53.3 (range 43-74) for the recurrent.

To further validate identified gene targets in cohorts 1 and 2, an independent set (test set) of serous papillary ovarian adenocarcinomas were interrogated. This additional cohort comprised of 13 serous papillary ovarian adenocarcinomas, 10 primary (P9-P18) and 3 recurrent (R9-R11) cases. An additional two patients (R12, R13) with different histological subtypes of recurrent ovarian cancer (one patient with well

differentiated clear cell carcinoma and one patient with dedifferentiated germ cell carcinoma) were also included in the test set.

All tumors were staged according to the International Federation of Gynaecology and Obstetrics standards (FIGO). Patients were optimally debulked (residual disease of <1cm in greatest diameter), had received no neoadjuvant treatment before surgery and they were all treated post operatively with paclitaxel and platinum. The two additional recurrent patients in the test set were optimally debulked, one received postoperative carboplatin/paclitaxel and the other bleomycin/etoposide/platinum.

All samples were removed as part of patient treatment for ovarian cancer at St James's Hospital, Dublin, Ireland. The study had approval of the hospital ethics committee and informed consent was obtained from each patient by the research team prior to surgery.
Specimens were snap frozen on collection within 1 hour of surgery and stored at -80°C. After tissue processing in a cryostat at -20°C, frozen sections were cut and mounted on slides. The slides were stained with H&E and examined by a pathologist to ensure >70% presence of tumor cells.

3.3.2. cDNA Arrays

cDNAs were performed as described in chapter 2. Briefly, samples were placed in liquid nitrogen, ground thoroughly with a mortar and pestle and homogenized in RLT buffer (Qiagen Ltd, UK). Total RNA was extracted using the Qiagen RNAeasy (Hilden, Germany) RNA Mini Kit and on-column RNase-free DNase digestion was performed according to the manufacturer's instructions. RNA quantity and quality was determined using Nanodrop spectrophotometer (Nanodrop Tehnologies).

Gene expression profiles were examined using the Applied Biosystems (ABI) (Foster City, CA, USA) Human Genome Survey Microarrays V2.0 system. These arrays contain 32,878 oligonucleotide probes (60 base pairs long) and target a complete annotated and fully curated set of 29,098 human genes from the public and Celera databases. Double stranded cDNA was prepared from 2 micrograms of total RNA using an oligo dT priming approach followed by in vitro transcription and labelling to

generate Digoxigenin (DIG) labelled cRNA (ABI Chemiluminescent RT-IVT Labelling Kit) according to the manufacturer's protocol.

Each microarray was first pre-hybridized at 55°C for 1 hr in hybridisation buffer with blocking reagent. 10μg of labelled cRNA targets were randomly fragmented by incubating with fragmentation buffer at 60°C for 30 min, mixed with internal control target (ICT, 24-mer oligo labelled with LIZ fluorescent dye) and then hybridized to each pre-hybridized microarray at 55°C for 16 hr. Following hybridisation, the arrays were washed with hybridisation wash buffer and chemiluminescence rinse buffer and stained with anti-DIG alkaline phosphatase, further enhanced with Chemiluminescence Enhancing Solution and finally with Chemiluminescence Substrate. Each array was then scanned on the ABI 1700 Platform for image collection. Technical replicates were performed on a subset of samples to ensure concordance and only those with greater than 90% concordance were considered valid.

3.3.3 Bioinformatics

Data Output

Microarray data analysis included both primary and secondary data analysis. The primary data analysis was performed using the software provided with the Applied Biosystems Expression Array System. For secondary analysis, the system software was compatible with both GeneSpring® and Spotfire® software application packages. The Expression Array System could also export microarray data in a flat-file format and industry standard MAGE-ML as per method.

3.3.3.1 Statistical analysis

The R statistical package, was used as per method for all the analysis (R Development Core Team, 2004) [342]. This program applied filtering methods to identify genes that showed differential expression across two study groups.

Data Analysis

Differential Gene Expression

Generally, the following three steps are used to determine differential gene expression:

Step 1: Regression analysis on biological replicates (and/or technical replicates), which rejects array outliers based on regression threshold. For example, the data point that has a correlation coefficient of $R2 < 0.75$ or $R2 < 0.95$ is used as threshold.

Step 2: Perform t-test/ANOVA analysis to determine differentially expressed genes based on p-value threshold (e.g. $p < 0.001$, $p < 0.01$ or $p < 0.05$). This is dependent on the confidence level researchers would like to select between test samples and normal samples.

Step 3: Determine fold change of genes by measuring the average ratios between test and normal samples using variable fold change cutoffs and associated p-values.

In general, each array is normalized by the median chemiluminescent signal (i.e. assay normalization signal from output); the data set is filtered using a threshold of $S/N > 3$; and fold change is determined by the ratio of test sample(s) vs. normal or control sample(s) and p-values that associate with each fold change based on ANOVA test.

3.3.3.2 Normalisation and filtering

Following quality control assessments, a two-step algorithm automatically processed raw image data, including gridding and quantification to remove control elements, such as hybridization controls, RT-IVT controls, so that genes were deemed undetectable if they had signal- to-noise (S/N) ratio threshold > 3 in 75% of the samples. Data were normalized with quantile normalization. The goal of the Quantile method applied in this microarray study is to make the distribution for each array in a set of arrays the same. The method implies that each array can be given the same distribution by taking the mean quantile substituting it as the value of the data item in the original dataset. In this respect, a quantile-quantile plot shows that the distribution

of two data vectors is the same if the plot is a straight diagonal line and not the same if it is other than diagonal.

3.3.3.3 Comparing samples

In sample comparison, non-parametric t-tests are used to generate p-values. The t-test looks at the mean and variance of the sample and control distributions and calculates the probability that the observed difference in means occurs when the null hypothesis is true. The null hypothesis states that the mean of the two distributions is equal. The aim is to look for genes that show a distinct difference in expression between the groups.

3.3.3.4 Fold change and adjusting p-values for multiple comparisons (FDR)

The p value (0.05, 0.01) has classically been used to control the rate of false positive values or the type 1 error rate. For example, a p value of 0.05 means that from 100 tests, 5 tests would never be statistically significant. This means that the use of this p value as a setting cut off would yield 1,500 false positive genes, a number rather unacceptable. A more strigent statistical method is that introduced by Benjamini and Hochberg to correct for multiple comparisons [343]. The FDR is the expected proportion of erroneously rejected null hypotheses among the rejected ones. However, if no or very few genes passed the Benjamini-Hochberg corrections, those with the smallest p value were evaluated, using $p<0.01$.

Fold change (FC) and log2 (FC) for detected probes were also calculated. FC compares the expression level of the same gene in both classes and assesses how many fold up- or downregulated the gene is in one class compared to the other. Only genes with a $FC>2$ were included in analysis.

Paired t and ANOVA tests were performed to generate p values for statistical differences between the two groups, with $p<0.05$ considered significant. The p values were further adjusted using more stringent Benjamini-Hochberg false discovery rate (FDR) at preset levels: 0.01, 0.1. Gene expression profiles were examined based on fold change, p and FDR values.

3.3.3.5 Hierarchical clustering

Clustering is the classification of similar objects into different groups, or more precisely the partitioning of a data set into subsets so that the data in each subset share some common trait according to some defined distance measure. Therefore, a key step in hierarchical clustering is to select a distance measure. We used the Euclidean distance in our experiment, the most commonly chosen type of distance, which is the geometric distance in the multidimensional space.

3.3.3.6 Analysis of Gene Lists and PANTHER

The R package, version 1.9.1 was used to visualize hierarchical clustering between differentially expressed genes and manipulate the final gene lists. Unsupervised hierarchical clustering was applied to the data set using the Unweighted Pair Group Method with Arithmetic Mean (UPGMA) based on Euclidean distance as the similarity measure. Functional classification of the data and gene ontology was defined by using the PANTHER Classification System. This is a unique resource that classifies genes by their functions, using published scientific evidence and evolutionary relationships to predict function even in the absence of direct experimental evidence [344]. Proteins are classified into families and subfamilies of shared function, which are then categorised by molecular function and biological process ontology terms.

Designed for PANTHER high-throughput analysis of protein sequences, the database provides a simplified ontology of protein function, which allows browsing of the database by biological functions. For an increasing number of proteins, detailed biochemical interactions in canonical pathways are captured and then can be viewed interactively. Biologist curators have associated the ontology terms with groups of protein sequences rather than individual sequences. Statistical models (Hidden Markov Models, or HMMs) are built from each of these groups. The advantage of this approach is that new sequences can be automatically classified as they become available. To ensure accurate functional classification, HMMs are constructed not only for families, but also for functionally distinct subfamilies. Multiple sequence alignments and phylogenetic trees, including curator-assigned information, are available for each family. The current version of the PANTHER database includes

training sequences from all organisms in the GenBank non-redundant protein database, and the HMMs have been used to classify gene products across the entire genomes of human, and Drosophila melanogaster.

A binomial statistical tool was employed to compare gene lists to a reference list (i.e. the complete human genome) to determine over- or under- representation of PANTHER classification categories. To further refine the gene lists, it was investigated if any of these genes were known to interact biologically. To this end, pathway analysis using the Ingenuity Pathways Analysis (IPA) tool was used which is a web-based software application that enables scientists to identify the biological mechanisms, pathways and functions most relevant to their experimental datasets or genes of interest [345].

Expression data from microarray and TaqMan® PCR data were correlated with nonparametric Spearman's correlation coefficient (r) to avoid distributional assumptions.

3.3.4 Validation of gene expression targets

RNA was initially reverse transcribed as per method. The mRNA levels of 31 overall differentially expressed genes were validated. All reactions were carried out on the ABI Prism 7000 Sequence detection system using the TaqMan® Universal PCR master Mix and Gene Expression Assays® (Applied Biosystems). Gene symbols and assay ID's are shown in Table 3.1 and 3.2. Relative quantitation was carried out using the ΔΔCt method with 18S ribosomal RNA as an endogenous control. Transcript quantification was performed in triplicate for each sample.

Table 3.1: List of gene targets selected for TaqMan® validation in cohort 1

Gene Symbol	Probe ID	P value	Array fold change	Expression in recurrent vs primary	Assay ID
CLDN16	163630	0.0068	9	Upregulated	Hs00198134_m1
S100B	114188	0.0001	6.12	Upregulated	Hs00389217_m1
CACNAID	127127	0.00012	3.9	Upregulated	Hs00167753_m1
BTC	112710	0.0006	2.67	Upregulated	Hs00156140_m1
IL27RA	145754	0.0005	1.82	Upregulated	Hs00175472_m1
CHORDC1	183675	0.0002	1.359	Upregulated	Hs00854389_m1
LASS4	155606	1.78E-05	9.02	Downregulated	Hs00226114_m1
STARD10	115998	4.26E-05	6.03	Downregulated	Hs00246405_m1
CSRP2	137165	0.0003	5.7	Downregulated	Hs00426717_m1
RNPC1	215065	0.0003	4.87	Downregulated	Hs00246405_m1
ARFRP1	118657	0.0003	4.85	Downregulated	Hs00182389_m1
ESM1	174810	0.005	4.68	Downregulated	Hs00199831_m1
CASK	143978	0.00035	4.42	Downregulated	Hs00177620_m1
WASF1	118398	0.0001	4.32	Downregulated	Hs00187514_m1
PVRL2	128369	0.0002	4.23	Downregulated	Hs00161054_m1
MGAT4B	186405	0.0002	4.13	Downregulated	Hs00365001_m1
LGALS3BP	185853	9.49E-05	4.12	Downregulated	Hs00174774_m1
PERP	141176	0.0004	3.52	Downregulated	Hs00751717_m1
PGM2L1	138177	0.0005	3.04	Downregulated	Hs00328100_m1
IFNGR1	190183	0.0003	2.57	Downregulated	Hs00166223_m1
USF2	144617	0.0005	1.94	Downregulated	Hs00231528_m1

Table 3.2: List of gene targets selected for TaqMan® validation in cohort 2

Gene Symbol	Probe ID	P value	Array fold change	Expression in recurrent vs primary	Assay ID
S100A8	196494	0.034	11.6	Upregulated	Hs00374263_m1
ZNF218	217273	0.002	6.06	Upregulated	Hs00542836_m1
MMP9	112640	0.0169	4.975	Upregulated	Hs00234579_m1
IL1R2	186009	0.038	4.46	Upregulated	Hs00174759_m1
SEPTIN6	122775	0.019	4.16	Upregulated	Hs00248408_m1
NRG2	170215	0.013	3.6	Upregulated	Hs00171706_m1
SPDEF	155169	0.005	2.87	Upregulated	Hs00171942_m1
TJP3	182089	0.013	2.7	Upregulated	Hs00274276_m1
FGF2	113042	0.03	2.7	Upregulated	Hs00266645_m1
FOXF1	145754	0.0015	6.58	Downregulated	Hs00230962_m1

21 genes were selected for our validation in cohort 1. We selected some of the most differentially expressed genes (FC>4) but we also included genes that had a 2-4 fold change and also some genes involved in the most differentially expressed pathways using the PANTHER binomial statistics tool.

In cohort 2, 10 targets were selected for validation. These included some of the most differentially expressed genes from both p value lists but also genes of known biological significance.

3.3.5 External and independent test set validation

Randomly selected genes identified in cohort 1 as upregulated in recurrent compared to primary samples (n=5) were validated against cohort 2 samples. Likewise, randomly selected genes identified in cohort 2 with a special emphasis on those again upregulated in recurrent versus primary (n=10) were tested against cohort 1 samples.

Validation of 12 upregulated genes in the recurrent samples from both cohorts was performed in an independent set of 10 primary and 3 recurrent serous papillary adenocarcinomas. An additional 2 recurrent samples of different histology were included.

3.4 Results

3.4.1 RNA sample analysis

The quality and quantity of RNA extracted from the primary and the recurrent fresh frozen ovarian tumours was examined prior to its inclusion in microarray analysis. Sample results from the Nano Drop are shown on Table 3.3.

Table 3.3 Nano Drop Analysis of primary (P) and recurrent (R) ovarian cancers

(Cohort 1)

Samples	RNA conc ng/µl	A260/280	A260/230
P1	1310.8	2.14	1.83
P2	746.3	2.15	1.83
P3	292.4	2.14	2
P4	783.5	2.15	1.88
P5	277.3	2.11	2.22
R1	297.4	2.13	1.95
R2	421	2.1	1.84
R3	388.1	2.10	2.10
R4	114.5	2.15	1.89
R5	480	2.1	2.07

(Cohort 2)

Samples	RNA conc ng/µl	A260/280	A260/230
P6	357.2	2.12	2
P7	138.4	2.15	1.87
P8	234.3	2.14	2.05
R6	138.1	2.15	1.80
R7	228.3	2.08	2.03
R8	323.6	2.09	1.92

3.4.2 Statistical analysis

3.4.2.1 Normalisation of Raw Data

The Quantile method of normalization was utilized in the study as per method 3.3.3.2. The goal of the Quantile method is to make the distribution for each array in a set of arrays the same [346].

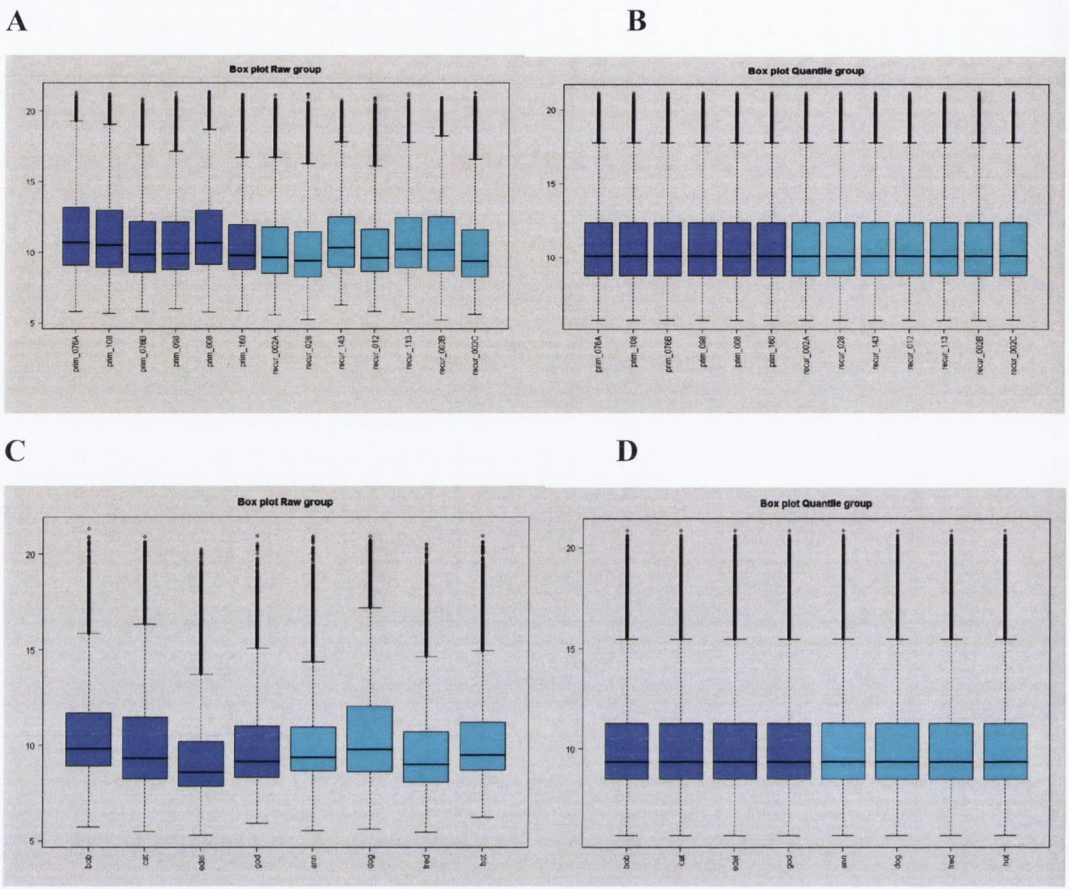

Figure 3.3 Quantile Normalisation of Raw Data in cohort 1 A) Box Plot of Raw Data before Quantile Normalisation B) Box Plot of Data after Quantile Normalisation. Quantile Normalisation in cohort 2. C) Box Plot of Raw Data before Quantile Normalisation D) Box Plot of Data after Quantile Normalisation.

The box plots for signal distribution range were divided into quartiles. Each of four quartiles describes the signal distribution of one fourth of the signal data for that sample (minus outliers). The box plot itself contains the middle 50% of the data. The dark line within the boxed region indicates the median value for the entire distribution of signals. The small black circles at the ends of the first of the first and fourth quartile ranges are probes having signal intensities greater than 2X the value of the interquartile range (boxed region). In general, the raw signal distributions of samples being compared in an analysis should have similar intensity distributions. Quantile normalization shifts all intensities so that the median value and intensity distributions are the same for all array samples included in the analysis (Figure 3.3).

Data distribution and expression variability between hybridizations for both cohorts is displayed in Figure 3.4.

A

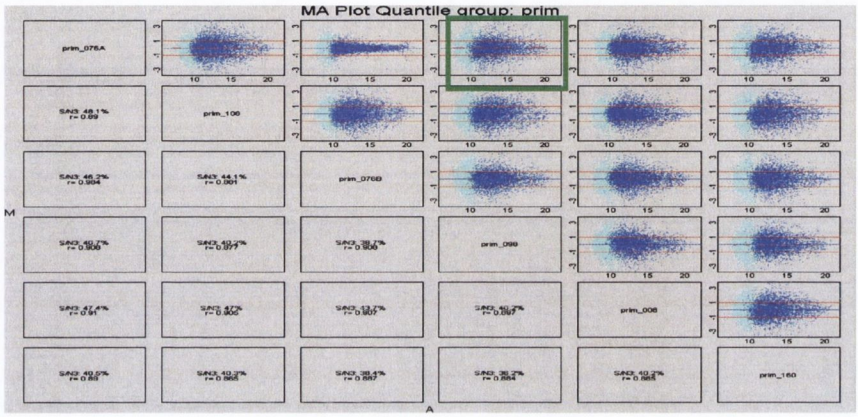

B

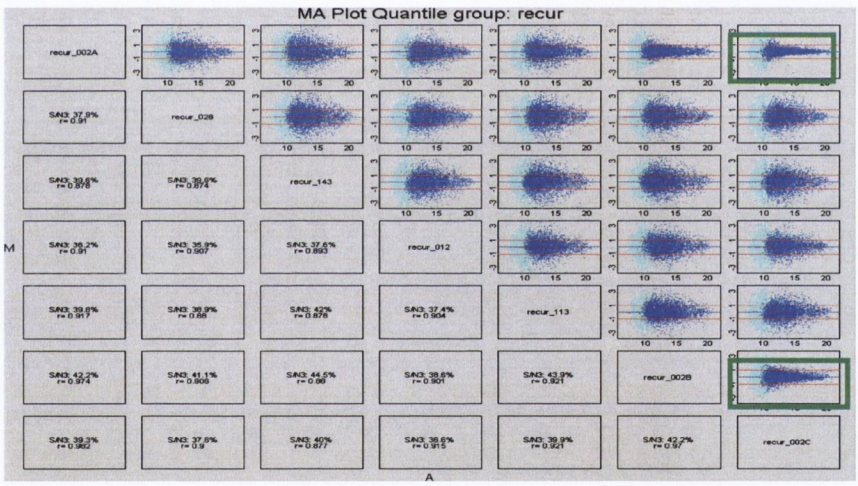

C

D

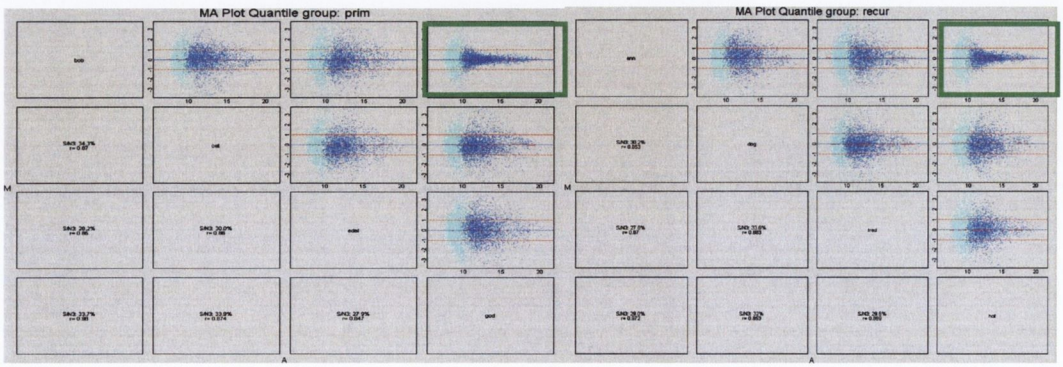

Figure 3.4 MA plots showing data distribution and expression variability between hybridizations. The plot shows all pairs of hybridization in the selected experimental inpool in cohort 1 A) primary samples B) recurrent samples and in cohort 2 C)

primary samples D) recurrent samples. MA plots for replicates are symmetrical around zero and show no appreciable difference (green boxes) whereas MA plots for two unrelated samples show more marked variation, in keeping with what would be expected for a comparison between technical replicates versus a comparison of two unrelated samples.

3.4.2.2 Detection Concordance

S/N detection concordance. The signal is detected if the probe shows S/N ratio equal or above a user defined threshold (default is 3). The S/N detection heatmap shows detection concordance between any pairs of hybridization (Figure 3.5).

A Cohort 1

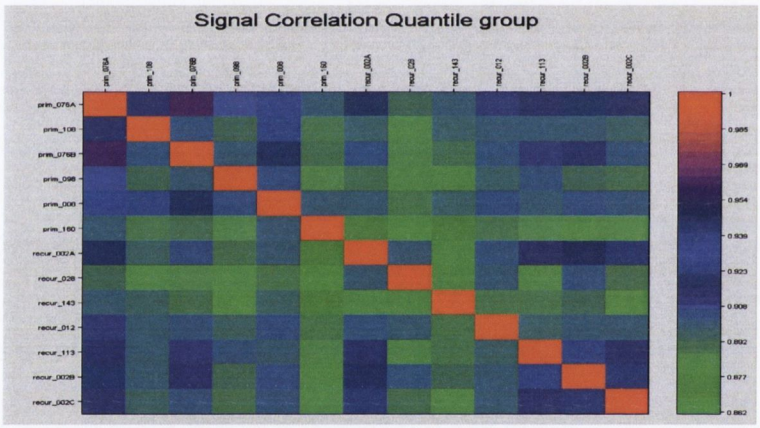

B Cohort 2

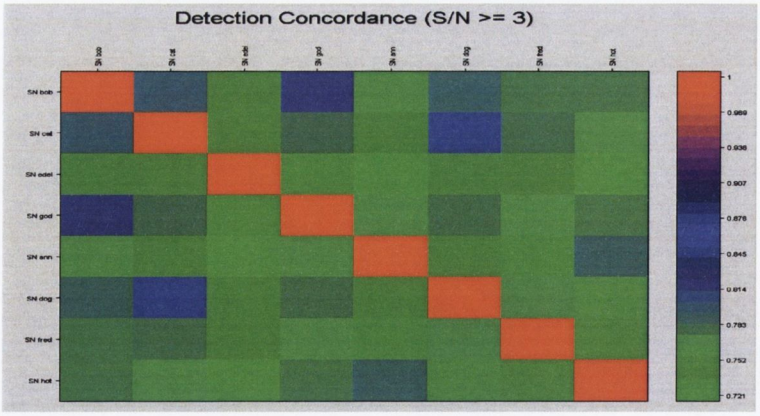

Figure 3.5 Detection concordance heatmap of the quantile normalized data for A) cohort 1 and B) cohort 2. The plots in the form of a heatmap represent all possible pair-wise combinations of samples used in the analysis. The signal is said to be detected if S/N ratio for the probe is equal to or above 3. The concordance value is calculated by taking the intersection of probes considered present (S/N>=3) in both

samples being compared and dividing the average number of genes considered present in both samples.

3.4.3 Gene expression profiling distinguishes primary and recurrent ovarian cancers

To identify potentially important mediators of recurrence in the most frequent histological pattern of ovarian cancer, we performed cDNA microarray experiments on a homogenous set of primary and recurrent serous papillary ovarian tumors (cohort 1).

Between patients results

Gene expression profiling revealed a total of 907 genes as differentially expressed between primary and recurrent samples at $p<0.01$. Using the more stringent false discovery rate (FDR 0.1), this list was narrowed down to 182 genes. Differential expression between primary and recurrent is displayed by scatter and volcano plots in figures 3.6 and 3.7. Included in this FDR list (with the exception of *CLDN16*, which was the top differentially expressed gene in the p value list), were *BTC, S100B, IL27RA, CSRP2, ARFRP1, PVRL2, WASF1, STARD10, LASS4, LGALS3BP, CASK, IFNGR1, PGM2L1, USF2, PERP, ESM, CHORDC1, RNPC1, MGAT4B* and *CACNA1D* which were selected for validation. Table 3.1 displays the fold changes observed for these genes, the corresponding probe identification and the p values.

A

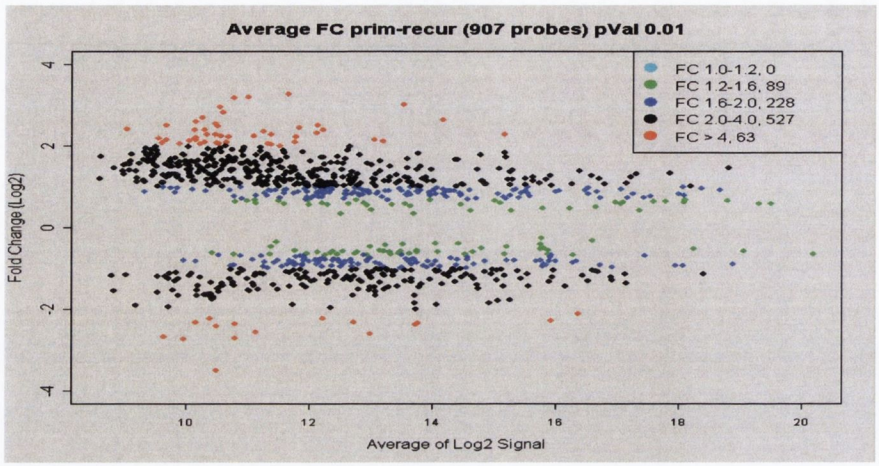

B

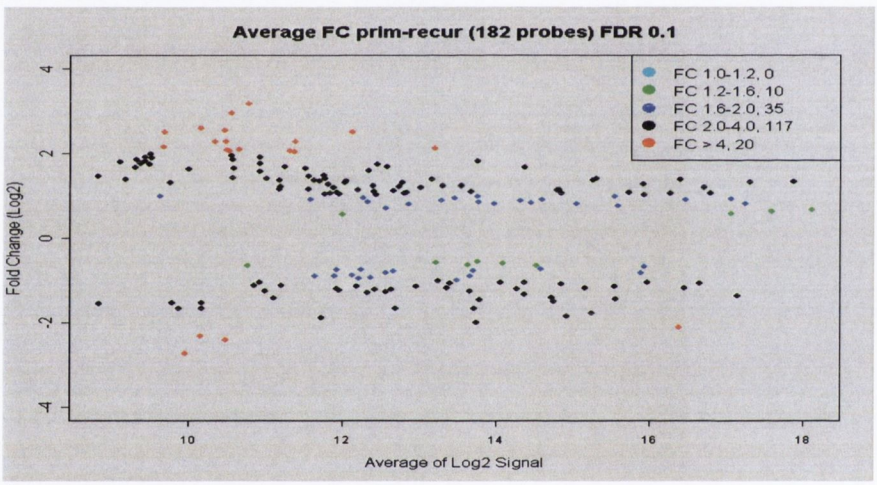

Figure 3.6: Detectable probes with A) p value 0.01 B) FDR 0.1 in primary versus recurrent ovarian cancers in cohort 1. Fold changes are plotted against the average of $\log_2$ signal of each gene.

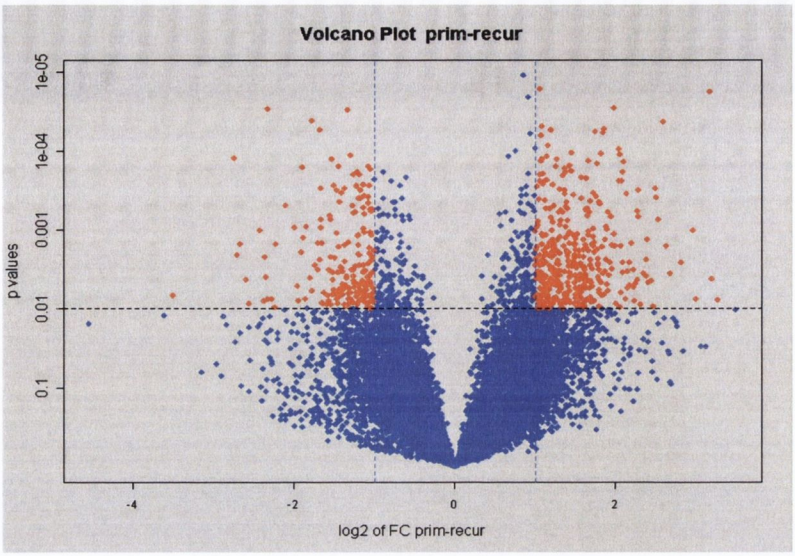

Figure 3.7 Volcano plot of fold changes and p values for differentially expressed genes between primary and recurrent ovarian cancers in cohort 1 for a p 0.01.

Within patients results

To address whether recurrence follows similar patterns and to avoid individual genetic variation, we profiled paired samples from the same patient (cohort 2). A total of 586 genes were differentially expressed between primary and recurrent at $p<0.05$ and this was reduced to 75 genes at $p<0.01$. Differential expression between primary and recurrent is displayed by scatter and volcano plots in figures 3.8 and 3.9. (Figure 3.8). Genes with a fold change greater than 4, upregulated in recurrent compared to primary tumors included: *Septin6, ZNF218, S100A8, MMP9, FOXF1* and *ILIR2* (Table 3.2).

A

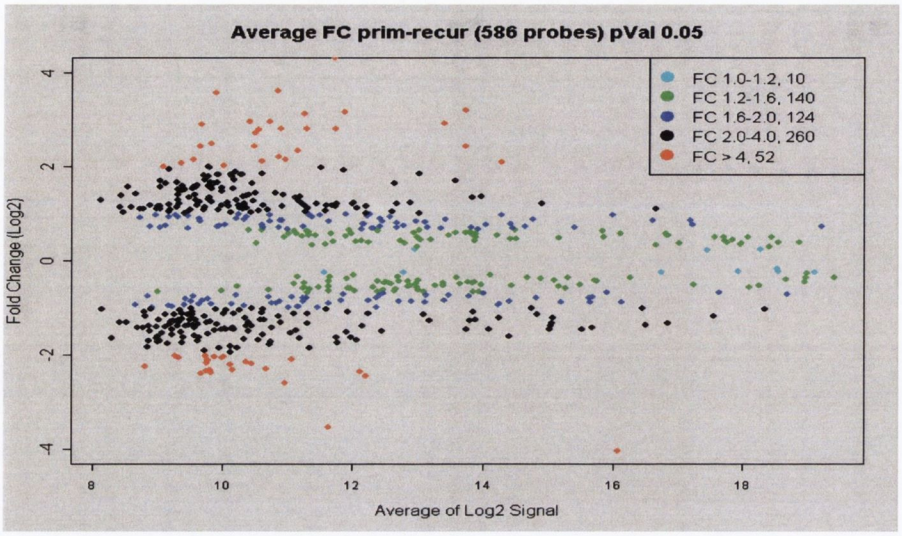

B

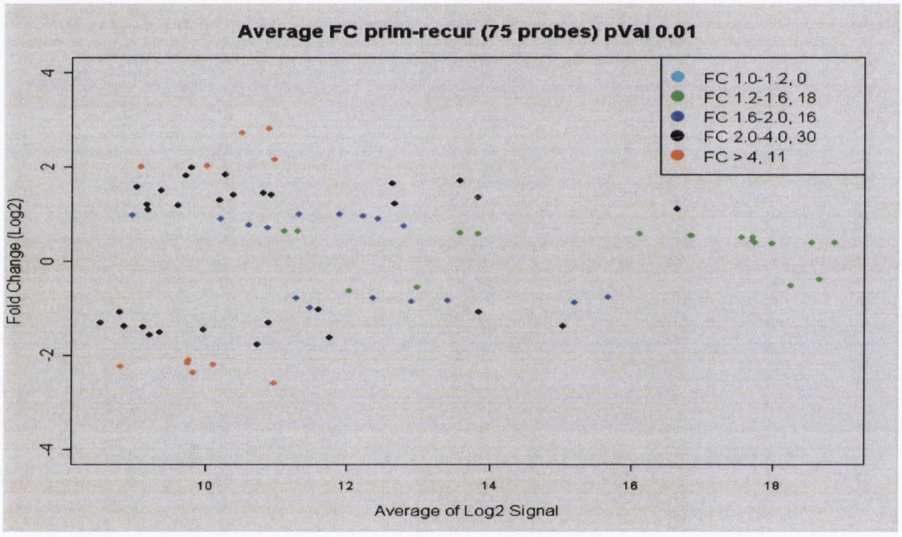

Figure 3.8 Detectable probes with A) p value 0.05 B) p value 0.01 in primary versus recurrent ovarian cancers in cohort 2. Fold changes are plotted against the average of log2 signal of each gene.

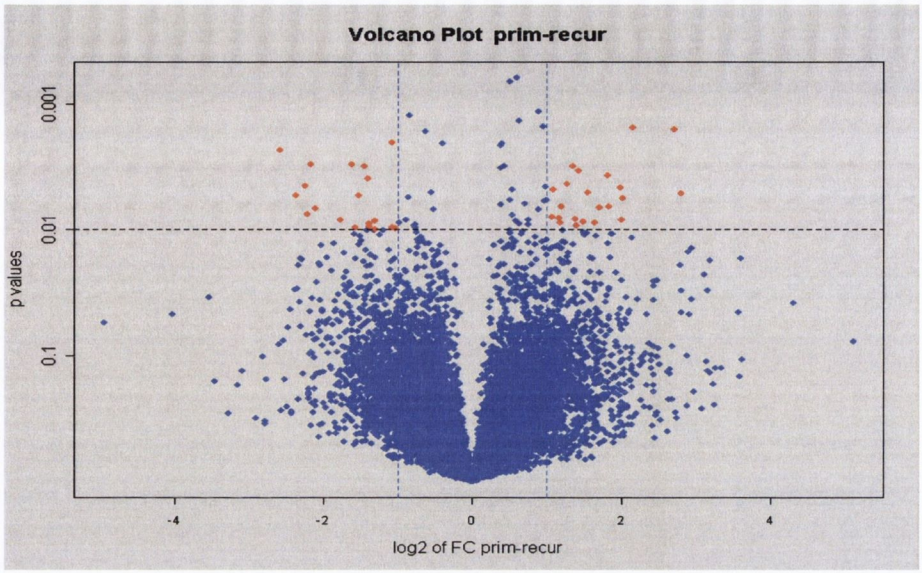

Figure 3.9 Volcano plot of fold changes and p values for differentially expressed genes between primary and recurrent ovarian cancers in cohort 2 for p 0.01.

Hierarchical heat maps, presented in Figures 3.10A and B, for both cohorts, demonstrated distinct gene expression patterns between primary and recurrent ovarian cancers.

A

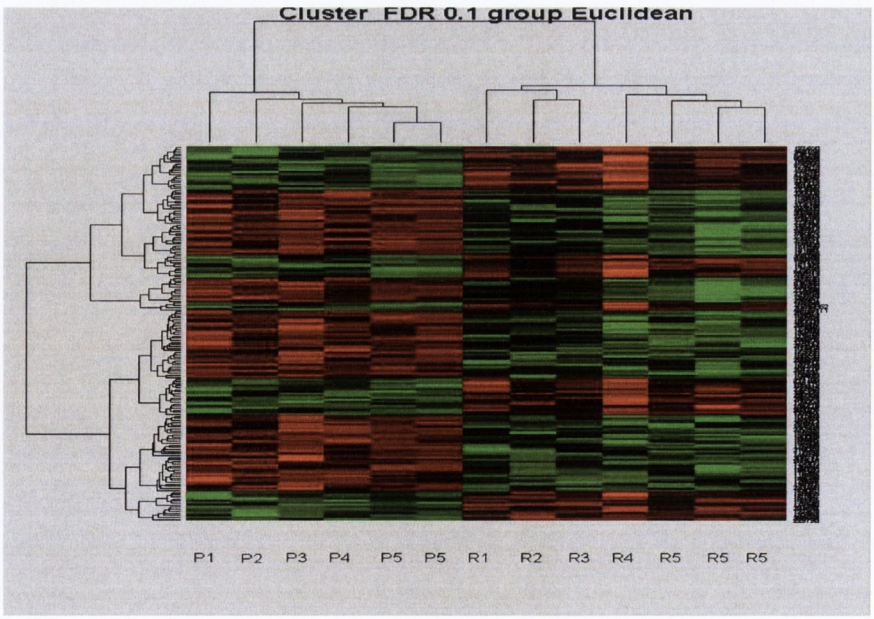

B

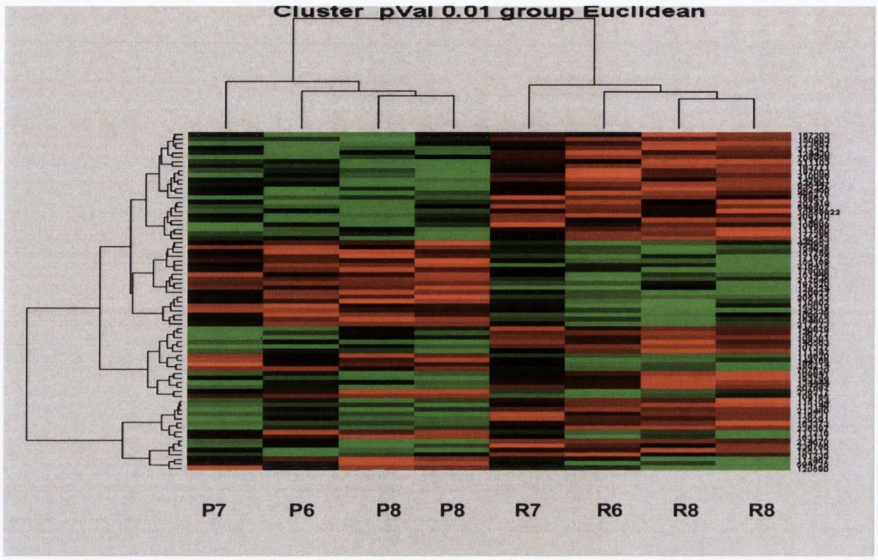

Figure 3.10 Hierarchical cluster heatmaps demonstrating distinct patterns of gene expression between primary and recurrent ovarian tumors. These are produced when less than 500 probes are differentially expressed for a particular threshold level. (a) Heatmap of the ovarian tumors in cohort 1 based on the FDR0.1 list with the primary clustering on the left and the recurrent samples on the right. Vertical bars represent the samples and the horizontal bars represent the genes. Green bars reflect downregulated genes and red bars upregulated genes. (b) Heat map discriminating recurrent (right) and primary (left) ovarian tumours in cohort 2 based on the p0.01 list. P, primary tumours; R, recurrent tumors.

Combined results

We then attempted to combine both cohorts to determine whether a distinct pattern of expression is maintained between primary and recurrent ovarian tumours independent of the histological type. Indeed, total of a 526 genes were differentially expressed between primary and recurrent at $p<0.01$ and this was reduced to 67 genes at FDR<0.25 (Figure 3.11 and 3.12).

A

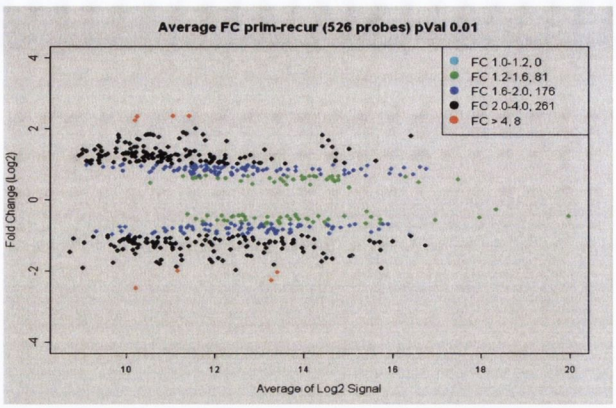

B

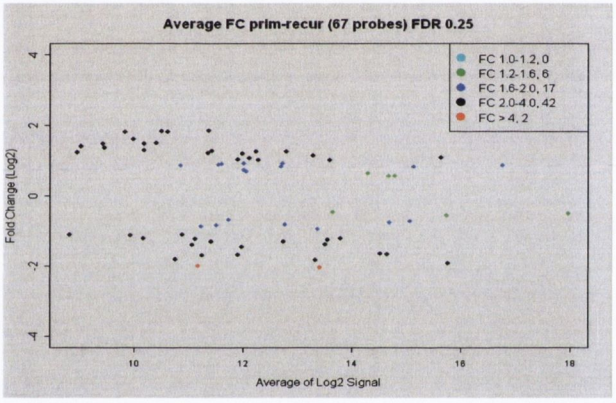

Figure 3.11 Detectable probes with A) p value 0.01 B) FDR 0.25 in primary versus recurrent ovarian cancers in combined cohorts 1&2. Fold changes are plotted against the average of log2 signal of each gene.

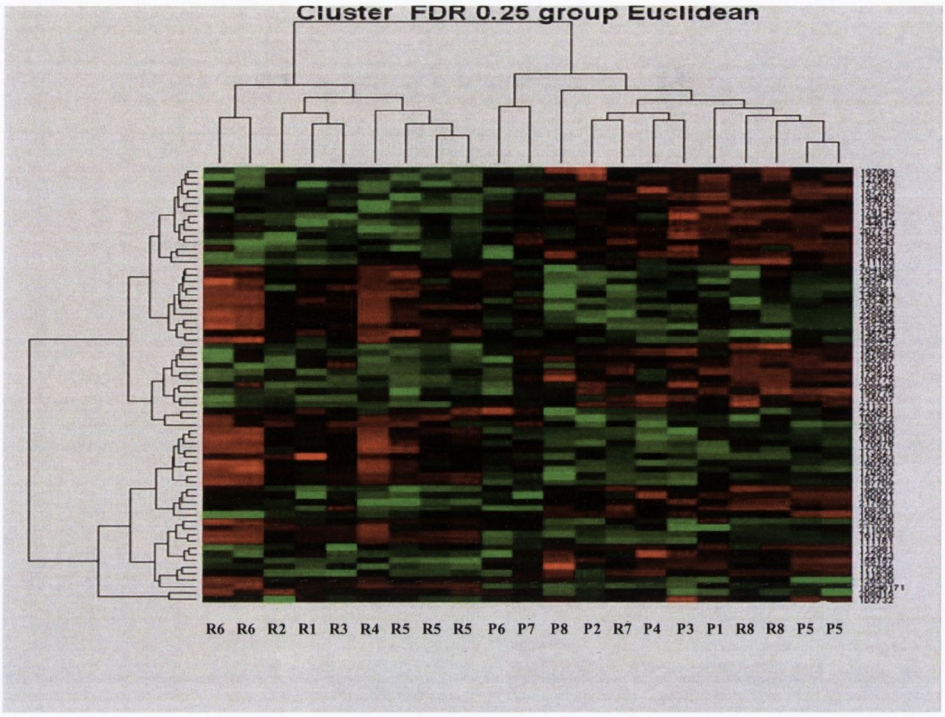

Figure 3.12 Example of a hierarchical cluster heatmap demonstrating distinct patterns of gene expression between primary and recurrent ovarian tumors in combined cohorts 1+2 based on the FDR 0.25 list.

We also aimed to identify which probes were commonly shared between the two cohorts. Surprisingly only two genes of known molecular functions were identified, namely *PVRL2* and *LASS4* but their fold changes were not statistically significant (p values of 0.93 and 0.97 respectively).

Notably, upregulated genes in the recurrent compared to primary tumors in cohort 1 and 2 segregated in the same gene families. Included among these genes are *S100B* and *S100A8* belonging to the *S100* family of calcium binding cytoplasmic proteins, *TJP3* and *CLDN16* belonging to the family of tight junction proteins, *BTC* and *NRG2* belonging to the family of *EGFR* ligands, and interleukin receptors *IL1R2* and *IL27RA* (Figure 3).

Upregulation of tight junction proteins and *EGFR* ligands, development of a cytokine response via interleukin receptors and intracellular signaling via calcium binding *S100* proteins appear to contribute to the "recurrent" signature and possibly have a role in drug resistance.

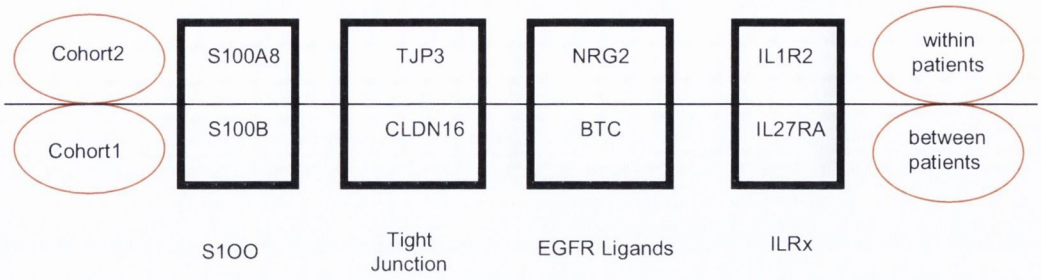

Figure 3.13 Gene families involved in the molecular regulation of recurrence in ovarian cancer. Some of the upregulated genes in recurrent compared to primary ovarian carcinomas that we validated in cohort 2 belong to the same gene families with some of the upregulated genes validated in cohort 1.

3.4.4 PANTHER

Final gene lists were uploaded and analysed in the online database known as PANTHER. Among its functions included are the ability to merge and differentiate genes within lists, to graphically breakdown the protein families of the selected genes and the ability to check for over/under representation of genes in a particular biological function.

3.4.4.1 Pathway Analysis

Final gene lists were uploaded and analysed using Panther. Its functions included the ability to merge and differentiate genes within lists and to graphically breakdown biological processes, molecular functions and "canonical" biological pathways based on the list of deregulated genes in primary versus recurrent ovarian cancers. Examples of biological pathways pie charts are dislplayed in Figures 3.14 and 3.15.

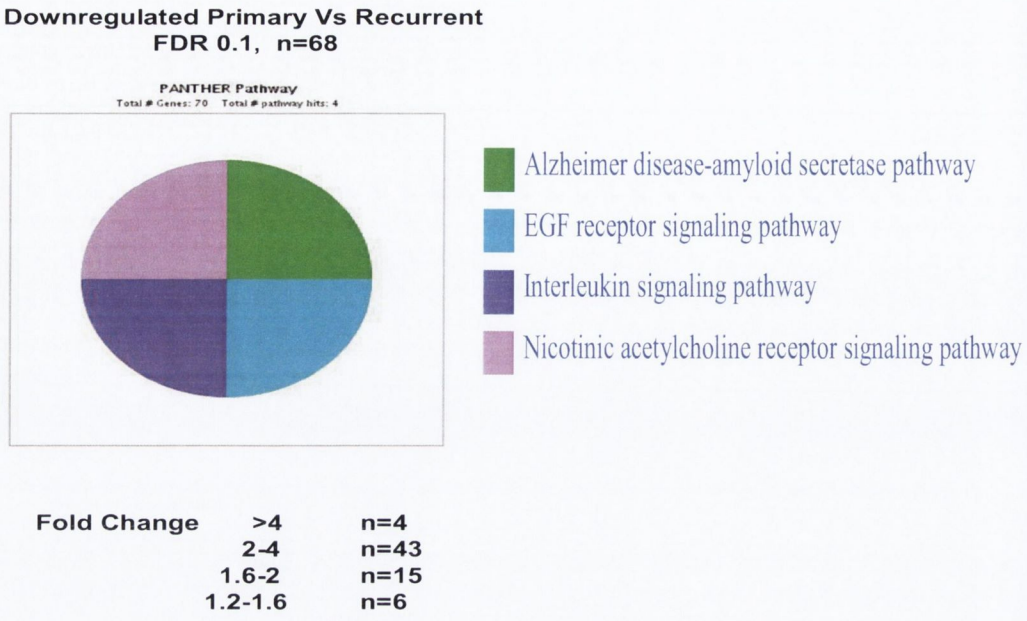

Figure 3.14 Example of a biological pathways pie chart of genes downregulated in primary versus recurrent (hence, upregulated in recurrent versus primary) in cohort 1 based on the FDR 0.1 list. A total of 68 genes were now upregulated in the recurrent compared to the primary samples with various fold changes as displayed. Upregulated pathways include Alzheimer disease-amyloid secrease pathway, *EGF* receptor signalling pathway, interleukin signaling and nicotinic acetylcholine receptor signalling pathway.

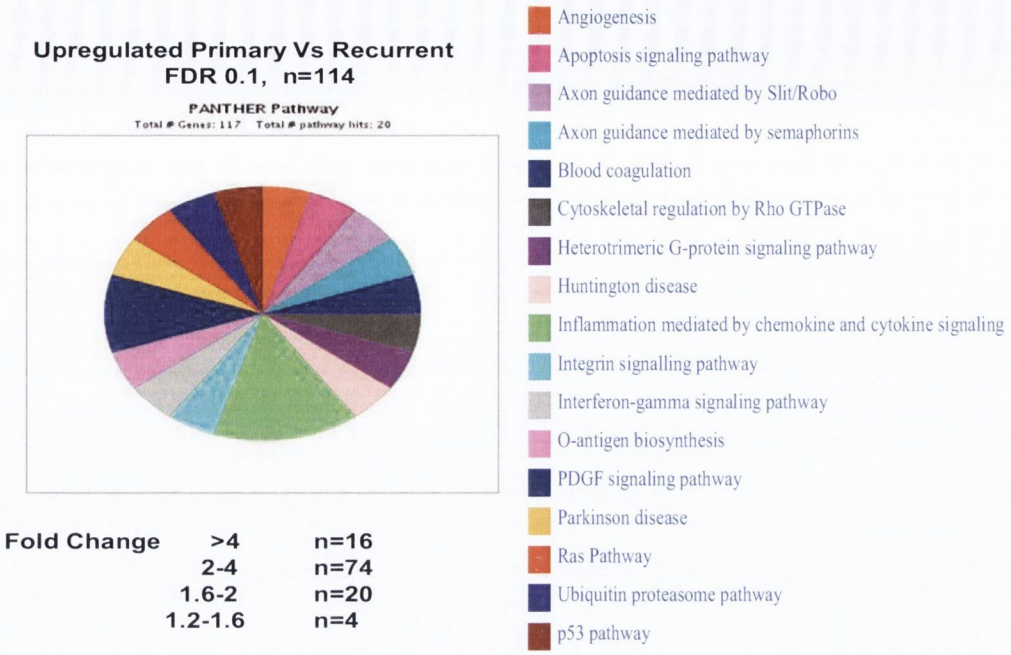

Figure 3.15 Example of a biological pathways pie chart of genes upregulated in primary versus recurrent in cohort 1 based on the FDR 0.1 list. A total of 114 genes were upregulated in the primary compared to the recurrent samples with various fold changes as displayed. The largest sector on the pie chart represents inflammation pathways.

3.4.5 Validation of gene expression by RT-PCR

A panel of genes from both cohorts was selected to confirm the reproducibility of the array data. Using TaqMan® PCR we validated dysregulated genes against different interrogation sets in order to select those likely to represent markers of recurrence (Figure 3.16). Gene selection for TaqMan® validation was based on the most differentially expressed genes from the p and FDR value list with a fold change > 4 but also included genes that had a 2-4 fold change and also some genes involved in the most differentially expressed pathways. Priority was given to selection of genes upregulated in recurrent compared to primary samples, which might provide "recurrence" signatures in ovarian cancer. Upregulated genes validated in both cohorts were alternatively interrogated (external validation) and further advanced for validation in the test set. Independent validation on a test set referred to completely distinct samples of serous histology that were not previously employed in marker development.

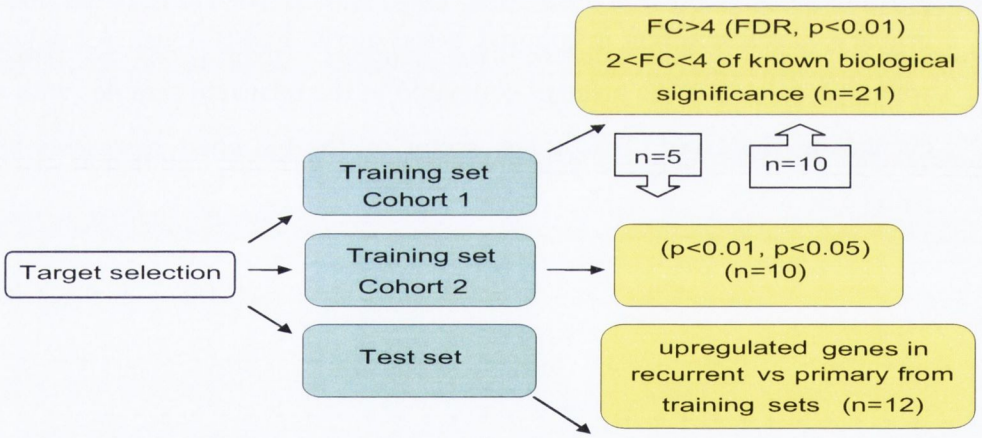

Figure 3.16 TaqMan® PCR validation of target genes in both training and test sets.

A list of the genes chosen for validation together with their molecular function and biological processes is shown in Table 3.4.

Table 3.4 List of selected genes differentially expressed in recurrent versus primary tumours in cohorts 1 and 2 with information about their molecular function, biological processes or pathways involved. Some of these genes have not been previously implicated in ovarian cancer. These genes were chosen to be validated as they might represent markers of recurrence).

Gene Symbol	Molecular function	Biological processes/pathways
Cohort 1		
CLAUDIN 16	Tight junction	Cell structure
S100B	Ca2+ related protein	Assembly of microtubules and intermediate filaments
CACNAID	Voltage gated Ca2+ protein	Transfer of cations,
BTC	*EGFR* binding ligand	*EGFR* signaling
IL27RA	Cytokine receptor	Inflammation, immunity
CHORDC1	Cysteine and histidine rich zinc binding protein	Transport signaling
LASS4	Ceramide synthesis	Lipid metabolism
STARD10	Transfer protein	Lipid and fatty acid transfer
CSRP2	Actin binding protein	Cell growth
RNPC1	Transcription factor RNA binding protein	Nucleic acid metabolism
ARFRP1	Small GTPase	Cadherin signaling

WASF1	Rho GTPase	*TK* receptors and cytoskeleton
PVRL2	Actin binding protein Receptor	Defense immunity Signal transduction
MGAT4B	Glycosyl transferase	Glycosylation, cell growth
LGALS3BP	Galectin binding protein	Cell adhesion signaling
PERP	*p53* induced protein related	Apoptosis
PGM2L1	Mutase	O antigen synthesis
IFNGR1	Receptor	Interferon signalling pathway
USF2	Transcription factor acid	Regulation of steroid, nucleic and lipid metabolism
CASK	Protein kinase	Phosphorylation, cell adhesion
ESM1	Endothelial cell specific growth factor	Cell structure

Cohort 2

S1OOA8	Ca2+ related protein	Assembly of microtubules and intermediate filaments
ZNF218	Transcription factor	Transcription regulation
MMP9	Extracellular matrix protein	Proteolysis

IL1R2	Cytokine receptor	Inflammation, immunity
SEPTIN6	Cytoskeletal protein	Cytokinesis
NRG2	*ERbB* receptor binding ligand	*ERbB* receptor signalling
SPDEF	*ETS* containing transcription factor	Transcription regulation
TJP3	Tight junction	Cell structure
FGF2	*FGF* binding ligand	*FGF* signaling pathway
FOXF1	Transcription factor	Cell cycle control, proliferation

Correlation was carried out using Spearman correlation co-efficient. The fold changes in the arrays were plotted against relative quantitation from the TaqMan® analyses of recurrent versus primary tumors. High concordance was revealed between TaqMan® and microarray experiments in cohort 1 ($r=0.874$, $p<0.01$) (Figure 3.17) and cohort 2 ($r=0.845$, $p<0.05$) (Figure 3.18).

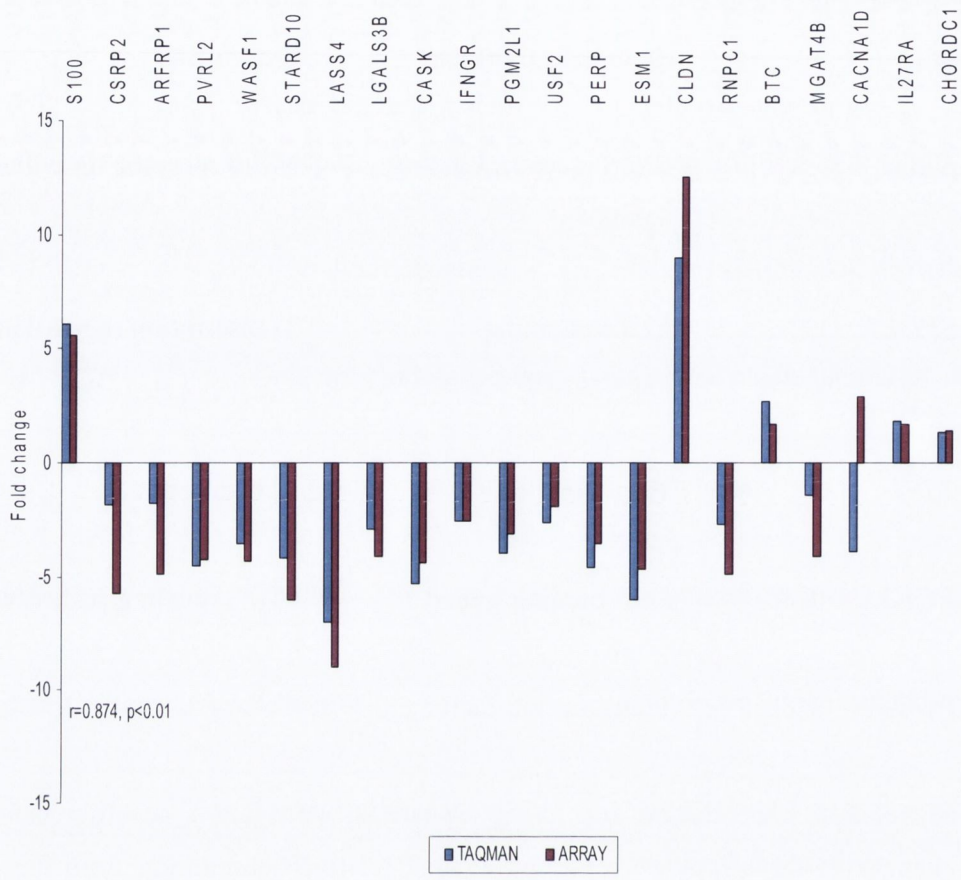

Figure 3.17 TaqMan® PCR validation of microarray experiments in cohort 1. The TaqMan® values are displayed in blue and the array results in red.

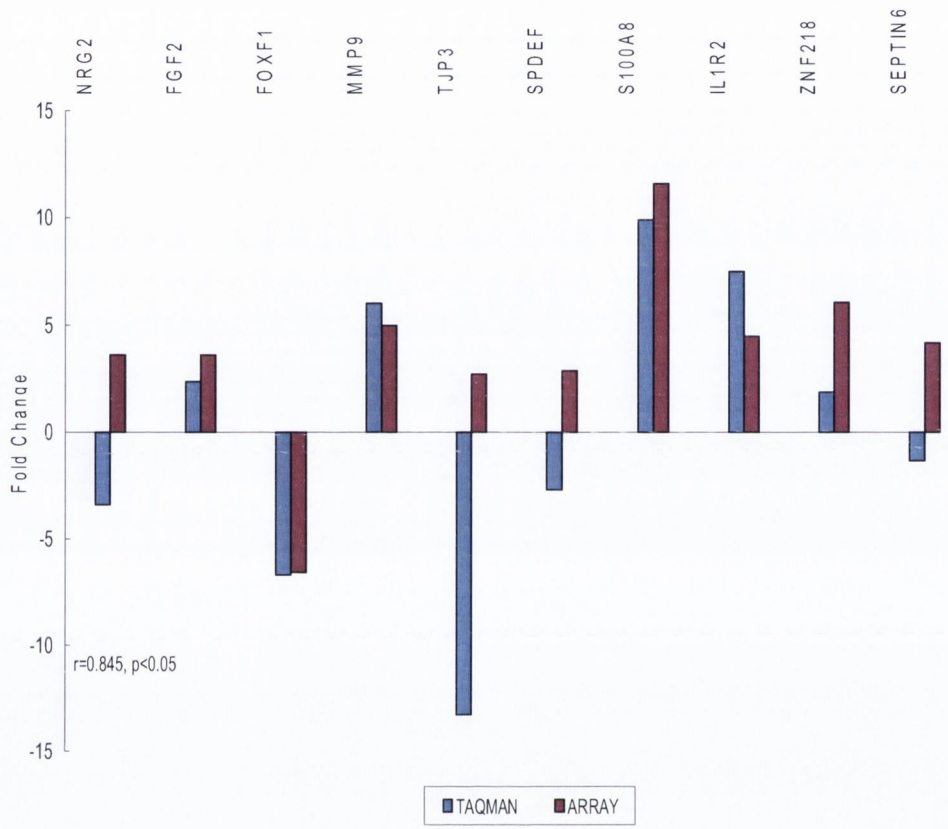

Figure 3.18 TaqMan® PCR validation of microarray experiments in cohort 2. A similar concordance was observed as in cohort 1.

IL1R2 and *ZNF218* identified in cohort 2 as upregulated in recurrent, when validated in samples from cohort 1, gave the best distinction with fold changes of 2.81 and 2.94 respectively (Figure 3.19). No significant difference was observed between recurrent and primary samples for the remaining 13 which is in accordance with the array results.

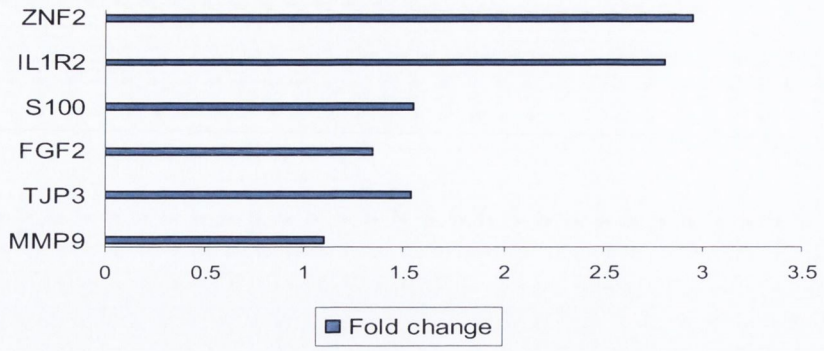

Figure 3.19 External validation of a subset of upregulated genes in cohort 2 that validated in cohort 1. Bars indicate the relative overexpression of target genes in recurrent vs primary tumors. *IL1R2* and *ZNF218* gave the best distinction between recurrent and primary tumors with greater than twofold changes.

Validation of candidate genes by RT-PCR from an independent set of specimens represents a more accurate method for measuring gene expression, as opposed to establishing a test set from the microarray data. Consecutively independent validation of a subset of the above genes (n=12) from both cohorts was carried out in our test set of primary and recurrent serous papillary adenocarcinomas (n=13) using TaqMan® PCR to identify if these targets were possible markers of recurrence for serous papillary adenocarcinomas (Figure 3.20). *BTC* and *FGF2* provided the best distinction between recurrent and primary tumors with fold changes of 2.8 and 2.71 respectively. Adding 2 recurrent samples of different histologies to the previously homogeneous histological sample cohort conferred no statistical significance for any of the validated genes (fold changes<2). These were subsequently excluded from the analysis to preserve homogeneity in the test set.

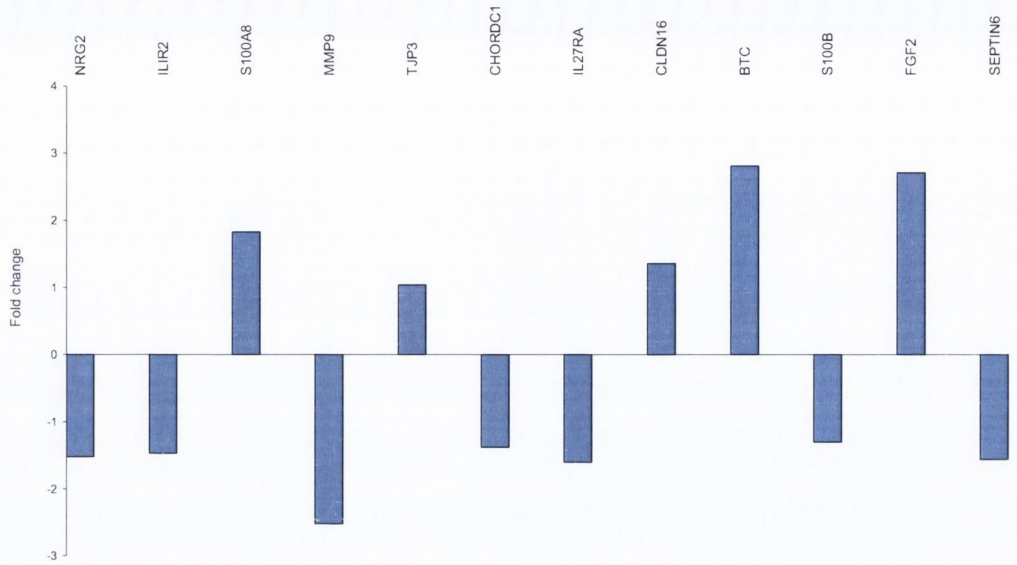

Figure 3.20 Independent TaqMan® PCR validation of a set of selected genes, upregulated in recurrent samples, from both cohorts in a test set of serous papillary adenocarcinomas of varying grade and stage. *BTC* and *FGF2* provided the best distinction between recurrent and primary tumours with fold changes of 2.8 and 2.71 respectively.

The results confirm the utility of the derived set of markers as potential markers of recurrence. The IPA software [345] was used to analyse the above upregulated genes from both cohorts in an attempt to integrate them in a single dynamic pathway. Recurrence is rather multifactorial as indicated by non identification of such a biochemical pathway to relate the above targets.

3.5 Discussion

This investigation demonstrates a distinct pattern of gene expression between primary and recurrent ovarian carcinomas in vivo and represents an effort to discover potentially important mediators of recurrence. It also addresses whether mechanisms of gene dysregulation in recurrent versus primary paired tumors are unique to those pairs. In order to address chemoresistance and minimise parameters introducing variations, well characterized tumors of the commonest histological subtype (serous papillary adenocarcinoma) were selected in cohort 1. In cohort 2, we used paired samples with identical genetic background (from the same patients). Such samples are valuable since second-look laparotomy in Europe is a rather uncommon practice in the treatment of ovarian cancer. To our knowledge, this dual approach of profiling primary and recurrent ovarian cancers in vivo has never been previously performed.

Unsupervised hierarchical clustering of the samples in both cohorts unambiguously separated primary and recurrent tumors. The substantial number of gene expression differences between the two groups, in particular cohort 2, reflects progression of the tumours from a primary to a relapsed state, but is also consistent with the hypothesis that tumor cells surviving chemotherapeutic treatment alter their gene expression allowing them to withstand the selective pressure of the drugs used. In fact, the "log kill" effect of cytotoxic chemotherapy significantly reduces tumor cells that are sensitive to the administered therapy [347]. Hence, one is inclined to think that recurrent tumors are enriched with resistant clones and likely to display molecular signatures more associated with acquired chemoresistance. Acquired resistance is likely to reflect changes in gene regulation rather than mutation-dependent clone selection [348], especially in solid tumors which have relatively low doubling rates.

Nonetheless, genes upregulated in recurrent compared to primary advanced ovarian tumors could be invoked as "recurrent metastasis virulent genes" that provide a selective advantage in recurrent sites but not in primary tumorigenicity [349]. This does not exclude the importance of genes identified and validated as upregulated in primary versus recurrent tumours as they can also signify mechanisms involved in recurrence/chemoresistance. To mention but a few, *CHORDC1*, has a less well established role in mediating chemotherapy resistance. The gene, located in 11q14.3 chromosome, encodes a zinc binding protein, a cysteine rich domain and by

facilitating cysteine entry in exchange to glutamate, it can regulate intracellular glutathione levels, which in turn may lead to drug inactivation and therefore chemoresistance [217]

STARD10, which encodes a *START* domain protein, was the most upregulated gene in our primary tumours. *STARD10* expression is abundant in liver, where it acts as a steroidogenic acute regulatory protein that mediates binding of lipids. Apart from a function in intracellular lipid transfer, *START* domains are hypothesized to act as lipid sensors with a regulatory role in signal transduction and transcription. For example, the *START* domain proteins *DLC1/2* are candidate tumor suppressors in hepatocellular cancer [350]. *STARD10* was identified as a protein overexpressed in breast cancer that cooperates with the *ErbB* family of receptor tyrosine kinases in cellular transformation [351]. Lower expression of *STARD10* and other (ie, *LASS4*, *DENND*, *TNSC*, *C1QTNF7*) tumour suppressor or anti-proliferative genes in the recurrent tumours would support the concept that a decreased proliferative state may be involved in the development of aquired chemoresistance.

Validation of targets was satisfactory as indicated by Spearman coefficients. Some variation may be due to differences in sensitivity between the two techniques, probably because of the number of absent cells made during normalisation of the microarray data or the asymmetry in the number of samples used in both cohorts.

We identified and validated genes upregulated in the recurrent tumors, which may be the signature expression pattern of drug resistant cancers (Tables 3.1 and 3.2). Some of the genes identified in the two cohorts belong to the same gene families corroborating the importance of several distinct gene families in the molecular regulation of ovarian cancer recurrence. Since all patients in both cohorts were treated with platinum based therapy and some of the identified genes are thought to be correlated to the mode of action of chemotherapeutic agents as discussed below, it is interesting to speculate that some of the mechanisms involved in recurrence are specific to the drugs used. Whether the genes represent etiologic causes of drug resistance or treatment failure remains to be further answered.

S100B was the most differentially upregulated gene in recurrent serous tumors (FDR 0.1). It constitutes a calcium binding cytoplasmic protein, involved in intracellular signaling. Historically used in the clinical management of malignant melanomas, it was found to be a negative regulator of *p53* [352]. If elevated *S100B* levels cause downregulation of *p53*, apoptotic pathways are not induced resulting in uncontrolled tumor growth or resistant phenotypes [353]. A recent proteomic study identified a putative S100 protein to be upregulated in cisplatin resistant cell lines [354]. Other members of the S100 family, including *S100A8*, identified in cohort 2, are overexpressed in common cancers. *S100B* is also involved in the assembly and disassembly of microtubules [355] and therefore might interfere with the mechanism of action of paclitaxel, which is currently used in the treatment of ovarian cancer.

CLDN16 was the most upregulated gene in the recurrent serous tumors ($p<0.01$) in cohort 1. It belongs to the family of claudins, tight junction (TJs) - associated proteins endowed with well-characterized roles in individual viability, epithelial differentiation and tumor growth probably by stabilizing tumor cell connection. A link between cisplatin exposure and cytoskeletal alterations has been reported [356]. Notably, *CLDN16* has been characterized as a novel human ovarian cancer-specific transcript using serial analysis of gene expression data [357].

Other members of the family, *CLDN3* and *CLDN4* are frequently overexpressed in ovarian cancer, as identified by both SAGE and microarray studies [358] [359] . In one of these studies, small interfering RNA (siRNA) analysis has also shown *CLDN3* expression to increase invasion and survival of ovarian tumor cells [358]. They have also been described to function as receptors for Clostridium Perfringens Enterotoxin [360], a finding that might open novel treatment approaches in ovarian cancer. *CLDN7* is significantly overexpressed in all main histologic types of EOC and in single neoplastic cells disseminated in peritoneal cavity and pleural effusions, suggesting its potential role as novel diagnostic marker in ovarian cancer [361]. Expression levels of *CLDN10* are associated with recurrence of primary hepatocellular carcinoma [362]. A proteomic study identified *CLDN4* as overexpressed in cisplatin resistance cell lines [354].

TJP3, another discriminatory gene identified in cohort 2, anchors to the cytoplasmic tail of claudins [363]. No studies on the relationship between TJs and chemotherapy response have been carried out. The functional role of *CLDN16* and *TJP3* in carcinogenesis is unknown. As loss of cell-cell contact has been noted to induce apoptosis [364], one would hypothesise that increased contact through tight junctions as a result of upregulation of these component proteins may favor tumor survival. Transmembrane proteins are also more likely to remodel the tumor microenvironment to favor drug resistance [365].

Of particular interest are putative markers among the coexpressed genes *ILIR2* and *ZNF218* that we validated in cohort 2 and they provided the best discrimination between primary and recurrent serous neoplasms in cohort 1. The role of cytokines and their receptors is well established in the epithelial cancer microenvironment [366] with *IL8* and *IL6* known to be involved in ovarian cancer pathogenesis [367]. A novel regimen of immunomodulatory cytokines and carboplatin show promising results on completion of a phase II clinical trial, in recurrent ovarian cancer [368]. The function of *IL1*, a proinflammatory cytokine, is closely associated with the interactions between B-Cells and T-Cells. *IL1* activates Antigen Presenting Cell and CD4+ lymphocytes affecting the differentiation of the B-Cells and T-Cells and other immunocompetent cells and takes part in the regulation of productions of other cytokines and Granulocyte-Macrophage Colony-Stimulating Factor [369]. *IL1*, is required for tumor invasiveness and angiogenesis in a variety of malignant lesions [370] and particularly in metastatic human tumor specimens [371]. Targeting *IL1R2* may be an appropriate therapeutic strategy for inhibiting tumor angiogenesis. *IL1R2* may provide an insight into the biology of recurrent ovarian tumors, suggesting an initial immune response to the relapsing neoplasm and may secondly represent a surrogate marker of recurrence in ovarian cancer.

ZNF 218 encodes for a newly described zinc finger protein located on chromosome 20q13.2 and has never been previously reported in ovarian cancer. Frequent amplification of DNA at 20q has been demonstrated by comparative genomic hybridization in ovarian cancer [372] and is associated with poor prognosis [373]. Given that amplification appears to be the predominant mechanism leading to

overexpression of genes, *ZNF 218* emerges as a strong candidate oncogene related to ovarian cancer [374].

External validation using independent sets of samples is a critical step in view of the potential for false-discovery using microarrays. In this regard, a test set of 13 serous papillary ovarian adenocarcinomas (primary and recurrent) of various stages and grades, given the same initial chemotherapy treatment, was used for relative quantitation of 12 targets upregulated in recurrent versus primary tumors. An elevated mRNA expression (FC>2) was observed for 2 out of 12 genes, namely *BTC* and *FGF2*, which bind to Epidermal Growth Factor Receptor (*EGFR* or *ErbB1*) and Fibroblast Growth Factor Receptor (*FGFR*) respectively. These genes gave the best distinction between primary and recurrent tumors in our test set of serous tumors. The inclusion of two tumors (n=2) of nonserous histologies (i.e. yolk sac and clear cell) in the previously homogenous test set conferred no statistical significance for any of the validated genes (FC<2), suggesting that various histological types may have variable chemosensitivities. Since *EGFR* and *FGFR* stimulate a similar repertoire of intracellular signaling pathways [375], this certain pattern of expression evident in the recurrent serous ovarian cancers deserves special consideration.

Despite the well established significance of *EGFR* in the progression of ovarian cancer [376], the role of *EGF* ligands in ovarian cancer is still poorly understood. Overexpression of *EGFR* is found in up to 75% of ovarian cancers and is associated with chemoresistance and poor prognosis [377]. Co-overexpression of *EGFR* and *HER2-neu* is also common in ovarian cancer [378]. Our study suggests that overproduction of ligands (*BTC* and *NRG2*), rather than overproduction of receptors could be the predominant mechanism that the *ErbB* pathway uses to generate cancer cell proliferation signals. Combined targeting of *ErbB* receptors and their ligands produces a synergistic antitumor effect [379] because of their non-overlapping functions.

BTC binding to *EGFR* initiates significant signal transduction pathways, such as MAPK and PI-3-kinase–Akt (PI3K/Akt) [380] in a metalloprotease dependent manner [381, 382]. The PI3K/Akt pathway promotes cell survival and has been identified as a potential contributor to drug resistance [383]. *MMP-9* co-upregulation was also observed in our study, which is in agreement with the finding that *MMP-9*

(and *MMP-14*) mRNA levels are selectively increased in response to *EGFR* activity in ovarian tumor cells [384]. Metalloproteases have also been described in a novel drug-resistant phenomenon [385]. Overexpression of stromal *MMP-9* is independently associated with shorter disease-specific survival (DSS) in EOC [207]. Evaluation of *MMP-9* expression seems to add valuable information for breast cancer prognosis [386]. *MMP-9* overexpression has been recently reported in human prostate cancer stem cells [387]. *EGFR* ligands and matrix metalloproteases constitute a vascular-remodeling program that facilitates pathological angiogenesis in mammary tumours [388].

FGF ligands are mitogenic growth factors, generally known to act in a local manner. Binding of the *FGFs* to their high affinity receptors cause the activation of intrinsic tyrosine kinase and a cascade of events, leading eventually to the induction of gene transcription and to cell proliferation. They also represent important tumour angiogenic and endothelial cell (ECs) survival factors. *FGF2* is responsible for extracellular matrix (ECM) production and release of MMPs for selective degradation and reorganization of ECM. This function seems to be implicated in cancer invasion and metastasis, probably through upregulation of *MMP9* [389], which was also upregulated in our study, as mentioned above. *MMP9* proteolytically cleaves and activates latent *TGF-β*, promoting tumour invasion and angiogenesis [390]. It has been described in prostate cancer [391] and hepatocellular carcinoma augmenting a *VEGF*-mediated angiogenesis [392]. *FGF2* also induces expression of the antiapoptotic proteins *bcl-XL* and *bcl-2* via the *MEK/ERK* signaling pathway and correlate with resistance to etoposide-induced apoptosis [393]. A recent study on the repertoire of mutated human cancer genes, based on the family of protein kinases, identified the *FGF* signaling pathway to confer growth advantage by the highest enrichment for kinases containing "driver" mutations [394]. *FGF2* critically modulates mesenchymal-to-epithelial transition, which is now widely accepted to contribute to carcinoma invasiveness [395]. These findings would explain the acquired metastatic capacity or recurrence pattern of advanced epithelial ovarian cancers, which are mesothelially derived and suggest a role for *FGF2* as an epithelial marker in strategies to block epithelialization of metastases.

Collectively, our data propose an integrative model for recurrence in ovarian cancer, in which tumor cells during relapse produce adhesion molecules to mediate attachment, cytokines and inflammatory mediators to stimulate survival and a variety of growth factors bound to their cognate receptors to fully proliferate in order to confront and modulate their immediate environment, which they must eventually overtake (Figure 3.21).

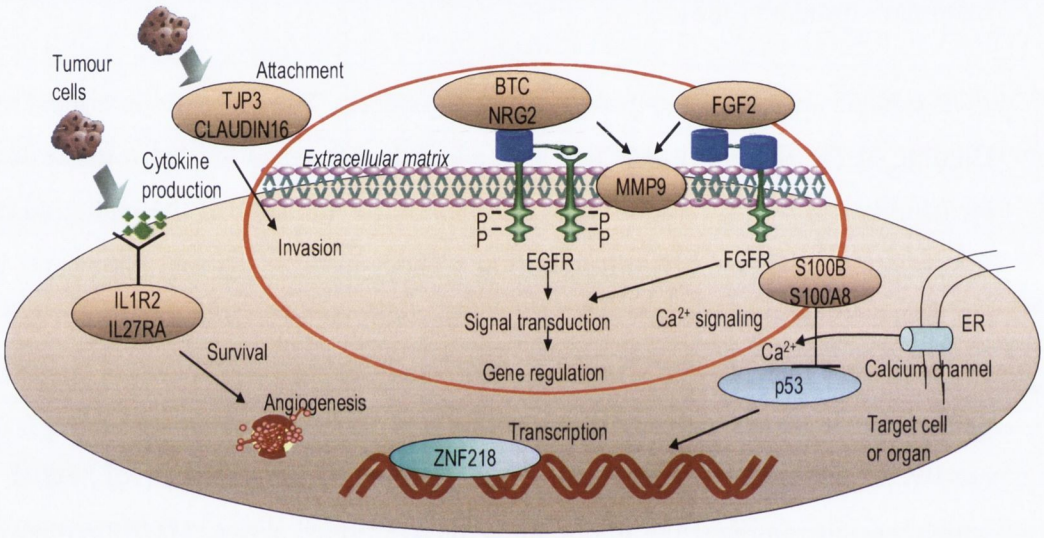

Figure 3.21 An integrative model for recurrence in ovarian cancer. Schematic representation of putative genes and gene families involved in the recurrence of ovarian carcinomas. According to our current working concept, tumour cells during relapse produce adhesion molecules to mediate attachment and invasion via co-overexpression of matrix metalloproteinases, cytokines and inflammatory mediators to stimulate survival and a variety of growth factors bound to their cognate receptors to fully proliferate in order to confront and modulate their immediate environment, which they must eventually overtake.

To date, the histological type of the ovarian cancer is not used as a factor to determine chemotherapy management. As the best strategy for second-line chemotherapy has not yet been defined, the proposed panel of genes could reduce at least in individual patients, unnecessary chemotherapy treatment and toxicity or

alternatively could be readily used for early detection of disease recurrence. Clearly, a definite role for the candidate targets will be provided by functionally investigating the mechanisms involved in the development of recurrence and drug resistance. These types of analyses may lead to novel approaches for the development of therapy aimed at reversing or decreasing drug resistance or alternatively optimization of the already available standard drugs [270]. A synchronous targeting of co-amplified genes may in the future offer better treatment for recurrent ovarian cancer.

CHAPTER 4

Potential role of miR-9 and miR-223 in recurrent ovarian cancer

4.1 Summary

Background: microRNAs (miRNAs) are small, noncoding RNAs that negatively regulate gene expression by binding to target mRNAs. miRNAs have not been comprehensively studied in recurrent ovarian cancer, yet an incurable disease.

Results: Using real-time RT-PCR, we obtained distinct miRNA expression profiles between primary and recurrent serous papillary ovarian adenocarcinomas (n=6) in a subset of samples previously used in a transcriptome approach. Expression levels of top dysregulated miRNA genes, miR-223 and miR-9, were examined using TaqMan PCR in independent cohorts of fresh frozen (n=18) and FFPE serous ovarian tumours (n=22). Concordance was observed on TaqMan analysis for miR-223 and miR-9 between the training cohort and the independent test cohorts. Target prediction analysis for the above miRNAs identified genes previously validated in our transcriptome study. Common biological pathways well characterised in ovarian cancer were shared by miR-9 and miR-223 lists of predicted target genes. This "recurrent metastatic signature" can predict progression free survival in ovarian cancer patients.We provide strong evidence that miR-9 acts as a tumour suppressor gene in recurrent ovarian cancer. Components of the miRNA processing machinery, such as Dicer and Drosha are not responsible for miRNA deregulation in recurrent ovarian cancer, as deluded by TaqMan and immunohistochemistry.

Conclusion: We propose a miRNA model for the molecular pathogenesis of recurrent ovarian cancer. Some of the differentially deregulated miRNAs identified correlate with our previous transcriptome findings. Based on integrated transcriptome and miRNA analysis, miR-9 and miR-223 can be of potential importance as biomarkers in recurrent ovarian cancer.

4.2 Introduction

A new and surprisingly abundant class of RNA regulatory genes known as microRNAs (miRNAs) has been found to confer a novel layer of genetic regulation in cells. They function as endogenous, highly conserved, non-coding small RNA's, 22 nucleotides long that silence gene expression by binding to target mRNAs. Their 5' end binds its target complementary sequence in the 3'–untranslated region (3'UTR) of mRNA and given the degree of complementarity, miRNA binding appears to result in translational repression, or in some cases, cleavage of cognate mRNAs, causing partial or full silencing of the respective protein-coding genes [310].

An accumulating body of evidence reveals critical functions for miRNAs in various biological processes as diverse as proliferation, apoptosis, and cell differentiation [396] and given their diversity and abundance, miRNAs appear to functionally interact with various components of many cellular networks. Almost 30% of the human genome is estimated to be regulated by miRNAs [397]. Therefore, they should be considered one of the largest classes of gene regulators. Figure 4.1 illustrates the miRNA biogenesis and evolution.

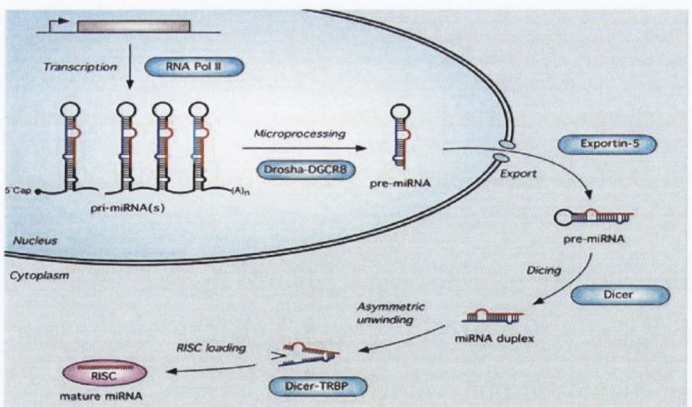

Figure 4.1 miRNA biogenesis and evolution.

In an attempt to understand the biology of recurrent ovarian cancer, we examined the expression of 180 miRNAs in primary and recurrent serous papillary adenocarcinomas, which were previously interrogated in a transcriptome study in recurrence [398, 399] as described in chapter 3. miRNAs with greatest changes in expression were further used in a larger group to predict progression free survival

(PFS) and overall survival (OS). The aim of this chapter is to investigate the role of miRNAs in recurrent ovarian cancer and to examine the expression levels of key components of the miRNA machinery. A flow chart of our experimental design is shown in Figure 4.2.

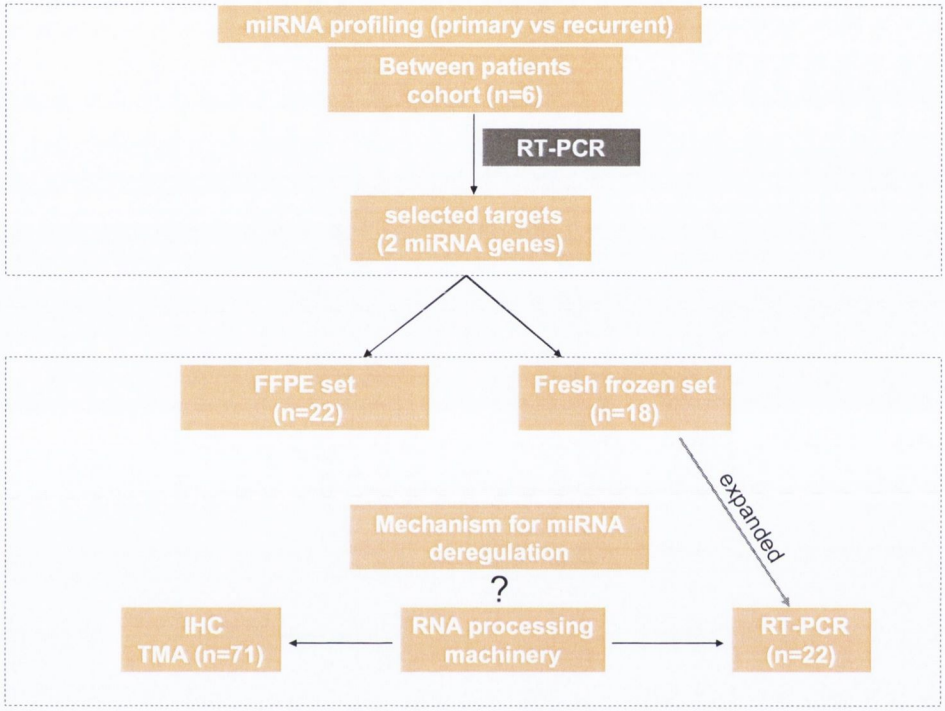

Figure 4.2 Flow chart of our study design. miRNA profiling was performed using TaqMan PCR in a homogenous set of 3 primary advanced and 3 recurrent serous papillary ovarian adenocarcinomas from different patients. Selected miRNA targets (n=2) were validated in two independent sets of primary and recurrent fresh frozen (n=18) and FFPE serous papillary adenocarcinomas (n=22). We also attempted to determine whether components of the miRNA processing machinery (Dicer and Drosha) are responsible for miRNA dysregulation in recurrent ovarian cancer.

4.3 Materials and methods

All samples were obtained at initial cytoreductive from patients treated for ovarian cancer at St James's Hospital, Dublin, Ireland. The study had approval of the hospital ethics committee and informed consent was obtained from each patient by the research team prior to surgery. All tumors were staged according to the International Federation of Gynaecology and Obstetrics standards (FIGO).

4.3.1 Patients and tissue samples (See Table 2.2 Materials and Methods).

A pilot study was undertaken to examine the expression of 180 miRNAs with the objective of generating a training set.

4.3.1.1 Fresh frozen samples

The initial cohort (training set) consisted of 3 (P2, P4, P5) fresh frozen primary serous papillary (stage III and grade III) and 3 (R1, R2, R4) fresh frozen recurrent serous papillary adenocarcinomas of the same grade but from different optimally debulked (residual disease of <1cm in greatest diameter) patients. The mean age in years for patients in the primary and the recurrent group was 63.3 (range 48-84) and 53.3 (range 45-68). Patients had received no neoadjuvant treatment before surgery and they were all treated postoperatively with platinum and/or paclitaxel.

A subset of miRNAs selected from the trainng set was further analyzed in fresh frozen and formalin fixed paraffin embedded (FFPE) cohorts.

The additional cohort of fresh frozen tissues, which were analysed with the putative signature miRNA panel comprised 18 serous papillary adenocarcinomas, 11 primary (P11-P18, P20-P22) and 7 recurrent (R3, R7,R8, R10-R12, R18) cases. This cohort was further expanded to 22 serous papillary adenocarcinomas-14 primary (P1-P5, P7, P9, P10, P12, P13, P15-P17, P19) and 8 recurrent (R1, R2, R4, R5, R7, R9-R11)- and used to examine the relative expression levels of Dicer and Drosha. An additional 2 primary (P6, P8) and 5 recurrent ovarian cancer patients of different histology (1 patient with small cell carcinoma (R6), 1 patient with mixed mullerian carcinoma (R8), 1 patients with poorly differentiated clear cell carcinoma (R12), 1 patient with

dedifferentiated germ cell carcinoma (R13) and 1 patient with adenosquamous (R14) differentiation) were subsequently added to the cohort (n=29).

Specimens were snap frozen on collection within 1 hour of surgery at -80°C. After tissue processing in a cryostat at -20°C, frozen sections were cut and mounted on slides. The slides were stained with H&E and examined by a pathologist to ensure >70% presence of tumour cells.

4.3.1.2 miRNA extraction from fresh tissues

miRNA was extracted from fresh tissues using the Ambion mirVana™ miRNA isolation kit (Ambion, Austin, TX) according to the manufacturer's recommendations as described in section 2.8.2.

4.3.1.3 Formalin-fixed paraffin-embedded (FFPE) tissues

An independent set of 22 ovarian serous carcinomas (OSC) tumours- 14 primary (P20, P24-P36) and 8 recurrent (R1, R3, R11, R12, R15, R16, R17, R19)- classified according to the FIGO system: stage (II-III) and grade 2-3, were selected from archival FFPE tissue, between the years 1996-2006 from St James's Hospital, Dublin. H&E slides of all tumors were reviewed by a histopathologist (RF) to confirm original diagnoses.

An additional paraffin tissue microarray (TMA) of 56 primary EOC and 15 recurrent OC was constructed, composed of tumors arrayed in quadruplicates as described for TMA Section.

4.3.1.4 miRNA extraction from formalin-fixed paraffin-embedded (FFPE) tissues

This was performed on the above mentioned independent set of OSC (n=22) using the Recoverall™ Total Nucleic Acid Isolation Kit (Ambion, Austin, TX). Where tumour cell density was >90% (n=16), whole sections were taken for miRNA analysis. In cases that tumour stroma component was significantly present (n=6), Laser Capture Microdissection (LCM) was performed to produce pure cell population for analysis. Up to 3 extractions were performed in parallel with one

pellet in each extraction. Following dissection from the blocks, these preparations were deparaffinized, followed by protease digestion for 3 hours at 50°C for RNA isolation, on column DNA digestion and elution as described in method 2.8.3.1.

4.3.1.5 Laser capture microdissection (LCM)

Laser Capture Microdissection was employed in six of the recurrent FFPE tumour samples as described in section 2.9.1.

4.3.1.6 miRNA expression analysis and Real-time TaqMan PCR using full miRNA panel

miRNA expression levels were examined using the Applied Biosystems TaqMan® MicroRNA Assay Human Panel Early Access kit (Applied Biosystems, Foster City, CA) consisting of 180 well characterized miRNAs. The kit uses gene-specific stem-loop reverse transcription primers and TaqMan probes to detect mature miRNA transcripts in a 2-step qRT-PCR assay as described for the Early Access kit protocol in section 2.8.6. Briefly, single stranded cDNA was generated from total RNA sample by reverse transcription using the Applied Biosystems High-Capacity cDNA Archive Kit (Applied Biosystems, CA, USA) as described in methods. RT reactions contained 10 ng of total RNA, 50 nM stem-looped RT primer, 1 × RT buffer, 0.25 mM each of dNTPs, 3.33 U/μl Multiscribe reverse transcriptase and 0.25 U/μ l RNase Inhibitor. PCR amplification was carried out using sequence specific primers on the Applied Biosystems 7900 Real-Time PCR system. The reactions were incubated in a 96-well optical plate at 95°C for 10 min, following by 40 cycles of 95°C for 15 s and 60°C for 10 min. The assay was run in triplicate for each case to allow for assessment of technical variability. let-7a was used as endogenous control. Four negative controls were also used, ath-mir159a, cel-lin-4, cel-miR-2 and cel-miR-124 as they show no expression in human tissue.

4.3.1.7 Selected miRNA expression analysis in independent cohorts using TaqMan MicroRNA Assays

The Applied Biosystems stem loop RT/PCR kit (AB) and TaqMan microRNA Assays were used to detect and quantify selected mature miRNAs in both fresh frozen and FFPE samples, as described in section 2.8.6.

4.3.1.8 TaqMan gene expression analysis of Dicer and Drosha

The expanded cohort of fresh frozen samples was used for this analysis. Dicer (Assay ID: Hs00203006_m1) and Drosha (Assay ID: Hs00229023_m1) were analysed using qRT-PCR as described in section 2.8.4.

4.3.1.9 Immunohistochemistry of eIF6 and Dicer on tissue microarrays (TMA)

4 μm sections of the OSC tissue array were cut and mounted on glass slides. For antigen unmasking, deparaffinized sections were boiled (eIF6) or microwaved (Dicer) in citrate buffer [10 mmol/L sodium citrate buffer (pH 6.0)] before incubation with primary antibodies. eIF6 (BD Biosciences, Belgium) and Dicer (Abcam, UK) protein levels were examined using mouse monoclonal antibodies at dilutions of 1:200 and 1:50 respectively. Antibody staining was done using the Biogenex Super Sensitive™ Link- Label IHC Detection system.

Intensity of eIF6 and Dicer immunoreactivity was recorded in the neoplastic glands for every specimen. The intensity of staining was graded on a scale from 0 to 3. "0" reflected a lack of immunoreactivity, "1" reflected weak immunoreactivity, "2" reflected moderate immunoreactivity and "3" reflected strong homogenous nucleocytoplasmic (eIF6) or cytoplasmic (Dicer) staining. Scores from all cores were averaged. Two pathologists (RF, CB) scored the stained slides.

4.3.1.10 Data analysis and bio-informatics in the pilot study

Relative quantitation using the ΔΔCt method in recurrent versus primary was carried out. Expression levels of each miRNA were normalized by calculating the ΔCt values based on substracting the Ct value of target miRNA from the CT of the internal

control (let 7-a) and fold changes were calculated for each gene. Replicates with a ct>40 were excluded.

4.3.1.11 Unsupervised classification

Spotfire® software [400] was used to visualize hierarchical clustering between differentially expressed genes. Unsupervised clustering was applied to the data set using the UPGMA mean based on Euclidean distance as the similarity measure. Target prediction analysis was carried out using the miRGen webserver (www.diana.pcbi.upenn.edu/miRGen). Functional classification of the data and gene ontology of the predicted mRNA targets was defined by using the PANTHER Classification System. A binomial statistical tool was employed to compare gene lists to a reference list (i.e. the complete human genome) to determine over- or under-representation of PANTHER classification categories [401].

4.3.1.12 Supervised classification

Prognostic miRNAs for recurrent versus advanced primary tumor class prediction were determined by using the Prediction Analysis of Microarays (PAM) [402]. PAM is a statistical technique for class prediction from gene expression data using nearest shrunken centroids. The method of nearest shrunken centroids identifies subsets of genes that best characterize each class. The technique is general and can be used in many other classification problems. It can also be applied to survival analysis problems. The algorithm was used for training set prediction, creating a multivariate predictor for determining which of the two classes (recurrent versus primary) a given miRNA belongs.

Correlations of miRNA expression levels were carried out using student's t-test for age and CA-125 and Fischer's test for debulking status with significance level set at $p<0.05$.

The traditional endpoints for the study were disease free survival (DFS) and overall survival (OS). DFS was calculated from date of primary surgery to the date of disease recurrence and OS until the date of death. The expression levels of miRNA genes were dichotomised as high or low, with the median values of normalised miRNA

expression as the cutoff points. Kaplan-Meier survival curves by clinical miRNA expression levels were calculated and compared using the log-rank test. Statistical tests were one or two-tailed with a significance level set at 5%. All statistical analyses were performed using the Analyze-It™ Software Ltd.

All statistical analysis of immunohistochemical studies was done with Analyse-It™ Software Ltd. Two sample comparisons (recurrent versus primary) were performed with the Mann-Whitney rank sum test.

4.4 Results

4.4.1 miRNA expression signature discriminates between primary and recurrent ovarian cancers (training set).

Using the Early Access Kit, 180 known miRNAs were examined for their expression levels and distinct expression signatures were identified between primary and recurrent ovarian cancers. 60 miRNAs were greater than 2-fold deregulated between primary and recurrent cases (Table 4.1 and Figure 4.3). A marked upregulation of miRNAs in recurrent tumours compared to primary was observed (52 miRNAs showed overexpression and 8 underexpression of >2 fold in recurrent versus primary tumours) (Figure 4.6). 12 miRNAs were not detectable in the ovarian samples. miR-223 and miR-9 were the top dysregulated in the recurrent versus primary samples. miR-147 was detected only in the recurrent specimens and was considered to be specific for recurrent ovarian cancer. Notably, we observed expression of miRNAs previously reported in other human cancers such as miR-155 [403], miR-21 [318], miR-221 and miR-222 [404].

Table 4.1 List of the miRNA genes differentially expressed between recurrent and primary serous papillary ovarian adenocarcinomas

Table shows numerical fold changes ranging from 2 to 11. Common miRNA genes highlighted in red have been identified as differentially expressed in diverse cancers. miRNAs highlighted in green were the top dysregulated in recurrent vs primary serous papillary adenocarcinomas in the training cohort.

miRNA Assay	Up in Recurrent	miRNA Assay	Up in Recurrent	miRNA Assay	Down in Recurrent
miR223	11.35571231	miR224	3.446998251	miR326	2.018085083
miR206	10.09241373	miR222	3.429526571	miR30d	2.139840206
let7i	8.246555615	miR29c	3.363029871	miR125b	2.142173482
miR30a3p	8.16742082	miR21	3.331135486	miR31	2.290207738
miR368	8.152857788	miR34c	3.158291208	miR99a	2.29788702
miR10b	7.727130269	miR139	3.14175359	miR100	2.318059102
miR338	7.704267522	miR197	2.937647789	miR137	2.974002788
miR195	7.166781978	miR15a	2.928993165	miR9	3.886456405
miR93	5.849476069	miR218	2.883622744		
miR23a	5.514310681	miR106a	2.815098885		
miR185	5.265698431	miR340	2.807685741		
miR22	5.149294678	miR219	2.797355288		
miR339	4.925213166	miR155	2.710428782		
miR321	4.81249158	miR92	2.701058863		
miR29b	4.778206067	let7g	2.606706081		
miR186	4.479887044	miR328	2.601412983		
miR128a	4.42675849	miR149	2.44190036		
miR374	4.369029661	miR23b	2.427274867		
miR193	4.002099215	miR221	2.389278913		
miR106b	3.971898585	miR150	2.284171328		
miR194	3.840507499	miR190	2.149257886		
miR370	3.76950678	miR107	2.106178095		
miR128b	3.536203171	miR331	2.091486666		
miR198	3.49349966	miR181c	2.072063046		
		miR133b	2.025726728		

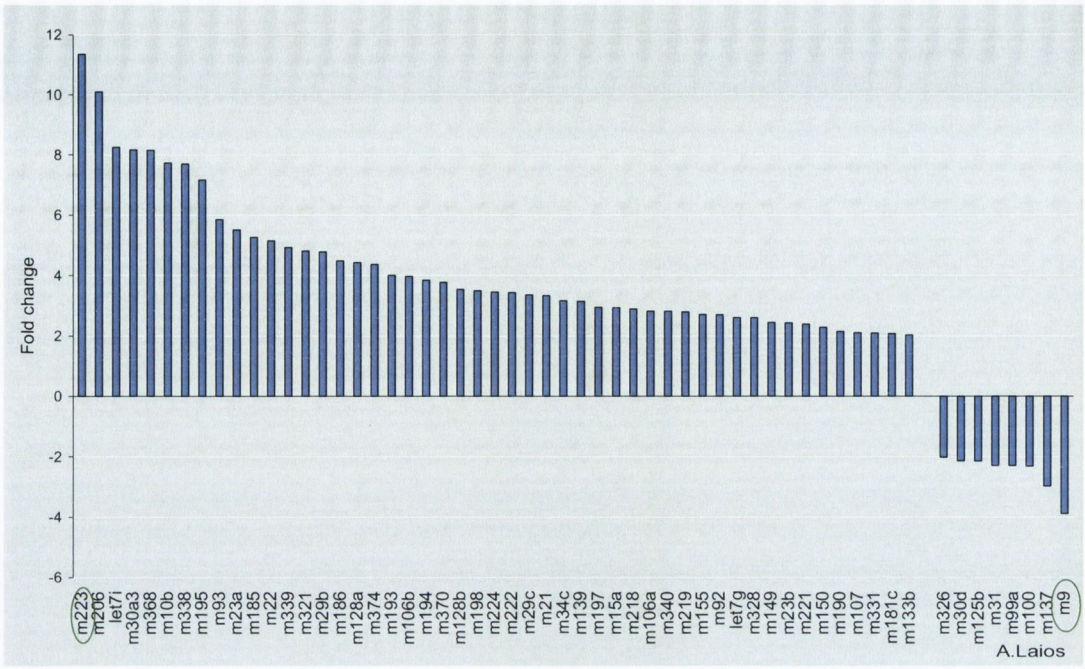

Figure 4.3 Relative fold changes are displayed on the y axis and the miRNAs are on the x axis. The most significant altered expression was observed for mir-223 with increased expression and mir-9 with decreased expression.

Unsupervised hierarchical clustering of the samples in our cohort, based on differentially expressed miRNA did not clearly separate primary and recurrent tumours. Interestingly, it segregated primary "chemosensitive" tumours while the primary "chemoresistant" tumour clustered together with the recurrent ones (Figure 4.4).

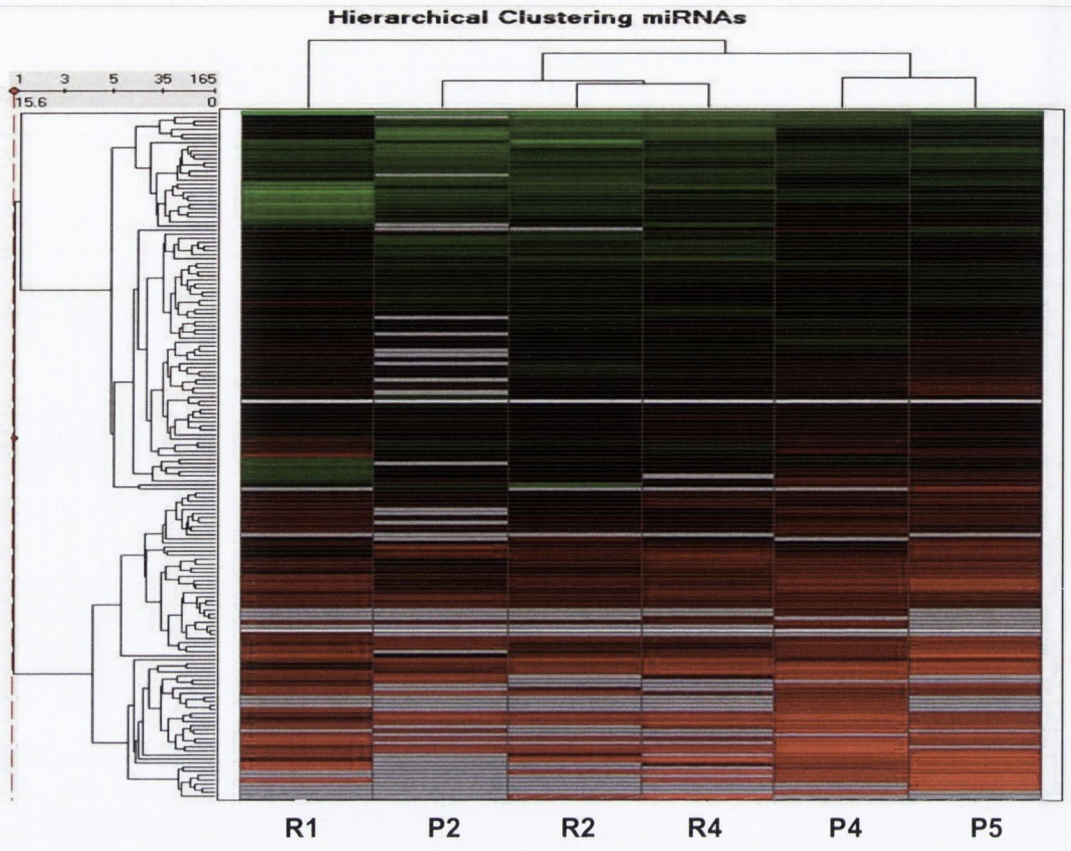

Figure 4.4 Unsupervised hierarchical cluster heatmap based on differential miRNA expression patterns identified in the initial cohort. Vertical bars represent the samples and the horizontal bars represent the miRNA genes. Green bars reflect downregulated genes and red bars upregulated genes. Interestingly, P2 clusters with the recurrent samples on the left of the heatmap. P2 relapsed within 6 months post completion of treatment and should be considered "chemoresistant" P, primary tumours; R, recurrent tumors.

4.4.2 PAM analysis

To identify the smallest set of predictive miRNAs differentiating between primary and recurrent ovarian cancer tissues we made use of the PAM software. A signature of least 5 miRNAs is needed to correctly predict the two types of tumours (Figure 4.5).

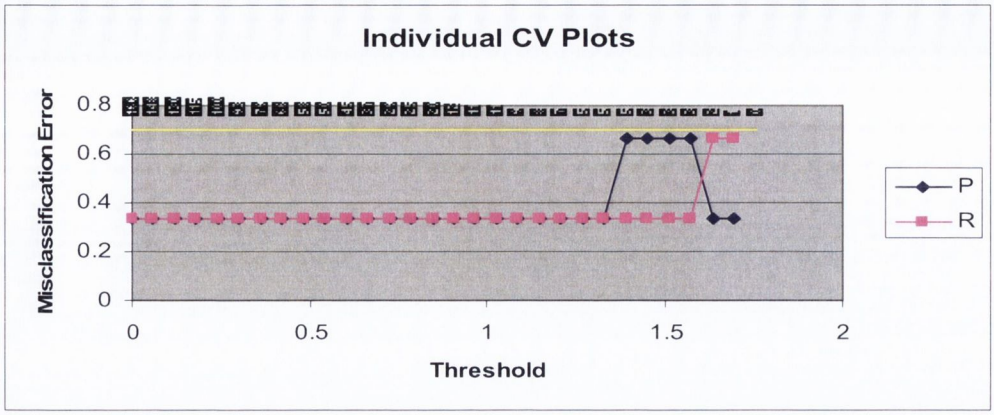

Figure 4.5 PAM prediction analysis in primary and recurrent ovarian samples. A balance 10-fold cross validation that minimizes classification errors to 50% enables choice of a threshold. Missclassification errors were plotted against various values of the threshold. 5 genes were needed to accurately predict between primary and recurrent ovarian cancers at a maximum threshold of 1.27.

However, 9 statistically significant genes for a given threshold of 1.1 that corresponds to an FDR<0.5 (Figure 4.6), accurately predicted the 2 classes (primary and recurrent) with a probability error of <20% for a given threshold (Figure 4.7).

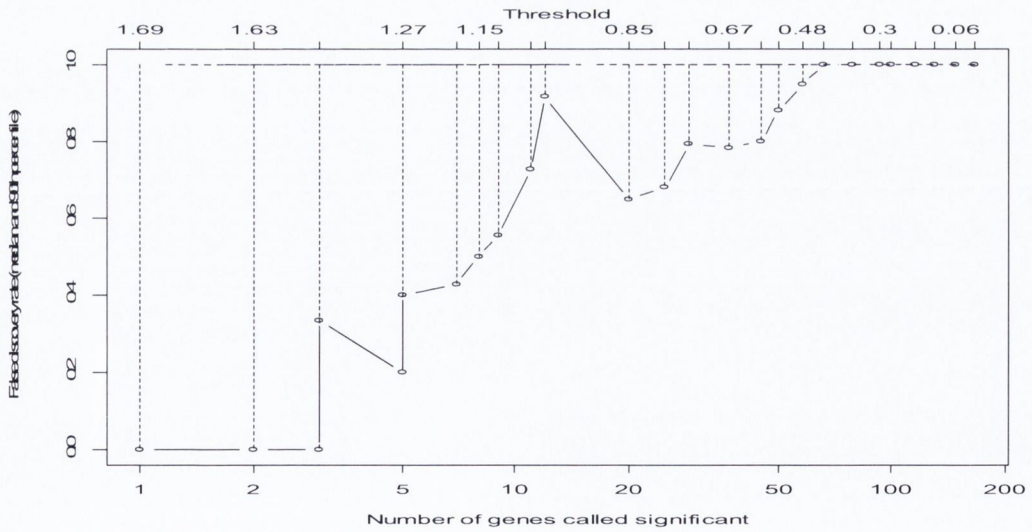

Figure 4.6 Esitmated FDRs for given thresholds plotted against the number of genes called significant. If FDR<0.5 (which corresponds to a p value ~0.05), data had to be thresholded at 1.1 and this provided with 9 statistically significant genes to perform classification prediction.

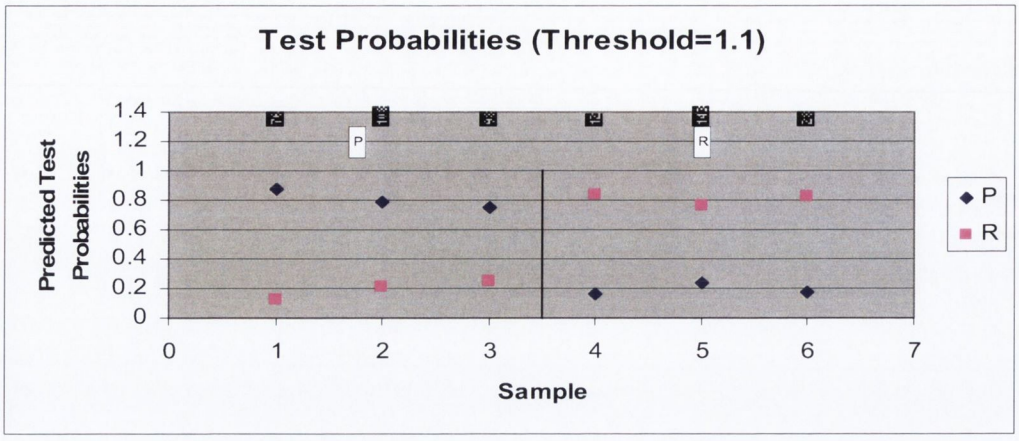

Figure 4.7 PAM class prediction analysis and test probabilities. For a threshold of 1.1 (FDR<0.5), there's less than 20% probability that training samples are not accurately clustered as primary and recurrent (classification rate ~80%).

Table 4.2 describes this set of genes, 6 upregulated in recurrent vs primary (miR-185, miR-338, miR-339, miR-10b, let-7i), 2 upregulated only in the primary samples (miR-211 and miR-189) and miR-147 upregulated only in recurrent samples. PAM analysis was in concordance with the unsupervised hierarchical clustering analysis in for as the primary "chemoresistant" tumour clusters with the recurrent ones (Figure 4.8).

Table 4.2 PAM list of significant miRNA genes for classification prediction in recurrent versus primary tumours. The PAM algorithm was used for gene identification at a threshold of 1.1 (FDR<0.5).

miRNA	P score	R score
miR185	0.2673	-0.2673
miR338	0.2236	-0.2236
miR211	0.206	-0.206
miR339	0.1397	-0.1397
miR93	0.1362	-0.1362
miR147	-0.065	0.065
miR189	0.0643	-0.0643
miR10b	0.0436	-0.0436
let7i	0.0094	-0.0094

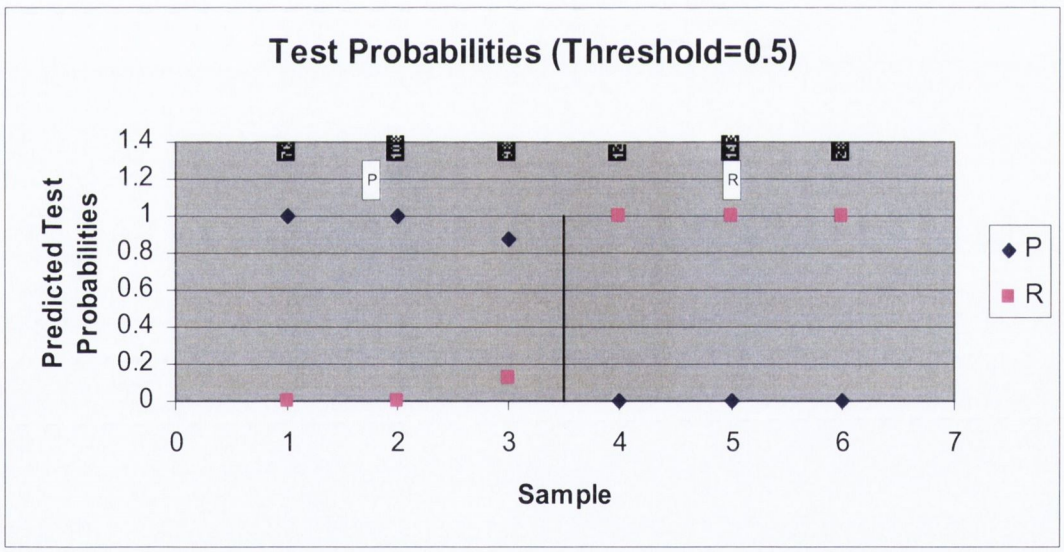

Figure 4.8 PAM class prediction analysis and test probabilities. For a threshold of 0.5, there's less than 10% probability that sample P3 is not clustered as primary but as recurrent. This is consistent with the unsupervised hierarchical clustering results.

4.4.3 miRNA expression in an independent set of fresh frozen (FF) tumours of the same histology

To determine the potential importance of the initially identified miRNAs, real time PCR was performed in an independent set of 11 advanced primary and 7 recurrent

serous papillary adenocarcinomas. 5 miRNAs were initially selected from the signature panel of 60 deregulated miRNAs; the top deregulated in the initial cohort miR-9, miR-223 and miR-206, and miR-93 and miR-147 randomly selected from the PAM class prediction miRNA list.

miR-147 was not amplified in either the primary or recurrent FF tumour tissues. miR-206, the second top upregulated miRNA in recurrent versus primary samples in the initial cohort, was detected in 2/3 of primary samples and 2/3 of recurrent ones in the initial cohort. It was then detected only in the recurrent samples in the wider cohort of FF samples. miR-93 was upregulated in recurrent versus primary and consistently expressed across all primary and recurrent samples. In the wider cohort of FF samples (n=18), it was consistently expressed across all the primary samples but only expressed in 3/6 (50%) of recurrent samples. Consequently, miR-147, miR-206 and miR-93 expression data were excluded from correlation analysis.

Based on initial training set data and following the above mentioned exclusion criteria, 2 miRNAs (miR-9 and miR-223) were selected from the signature panel of 60 miRNAs according to a) their degree of dysregulation (they demonstrated the greatest changes in expression levels) b) their consistent expression across all the tested samples c) their predicted target miRNAs.

A similar pattern of dysregulation was observed for miR-9 and miR-223 on TaqMan analysis between independent and training cohort (Figure 4.9).

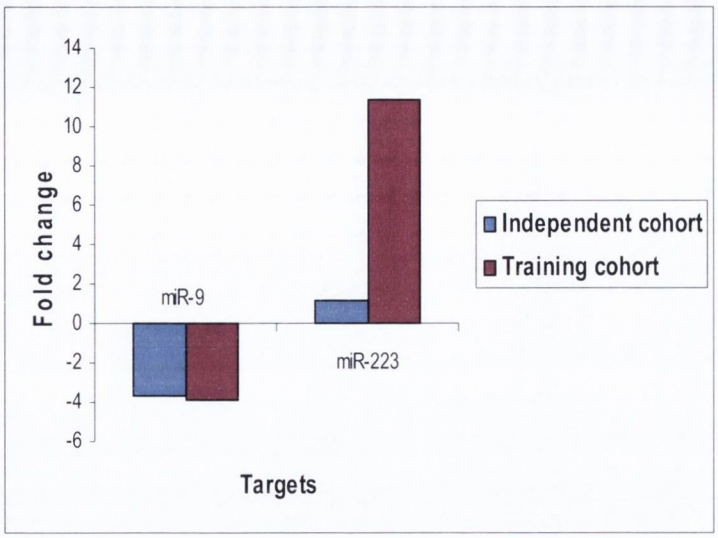

Figure 4.9 TaqMan PCR analysis of top dysregulated miRNAs. The relative quantitation from TaqMans in recurrent vs primary are plotted for miR-223 and miR-9. Concordance was observed on TaqMan analysis between the training and expanded independent cohort of serous ovarian papillary adenocarcinomas (comprised of snap frozen tissues).

4.4.4 miRNA expression in FFPE ovarian adenocarcinomas correlates with training cohort

miRNA expression analysis for the 2 selected miRNAs was carried out using real-time PCR in an independent cohort of 14 primary and 8 recurrent FFPE tissues (n=22). TaqMan data corroborated with the results obtained from the initial cohort in so far as miR-223 was upregulated and miR-9 downregulated (Figure 4.10).

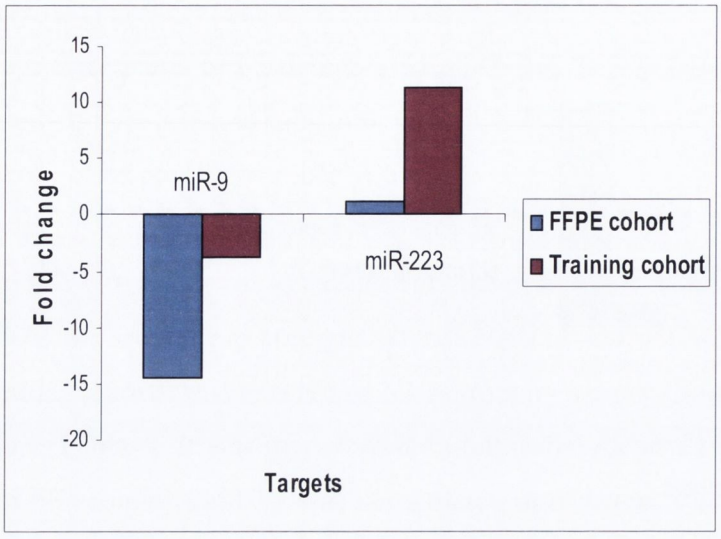

Figure 4.10 TaqMan analysis of top dysregulated genes in training cohort and FFPE cohort. Likewise, concordance was observed for miR-223 and miR-9 between the 2 cohorts.

4.4.5 Predicted and confirmed mRNA targets

To investigate the biological consequence of altered miRNAs, we analyzed the predicted gene targets of the top dysregulated miRNA genes identified in our cohort. The analysis was conducted using the miRGen webserver, an online tool that takes sets of target genes, predicted by the individual programs and presents compiled lists of the intersection of miRanda and TargetScan algorithms.

Table 4.3 List of important miRNA genes differentially dysregulated in recurrent vs primary ovarian cancers with their predicted gene targets. These represent genes well characterised in ovarian carcinogenesis. Genes highlighted in italics were also identified in the earlier transcriptomic study as described in chapter 3.

miRNAs	FOLD CHANGE	POTENTIAL TARGET GENES	REC vs PRIM
miR-223	11.35571231	*SEPTIN6, FGFR2, MMP9, EGF, S100A3, USF2, KRAS, TGFB2, E2F1*	UP
miR-206	10.09241373	*E2F5, GTF2B*	UP
miR-10b	7.72713	*PIK3CA*	UP
let-7i	8.246555615	*TJP3, ABCC5, COL3A1*	UP
miR-106a	2.815098885	*IL27RA*	UP
miR-93	5.849	*PTEN, HIFIA, CDK2, ERBB4, MAPK9, n-MYC*	UP
miR-9	3.886456405	*FGF18, FGF10, BCL2, BCL6, BRAF, ZNFS, CLDN14, CLDN6, SEPTIN10, PVRL2, LASS4*	DOWN

4.4.6 mRNA (transcription) and miRNA (regulation) expression correlation

Analysis and validation of cDNA microarray data as described in chapter 3 identified a group of genes that were upregulated in recurrent compared to primary ovarian cancers. Comparing this list of genes with the list of putative miRNA targets yielded from MIRGEN, showed that several of the differentially expressed genes in each comparison are targeted by several miRNAs identified in the subcohort of patients (Table 4.3 and 4.4). *ZNF218* was excluded as no putative miRNA targets were identified from the prediction analysis.

NRG2	*BTC*	*S100B*	*S100A8*	*CLDN16*	*TJP3*	*IL27RA*	*IL1R2*	*MMP9*	*FGF2*
miR129	miR154	miR26a	miR135a	let7e	let7	miR106a	miR379	miR133a	miR9
miR133a	miR199a	miR26b	miR135b	miR224	miR125a	miR106b	miR454-p	miR133b	
miR133b	miR199b	miR340	miR187	miR548a	miR138	miR10	miR494	miR149	
miR138	miR217	miR565	miR202		miR184	miR140	miR616	miR183	
miR187	miR3a	miR615	miR24		miR197	miR17-5p		miR184	
miR208	miR378	miR632	miR326		miR205	miR182		miR185	
miR308	miR487a	miR671	miR423		miR345	miR20a		miR191	
miR431	miR487b		miR496		miR453	miR20b		miR204	
miR450	miR490		miR544		miR517	miR22		miR205	
miR517a	miR587				miR520c	miR296		miR223	
miR517b					miR520d	miR320		miR24	
miR517c					miR526b	miR324		miR299-5p	
miR551a					miR553	miR372		miR300-3p	
miR551b					miR555	miR373		miR320	
miR586					miR598	miR383		miR324-3p	
miR599					miR612	miR500		miR330	
miR611					miR658	miR512-3p		miR337	
miR615					miR765	miR512-5p		miR339	
miR668						miR518f		miR340	
						miR520g		miR518e	
						miR93		miR345	

Table 4.4 mRNAs and predicted miRNA targets.

The list of mRNAs used for prediction analysis included those identified and validated as upregulated in recurrent versus primary ovarian cancers as described in chapter 3.

Conversely, to determine whether any of the identified miRNAs coexpressed with their putative mRNA targets, we compiled our previous microarray data from the same cohort of patients. Putative targets for miR-9, previously identified and validated in our transcriptome study, as described in chapter 3, included *LASS4* and *PVRL2*. Likewise, *USF2* was the only putative target for miR223. No inverse pattern was observed between paired miRNA and mRNA expression signatures as expected.

4.4.7 miR-9 and miR-223 gene prediction analysis identifies common significant biological pathways

The list of predicted targets for both miR-223 and miR-9 was further uploaded into Panther classification system and examined against the H. sapiens reference list to determine what percentage of genes were present compared to that expected and to determine whether any relevant biological pathways were statistically significant at a p value of 0.01 and 0.05. Common significant pathways were observed for the "miR-223 list" and "miR-9 list" of predicted gene targets at a $p<0.05$; namely angiogenesis, Ras, integrin signalling, Notch signalling and a dynamic signalling pathway involving actin and tubulin, well known to interfere with the mechanism of action of paclitaxel (taxol®) (Figure 4.11).

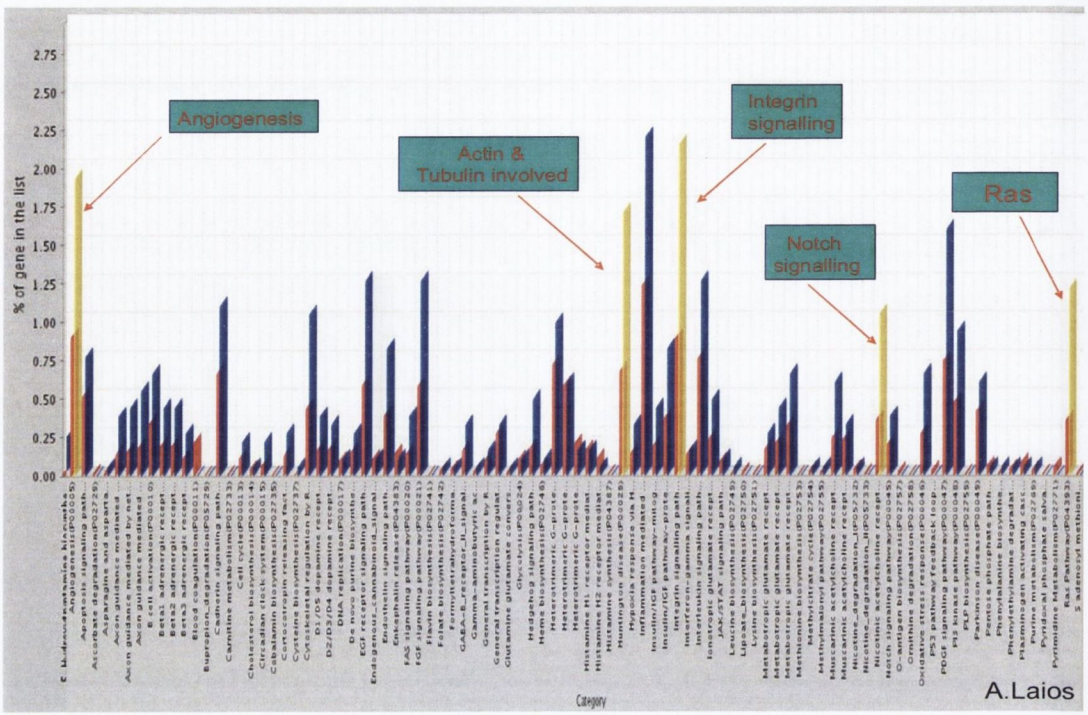

Figure 4.11 Common significant biological pathways observed for miR9 and miR223 based on comparison between percentage of miR9 and miR223 predicted genes and expected genes from the H.Sapiens reference list; namely angiogenesis, Ras, integrin signalling, Notch signalling and a pathway involving actin and tubulin.

4.4.8 miRNA signature predicts progression free survival in an independent set of ovarian adenocarcinoma patients

To test the ability of miRNAs to predict survival outcomes such as PFS and OS, we measured expression of 3 miRNAs (miR-223, miR-9 and miR-93) in the set of fresh frozen (FF) and 11 of the FFPE primary ovarian tumour samples. This panel of genes was chosen based on their pattern of expression (for top deregulated genes miR-223 and miR-9) and their consistent expression across all the primary samples, that would allow for analysis to perform (miR-93). Table 4.5 displays the survival data and clinicopathological details for these specimens. For mean centered values, a log-rank test demonstrated no miRNAs as statistically significant when related to patient's progression free survival and overall survival (Figures 4.12-4.23).

Table 4.5 Survival Data and clinicopathological details

A Fresh Frozen

Sample	Age	Stage	Grade	CA-125	PFS	OS	Debulking
P11	74	3C	3	1051	5+	5+	1
P12	60	3C	3	2310	0	9	2
P13	44	3A	3	12618	7	16+	2
P14	64	3C	3	2895	22+	22+	2
P15	74	3C	3	3533	9	23	1
P16	68	3C	3	2719	0	5	2
P17	54	3C	3	883	15	18+	1
P19	86	3C	3	3621	6	17	1
P20	86	3C	3	2310	7	30	2
P21	59	3C	3	758	3	4	1
P22	63	3C	2	679	8+	8+	1

+: Still alive, 1: Optimal Debulking, 2: Sub-optimal debulking

B Formalin Fixed Paraffin Embedded

Sample	Age	Stage	Grade	CA-125	PFS	OS
P20	86	3C	3	2310	7	9
P24	66	2	3	380	24	24
P25	71	1C	3	1635	22	22+
P26	63	2C	3	463	16	17
P27	59	3C	2		22	22+
P28	55	4	2		9	9+
P30	45	3C	2		10	11
P31	59	3C	3		11	25
P33	47	4	3		9	9+
P36	59	3C	3		8	11

Survival curves for FFPE samples

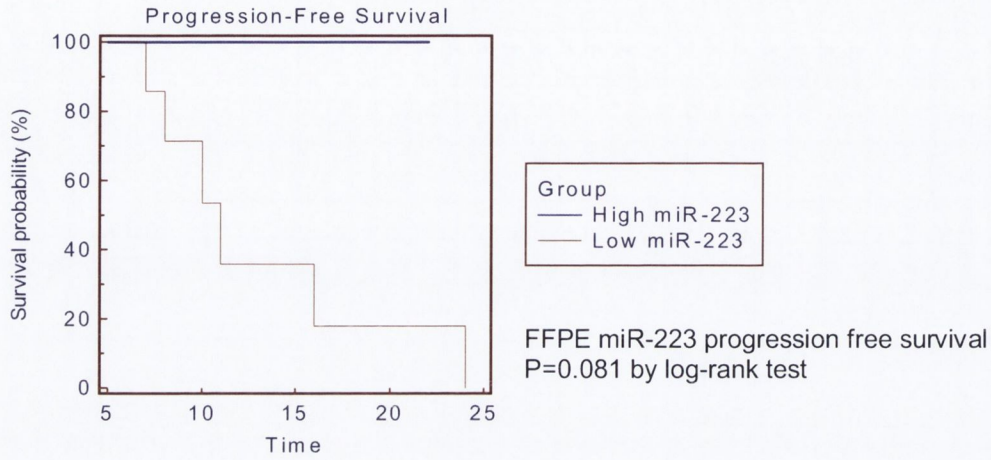

Figure 4.12 Progression free survival curves in FFPE primary ovarian tumours in relation to miR-223 expression levels.

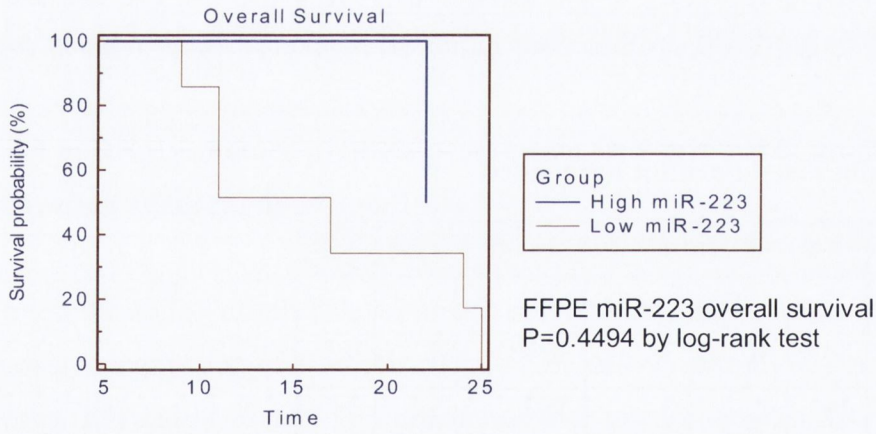

Figure 4.13 Overall survival curves in FFPE primary ovarian tumours in relation to miR-223 expression levels.

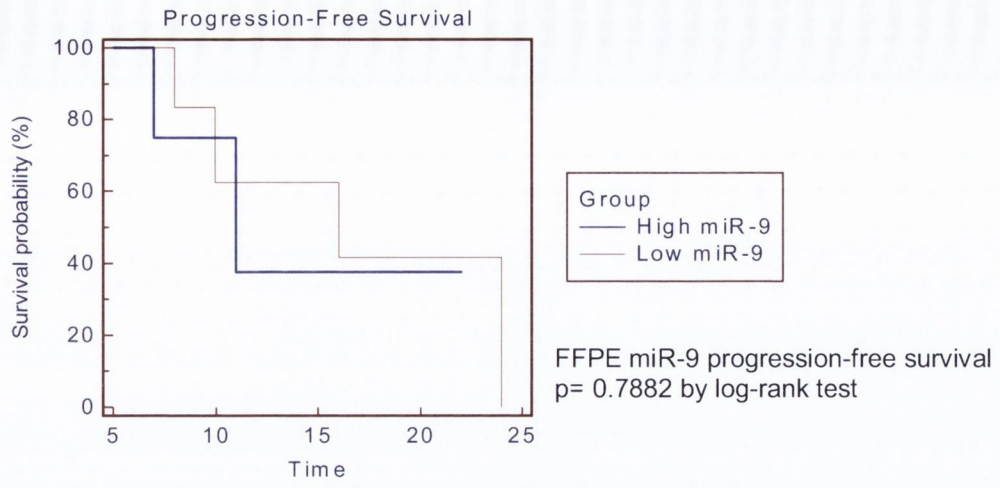

Figure 4.14 Progression free survival curves in FFPE primary ovarian tumours in relation to miR-9 expression levels.

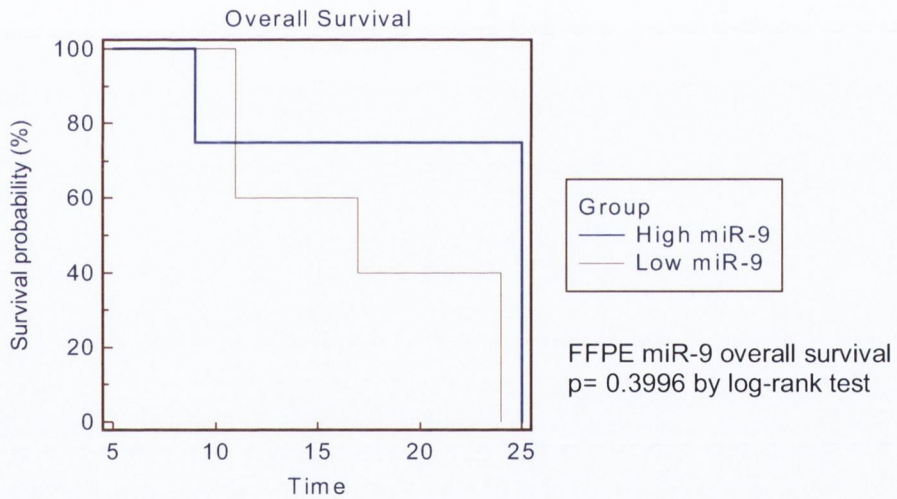

Figure 4.15 Overall survival curves in FFPE primary ovarian tumours in relation to miR-9 expression levels.

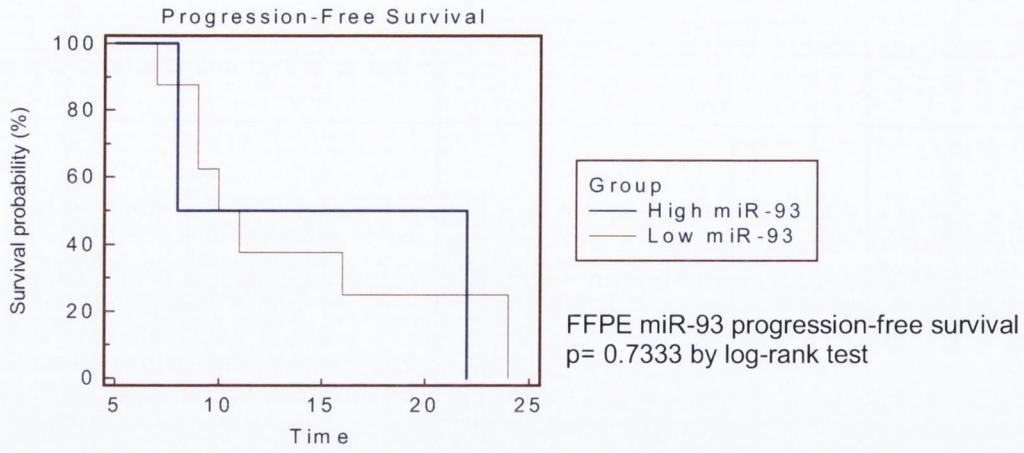

Figure 4.16 Progression free survival curves in FFPE primary ovarian tumours in relation to miR-93 expression levels.

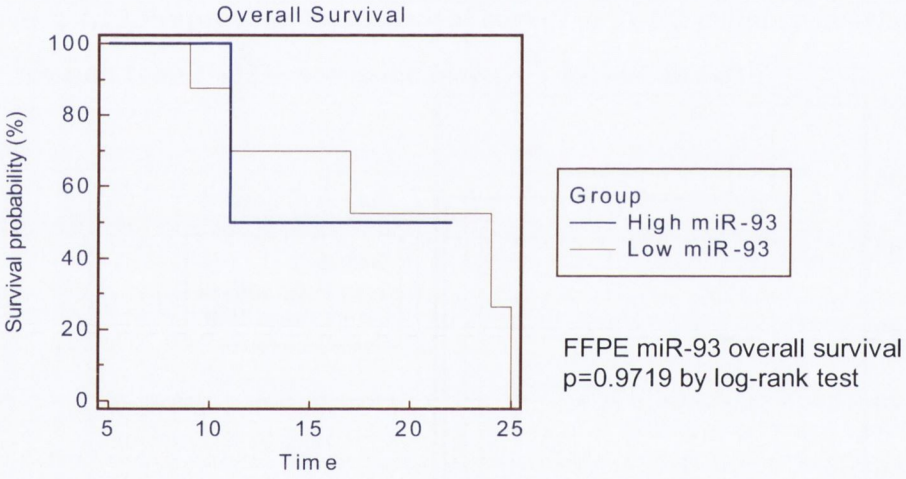

Figure 4.17 Overall survival curves in FFPE primary ovarian tumours in relation to miR-93 expression levels.

Survival curves for fresh frozen (FF) samples

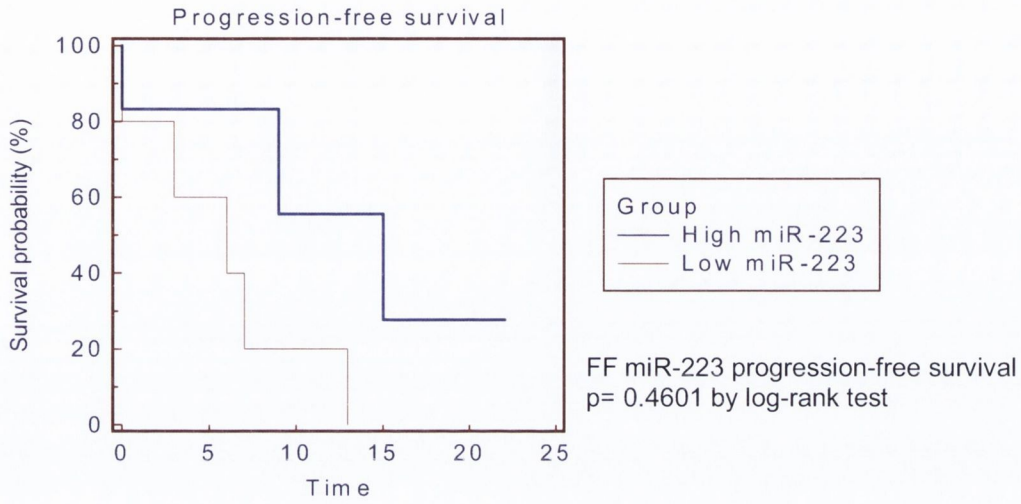

Figure 4.18 Progression free survival curves in FF primary ovarian tumours in relation to miR-223 expression levels.

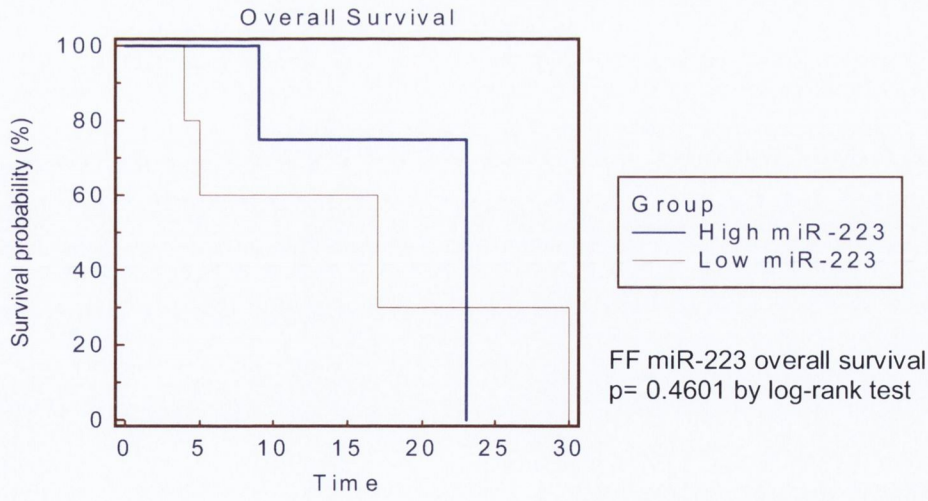

Figure 4.19 Overall survival curves in FF primary ovarian tumours in relation to miR-223 expression levels.

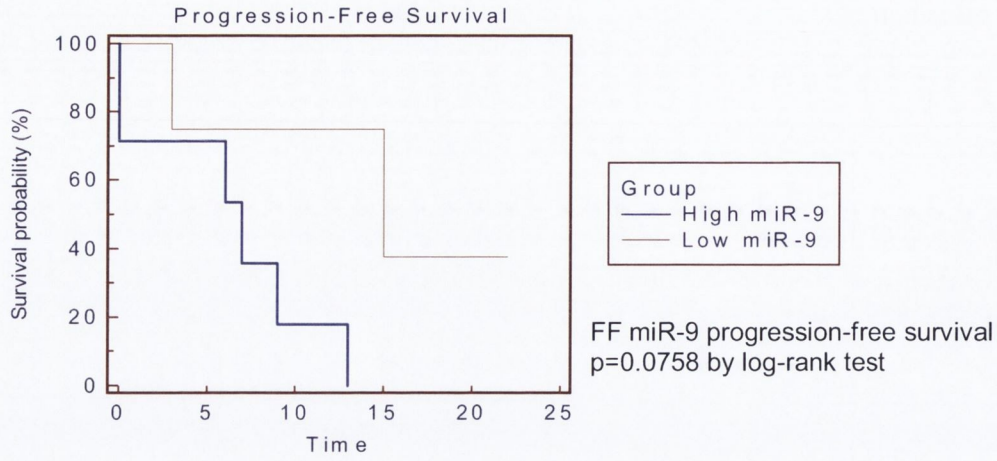

Figure 4.20 Progression free survival curves in FF primary ovarian tumours in relation to miR-9 expression levels.

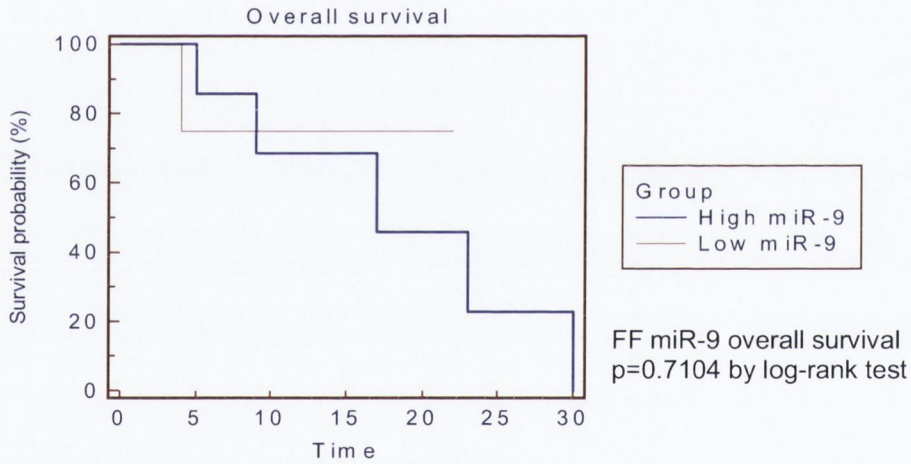

Figure 4.21 Overall survival curves in FF primary ovarian tumours in relation to miR-9 expression levels.

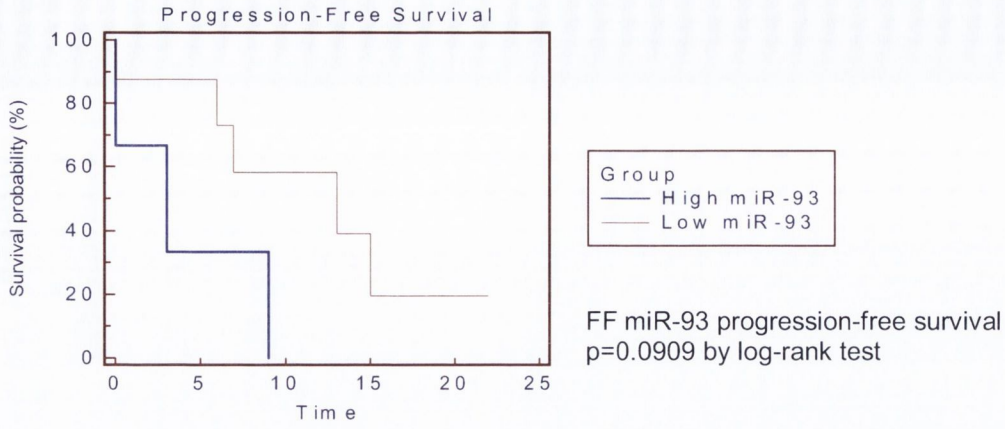

Figure 4.22 Progression free survival curves in FF primary ovarian tumours in relation to miR-93 expression levels.

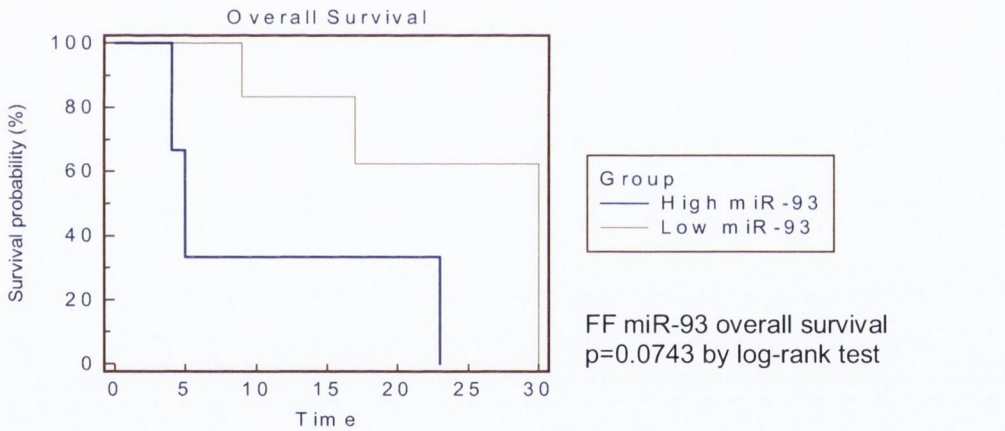

Figure 4.23 Overall survival curves in FF primary ovarian tumours in relation to miR-93 expression levels.

We then attempted to combine the results from individual log-rank tests used in survival analysis to obtain a p value from a chi-square distribution with 3 degrees of freedom (where 3 is the number of miRNAs used for survival outcome correlation). A one-sided test with mean centered data on fresh frozen ovarian cancer tissues demonstrated statistical significance for PFS if miR-9 is combined with miR-93 or miR-223 or alternatively miR-93 with miR-223 ($p<0.05$). The most significant P value was obtained by combining all three miRNAs together ($p<0.025$). For median centered data on the above fresh frozen tissues, there is statistical significance for PFS when combining miR-9 and miR-223 ($p<0.05$) (Table 4.6).

Table 4.6 One-sided test analysis of two miRNA signatures

a) n=3 and b) n=2 and PFS in the cohort of FF primary ovarian cancer samples.

a)

DF*	miR	p-value	Chi-square	Sum	p-value
n=1	9	0.0758	3.1517		
n=2	93	0.0909	2.8592	6.0109	<0.05
n=3	223	0.0663	3.3729	9.3838	<0.025

One-sided test

*DF: degrees of freedom

b)

DF*	miR	p-value	Chi-square	Sum	p-value
n=1	9	0.0908	2.861		
n=2	223	0.0663	3.3729	6.2339	<0.05

One-sided test

*DF: degrees of freedom

Collectively, a miRNA signature comprising of miR-9 and miR-223 or miR-93 or both can be the best predictor of PFS but not OS in our validation sets.

Statistical analysis of clinical variables including age, CA-125 and debulking status did not prove significant when correlated with expression levels of miR-223 and miR-9 (Table 4.7).

Characteristics	Cases	miR-9 expression levels			Cases	miR-223 expression levels		
		High	Low	P value*		High	Low	P value*
Age								
>50	3	5	3	1.00	3	5	3	1.00
<50	8	2	1		8	2	1	
Debulking status								
Optimal	6	3	3	0.697	6	4	2	0.7835
Suboptimal	5	4	1		5	2	3	
CA 125								
>2310	10	4	1	0.697	10	1	3	0.697
<2310	1	3	3		1	5	2	

* Fischer's Exact Test

Table 4.7 Correlation of expression levels of top dysregulated miRNA genes with clinicopathological variables for primary tumours. No statistical significance was proven.

4.4.9 qRT-PCR analysis of Dicer and Drosha

In order to elucidate the mechanism of miRNA dysregulation in the recurrence of ovarian cancer, we characterised the alteration in expression of genes encoding proteins of the miRNA machinery, namely Dicer and Drosha, in 14 primary and 8 recurrent OSC, using qRT-PCR. Fold changes less than 2 were observed for both genes (Relative fold changes prim vs rec: Drosha FC=0.91 (2-tailed p=0.484) Dicer FC=1.19 (2-tailed p=0.968). Our test set was further expanded to 16 primary and 13 recurrent samples by adding tumours of other than OSC histological subtypes. Fold changes of 1.78 (2-tailed p=0.496) and 1.49 (2-tailed p=0.11) were observed for Drosha and Dicer respectively, but in the opposite direction (rec vs primary).

4.4.10 Immunohistochemical analysis of eIF6 and Dicer expression in primary versus recurrent serous ovarian adenocarcinomas

We also aimed to examine the relative expression levels of eIF6 and Dicer in 56 primary OSC and 15 recurrent and to determine whether any correlation exists between the two (Figures 4.24 and 4.25). In this respect, we wanted to examine functionality of the "mature" part of the miRNA machinery at a protein level. No statistically significance was observed in relative expression for both eIF6 (Mann-Whitney U, 2-tailed p=0.4374, 95.1% CI) and Dicer (Mann-Whitney U, 2-tailed p=0.4773, 95.1% CI).

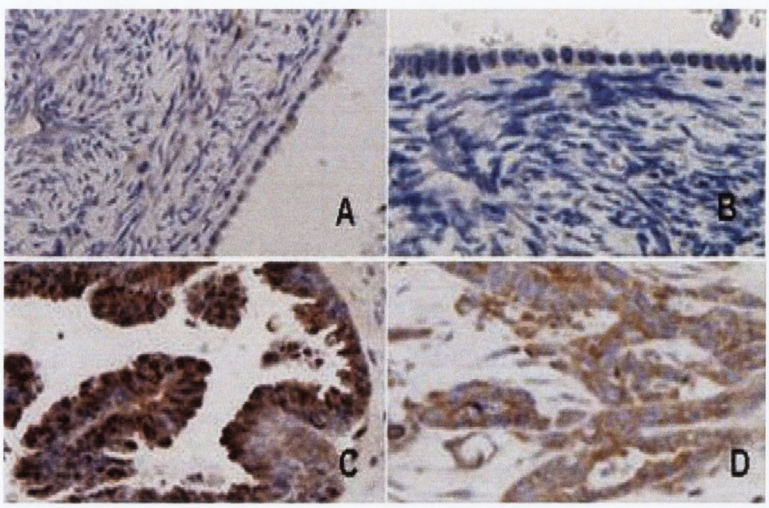

Figure 4.24 Expression of eIF6 and Dicer in normal ovarian surface epithelium and ovarian serous adenocarcinoma (x40): No staining ('0') for eIF6 (A) and Dicer

(B) in normal ovarian surface epithelium. Strong ('3') staining for eIF6 (C) and Dicer (D) in ovarian serous adenocarcinoma.

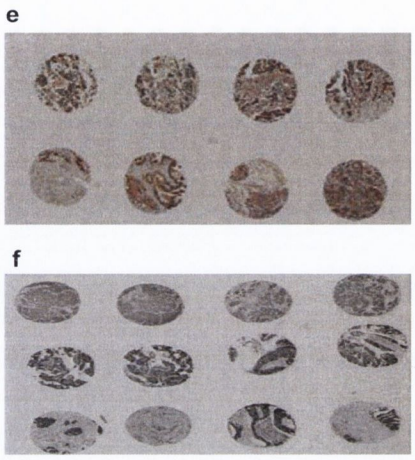

Figure 4.25 Global staining pattern for (e) eIF6 and (f) Dicer in TMA of primary serous papillary ovarian adenocarcinomas. Global staining pattern for eiF6 and Dicer in recurrent ovarian tumours is not shown.

4.5 Discussion

Not surprisingly, a variety of studies have linked aberrant microRNA expression to carcinogenesis where they act as both oncogenes and tumour suppressor genes [405]. Unique miRNA expression profiles have been able to classify various cancers. In one study, for example, the expression pattern of 217 microRNAs identified cancer type more accurately than mRNA [406].

A recent study reported aberrant miRNA expression profiles in ovarian cancers compared to normal ovary [323]. The *p53* protein, the most frequently mutated transcription factor in ovarian cancer, has been recently linked with suppression of critical miRNA components in EOC proliferation [407] In addition, direct evidence that miRNA is of critical importance in chemoresistance of human ovarian cancer has just been published [408].

This investigation demonstrates discrete miRNA signatures between primary and recurrent serous papillary adenocarcinomas on a homogenous set of ovarian tissues from different patients with a view to identifying a miRNA signature that could be used in the prediction of ovarian cancer relapse. Real-time PCR can be employed to quantify miRNA expression profiles and study the potential function of miRNAs as well as miRNA precursors in cancer pathogenesis [341]. We utilized a novel stem-looped TaqMan RT-PCR method to quantify the expression profiles of 180 mature miRNAs in a collection of primary and recurrent serous papillary adenocarcinomas. This method offers several distinct advantages over conventional miRNA detection methods including a higher sensitivity, enhancing specificity for mature miRNAs and a fast and simple methodology [333].

The data showed aberrant miRNA expression in recurrent compared to primary serous papillary adenocarcinomas. Traditionally, a change in expression of >2-fold is considered sufficient to assert that the change was significant [409]. Therefore, we conventionally used a twofold change as a cut-off for differential expression, although one would argue, much smaller changes could also be significant, reflecting the fact that miRNAs target many genes of even similar function, so that disruption of cooperating genes can be a likely event [410]. Marked upregulation of miRNAs in recurrent compared to primary cancers supports a progressive model for miRNA gene

expression consistent with progression from primary to relapse cancer stage and functionally related to drug resistance. We employed both unsupervised and supervised algorithms to generate a set of candidate genes that could serve as a classifier for tumour malignancy. However, segregation of samples in primary and recurrent was not observed in unsupervised hierarchical clustering. Instead, the primary "chemoresistant" tumour clustered together with the recurrent ones, a finding that suggests potential advantage of utilizing miRNA expression patterns to predict relapse in ovarian cancer.

Because the expression of some miRNAs is highly tissue specific [313], it was actually expected that not all of the miRNAs would be detected in ovarian cancer samples. Furthermore, because of the tissue specificity, different sets of miRNAs are likely to be deregulated in cancers of different cellular origin, although it has been reported that the miRNA signatures of different cancer types could share some individual miRNAs [317]. Of the miRNAs we detected here as dysregulated, many are similarly dysregulated in other cancers: down-regulation of miR-125b in breast cancer [322], the let-7 miRNA family in lung cancer [324], miR-21 which activates PTEN in hepatocellular cancer [318], miR-155 in B cell lymphomas [411] and miR-221 in PTC [404]. miR-21 was shared by the signatures of six solid cancers (breast, colon, lung, pancreas, stomach, prostate)in a large scale miRnome analysis [317]. This signifies that specific miRNAs are involved in common molecular pathways. However, the majority of the differentially expressed miRNAs detected in this study have not been commonly reported to be deregulated in other cancers, suggesting that primary and recurrent ovarian cancers may have miRNA signatures specific for this cancer type.

We then set out to determine the expression patterns of selected miRNAs across a large panel of FFPE pathological tissues representing primary and recurrent serous ovarian adenocarcinomas, routinely seen in the hospital pathology laboratories. Unlike mRNAs, miRNAs remain largely intact in these routinely collected clinical samples [329]. "Recurrent" samples are rather limited, thus valuable, in common clinical practice therefore, LCM was performed in a subset of recurrent samples, as it can harvest tumour cells of interest under direct microscopic visualization, in order to give histologically pure enriched cell populations [412]. Few earlier studies have

addressed the expression characteristics of miRNA genes from FFPE tissues [329]. Our results share the obvious advantage of analyzing tissues from the more voluminous archive of human pathological specimens long after surgery, so that survival data can be accumulated.

The comparison of miRNA expression levels between primary and relapsed patients from independent datasets is a feasible approach for the identification of relapse-related miRNAs, however further comparison with respect to clinical outcomes provides indirect but strong evidence that a specific miRNA signature are consistent with drug resistance in ovarian cancer.

Individual miRNAs and miRNA fingerprints have already been shown to have prognostic value in some cancers, such as chronic lymphatic leukemia, diffuse large B-cell lymphoma, and lung carcinomas [317, 413, 414]. In our study, a 3-miRNA signature comprised of miR-223, miR-9 and/or miR-93, identified in the snap frozen samples, can predict DFS but not OS, probably because OS requires even more prolonged follow-up as an endpoint or alternatively takes into consideration comorbidities that might or might not reflect the impact of first-line therapy or might be confounded by the effect of second line therapies. This signature may have the capacity to detect patients resistant to conventional drug therapy. To our knowledge, this is one of the first studies attempting to predict survival in ovarian cancer based on a miRNA "recurrent metastatic signature". Deregulation of miRNA is a recurrent event in human ovarian cancer and a recent study showed miR-214 to induce cisplatin resistance through targeting the PTEN-Akt pathway [415]. In this respect, our signature may deserve some special consideration.

miR-223 was the most upregulated in recurrent cancers when compared to primary. Recent work by Chen *et al.* identified among others miR-223 as a murine hematopoietic-specific miRNA and showed functionality of these miRNA through in vitro and in vivo overexpression studies [416]. miR-223 was highly expressed in cell lines of myeloid origin suggesting important regulatory roles of in human hematopoiesis and oncogenesis [417]. More recently, it has been reported that miR-223 is a key member of a regulatory circuit involving C/EBPa and NFI-A genes that control granulocytic differentiation and clinical response of acute promyelocytic leukemia (APL) blasts to all-trans retinoic acid (ATRA) [418]. Its intriguing

"myeloid" pattern appears to be evolutionarily conserved [419]. microRNA-223 is commonly repressed in hepatocellular carcinoma and potentiates expression of Stathmin1 [420].

miR-9 was the most downregulated in recurrent cancers and appears to play a functional role in the determination of neural fates in embryonic stem cell differentiation [421]. miR-9 was also transcriptionally downregulated in a methylation-dependent way, in early breast cancer development [422]. Epigenetic inactivation of microRNA gene miR-9 is an early and frequent event in human breast cancer [423].

The first report describing complete miRNA expression profiles in ovarian cancer has just been published, reporting an aberrant miRNA expression in ovarian cancers compared to normal [323]. Specifically, in the serous histotype, 37 of 41 differentially expressed miRNAs were down-regulated relative to normal ovary. In particular, miR-147 and miR-9 were among differentially expressed genes between ovarian tumours and normals, a finding partly in concordance with our results. The absence of other common miRNAs between the two studies suggests that different miRNAs are involved in different stages of ovarian carcinogenesis. A distinct miRNA fingerprint was also identified in drug-resistant ovarian cancer cells [424].

Gene expression levels in the training sample were previously examined as documented in chapter 3 and over/ under represented genes identified with full functional annotation. In this study, miRGen webserver was used to determine lists of putative mRNA targets of differentially expressed miRNAs. Although these lists may contain an unpredictable number of false positives, miRGen appears superior to other approaches, providing higher specificity for a particular miRNA [425]. It was interesting to observe that some of the differentially regulated miRNAs in this study correlate with our transcriptome findings [426] as rather few studies have attempted to link mRNA with microRNA data in different cancers [427, 428].

Similarly, our list of predicted targets for both miR-223 and miR-9 was further uploaded into Panther classification system and examined against the H.sapiens reference list to determine what percentage of genes were present compared to that expected and to determine whether any relevant biological pathways were statistically significant at a p value of 0.01. No pathway was observed for the "miR-223 list" of predicted gene targets against the reference list. However, for miR-9, five pathways, well characterized in the pathogenesis of ovarian cancer and chemoresistance, were identified; namely angiogenesis, Ras, integrin signalling, Notch signalling and a pathway involving actin and tubulin, well known to interfere with the mechanism of action of taxanes (Figure 4.11). It appears that these pathways at a statistically significant level contain traits that distinguish primary and recurrent ovarian cancers. If downregulated miRNAs are expected to activate overexpression of mRNA targets, it is fair to suggest that miR-9 downregulation can possibly lead to drug resistance.

The target list for miR-223 and miR-9 was interestingly enriched for genes involved in FGF cell signaling (*FGFR2* and *FGF* respectively), which is in concordance with our transcriptomic results. This is also consistent with the very latest discovery that FGF signaling is crucial for collective invasion of carcinomas cells following the tracks generated by fibroblasts [429]. FGF-mediated signalling also negatively regulates the initiation of miR-206 gene expression [430].

To elucidate the mechanism of miRNA dysregulation in the recurrence of ovarian cancer we characterised the alteration in expression of genes encoding proteins of the miRNA machinery, namely Dicer, Drosha and eIF6 that appear to have a role in miRNA-mediated post-transcriptional regulation. Knocking down Drosha and Dicer, reduces the production of mature miRNAs in cell lines [209]. Individually, tissue-specific mammalian miR processing has been recently shown to be regulated by Dicer [431]. Dicer upregulation increases expression of miR species in prostate cancer and is associated with aggressive features [432]. Human Dicer is mapped to chromosome 14q where LOH occurs in ovarian cancer at a rate of 49% [17]. Gene expression analysis in primary tumours indicated that the widespread downregulation of miRNAs observed in cancer is due to a failure at the Drosha processing step [433]. EIF6 is a ribosome inhibitory protein, essential for ribosome biogenesis, assembly and initiation of protein translation. Fold changes <2 were observed for Dicer and Drosha at an

mRNA level. To determine whether the observed gene expression pattern was altered at the protein level, primary and recurrent ovarian tumors (n=71) were analysed immunohistochemically on TMA constructs containing multiple histologic sections, using specific antibodies for Dicer and EIF6. They are both cytoplasmic and responsible for processing of mature miRNA, which is the only active in the miRNA-mRNA interplay.

Our results show that Dicer, Drosha and eIF6 may not have a role in recurrent ovarian cancer and may only be involved in early tumorigenesis [432]. We are unsure whether this represents a delay in processing or a complete block on the miRNA machinery, but it is possible that altered miRNA machinery is still functional and other components also participate. Our data do not exclude other important mechanisms, such as DNA copy number alterations [434] or disrupted epigenetic regulation [311], but rather suggest a multistep model for the control of miRNA dysregulation. The exact nature of the regulatory mechanism awaits further investigation.

In summary, a miRNA model is proposed for the molecular pathogenesis and clinical cancer progression in recurrent ovarian cancer (Figure 4.26). Some of the differentially deregulated miRNAs identified correlate with previous transcriptome findings. A molecular signature of 3 miRNAs is a predictor of cancer relapse but not survival in ovarian cancer.

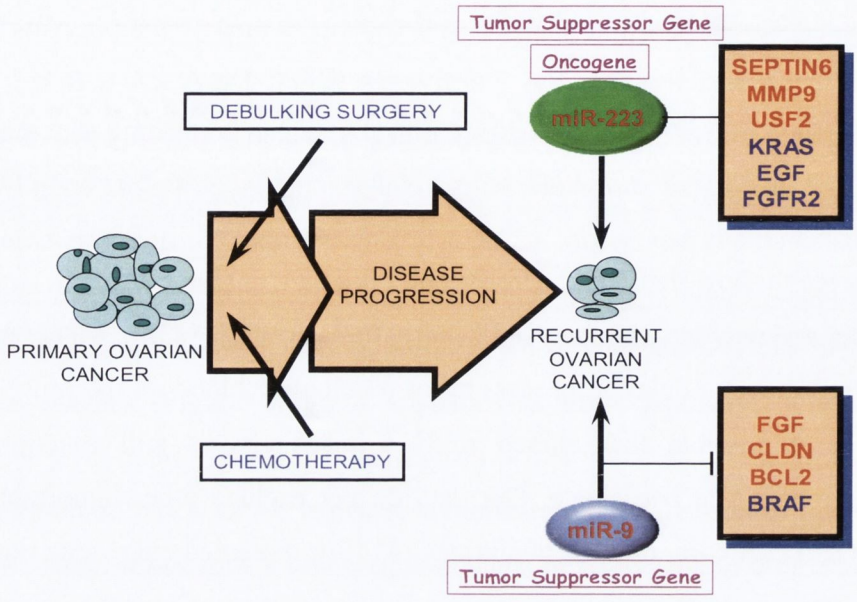

Figure 4.26 A miRNA model for the molecular pathogenesis of recurrent ovarian cancer. Based on integrated transcriptome and miRNA analysis, we identified a "recurrent metastatic signature" comprised of top dysregulated miRNAs, miR-9 (down) and miR-223 (up) that correlated with our previous transcriptome findings. miR-9 appears to be a tumour suppressor gene and when downregulated, it can lead to drug resistance. miR-223 can act either as oncogene or tumour suppressor gene. Genes highlighted in red were previously identified in our transcriptome study. Genes in blue have been well characterised in ovarian cancer. FGF signalling pathway appears to be commonly shared between our identified miRNAs.

Not surprisingly, a significant overlap was observed between putative mRNA targets and genes identified in the previous transcriptome study for the same subcohort of patients. No inverse pattern of correlation was noticed; it remains difficult to identify the precise target mRNA of each miRNA species. Therefore, without further experimental investigation, any mRNA:miRNA partners are essentially speculative and selection involves a degree of subjectivity.

Our findings highlight the potential importance of certain miRNA molecules as biomarkers in recurrent ovarian cancer, given their abundance, stability and easy detection. Future use of this miRNA signature as a blood-based diagnostic and prognostic tool can ultimately be translated into designing drugs that might offer a promising treatment to selected ovarian cancer patients.

CHAPTER 5

Evaluation of *MMP-9* inhibitor and cisplatin cytotoxicity in ovarian cancer cell lines using high content screening (hcs) cell-based assays

5.1 Summary

Background Resistance to cytotoxic drugs principally limits long-term treatment success against ovarian cancer. We previously identified *MMP-9* as a potential marker of recurrence/chemoresistance. We hypothesized that using a chemical inhibitor of *MMP-9* (*MMP-9*i) alone or in conjunction with cisplatin the chemoresistance phenotype seen in ovarian cancer cells could be overcome.

Materials and Methods A2780cis (cisplatin-resistant) and A2780 (cisplatin-sensitive) human ovarian carcinoma cell lines were used. We initially carried out TaqMan PCR on 10 gene targets, previously upregulated in recurrent versus primary ovarian cancers, in our chemoresistant versus chemosensitive ovarian cancer cell lines. The cytotoxic effect of *MMP-9*i and *MMP-9*i+cisplatin in combination was determined using the multiparameter cytotoxicity 1 Kit by Thermo Fisher. Cells were plated in triplicate in 96-well plates overnight and then treated with various concentrations of drugs for 3, 6 and 24 hours. A pre-incubation for 3 hours with *MMP-9*i prior to treatment with cisplatin was also assessed and cytototoxicity was observed at 3 hours and 6 hours. Cells were then stained with three fluorescent dyes to image nucleus, cell permeability and lysosomal mass/pH respectively. Image acquisition analysis was performed by using HCS tool (an automated fluorescent microscope) and the optimized software. The relative fluorescent intensity was used to quantify the above changes.

Results *NRG2* and *MMP9* were consistently upregulated for an average of 3 passages in A2780cis versus A2780 cell lines. *MMP-9*i alone had a cytotoxic effect in cisplatin-resistant cells at high doses (260-520uM) at 3h, 6h and 24h time points but also at an early time course (3h) even at a low dose (52um) The combined treatment of *MMP-9*i+cisplatin enhanced cytotoxicity compared to cisplatin alone. Preincubating cells with *MMP-9*i for 3h at all doses were significantly cytotoxic followed by treatment with cisplatin for 3h but not 6h suggesting an early apoptotic response. Pre-incubating sensitive ovarian cancer cells with *MMP-9*i for 3h resulted in more enhanced cytotoxicity for the 3h incubation with cisplatin compared to the 6h incubation and appeared to be more effective than co-incubation at early time in a concentration dependent way.

Conclusion Highly selective *MMP-9*i might have a place in treatment of recurrent/chemoresistant ovarian cancer but their role *in vivo* remains to be evaluated.

5.2 Introduction

Platinum compounds, given as combination of cis-and/or carboplatin, constitute the most active and standard chemotherapy treatment for nearly all women diagnosed with ovarian cancer. Despite its efficacy, resistance to chemotherapy, both intrinsic and acquired, is a major cause of treatment failure. Resistance to cisplatin occurs in roughly one-third of women during primary treatment and in almost all patients treated for recurrent disease [435]. New approaches are clearly needed. Thus, the concept of maintenance or consolidation therapy after optimal first line treatment is of potential interest.

Inactivation of pathways rather than dysregulation of single genes has been proposed for resistance. Currently, resistance can only be determined retrospectively after patients have experienced the burden and toxicity of ineffective therapy. Thus, it remains a critical point requiring extensive investigation in cell lines and validation in clinical specimens.

The mechanisms by which tumours can develop cisplatin resistance appear to be multifactorial and can be arbitrarily grouped into two broad categories: 1) the mechanisms affecting the amount of DNA damage and 2) the mechanisms affecting the response of cells to damage. It is believed that cisplatin resistance in a given tumour arises through multiple mechanisms.

5.2.1 Matrix Metalloproteinases (MMPs)

MMPs comprise a family of calcium and zinc-dependent endopeptidases that consist of 21 human MMPs and numerous homologues from other species. They are synthesized as inactive zymogens and activated by proteinase cleavage. Their activity is regulated by endogenous inhibitors, including A2-macroglobulin and tissue inhibitors of metalloproteinases (TIMPs). TIMPs regulate the function of MMPs either by inhibiting active MMPs or by controlling their activation process. They form tight, non-covalent inhibitory complexes with MMPs (K_d = 10 to 50 pM).

They are characterized by the presence of a zinc ion in the active site, which is required for their catalytic activity. Historically, they are divided into collagenases,

gelatinases, stromelysins and matrilysins on the basis of their specificity for ECM components and the common names of the MMPs reflect this classification (Figure 5.1). *MMP9* belongs to the subfamily of gelatinases which are highly active against collagens and is predominantly secreted by stromal rather than tumour cells. However, the list has grown thus far and 28 different types of MMPs (secreted or transmembrane enzymes) have been identified and classified based on their protein domain structures derived from genomic data. Of these, 23 MMPs have been found to be expressed in human tissues.

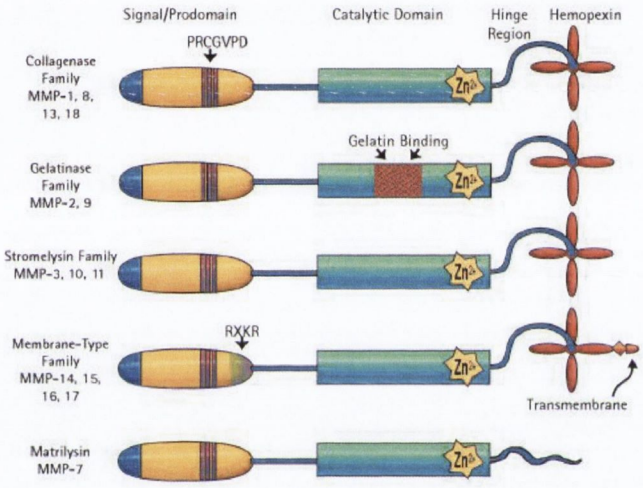

Figure 5.1 Classification of MMPs based on their specificity for ECM components

All MMPs sequenced to date have at least three domains in common. The prodomain contains a highly conserved segment of eight amino acids that fold over to cover the catalytic site and helps to maintain the inactive conformation following the release of MMPs. Cleavage of the prodomain destabilizes the inhibitory interaction between the unpaired cysteine in the sequence and the active site zinc. The catalytic domain contains the conserved structural metal binding sites consisting of 106 to 119 residues. The highly conserved zinc-binding active site domain contains 52 to 58 aminoacids.

MMPs have been primarily associated with matrix remodelling, an essential component of invasion. This is accomplished by the ability of MMPs to modulate the availability and activity of growth factors and cytokines or their receptors, and to process adhesion and signaling receptor targets [436].

Recent studies confirmed that MMP activity involves precise MMP localization on a cell's invasive front, exposure of key components in the extracellular matrix which transform it from a barrier into a scaffold for invasion and cleavage of growth factors which result in cell growth, division and inhibition of apoptosis [437].

For tumour invasion to occur there must be degradation of the extracellular matrix and connective tissue surrounding the tumour cells. MMPs comprise a family of highly specialized enzymes that are able to degrade most components of the extracellular matrix. In this respect, they can regulate the tumour microenvironment and their expression is increased in almost all human cancers compared to normal tissue. They are expressed in cell- or tissue-specific patterns. MMPs also play an important role in wound healing, angiogenesis, and embryogenesis.

Functions of MMPs also underlie all fundamental hallmarks of cancer progression. Originally, MMPs were considered to facilitate exclusively tumor cell invasion and metastasis by at least three distinct mechanisms: (a) by eradicating physical barriers to invasion through degradation of collagens, laminins, and proteoglycans in the ECM, (b) by modulating cell adhesion and enabling cells to form new cell-to-cell and cell-to-matrix attachments while breaking the existing ones, and (c) by acting on ECM components and other proteins to expose hidden biological activities, such as release of angiostatin from plasminogen. In normal adults, MMP expression is very low except in rapidly remodeling tissue, such as wound healing and menstrual endometrium.

However recent studies document that MMPs are involved in several steps of cancer development (Reviewed in [438] and illustrated in Figure 5.2). These include cancer cell growth, EMT or differentiation, apoptosis, migration and invasion and the regulation of tumour angiogenesis and immune surveillance. MMPs have both cancer-promoting and cancer inhibiting functions and pathways with opposing effects on cancer progression are sometimes initiated by cleavage of the same substrate.

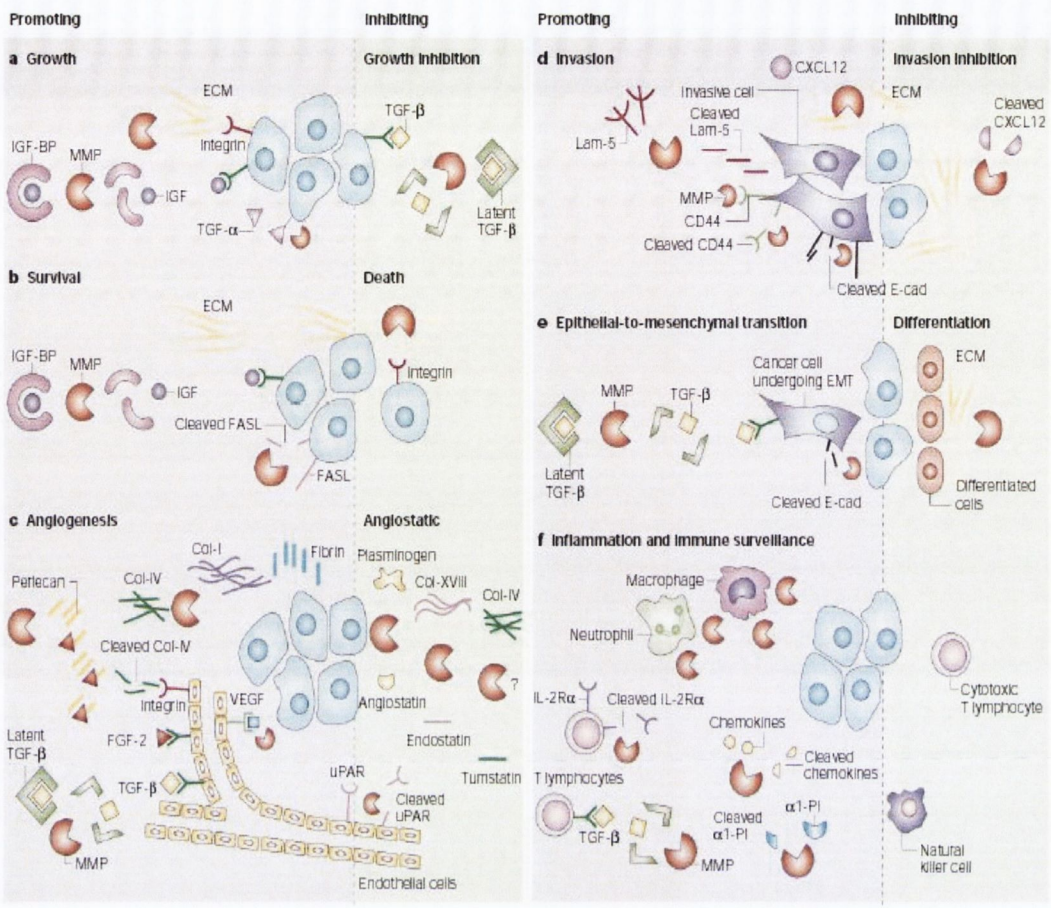

Figure 5.2 Functions of MMPs in cancer progression Are MMPs good or bad? Their basic mechanism of action- "degradation of proteins"- regulates various cell behaviours with relevance for cancer biology (Adapted from [438]).

5.2.2 MMP inhibition in anticancer therapy

Several agents have been developed, that block the synthesis of MMP, preventing them from interacting with molecules that direct their activities to the cell surface or inhibiting their enzymatic activity.

MMP synthesis is directly inhibited by transfecting cells with antisense mRNA or by targeting mRNA with ribozymes. In mouse models, downreglation of *MMP9* by these means results in reduced glioblastoma tumour burden [439].

MMPs can hypothetically be inhibited by blocking their interactions with other proteins [440]. This simple type of strategy has not been yet tested in clinical practice. To take advantage of the increased MMP activity in tumours, cytotoxic agents that are activated by MMPs have been developed. These include recombinant toxin proteins that are activated by MMP cleavage and then internalized by the cell, leading to cell death [441].

A more straightforward way is by blocking their enzymatic activity. Natural inhibitors, such as TIMP-2 and TIMP-4 have shown efficacy in experimental models [442] but systematically administered, can also promote cancer growth [443]. A membrane-anchored glycoprotein, RECK, negatively regulates *MMP-9* and inhibits tumor invasion and metastasis [444].

Instead, five categories of synthetic MMP inhibitors have been developed:

- The collagen peptidomimetics (Batimastat and Marimastat that mimic the cleavage sites of MMP substrates).
- The collagen non-peptidomimetics (synthesized on the basis of the conformation of MMP active group, eg Bay 12-9566, BMS 275291).
- The tetracycline derivatives (Metastat that inhibits both activity and synthesis of MMPs without any antibiotic activity).
- Small peptides: These can be selected for high specificity for individual MMPs and one such peptide that inhibits gelatinase (both *MMP-2* and 9) enzymatic activity showed promising effect in animal experiments [445].
- Unconventional MMP inhibitors (a component in green tea acts as an *MMP-2* and *MMP-9* inhibitor [446].

A novel anthralinic-acid based *MMP-9* Inhibitor 1 (Calbiochem-Novabiochem Corp., San Diego, CA, USA) is a potent and selective inhibitor of *MMP-9*, which also inhibits *MMP-1* and *MMP-3* at higher concentrations [447]. An *MMP-2*/*MMP-9* inhibitor, 5a, enhances apoptosis induced by ligands of the TNF receptor superfamily in cancer cells [448]. Treatment with Batimastat, a nontoxic to cells synthetic MMP inhibitor, potentiates the antitumour activity of cisplatin in ovarian carcinoma xenografts [449].

Results from initial clinical trials have proved rather disappointing due to either lack of benefits or major adverse effects or even non ideal design. However, an appreciation of their many functions because of the current understanding of their diverse role in cancer progression –often acting in opposing directions – is needed.

MMP inhibitors have been compared with cytotoxic drugs and tested in patients with late stage tumours. Evidence also suggests their usefulness as preventive drugs because they are cytostatic. Moreover, MMP inhibitors have also an important role in tumour angiogenesis, therefore treating recurrent tumours, one would expect to result in tumour shrinkage.

Most trials also used the maximum tolerated dose of inhibitors. However, at maximum tolerated doses, apart from the obvious adverse effects, some inhibitors might lose selectivity for specific MMPs. This necessitates either reduced dosing or highly selective targeting or even use in earlier stage than conventional chemotherapeutics.

Research has been devoted to the development of *in vitro* methods to accurately predict the chemosensitivity of human tumours in vivo [450]. The advantages and disadvantages of these methods have been widely discussed [451]. We recently used the 3-(4,5-dimethylthiazol-2yl)-5-(3-carboxymethoxyphenyl)-2-(4-sulfophenyl)-2H-tetrazolium, inner salt (MTS) assay to determine the chemosensitivity/resistance of ovarian cancers [452] [453]. Novel screening methods have been since developed, including flow cytometry and HCS.

5.2.3 HCS and Cytotoxicity screening

Multiparametric analysis of drug toxicity at the level of individual cells using cellular imaging-based approach such as HCS plays a key role in the detection of toxicity and classification of cytotoxic compounds. Historically, cellular toxicity screening has relied on the use of single-parameter readouts for toxicity markers such as cell proliferation, mitochondrial activity or membrane permeability. However, parallel analysis of multiple markers for cytotoxicity allows early reversible and late irreversible effects to be distinguished and in this way, it provides a more sensitive interpretation of compound-induced toxicity [338].

HCS-based cytotoxicity assays analyze the effects of compounds on a number of parameters such as nuclear morphology, cell membrane permeability, lysosomal mass/pH and cell density, offering increased specificity and selectivity for toxic events.

MMP-9 was previously identified as a potential marker of recurrence/chemoresistance as described in chapter 3. We hypothesized that using a chemical inhibitor of *MMP-9* (*MMP-9*i) alone or in conjunction with cisplatin the chemoresistance phenotype seen in ovarian cancer cells could be overcome. The cytotoxicity of the above compounds was evaluated by application of HCS multiparametric cytotoxicity assay.

5.3 Materials and methods

5.3.1 Cell cultures

A2780 and A2780cis (cisplatin-resistant) human ovarian carcinoma cell lines were purchased from ECACC and cultured as described in section 2.11.

5.3.2 Chemicals

MMP-9/MMP-2 inhibitor, (2R)-2-[(4-Biphenylylsulfonyl)amino]-3 phenylpropionic Acid (C21H19NO4S), was purchased from Calbiochem (Merck, Darmstadt, Germany). It is described as a potent inhibitor of *MMP-2* (IC_{50} = 310 nM) and *MMP-9* (IC_{50} = 240 nM) [454] (Figure 5.3).

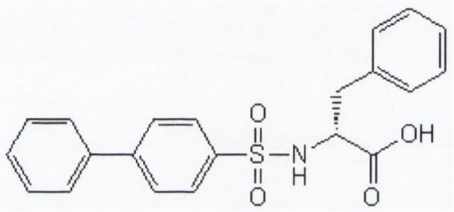

Figure 5.3 (2R)-2-[(4-Biphenylylsulfonyl)amino]-3-phenylpropionic Acid with a molecular weight (MW): 381.5.

Table 5.1 displays the concentrations of cytotoxic drugs used in our study, alone or in combination. A 520mM stock solution was prepared in DMSO (by dissolving 5mg in 250μL DMSO) and escalated concentrations were prepared by further diluting the stock dilution in DMSO so that IX refers to the IC50 for *MMP-9* inhibition (IC50= 240nm or 0.24μM). 5X and 10X concentrations were also selected that one would expect maximum concentrations. Cisplatin, (Pt(NH3)2Cl2) was obtained from Sigma-Aldrich (Sigma-Aldrich, Ireland Ltd). A 10μM stock solution was prepared in Phosphate Buffer Saline (PBS) by dissolving 25mg in 8ml of PBS immediately before use. DMSO was used as a positive control.

Table 5.1: List of concentrations of Cisplatin and *MMP-9*i; 1X refers to IC50 for MMP-9i. 2X refers to the PPC for cisplatin. Concentrations refer to the stock solutions prepared for the cytotoxic drugs.

*MMP-9*i (μM)	Cisplatin (μM)
52 (1X)	1 (1X)
260 (5X)	2 (2X)
520 (10X)	10 (10X)

5.3.3 TaqMan PCR analysis of selected candidates

11 genes previously identified and validated as upregulated in recurrent compared to primary ovarian cancers, using a transcriptomic approach, as described in chapter 3, were selected for TaqMan PCR analysis. This is described in Material and Methods (Chapter 2).

All reactions were carried out on the ABI Prism 7000 Sequence detection system (Applied Biosystems, Applera UK, Cheshire, UK) using the TaqMan® Universal PCR master Mix and TaqMan® Gene Expression Assays (Applied Biosystems). Gene symbols and Assay ID's for the 11 genes are shown in Table 5.2. Relative quantitation in A2780cis compared to A2780 cells was carried out using the ΔΔCt method with 18S ribosomal RNA as an endogenous control. Transcript quantification was performed in triplicate for each sample.

Table 5.2 List of selected genes for TaqMan analysis in the cell lines with their assay ID's. These genes were previously identified in the transcriptomic study as described in chapter 3.

Gene Symbol	Probe ID	P value	Array fold change	Expression in recurrent vs primary	Assay ID
CLDN16	163630	0.0068	9	Upregulated	Hs00198134_m1
S100B	114188	0.0001	6.12	Upregulated	Hs00389217_m1
BTC	112710	0.0006	2.67	Upregulated	Hs00156140_m1
IL27RA	145754	0.0005	1.82	Upregulated	Hs00175472_m1
FGF2	113042	0.03	2.7	Upregulated	Hs00266645_m1
NRG2	170215	0.013	3.6	Upregulated	Hs00171706_m1
S100A8	196494	0.034	11.6	Upregulated	Hs00374263_m1
ZNF218	217273	0.002	6.06	Upregulated	Hs00542836_m1
MMP9	112640	0.0169	4.975	Upregulated	Hs00234579_m1
TJP3	182089	0.013	2.7	Upregulated	Hs00274276_m1
IL1R2	186009	0.038	4.46	Upregulated	Hs00174759_m1

5.3.4 Cytotoxicity assay

The cytotoxicity effect of *MMP-9*i (cytostatic) and cisplatin (cytotoxic) alone or/and simultaneous co-incubation of *MMP-9*i+cisplatin was determined using the multiparameter cytotoxicity 1 kit by Thermo Fisher® as described in Section 2.13. A preincubation for 3h with *MMP-9*i prior to treatment with cisplatin for 3h and 6h was also assessed. The HCS assay was used to analyze the results of cytotoxicity after addition of drugs to cells.

All treated cells were assayed in triplicates and results were expressed as mean percent surviving cells. DMSO was used as an endogenous control. Error bars

represented the coefficient of variation for the findings in the replicate wells. Statistical significance was considered at $P < 0.05$.

5.3.5 Statistical analysis

Results were expressed as the mean+-SD (n=3 wells). Statistical analysis was carried out by t-test or two-way ANOVA was carried out using the PRISM® software. Statisical significance was inferred at $p<0.05$.

5.4 Results

5.4.1 RNA sample analysis from cell lines

The quality and quantity of RNA extracted from A2780cis and A2780 ovarian cancer cells was determined prior to TaqMan analysis. No more than $5x10^5$ cells were used for RNA extraction. Sample results from the Nano Drop are shown on Table 5.3A and B. A2780cis cell line was obtained at passage P6 and A2780 cell lines at passage 8. Passages 6 and 8 were selected respectively for "within passage" RNA extraction. In passage 8 A2780cis cell line is expected to maintain its resistance without any cisplatin addition as per manufacturer's instructions.

Table 5.3A Nano Drop Analysis of A2780cis (resistant) and A2780 (sensitive) ovarian cancer cells

Samples	RNA conc (ng/ml)	A260/280	A260/230
A2780cis			
Passage 6	1276	2.15	1.83
Passage 7	320	2.14	1.83
Passage 8	86	1.89	1.74
A2780			
Passage 7	87.5	2.21	1.74
Passage 8	2650	2.1	1.94
Passage 10	2255	2.10	2.10

Table 5.3B: Nano Drop Analysis of A2780cis (Passage 6) and A2780 (Passage 8) ovarian cancer cells

Samples	RNA conc (ng/ml)	A260/280	A260/230
A2780cis (passage 6)			
Replicate 1	1276	2.15	1.83
Replicate 2	686	1.94	1.88
Replicate 3	88	1.89	1.65
A2780 (passage 8)			
Replicate 1	3830	2.09	2.1
Replicate 2	2650	2.1	1.94
Replicate 3	1956	1.84	2.15

5.4.2 RT-PCR analysis of selected candidates

TaqMan PCR was carried out on previously selected targets (n=10) as discussed in chapter 3 and Table 5.1. Relative quantitation was carried out in A2780cis versus A2780 ovarian cancer cells. *MMP9* and *NRG2* were identified as upregulated in "resistant" versus "sensitive" cells with fold changes of 2.12 and 4.37 respectively. Upregulation was observed for an average of three passages in A2780 cis compared to A2780 cell line. BTC was excluded from analysis as it was not detected in either cell lines. Technical replicates were also performed for a representative passage for each line. Each individual passage followed the same overall pattern for the upregulated genes.

Clustering of selected targets was performed using both heatmaps and K-means clustering and the Euclidean distance was used to measure the similarity or dissimilarity between the individual genes to reflect their fold changes in A2780cis vs A2780 cell lines. *MMP9* and *NRG*" skewed the "cluster" group for any type of unsupervised or supervised clustering. (Figures 5.4, 5.5 and 5.6).

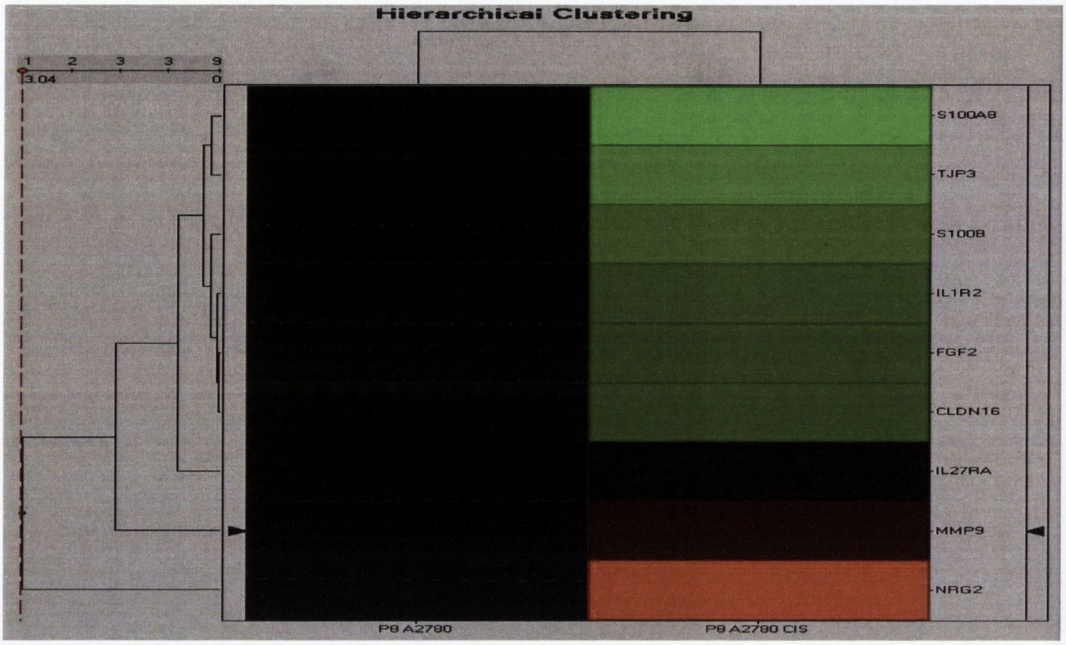

Figure 5.4 Heatmap demonstrating two-dimensional hierarchical clustering of selected gene targets based on their relative quantitation (RQ) in A2780cis vs A2780 cell lines for an average of three passages. The A2780 cell line was used as a calibrator, so that RQ=1 for each assay. Colour changes other than bright green represent varying degrees of upregulation as was observed for *NRG2* (red) and *MMP9* (brown) that correspond to fold changes of 4.37 and 2.12 respectively.

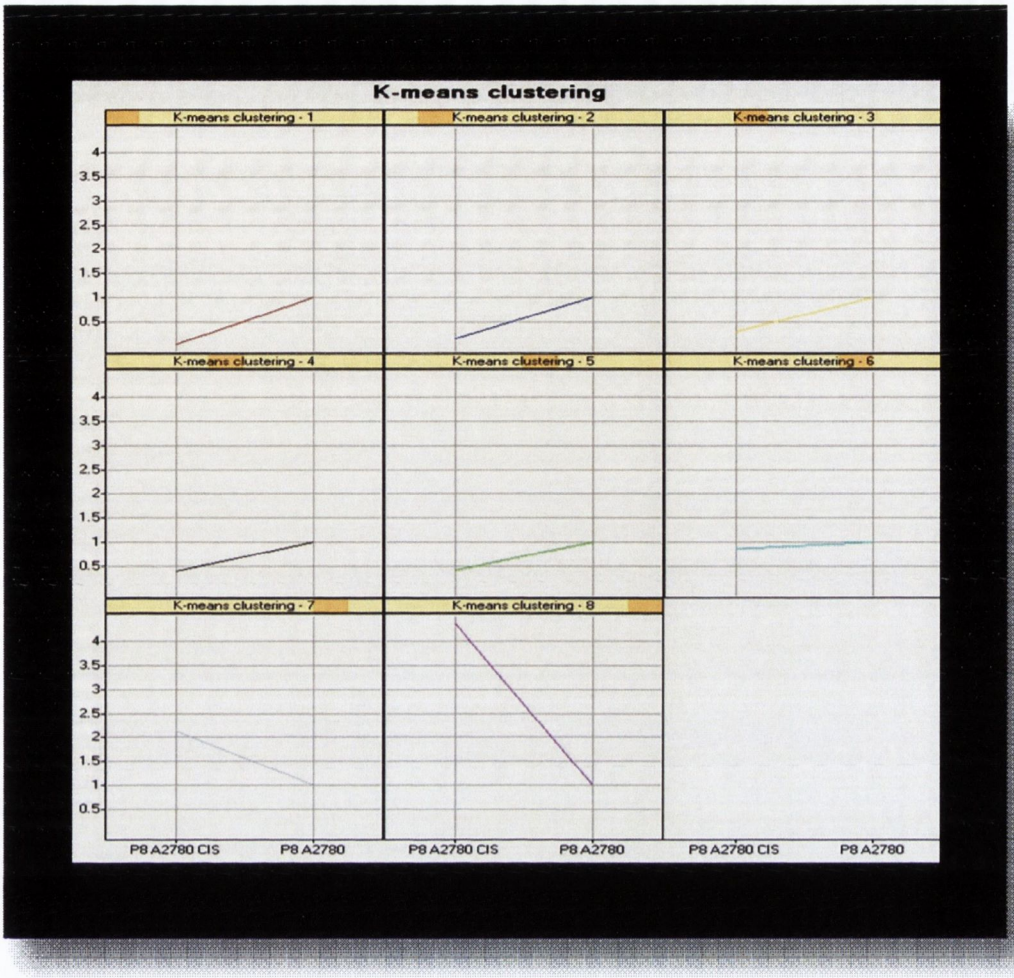

Figure 5.5 K-means unsupervised clustering of the 8 deregulated genes in A2780 vs A2780 cell lines. It validates the heatmap clustering and clusters the upregulated genes separately (K=3). The slope of the graphs indicates the RQ of the above genes in A2780cis vs A2780 cell lines. Since we focused on the upregulated genes, S100A8 was omitted from analysis as it was highly downregulated in A2780cis vs A2780 cells. Fold changes for upregulated genes *NRG2* and *MMP9* (highlighted in red) were 4.37 and 2.12 respectively.

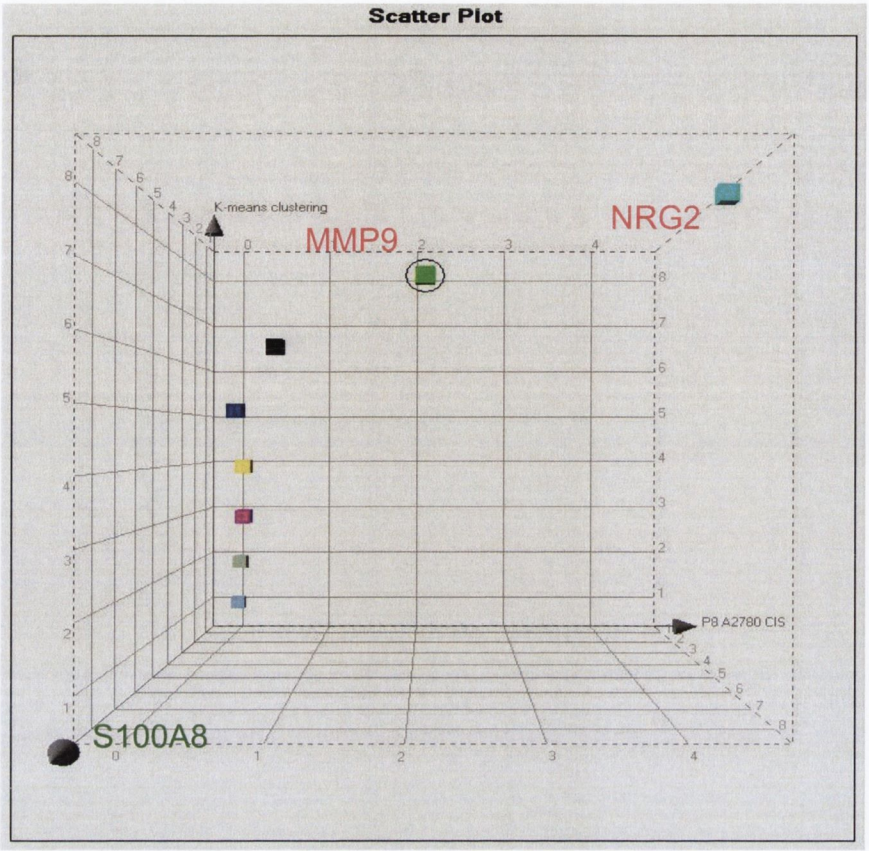

Figure 5.6 Scatter plot three dimensional clustering of tested genes based on their fold changes in A2780cis compared to A2780 cell lines. Each gene represents one point with 3 attributes (x; A2780cis, y; A2780, z; Hierarchical clustering) and is placed as a coordinate in an attribute space based on Euclidean distance measurements. The scatter plot demonstrated a main group of genes with similar fold changes. *MMP9* and *NRG2* appeared to "skew" from that main group given their upregulation pattern in A2780cis vs A2780 cells.

5.4.3 *MMP-9*i induces cell death in chemoresistant ovarian cancer cells

A flowchart of our cytotoxicity experiment is shown in figure 5.7.

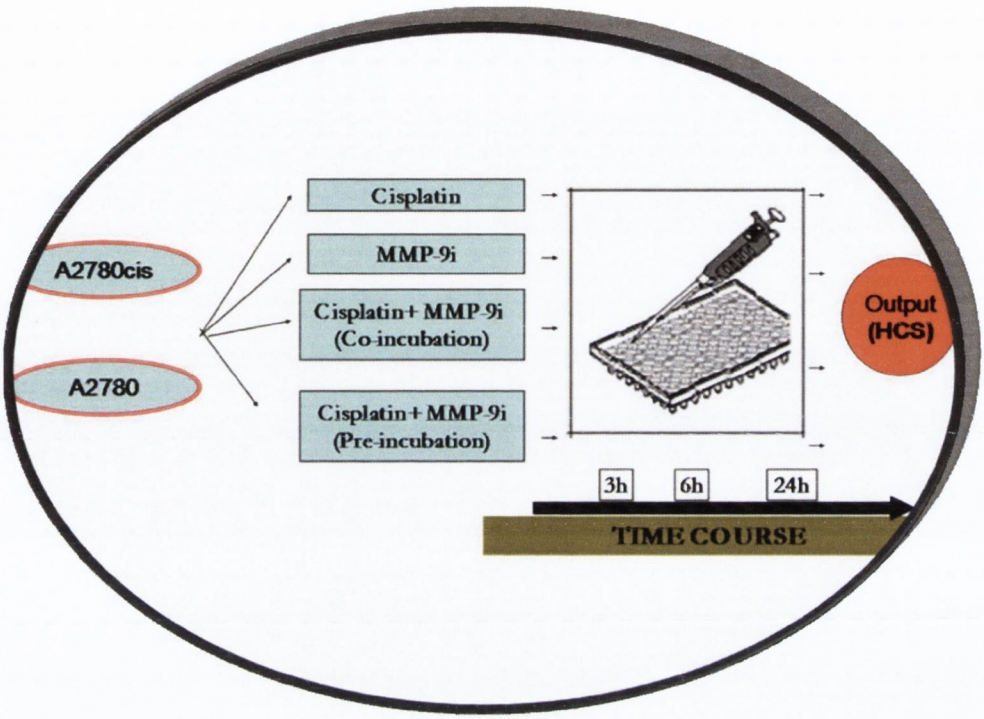

Figure 5.7 Flow chart of our dose and time response experiments using the cytotoxicity assay in A2780 cis and A2780 cell lines. Cells were treated with cisplatin or *MMP-9*i alone or in combination at different time points (3h, 6h and 24h). Cytotoxicity parameters were assessed using the HCS tool.

We first screened the A2780cis cell line for resistance to cisplatin-induced apoptosis. As shown in figure 5.8, cisplatin induced cell death in 17%-18% of A2780cis cells following 3h incubation, up to 30% of A2780cis cells following 6h incubation and in 47%-66% of A2780cis cells following 24h incubation, however, the proportion of apoptotic cells was not significantly different. Changes in cytotoxicity parameters such as cell density, cell membrane permeability, lysosomal mass/pH, nuclear morphology were assessed. Although there was no effect in lysosomal mass/pH and cell membrane permeability, cisplatin induced significant nuclear morphology changes that were more pronounced at the longest incubation time (24hr) (Figure 5.8A-E).

A

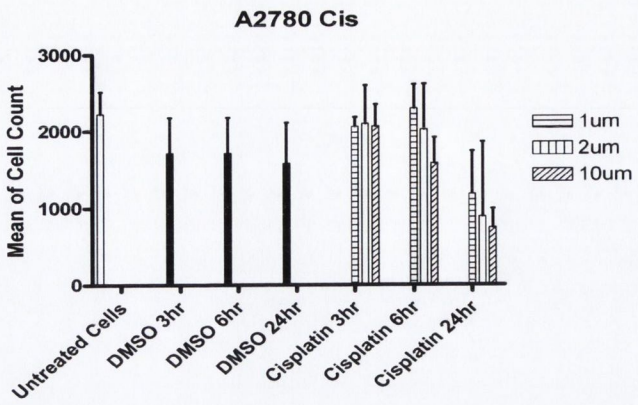
A2780 Cis
Mean of Cell Count
3000
2000
1000
0
1um
2um
10um
Untreated Cells
DMSO 3hr
DMSO 6hr
DMSO 24hr
Cisplatin 3hr
Cisplatin 6hr
Cisplatin 24hr

B

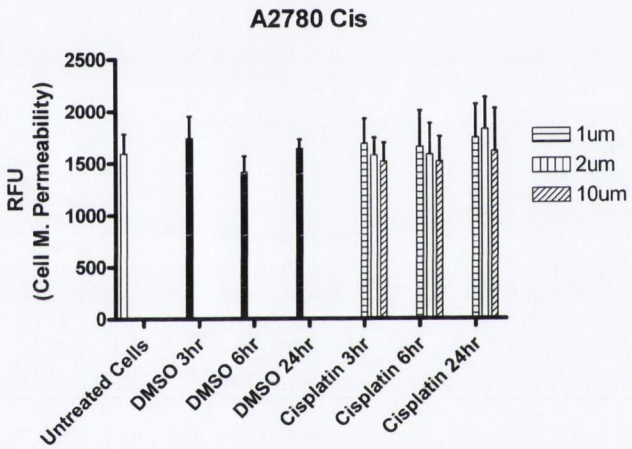
A2780 Cis
RFU
(Cell M. Permeability)
2500
2000
1500
1000
500
0
1um
2um
10um
Untreated Cells
DMSO 3hr
DMSO 6hr
DMSO 24hr
Cisplatin 3hr
Cisplatin 6hr
Cisplatin 24hr

C

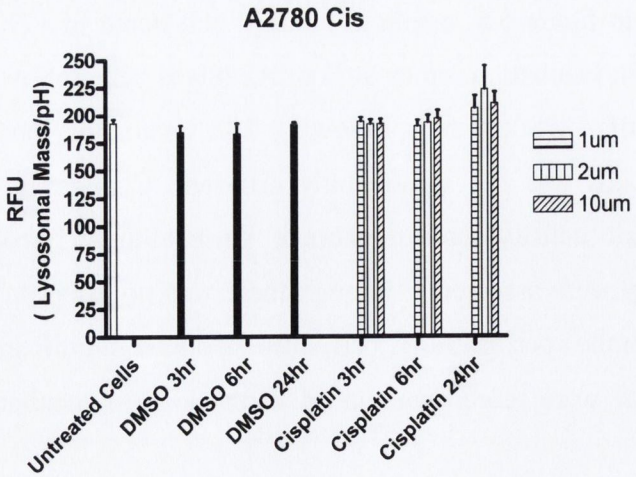
A2780 Cis
RFU
(Lysosomal Mass/pH)
250
225
200
175
150
125
100
75
50
25
0
1um
2um
10um
Untreated Cells
DMSO 3hr
DMSO 6hr
DMSO 24hr
Cisplatin 3hr
Cisplatin 6hr
Cisplatin 24hr

D

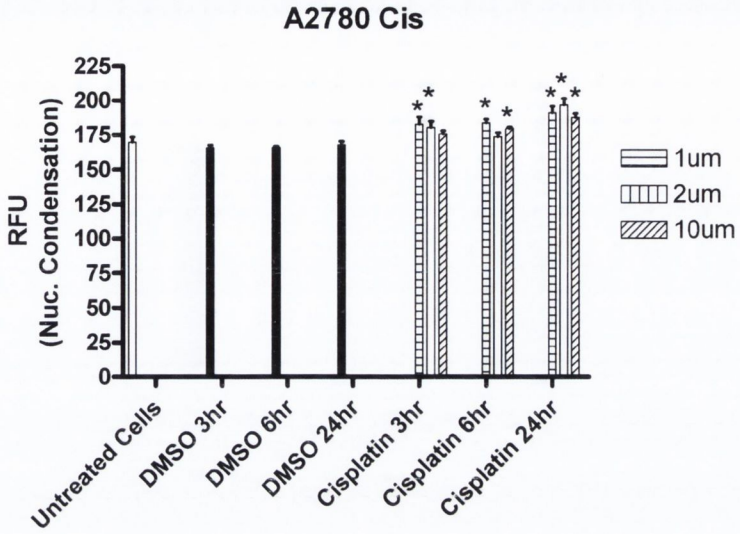

E

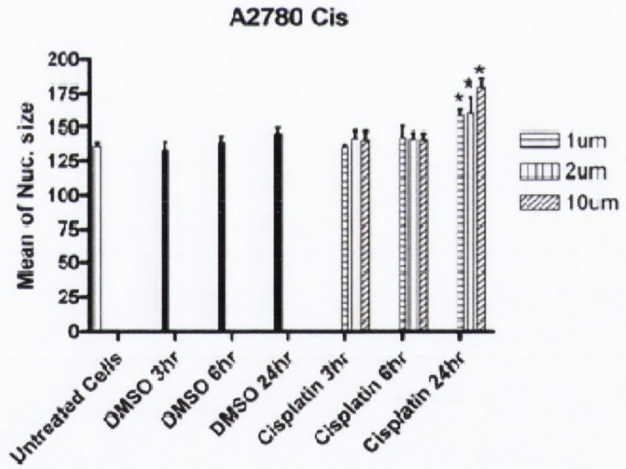

Figure 5.8(A-E) Simultaneous monitoring of changes in A) cell density B) cell membrane permeability C) lysosomal mass/pH D) nuclear condensation and E) nuclear size following treatment of the A2780cis cells with cisplatin (1μM, 2μM, 10μM) and incubation for different time points 3h, 6h and 24h. DMSO was used as a vehicle control. Representative data are shown as means +-SD (n=3 wells).

To determine if *MMP-9*i alone was cytotoxic to resistant ovarian cells *in vitro*, cells were treated with or without *MMP-9*i at titrated concentrations (52μM, 260μM, 520μM) for different time points, 3h, 6h and 24hr. Effects in cytotoxicity are shown in figure 5.9A-E.

There was no significant effect of *MMP-9*i alone in cell density. *MMP-9*i induced cell death in 22%-49% of A2780cis cells. The apoptotic effect was similar following 6h and 24h incubation (45%-50% vs 44%-53%). Increase in cell membrane permeability was significant following treatment with 260um at 24h, as displayed in figure 5.9B. Lysosomal mass increase was significant at all concentrations after treatment for 24h (Figure 5.9C).

Treatment with 260μm of *MMP-9*i caused a significant increase in nuclear condensation at 3h and 24h but the effect was also significant at 52μm and highest (520m) concentrations 6h post incubation. An increase in nuclear size (nuclear swelling) was significant for *MMP-9*i at high toxic concentrations (260-520μM) at an early time course (3h). Treatment with *MMP-9*i vs DMSO was not significant at all doses and all time points.

A

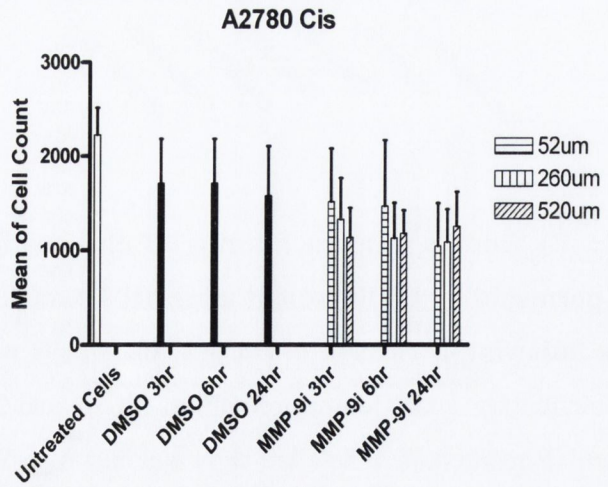

B

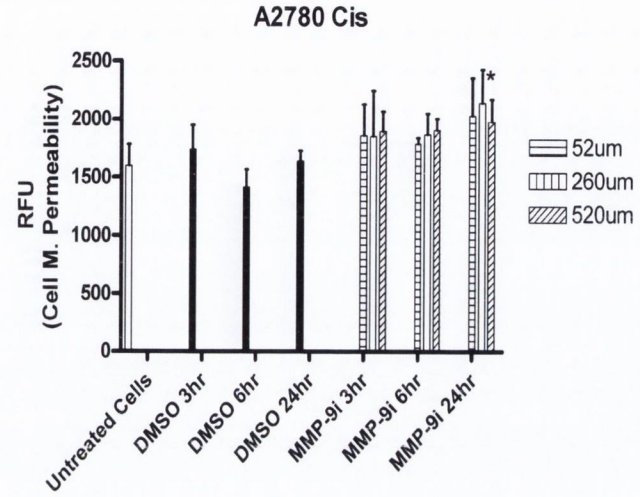
A2780 Cis
RFU
(Cell M. Permeability)
2500
2000
1500
1000
500
0
*
52um
260um
520um
Untreated Cells
DMSO 3hr
DMSO 6hr
DMSO 24hr
MMP-9i 3hr
MMP-9i 6hr
MMP-9i 24hr

C

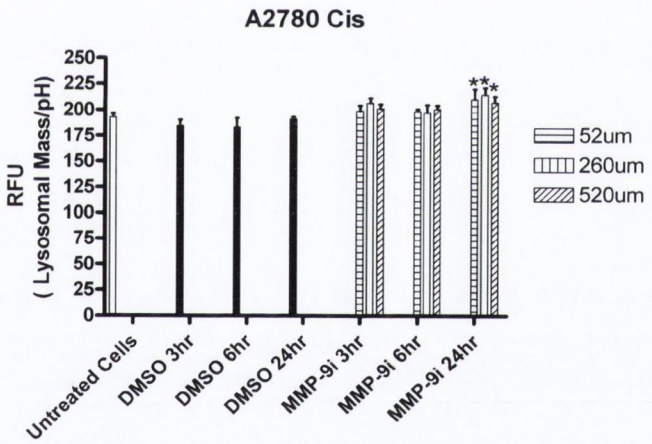
A2780 Cis
RFU
(Lysosomal Mass/pH)
250
225
200
175
150
125
100
75
50
25
0
**
*
52um
260um
520um
Untreated Cells
DMSO 3hr
DMSO 6hr
DMSO 24hr
MMP-9i 3hr
MMP-9i 6hr
MMP-9i 24hr

D

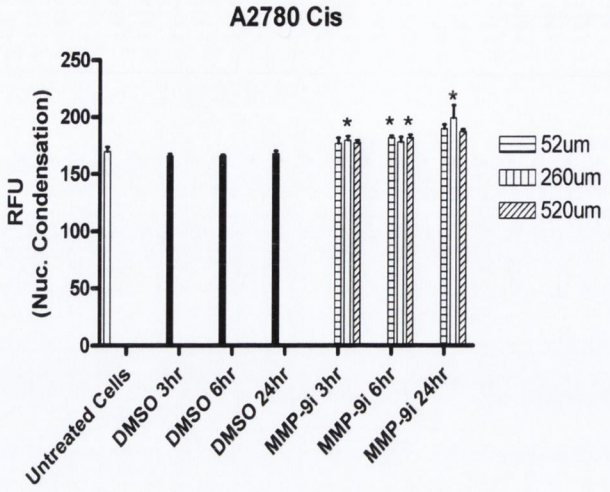

E

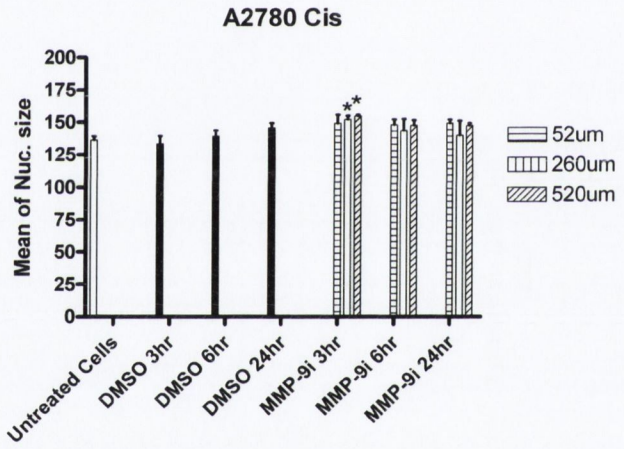

Figure 5.9(A-E) Simultaneous monitoring of changes in cell density, cell membrane permeability, lysosomal mass/pH, nuclear condensation and nuclear size following treatment of the A2780cis cells with *MMP-9*i (52μM, 260μM, 520μM) and incubation for different time points 3h, 6h and 24h. DMSO was used as a vehicle control. Representative data are shown as means +-SD (n=3 wells).

5.4.4 Drug cytotoxicity in the A2780cis cell line and changes in cell morphology

Using the HCS, we observed changes in morphology of cisplatin and *MMP-9*i treated cells as demonstrated in Figure 5.10. A2780cis cells were incubated with DMSO (vehicle control) (E), cisplatin (B, C, D) and MM-9i (F, G, H). Untreated cells were also shown (A). HCS images were obtained following 3h treatment (X10). Negative control wells had more cells, whereas wells with toxic doses of drugs had fewer cells measured per field, depending on the cytotoxicity of the drugs. A decrease in cell density was observed following treatment with ciplatin or *MMP-9*i in a concentration dependent manner.

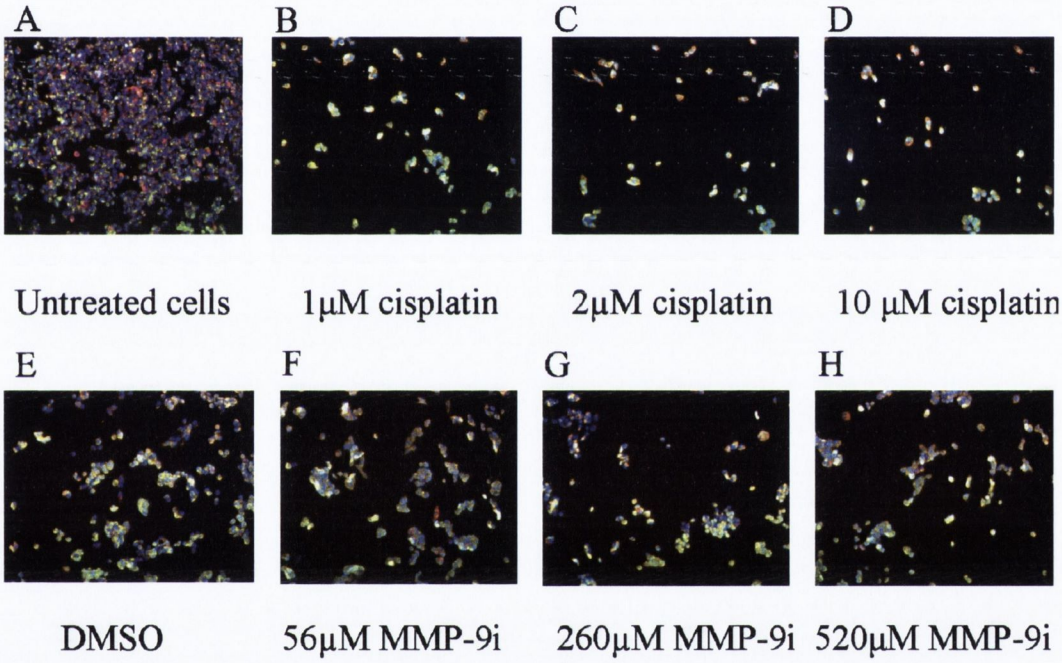

Figure 5.10 Morphology of cisplatin and *MMP-9*i treated cells as demonstrated by HCS image analysis.

5.4.5 *MMP-9*i enhances cisplatin-induced cell death in chemoresistant ovarian cancer cells at an early time point

We then sought to determine whether co-treatment of ovarian cancer cells could enhance cisplatin-induced apoptosis at 3h and 6h. Resistant ovarian cancer cells were coincubated along with varying concentrations of *MMP-9*i (52-520μm). 1μm cisplatin/260μm *MMP-9*i was significantly cytotoxic in 40% of A2780cis cells at 3h. Highest cytotoxicity (~55%) was observed at maximum concentrations of cisplatin

(10μM) and *MMP-9*i (520μM) at 3h but was not significant. No significant result in cell density was observed at 6h for any dose combination.

Co-incubation of a subtoxic dose (1μM) of cisplatin with 260uM *MMP-9*i at 3h appeared to result in significantly greater cytotoxicity as compared to cisplatin or *MMP-9*i treatment alone (Figures 5.11A, C, E, G, I compared to 5.11 B, D, F, H, J and figures 5.8A and 5.9A).

A

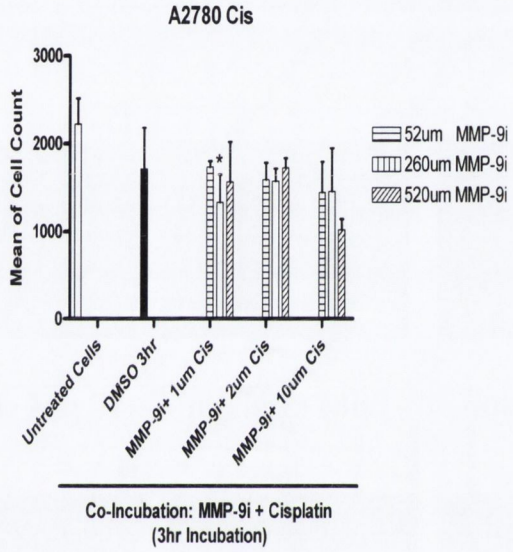

B

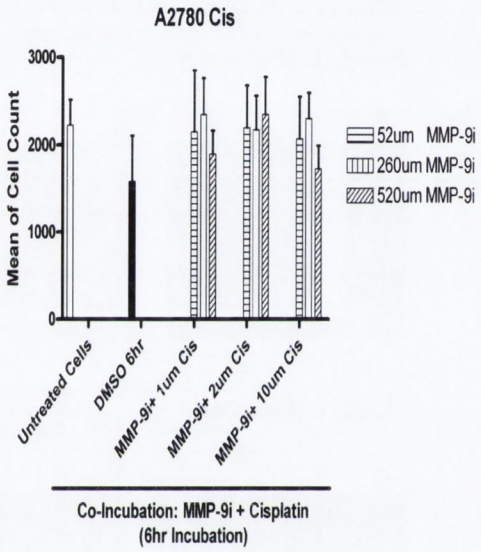

C

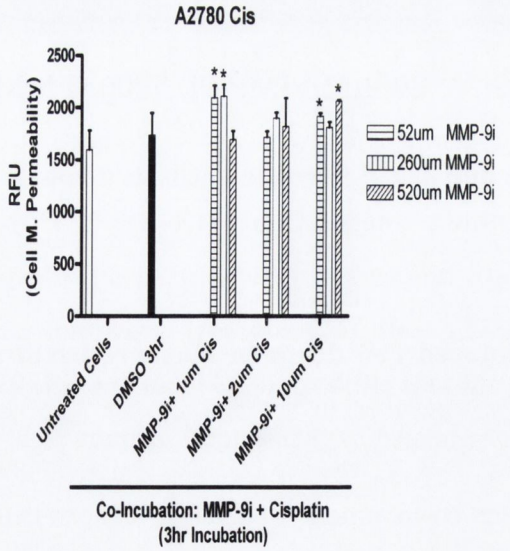

D

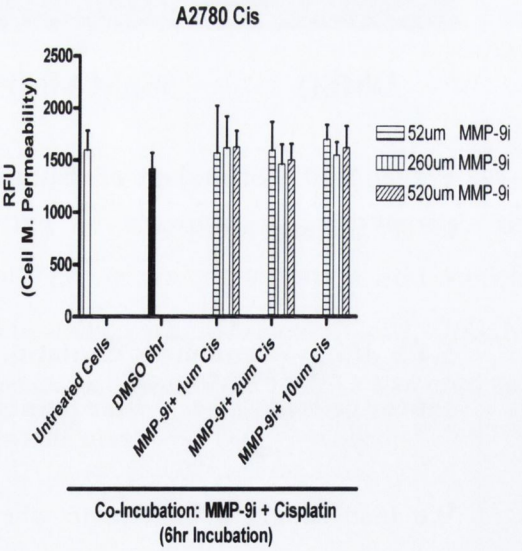

E

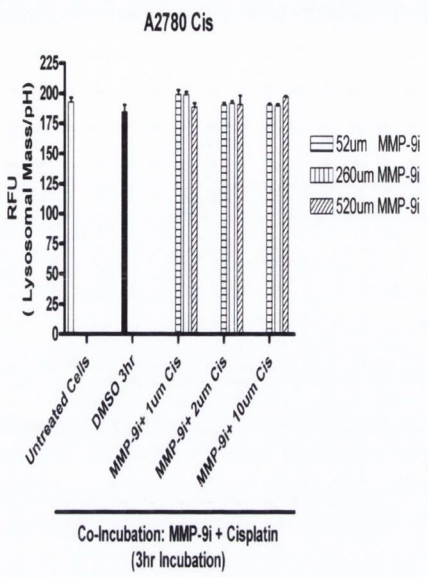
A2780 Cis
RFU
(Lysosomal Mass/pH)
225
200
175
150
125
100
75
50
25
0
52um MMP-9i
260um MMP-9i
520um MMP-9i
Untreated Cells
DMSO 3hr
MMP-9i+ 1um Cis
MMP-9i+ 2um Cis
MMP-9i+ 10um Cis
Co-Incubation: MMP-9i + Cisplatin
(3hr Incubation)

F

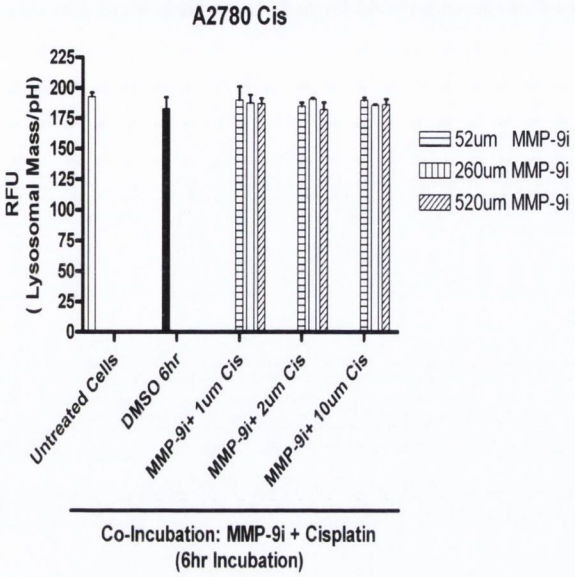
A2780 Cis
RFU
(Lysosomal Mass/pH)
225
200
175
150
125
100
75
50
25
0
52um MMP-9i
260um MMP-9i
520um MMP-9i
Untreated Cells
DMSO 6hr
MMP-9i+ 1um Cis
MMP-9i+ 2um Cis
MMP-9i+ 10um Cis
Co-Incubation: MMP-9i + Cisplatin
(6hr Incubation)

G

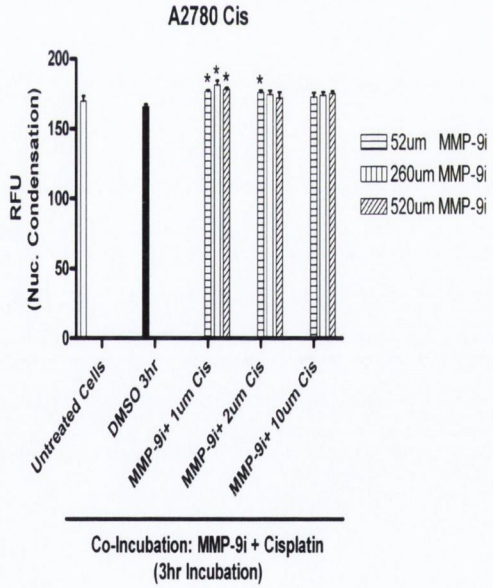
A2780 Cis
RFU
(Nuc. Condensation)
200
150
100
50
0
52um MMP-9i
260um MMP-9i
520um MMP-9i
Untreated Cells
DMSO 3hr
MMP-9i+ 1um Cis
MMP-9i+ 2um Cis
MMP-9i+ 10um Cis
Co-Incubation: MMP-9i + Cisplatin
(3hr Incubation)

H

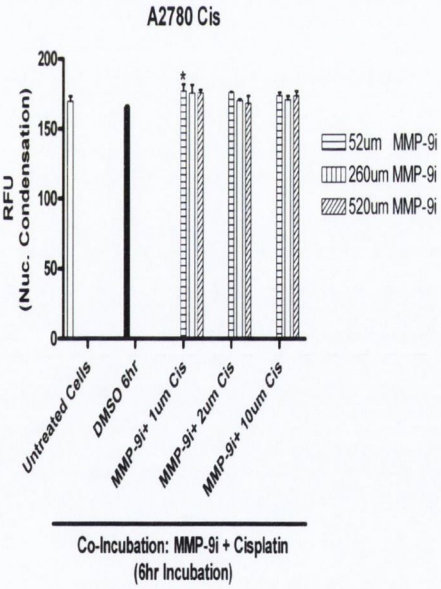
A2780 Cis
RFU
(Nuc. Condensation)
200
150
100
50
0
52um MMP-9i
260um MMP-9i
520um MMP-9i
Untreated Cells
DMSO 6hr
MMP-9i+ 1um Cis
MMP-9i+ 2um Cis
MMP-9i+ 10um Cis
Co-Incubation: MMP-9i + Cisplatin
(6hr Incubation)

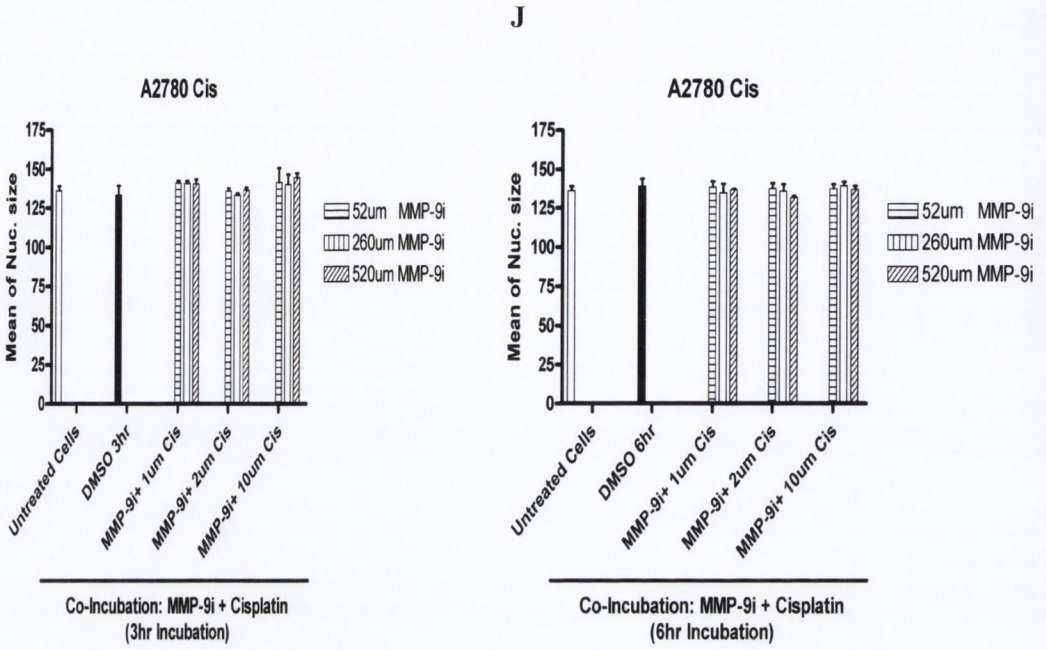

Figure 5.11(A-J) Effects on cytotoxicity following co-incubation of A2780cis cells with cisplatin and *MMP-9*i for 3h and 6h.

We then decided to investigate whether preincubating resistant ovarian cancer cells with *MMP-9*i for 3h may result in more enhanced cytotoxicity. Indeed, preincubation with *MMP-9*i followed by treatment with cisplatin at all concentrations for 3h was significantly cytotoxic (Figure 5.12A, C, E, G and I). Less significant cytotoxicity was observed with at 6h incubation time (Figure 5.12B, D, F, H and J).

Pre-incubation of 1μM of cisplatin with 260μM *MMP-9*i at 3h appeared to result in significantly greater cytotoxicity as compared to cisplatin or *MMP-9*i treatment alone (Figures 5.12 A compared to 5.8A and 5.8B).

1μm cisplatin/260μm *MMP-9*i was significantly cytotoxic in 40% of A2780cis cells at 3h. Highest cytotoxicity (~55%) was observed with maximum concentrations of cisplatin (10μM) and *MMP-9*i (520μM) at 3h but was not significant Figure (5.12A). No significant result in cell density was observed at 6h for any dose combination (Figure 5.12B).

A

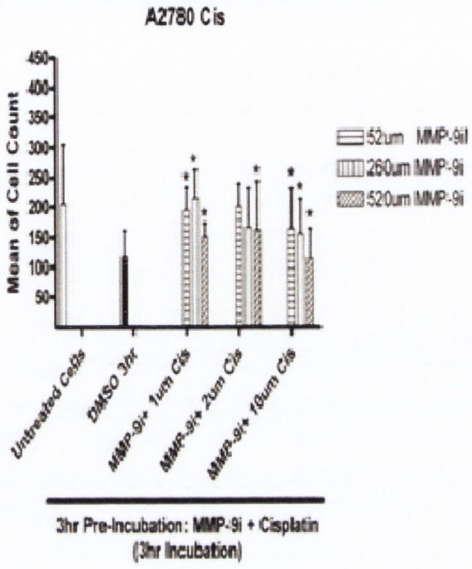
A2780 Cis
Mean of Cell Count
52um MMP-9i
260um MMP-9i
520um MMP-9i
Untreated Cells
DMSO 3hr
MMP-9i+ 1um Cis
MMP-9i+ 2um Cis
MMP-9i+ 10um Cis
3hr Pre-Incubation: MMP-9i + Cisplatin
(3hr Incubation)

B

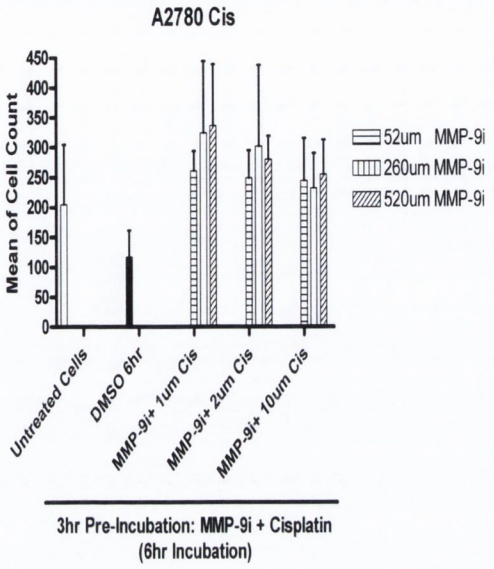
A2780 Cis
Mean of Cell Count
52um MMP-9i
260um MMP-9i
520um MMP-9i
Untreated Cells
DMSO 6hr
MMP-9i+ 1um Cis
MMP-9i+ 2um Cis
MMP-9i+ 10um Cis
3hr Pre-Incubation: MMP-9i + Cisplatin
(6hr Incubation)

C

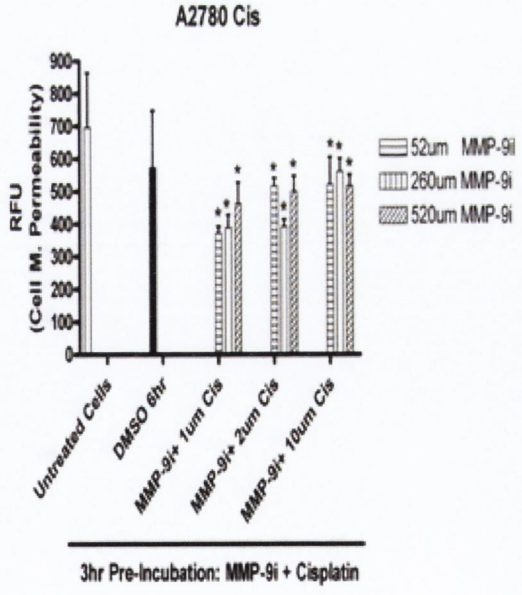
A2780 Cis
RFU
(Cell M. Permeability)
52um MMP-9i
260um MMP-9i
520um MMP-9i
Untreated Cells
DMSO 6hr
MMP-9i+ 1um Cis
MMP-9i+ 2um Cis
MMP-9i+ 10um Cis
3hr Pre-Incubation: MMP-9i + Cisplatin

D

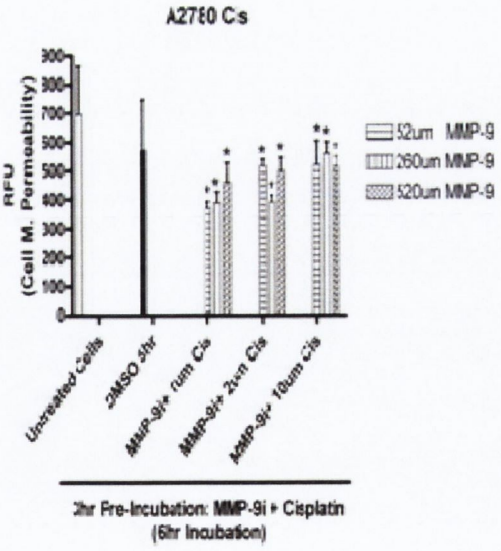
A2780 Cis
RFU
(Cell M. Permeability)
52um MMP-9
260um MMP-9
520um MMP-9
Untreated Cells
DMSO 3hr
MMP-9i+ 1um Cis
MMP-9i+ 2um Cis
MMP-9i+ 10um Cis
3hr Pre-Incubation: MMP-9i + Cisplatin
(6hr Incubation)

E

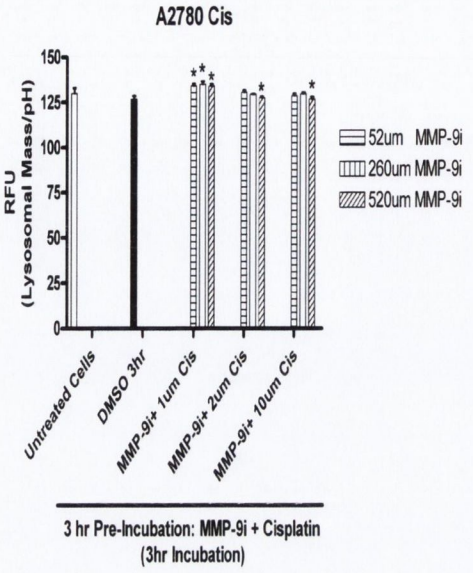
A2780 Cis
RFU
(Lysosomal Mass/pH)
150
125
100
75
50
25
0
52um MMP-9i
260um MMP-9i
520um MMP-9i
Untreated Cells
DMSO 3hr
MMP-9i+ 1um Cis
MMP-9i+ 2um Cis
MMP-9i+ 10um Cis
3 hr Pre-Incubation: MMP-9i + Cisplatin
(3hr Incubation)

F

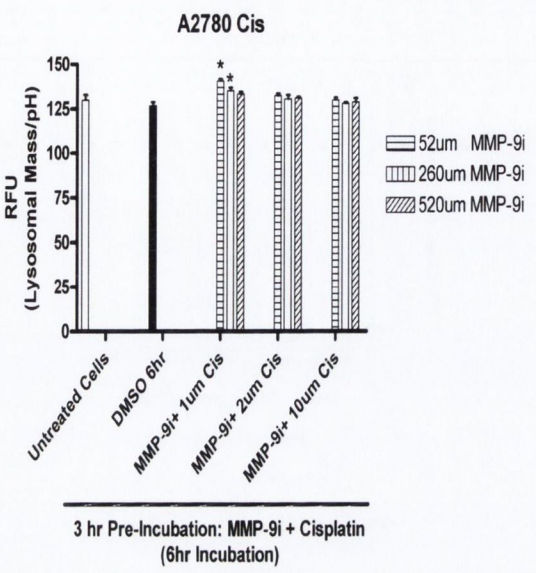
A2780 Cis
RFU
(Lysosomal Mass/pH)
150
125
100
75
50
25
0
52um MMP-9i
260um MMP-9i
520um MMP-9i
Untreated Cells
DMSO 6hr
MMP-9i+ 1um Cis
MMP-9i+ 2um Cis
MMP-9i+ 10um Cis
3 hr Pre-Incubation: MMP-9i + Cisplatin
(6hr Incubation)

G

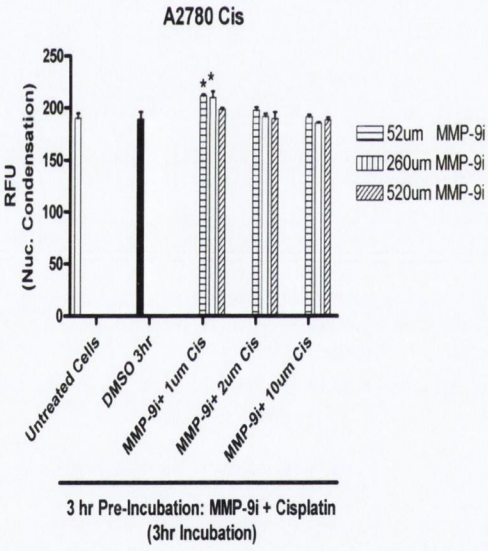
A2780 Cis
RFU
(Nuc. Condensation)
250
200
150
100
50
0
52um MMP-9i
260um MMP-9i
520um MMP-9i
Untreated Cells
DMSO 3hr
MMP-9i+ 1um Cis
MMP-9i+ 2um Cis
MMP-9i+ 10um Cis
3 hr Pre-Incubation: MMP-9i + Cisplatin
(3hr Incubation)

H

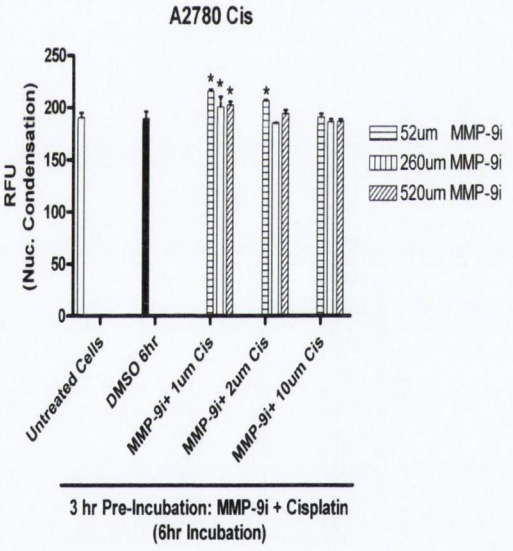
A2780 Cis
RFU
(Nuc. Condensation)
250
200
150
100
50
0
52um MMP-9i
260um MMP-9i
520um MMP-9i
Untreated Cells
DMSO 6hr
MMP-9i+ 1um Cis
MMP-9i+ 2um Cis
MMP-9i+ 10um Cis
3 hr Pre-Incubation: MMP-9i + Cisplatin
(6hr Incubation)

I

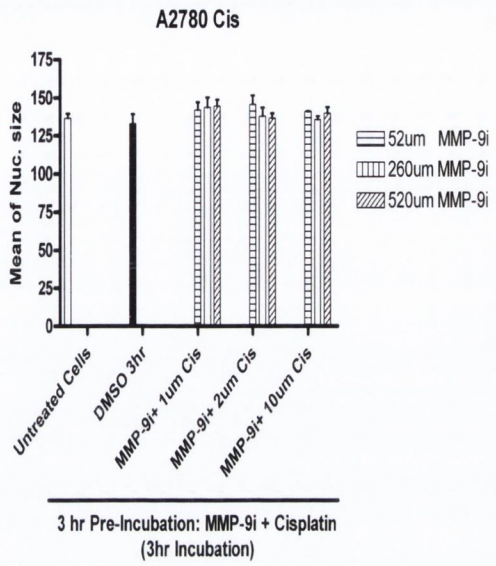

J

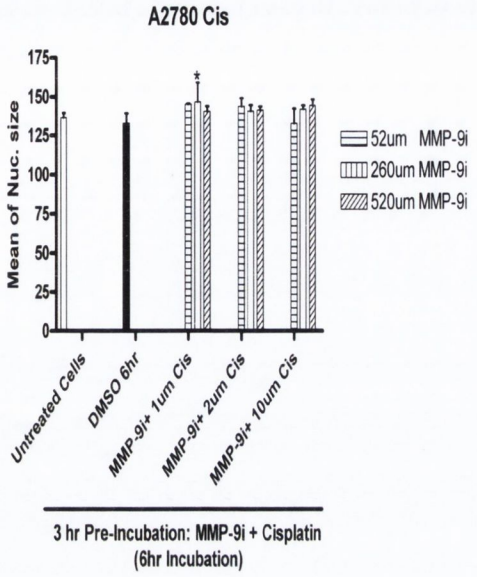

Figure 5.12(A-J) Preincubation of A2780cis cell line with *MMP-9*i for 3h enhances cytotoxicity. Resistant cells were incubated with MMP9-i for 3h prior to addition of cisplatin and incubation for 3h and 6h.

Next, we compared the cytotoxic effect of combination treatment (simultaneous cisplatin and *MMP-9*i) with pre-treatment (preincubation with *MMP-9*i for 3h followed by treatment with cisplatin for 3h and 6h). Significant results from combination comparisons are displayed in Table 5.4 and Figure 5.13A-D).

No significant results were observed for cell membrane permeability. The most significant cytotoxicity was observed for lysosomal mass with a preincubation combination 52μM or 260μM MMP-9i followed by 2μM Cisplatin versus coincubation with 2μM Cisplatin +52μM MMP-9i ($p<0.01$) (Table 5.4).

Table 5.4 Incubation comparisons between pre-incubation versus co-incubation treatments (3h) with their p values.

Cytotocicity parameters	pre-incubation (3h)	co-incubation (3h)	p value
Cell density	1μM Cisplatin +520μM *MMP-9*i	1μM Cisplatin +260μM *MMP-9*i	<0.05
Lysosomal mass/pH	1μM Cisplatin +260μM *MMP-9*i	1μM Cisplatin +52μM *MMP-9*i	<0.05
	1μM Cisplatin +260μM *MMP-9*i	1μM Cisplatin +260μM *MMP-9*i	**<0.01**
	1μM Cisplatin +52μM *MMP-9*i	1μM Cisplatin +520μM *MMP-9*i	**<0.01**
Nuclear condensation	2μM Cisplatin +520μM *MMP-9*i	2μM Cisplatin +260μM *MMP-9*i	<0.05
	2μM Cisplatin +260μM *MMP-9*i	2μM Cisplatin +52μM *MMP-9*i	<0.05
Nuclear size	1μM Cisplatin +52μM *MMP-9*i	1μM Cisplatin +52μM *MMP-9*i	<0.05

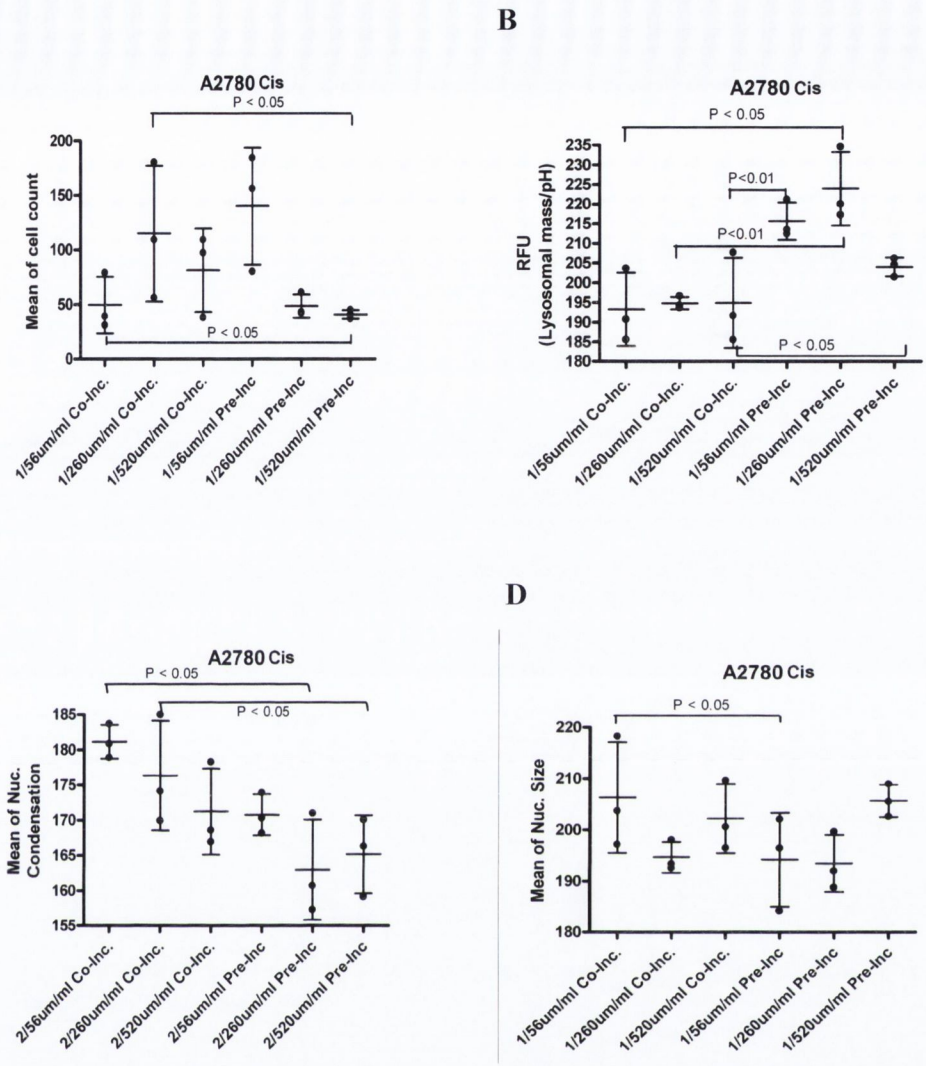

Figure 5.13(A-D) Pre-incubation with *MMP-9*i compared to co-incubation for the A2780cis cell line (3h incubation).

Preincubation with *MMP-9*i for 3h did not result in any significant decrease in cell density compared with co-incubation for the same period of time. In fact, combination treatments with cisplatin (2μM) and *MMP-9*i (52μM and 260μM) proved more significant than pre-treatment with the same concentrations (Table 5.5 and Figure 5.14).

Table 5.5 Incubation comparisons between pre-incubation vs co-incubation treatments for 6h with their p values.

Cytotocicity parameters	pre-incubation (6h)	co-incubation (6h)	p value
Lysosomal mass/pH	10μM Cisplatin +52μM *MMP-9*i	10μM Cisplatin +520μM *MMP-9*i	<0.05
	1μM Cisplatin +52μM *MMP-9*i	1μM Cisplatin +52μM *MMP-9*i	<0.01
	1μM Cisplatin +260μM *MMP-9*i	1μM Cisplatin +52μM *MMP-9*i	**<0.001**
	1μM Cisplatin +520μM *MMP-9*i	1μM Cisplatin +52μM *MMP-9*i	<0.05
	2μM Cisplatin +52μM *MMP-9*i	2μM Cisplatin +52μM *MMP-9*i	<0.05
	2μM Cisplatin +260μM *MMP-9*i	2μM Cisplatin +52μM *MMP-9*i	**<0.001**
	2μM Cisplatin +520μM *MMP-9*i	2μM Cisplatin +52μM *MMP-9*i	<0.01
Nuclear condensation	1μM Cisplatin +260μM *MMP-9*i	1μM Cisplatin +52μM *MMP-9*i	<0.05
	1μM Cisplatin +520μM *MMP-9*i	1μM Cisplatin +52μM *MMP-9*i	<0.05
	2μM Cisplatin +260μM *MMP-9*i	2μM Cisplatin +52μM *MMP-9*i	**<0.001**
	2μM Cisplatin +520μM *MMP-9*i	2μM Cisplatin +52μM *MMP-9*i	<0.01
Nuclear size	2μM Cisplatin +52μM *MMP-9*i	2μM Cisplatin +520μM *MMP-9*i	<0.05
	10μM Cisplatin +52μM MMP	10μM Cisplatin +520μM MMP	<0.05

Lysosomal mass was by far the parameter most frequently affected by 3h pre-incubation versus co-incubation for the 6h timepoint (Figure 5.20A-C). Pretreatment with *MMP-9*i for 3h followed by treatment with 1μM or 2μM of cisplatin for 6h was more significant than co-treatment for 6h with exactly the same concentrations (Figure 5.20C). The most significant effects were observed with pre-incubation

treatment of 260μM *MMP-9*i followed by 1μM or 2μM cisplatin compared to co-incubation of 52μM of *MMP-9*i with 1μM or 2μM of cisplatin ($p<0.001$) (Figures 5.20C-F).

A

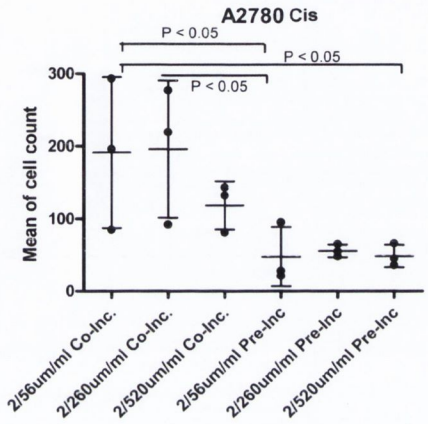

B

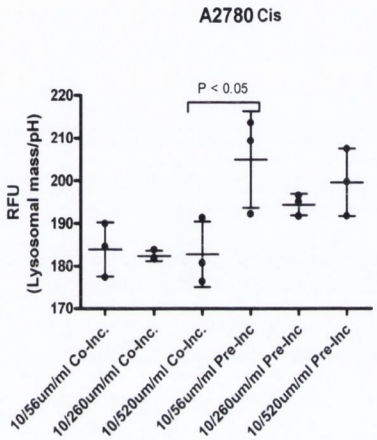

C

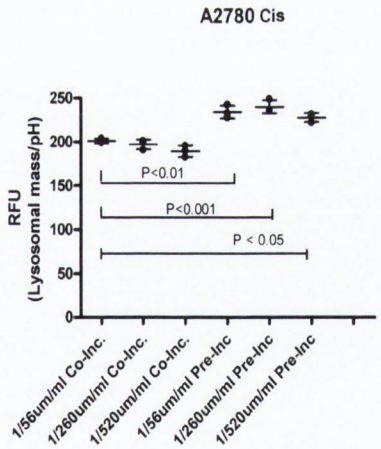

D

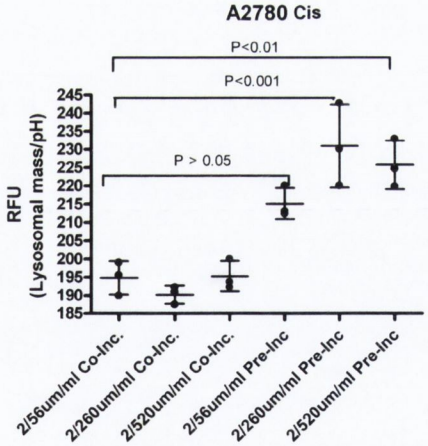

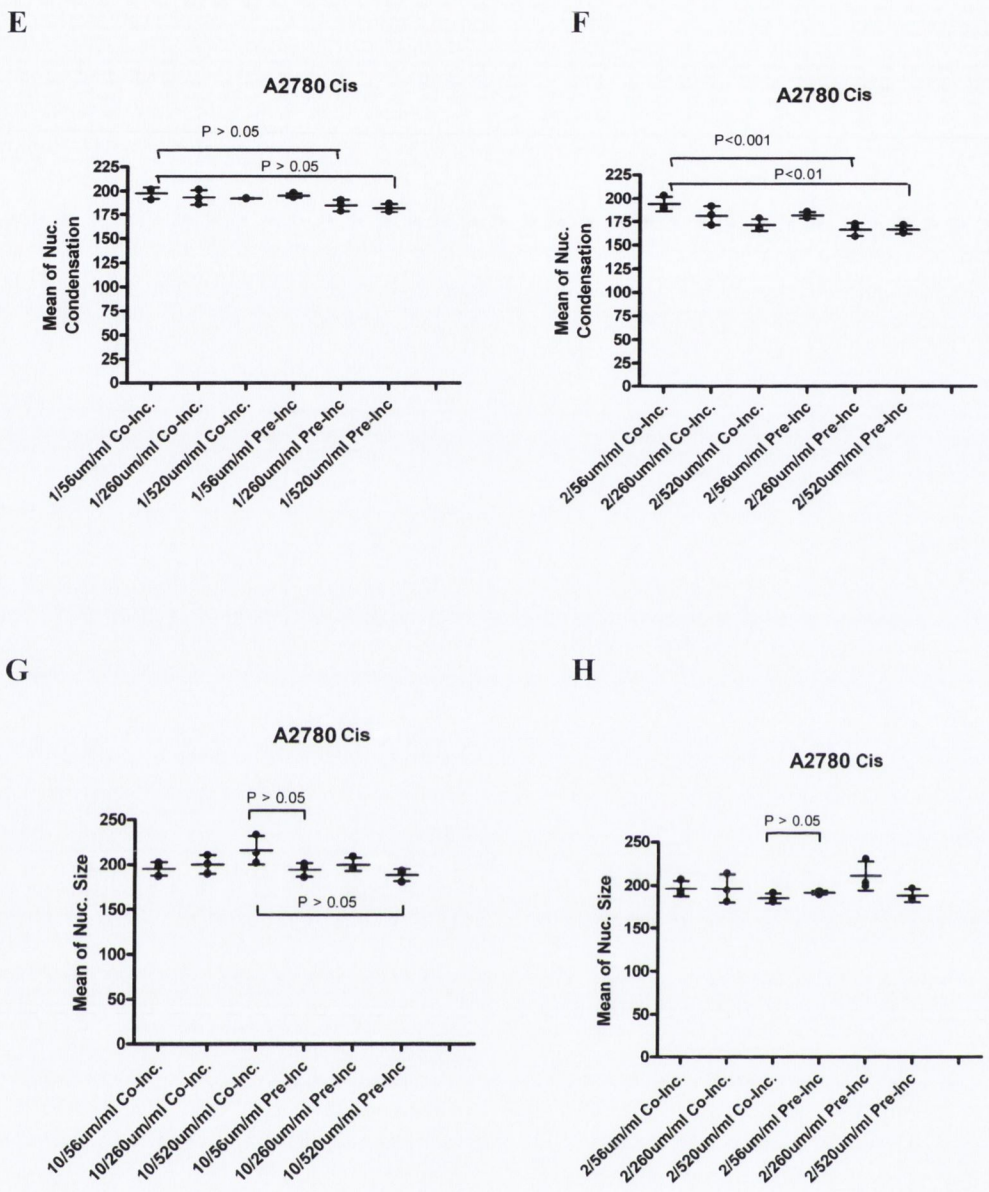

Figure 5.14(A-H) Pre-incubation with MMP-9i compared to co-incubation for the A2780cis cell line (6h incubation).

5.4.6 *MMP-9*i induces cell death in chemosensitive ovarian cancer cells

Time and dose course experiments were initially performed in the A2780 cell line to determine the sequence of changes in cytotoxicity parameters. At a threshold concentration of cisplatin (10μM), cytotoxicity effects progressively increased with time of incubation (Figure 5.15A).

Time course experiments on cisplatin cytotoxicity indicated that a decrease in cell density was significant at the highest concentration (10μM) after 24h incubation (Figure 5.15A). 24h incubation with cisplatin also significantly increased lysosomal mass and nuclear condensation (Figure 5.15B-C). The highest concentration of cisplatin (10μM) significantly altered 3 out 5 cytotoxicity parameters, namely cell density, lysosomal mass and nuclear condensation.

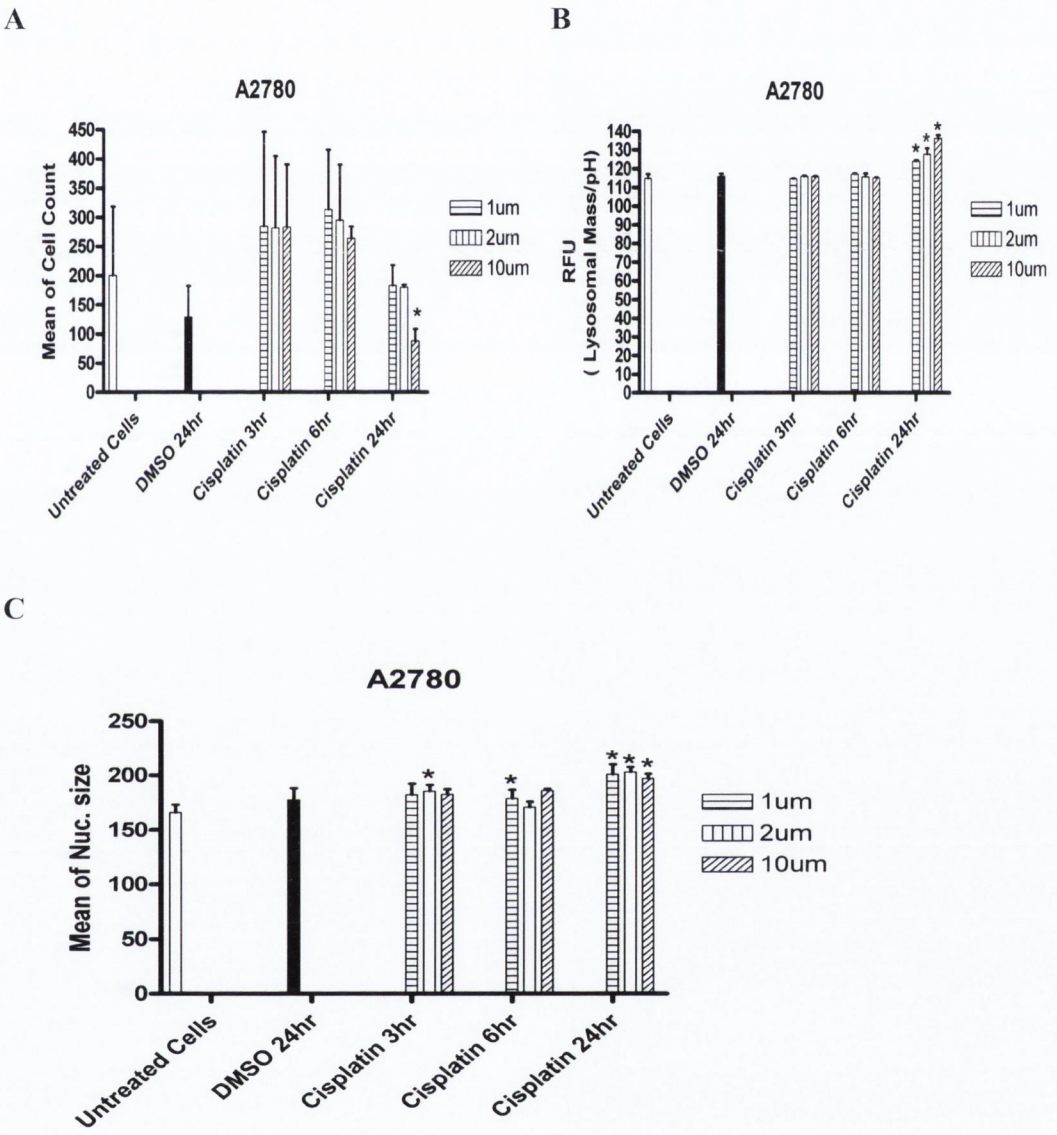

Figure 5.15(A-C) Simultaneous monitoring of changes in A) cell density B) lysosomal mass/pH C) nuclear size following treatment of the A2780cis cells with cisplatin (1μM, 2μM, 10μM) and incubation for different time points 3h, 6h and 24h. DMSO was used as a vehicle control. Representative data are shown as means +-SD (n=3 wells).

To determine whether *MMP-9*i alone was cytotoxic to sensitive ovarian cancer cells, time and dose experiments in *MMP-9*i cytotoxicity were performed in chemosensitive A2780 ovarian cancer cells. Changes in cell density, lysosomal mass/pH, cell membrane permeability and nuclear morphology were measured after treatment with *MMP-9*i.

Treatment with *MMP-9*i for 3h significantly decreased cell density (Figure 5.16A). The concentration-response curve was characterised by early positive response at 3h, an effect that is known as hormesis. Nuclear condensation was observed following 24h incubation with *MMP-9*i (Figure 5.16B). Changes in lysosomal mass/pH, cell membrane permeability and nuclear morphology were observed in a concentration-dependent manner (Figure 5.16C-D). A 52μM concentration of *MMP-9*i following 3h incubation and 52μM or 260μM of MMP-9i following 24h incubation were the best indicators of cytotoxicity in A2780 cells (Figure 5.16A-D).

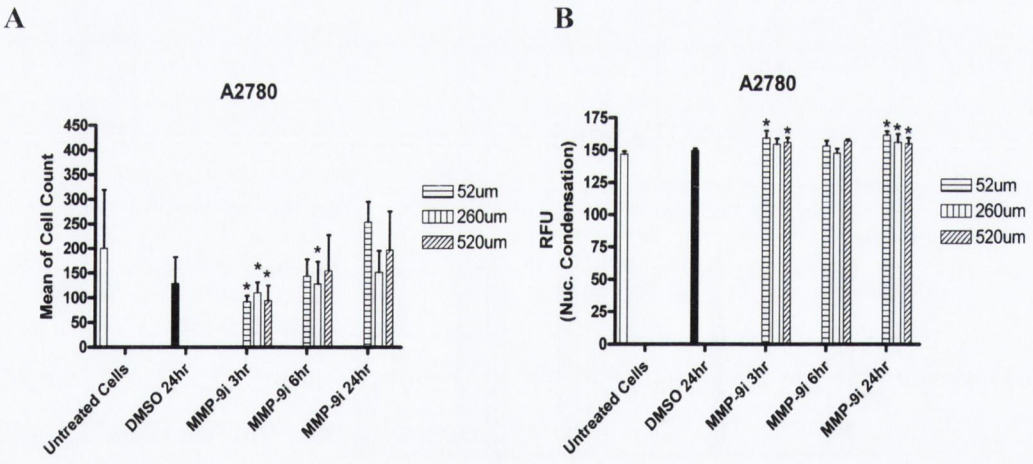

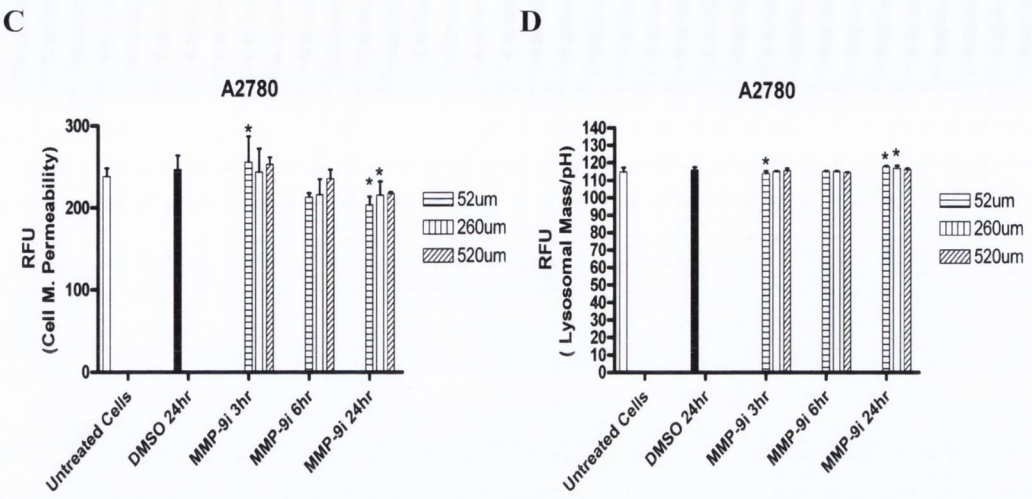

Figure 5.16 Simultaneous monitoring of changes in A)cell density B) nuclear condensation C) cell membrane permeability D) lysosomal mass/pH, following treatment of the A2780 cells with MMP-9i (52μM, 260μM, 520μM) and incubation for different time points 3h, 6h and 24h. DMSO was used as a vehicle control. Representative data are shown as means +-SD (n=3 wells). Only significant results are shown.

We sought to determine whether co-treatment of sensitive ovarian cancer cells could enhance cisplatin-induced cytotoxicity. Simultaneous incubation of A2780 cells with cisplatin and *MMP-9*i induced a significant decrease in cell density after 3h incubation (Figure 5.17A-B). The effect was more prominent for 3h than 6h incubation period and follows a dose response pattern (Figure5.18A-B).

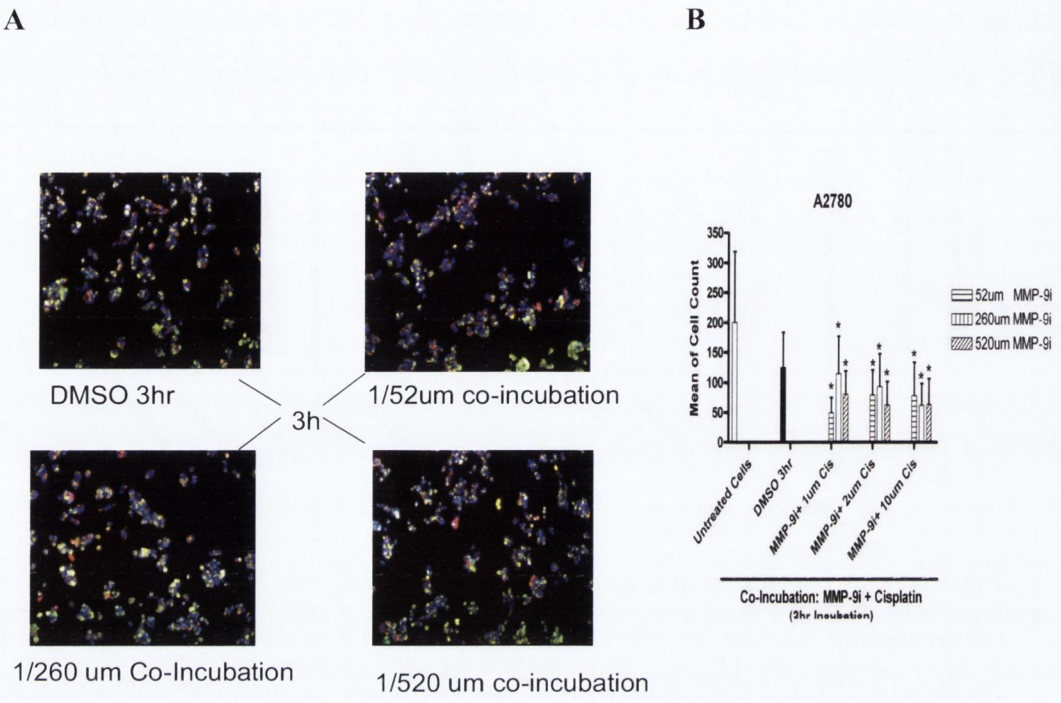

Figure 5.17(A-B) A) Morphology of cisplatin and MMP-9i chemosensitive ovarian cancer treated cells as demonstrated by HCS image analysis. B) Co-incubation of A2780 cells for 3h induced a significant decrease in cell density.

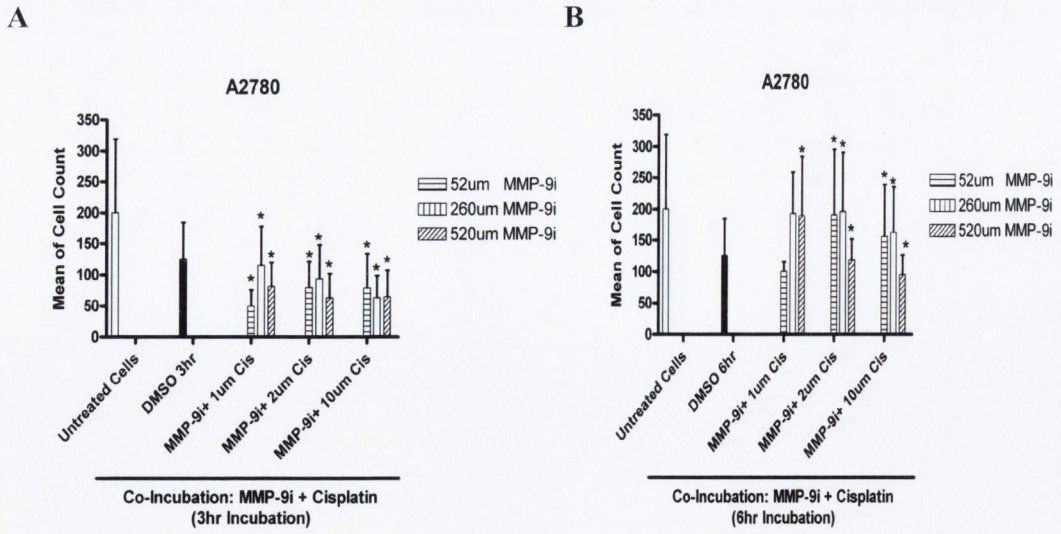

Figure 5.18(A-B) Efffect on cell density following co-incubation of A2780 cells with cisplatin and MMP-9i for 3h and 6h.

Lysosomal mass was significantly increased when coincubating cisplatin (1μM) with *MMP-9*i (520μM) at 3h (Figure 5.19A). Changes in cell membrane permeability, nuclear size and nuclear condensation were not significant.

Nuclear condensation and an increase in lysosomal mass were observed with X doses of drugs (cisplatin 1μM and *MMP-9*i 52μM) following 6h incubation (Figure 5.19A-B). Similarly, an increase in cell membrane permeability was significantly observed 6h following coincubation with cisplatin (2μM) and *MMP-9*i (520μM) (Figure 5.19C).

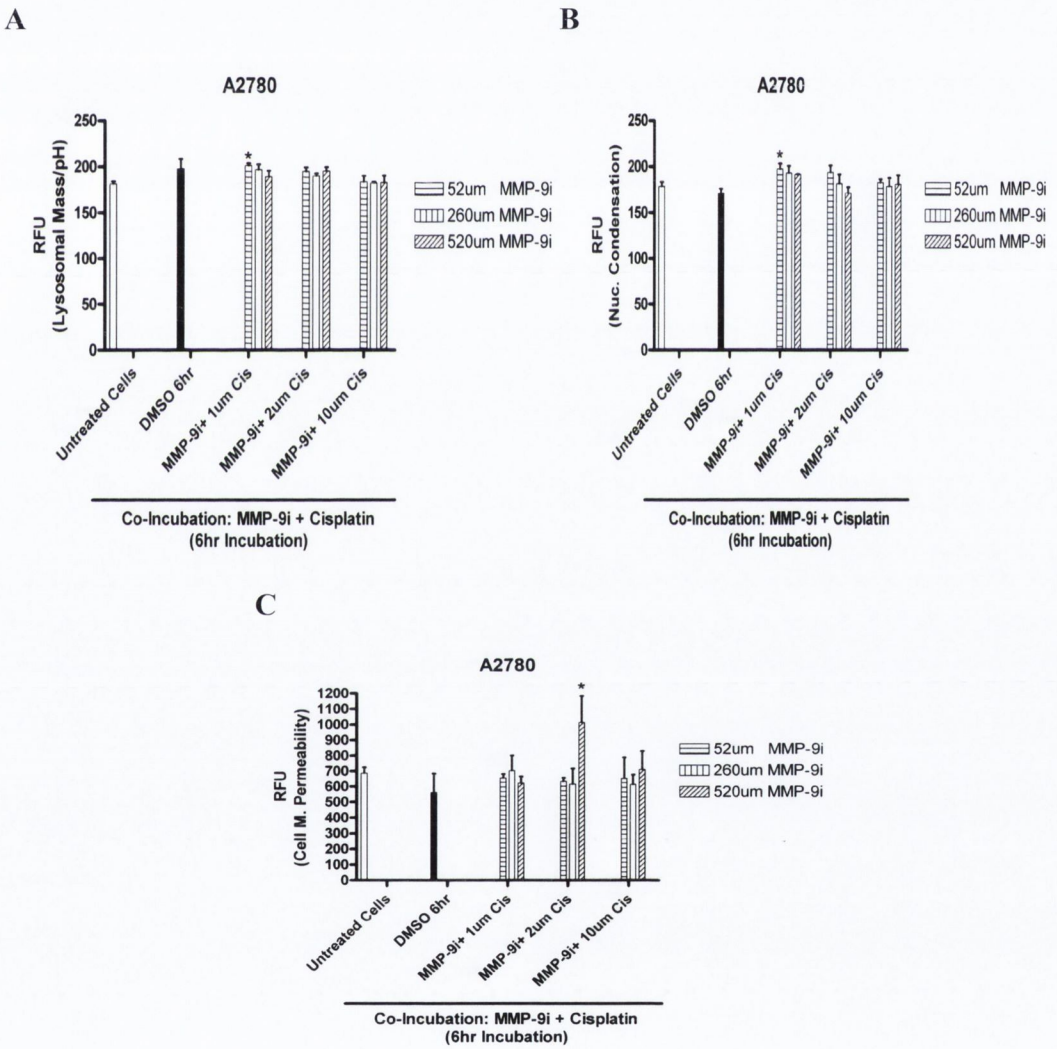

Figure 5.19(A-C) Effects on A) lysosomal mass/pH B) nuclear condensation C) cell membrane permeability following co-incubation of A2780 cells with cisplatin and MMP-9i for 6h.

Co-incubation of cisplatin with *MMP9*-i appeared to result in significantly greater cytotoxicity compared to cisplatin alone for the 3h and 6h incubation period as observed by a decrease in cell density and increase in lysosomal mass and cell membrane permeability (Figures 5.18 and 5.19 compared to figure 5.15 A-B).

Co-incubation of *MMP9*-i with 2μM and 10μM cisplatin for 6h resulted in greater cytotoxicity than either the IC50 or highest cytotoxic dose of *MMP-9*i alone for the same incubation period as observed by a decrease in cell density, increase in lysosomal mass, increase in cell membrane permeability, nuclear size and nuclear condensation for the same incubation time. Combined treatment with *MMP-9*i (520μM) and cisplatin (10μM) resulted in significant cytotoxicity compared to the highest dose of *MMP-9*i (520μM) alone as indicated by changes in all cytotoxicity parameters.

We then reasoned that preincubating sensitive ovarian cancer cells with *MMP-9*i may result to more enhanced cytotoxicity. Indeed, preincubation with *MMP-9*i for 3h followed by treatment with cisplatin for 3h rendered a significant decrease in cell density (compared to untreated cells) for almost all the combination concentrations compared to preincubation for 3h followed by treatment with cisplatin for 6h (Figures 5.20A compared to 5.20B).

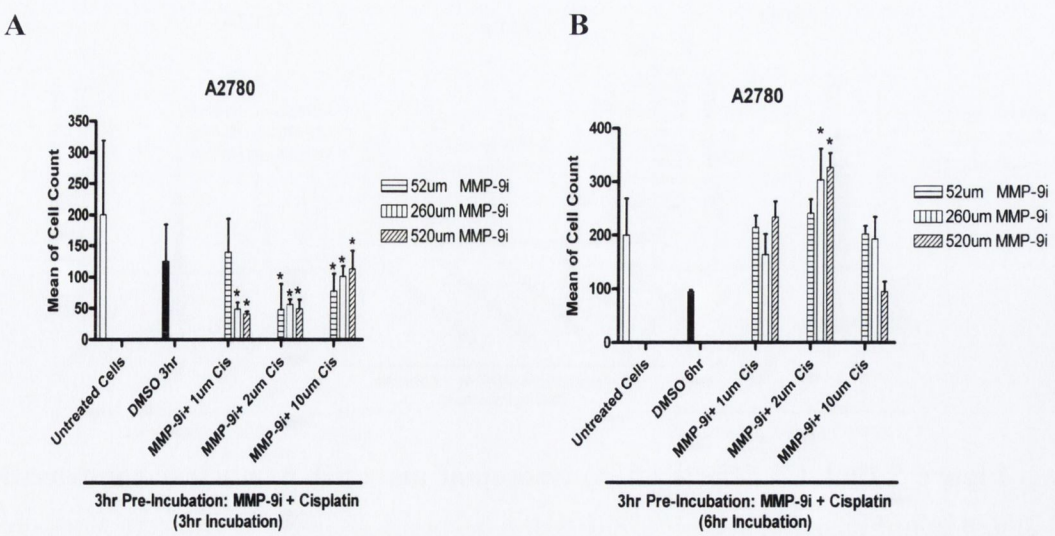

Figure 5.20(A-B) Preincubation of A2780 cell line with *MMP-9*i for 3h followed by treatment with cisplatin and incubation for 3h and 6h.

5.5 Discussion

The major goal of cancer chemotherapy is to commit tumour cells to apoptosis following exposure to antitumour agents. Tumour resistance to chemotherapy is a well known clinical phenomenon, now yielding its secrets to investigation at the molecular level. Several mechanisms have been implicated as determinants of cellular resistance to drugs, with alterations in genes controlling cell cycle progression and apoptosis as well as modulators of signal transduction pathways appearing to play the major roles [455].

Cell culture systems have been pivotal in defining the molecular and cellular mechanisms responsible for the drug-resistance phenotype. Studies in cell lines do not always correlate with results from tissue tumours [456]. Although mechanisms of resistance have been largely derived from tissue culture studies, there is good evidence for a general agreement [457]: only cells that withstand drug-induced pressure will regrow.

Combination therapy (carboplatin or cisplatin with paclitaxel) is the standard treatment for patients with ovarian cancer but cisplatin and paclitaxel might have opposite effects on the expression of certain proteins.

The major mechanism of cisplatin tumour killing is via induction of apoptosis [458]. Although cisplatin is a very potent inducer of apoptosis, resistance develops and is implied when cells fail to undergo apoptosis at clinically relevant drug concentrations. This resistance can be acquired through chronic drug exposure or present as an intrinsic phenomenon. With the understanding that the cytotoxic effect of cisplatin is a complex process, extending from initial drug entry into cells to the final stages of apoptosis, it follows that intracellular events interfering with any stage of this process will inhibit apoptosis and lead to drug resistance. Therefore, resistance is multifactorial; mechanisms to explain cisplatin resistance include the reduction of cisplatin accumulation inside cancer cells, the ability to detoxify cisplatin, faster repair of cisplatin-DNA adducts, modulation of apoptotic pathways, upregulation in transcription factors and a higher concentration of glutathione and metallothioneins [459].

The exact level of cisplatin resistance in patients is difficult to define, but at least a twofold resistance is inferred from clinical studies, when the standard clinical dose of cisplatin is doubled in drug-intensive therapy protocols [460]. In general, resistance to cisplatin may be substantially greater, as judged from studies with cell line established from clinically refractory tumours, which require cytotoxic concentrations as much as 50-100 fold in excess of those needed for sensitive tumour cells [461]. The extent of cellular sensitivity to platinum drugs has been extensively evaluated in vitro, most commonly by use of growth-inhibiting assays [462].

Genes that are differentially expressed between cisplatin-resistant and cisplatin-sensitive ovarian cancer cell lines are likely to be involved in pathways that modulate the sensitivity of ovarian cancer to cisplatin and therefore can be sensible candidates for treatment response and therapeutic targets. Gene Ontology reveals biological processes involved in RNA splicing, processing and DNA replication were over represented in cisplatin resistant cells [463]. Increased activities in these biological processes may allow faster repairs of cisplatin-induced damages such as cisplatin-DNA adducts, thus resulting in a resistant phenotype.

In recent years, much attention has been focused on the function of MMP enzymes, given their sophisticated pattern of modulating opposite effects in cancer progression (Figure 5.21). Unlike classical oncogenes, MMPs are not upregulated by gene amplification or activating mutations. Therefore, increased MMP expression in tumours is probably due to transcriptional changes rather than genetic alterations. This might be the result of activation of oncogenes or loss of tumour suppressors. Cancer cells, stromal cells and cells undergoing EMT synthesize MMPs in a paracrine manner through secretion of interleukins and growth factors [464].

A subgroup of those, the gelatinases (*MMP-2* and *MMP-9*), appear as key regulators of tumor angiogenesis and therefore as potential targets for therapeutic intervention in cancer.

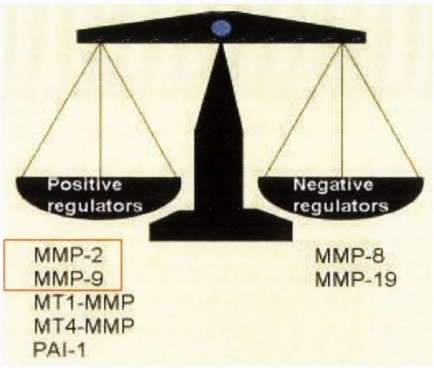

Figure 5.21. MMPs can be viewed as sophisticated modulators, positive or negative regulators of cancer development and metastatic dissemination.

The expression and activity of MMPs are increased in almost every type of human cancer [465] and this correlates with increased invasion and metastasis and shortened survival [466]. As a resulty, the antimetastatic prospensity of MMPs was further investigated by the development of MMP inhibitors (MMPIs) as a new class of anticancer drugs. Despite extensive research, very few inhibitors specific for the gelatinases have been described to date, the most potent also inhibit several other MMP family members. Nonspecific inhibitors could cause side effects during antitumour therapy because of disruption of several physiological processes.

The exact mechanism of their action is not yet completely understood. Apoptosis is induced by many but not all endogenous inhibitors and not necessarily by synthetic MMP inhibitors, thus suggesting that the mechanism may not rely on the inhibition of a MMP [467]. Synthetic MMP inhibitors appear to mimick most of the actions of TIMPs including MMP inhibition but also cell growth and proliferation [468, 469]. In sharp contrast, differing effects of endogenous and synthetic MMPs have been demonstrated in gastrointestinal cancers [470], that supports the idea that synthetic inhibitors are unlikely to have actions other than MMP inhibition.

We observed a consistently higher level of *MMP-9* and *NRG2* in A2780cis compared to the A2780 ovarian cancer cell line for a given passage. However, this higher level of expression was maintained for successive passages and before treatment of the A2780cis cell line with cisplatin to maintain chemoresistance. *In vivo*, it is well known that both proteins are also produced by peritumoural (microenvironmental)

factors, suggesting that microenvironmental factors are necessary for *MMP-9* and *NRG2* production.

Co-expression of *NRGs*, cognate ligands for *ErbB* receptors, has been observed in solid tumours, such as breast [471] and ovarian [472]. *NRG2* binds both *ErbB-3* and *ErbB-4* and is linked with direct induction of *PI3K* pathway [473]. An increase in cisplatin sensitivity can be achieved achieved experimentally by certain signal transduction inhibitors of *PKC* or *EGFR* [474].

MMP-9 was more prevalent than *NRG2*, suggesting that ovarian tumours have alternative *MMP-9* sources and mechanisms of regulation. In ovarian cancer, *MMP-9* is expressed in both the stroma and the ovarian epithelial tumour cells and *MMP-9* expression in either compartment is indicative of poor prognosis [475].

Other authors have demonstrated ovarian carcinoma cell lines (OVCA 429 and OVCA 433) also produce *MMP-9* [476], so the presence of *MMP-9* in ascites and tumour cell, regardless of the cellular source suggests that *MMP-9* might also contribute to the pathology of ovarian carcinoma. The high expression levels for both *MMP-2* and *MMP-9* have been clearly documented in early passage cultures of ovarian carcinoma cells and their importance was clearly demonstated in studies examining the effect of their synthetic inhibitor (Batimastat) on human ovarian carcinoma xenografts growing in nude mice, with resolution of ascites and prolonged survival.

Elevated *EGFR* activation in ovarian cancer is associated with poor patient outcome. Numerous activators of *EGFR* exist in the ovarian cancer microenvironment including *NRG2*. *EGFR* engagenent by ligand results in activation of signaling pathways. One consequence of *EGFR* activation is induction of *MMP-9 in vitro* and *in vivo*. A recent study supports concomitant activation of *EGFR* and *MMP-9* in ovarian cancer cells triggering down-modulation of E-cadherin [477].

In this study, we used a novel gelatinase inhibitor, derived from N-sulfony-lamino acid [454], for which inhibition of gelatinase activity in implanted tumour tissues has been demonstrated by means of film in situ zymography (ISZ) [478]. Such inhibitors

appear to have two levels of specificity. First, they specifically inhibit *MMP-9* and to a lesser extent *MMP-2*; second, they selectively target tumours because these enzymes are overexpressed and also accessible for homing in the tumour vasculature. Their combination of tumour targeting, antiangiogenic and anti-invasive properties renders them a potential lead compound (Figure 5.2).

Dose selection for our experiment renders a real challenge. Large trials use a maximum tolerated dose of MMP inhibitors. However, at the highest tolerated doses, the inhibitors might loose selectivity for specific MMPs. To investigate the molecular changes that occur during cisplatin exposure, analysis was not extended to late time points where apoptosis becomes significant or non specific [479] and may mask cisplatin or *MMP-9i*-dependent gene expression changes. Assays that target late events in the process of cell injury are more likely to miss toxicities that require chronic exposure or exert adverse but not lethal effects, therefore they have low sensitivity.

Detailed knowledge about mechanisms of toxicity can be obtained by examining the multiparametric responses at the level of individual cells, as most cellular processes, if not all, require a spatial and temporal context. The multiparametric cytotoxicity assay involved the performance of $>8x10^3$ individual cellular measurements, of which a subset was relevant to analysis of cytotoxicity. The analysis was made possible for each individual cell by use of fluorescent reagents in a format that reports on averages from large cell populations. Hoechst 33342 appears to be the best marker for monitoring multidrug resistance transporters efflux in cancer-stem cells (CSC) [480]. The model of ovarian cancer stemness has not been fully dissected and it would be interesting to determine whether *MMP-9i* represents a cancer stem marker by use of HCS tools. On exposure to toxic compounds, cells can respond by exhibiting changes in nuclear size and shape, increased cell permeability, increases in lysosomal mass/pH and decrease in cell density.

Nuclear condensation occurred on a variable timescale, often accompanying membrane permeability but occasionally beginning before it. In general, a dose and time response heterogeneity in cellular responses was observed in every case.

The combined treatment of *MMP-9*i and cisplatin enhanced cytotoxicity compared to cisplatin or *MMP-9*i alone. Preincubating cells with *MMP-9*i for 3h at all doses were significantly cytotoxic following treatment with cisplatin for 3h but not 6h suggesting an early apoptotic response.

Our time course results support the notion that if *MMP-9* is considered a chemoresistant marker, the ability to acquire drug resistance arises early during the tumorigenesis process, as recently proposed and validated in an ovarian cancer model [481] and is assococitated with immediate adaptive response to treatment.

Out inhibitor has been shown to possess a novel proapoptotic function when combined with *TNFa*, *TRAIL* or *FAS* ligands [448]. This alternative mechanism could explain the enhanced apoptosis observed with synergistic interaction between our inhibitor and cisplatin, although the proposed antineoplastic mechanism has not been tested in an ovarian cancer model.

A similar inhibitor, marimastat, has been assessed in Phase I trials at doses X6 the IC50 for *MMPs* and despite increasing effect with increasing dose, it was associated with dose limiting toxicities [482]. Tanomastat administration to advanced ovarian cancer patients after optimal response to first-line therapy showed no evidence of an impact on either PFS or OS [483]. A new trial is now under way for ovarian cancer patients achieving at least a partial response to second line carboplatin therapy [484]. A novel inhibitor of *MMP-2* and *MMP-9*, BAY 12-9566 appears to have a more favourable toxicity profile by perturbation of the cell cycle [485]. Oral treatment with the highly selective MMPI RO 28-2653 decreases the incidence of liver metastases due to reduced *MMP-2* and *MMP-9* concentration in a pancreatic cancer model [486]. No mechanism of action was proposed in the above studies. It remains to be determined whether proapoptotic activity is related to inhibition of gelatinases.

In conclusion, we report a successful adaptation of HCS for cytotoxicity using a novel *MMP-9*i/*MMP-2*i alone and in combination with cisplatin and we provide evidence regarding MMPI involvement in the treatment of ovarian cancer (Figure 5.22). An enhanced early time and concentration-dependent cytotoxic/apoptotic effect

has been observed, consistent with a hormetic effect. Manipulation of doses and use of antisense molecules to create highly selective MMPIs might be useful in the preclinical setting of these markers. However, a major advantage with many of these settings is that drug exposure may not have to be long-term and/or systemic thus reducing the possibility that side-effects. It may be also most effective for minimal residual disease and in addition is suited to chronic oral administration and associated with minimal toxicity [487].

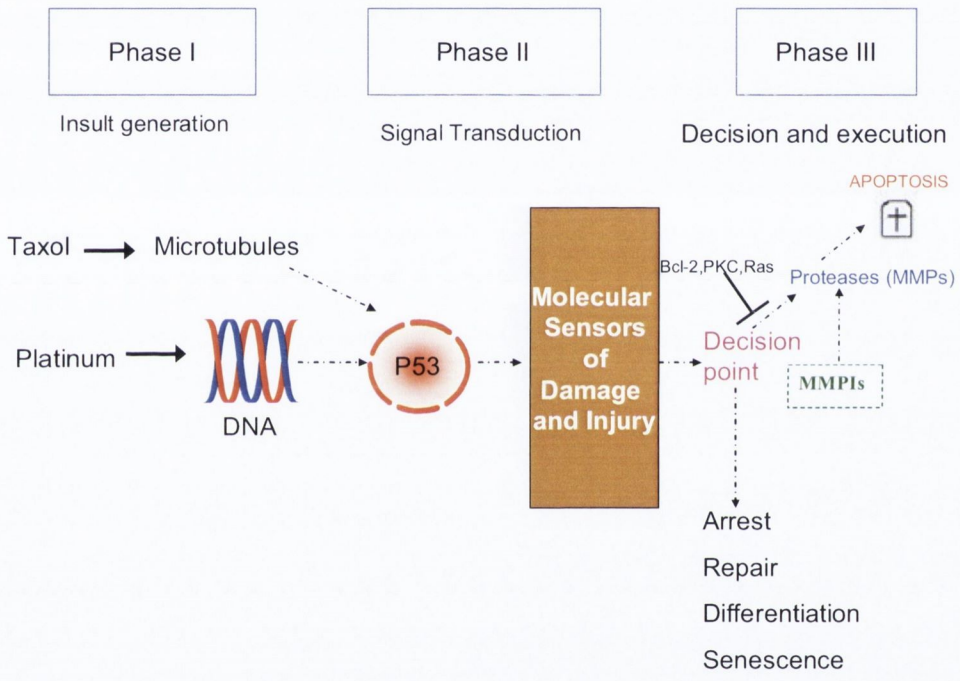

Figure 5.22 A model of possible implication of MMPIs in the treatment of ovarian cancer. Hypothesized phases in the induction of apoptosis in response to common chemotherapeutic agents in ovarian cancer. In phase I, cytotoxic agents impart damage to a critical component of the cell such as DNA or microtubules. In phase II, the cell recognizes the damage through signalling mechanisms. In phase III, the cell assesses the extent of damage and decides the appropriate response. In most cancer cells, the preferred response is the induction of apoptosis, whereas the response can also involve growth arrest to allow for repair or senescence or terminal cell differentiation. Cancer cells may acquire resistance to apoptosis at several points in this pathway. MMPs appear to induce the irreversible phase of apoptosis. Highly selective MMPIs may have a complementary role in the treatment of ovarian cancer.

CHAPTER 6
General Discussion

6.1 Introduction

Ovarian cancer is a devastating disease. Conventional chemotherapy in ovarian cancer is still unsatisfactory as it ignores aspects of tumor biology during recurrence. The identification of new markers of recurrence/chemoresistance in selected patients undergoing unnecessary chemotherapy would greatly assist their individualised treatment.

In this study we used cDNA and miRNA gene expression patterns as a set of data that may augment the use of HCS to help determining novel cytotoxicity compounds in primary and recurrent ovarian cancer.

6.2 Molecular profiling of recurrent versus primary ovarian cancers

The main focus of this thesis was centered on addressing chemoresistance in the commonest histological type of ovarian cancer and tumour heterogeneity. A dual transcriptomic approach of profiling primary and recurrent ovarian tumours was undertaken and distinct expression profiles were identified. These would reflect the natural history of the disease as well as chemoresistance. We observed that most of the genes identified in our microarray experiments had a higher expression in the recurrent compared to the primary tumours. A similar imbalanced distribution has been observed for chemotherapy-based discovery sets [285]. We therefore propose that the overexpression of discriminatory genes is more often associated with chemotherapy resistance than sensitivity.

A significant number of the identified genes were functionally involved in the regulation of gene expression, including mainly transcription factors that bind DNA, thus allowing faster repairs of drug induced DNA damages, suggesting that nucleic acid proteins may have even a predicitive role in conferring drug resistance in ovarian cancer [488].

The observation that some of the genes identified in different cohorts belong to the same gene families corroborates the importance of several distinct gene families in the

molecular regulation of recurrence in ovarian cancer. This likely represents the fact that gene families are activated as part of common signaling pathways or that extensive cross-talk exists between several pathways in ovarian cancer. Co-upregulation of genes rather than gene families has been previously reported in ovarian cancer using a statistical model [489]. Some of the identified genes are thought to be correlated to the mode of action of chemotherapeutic agents. It appears that some of the mechanisms involved in recurrence are specific to the drugs used, however cisplatin and paclitaxel might have opposite effects on the expression of certain genes, even within the same gene family.

The interactions between the "ovarian cancer recurrence" signatures have not been extensively explored. Cell-to-cell growth signalling is likely to operate in the vast majority of human tumours as well. In this respect, tumours should be regarded as complex tissues in which mutant cancer cells coexist with normal cell types that serve as collaborators in their neoplastic agenda. Successful tumour cells are those that acquire the ability to co-opt their normal neighbors by inducing them to release growth stimulating signals, in which the stromal microenvironment plays a crucial role [490]. Inflammatory cells or cells meditating immune response are typical examples of normal cells that can enhance tumour growth potential [491].

The relationship between Ca2+ binding proteins such as *S100B* and chemoresistance has not been studied. Moreover, the relationship between increased *CLDN16* protein expression and cisplatin resistance is also unclear at present. Indeed to our knowledge, no studies on the relationship between tight junction and chemotherapy response have been carried out. It is proposed that claudin-mediated increased cancer cell invasion might be mediated through the activation of MMP proteins [492]. A reasonable hypothesis could be that *CLDN16* can alter the balance of cellular uptake and export of cisplatin; a change in the intracellular levels of cisplatin can result.

6.3 miRNA profiling of recurrent versus primary ovarian cancers

Identification of the molecular pathways involved in drug resistance plays a prominent role in the establishment of rational therapeutic approaches aiming to

circumvent or retatd the acquisition of drug resisance phenotype. In this context, the recent identification of the regulatory role of miRNAs has extended the spectrum of possible key factors involved in these processes. In fact, miRNAs are involved in various biological processes through the fine tuning of gene expression [493].

miRNAs have not been comprehensively studied in recurrent ovarian cancer, yet an incurable disease. Very few reports are also available on the characterization of the miRNAs involved in the ovarian cancer drug resistance mechanisms [424]

The comparison of miRNA expression levels between primary and relapsed cancers from independent datasets is a feasible approach for the identification of relapse-associated miRNAs. We attempted to predict survival in ovarian cancer based on a miRNA "recurrent metastatic signature", consisted of the top deregulated genes, miR-223 and miR-9. This signature can predict PFS but not OS in ovarian cancer patients, possibly because it is also included in a bigger list associated with human cancer metastasis [494].

.

The therapeutic potential of miRNAs is still unexplored and miRNA-based cancer gene therapy offers the theoretical appeal of targeting multiple gene networks that are controlled by a single miRNA. Strategies of "in patients" delivery of miRNAs are currently in advanced preclinical development and are expected to enter soon in clinical experimentation [495].

To this end, the combination of miR-9 and miR-223 is an attractive candidate to circumvent drug resistance in ovarian cancer. We propose a miRNA model for the molecular pathogenesis of recurrent ovarian cancer (Figure 4.10). Some of the differentially deregulated miRNAs identified correlate with our previous transcriptome findings. miRNAs, unlike mRNA targets, remain largely intact in routinely collected FFPE clinical samples, enhancing their potential utility and suggesting their overall levels are unlikely to be affected by storage or collection procedures.

6.4 HCS cytotoxicity screening

We implemented a live-cell multiparametric HCS cytotoxicity assay measuring cell density, nuclear morphology, lysosomal mass and cell membrane integrity. These represent principle parameters of compromised cell health. In this respect, knowledge of the behaviour of individual cells within a population is critical for detailed characterisation of cellular processes. Whereas drug-induced cytotoxicity may indicate potential for in vivo cytotoxicity, it is not predictive of such. Cytotoxic effects in vivo may be limited or even aggravated, compared to those occurring in vitro. A cytotoxicity model rather ignores cell types, cell structures or interactions within a tissue, organ, even the whole body; toxicity may occur secondary to direct cytotoxicity due to other processes such as, inflammation, innune mediated hypersensitivity, volume expansion and endocrine effects.

An important finding in the study is that early measurements of toxicity mechanisms are probably critical. Conventional cytotoxicity assays (eg, LDH release, cell rupture, membrane blebbing) usually observe late-stage toxicity and cellular events associated with a lethal apoptotic or necrotic effect [479].

Further studies are also needed to enhance assay sensitivity; to determine which additional cell health parameters are necessary to assemble a cytotoxicity assay that is more or less sensitive to agents that are cytotoxic in humans. This will require performance of studies where different combinations of cell health indicators are measured simultaneously. However, in a screening environment, it may be more practical to apply specific mechanistic assays such as DNA damage, apoptosis and cell cycle inhibition as follow-up assays given the intensive nature of data analysis when high multiplexed assays are implemented. In any case, the process of data analysis described here, presents a significant bottleneck in the rapid application of this assay to even small sets of compounds.

6.5 Recommendations for future research

The identification of robust biomarkers for ovarian cancer that can predict response/resistance to chemotherapy or be used as diagnostic markers is a recognised priority in the field.

The analysis of primary and recurrent ovarian cancers as described in chapter 2 provided a long list of differentially expressed genes. A subset of 31 such genes was selected for TaqMan® validation with a special emphasis on the mRNA targets that were upregulated in recurrent versus primary tumours, as they might represent markers of recurrence/chemoresistance. However, to investigate fully the genes discussed in chapter 3, it will be necessary to conduct further validation at the protein level in a larger cohort of FFPE samples. IHC is such an alternative validation method in conjunction with a TMA. A TMA could potentially contain hundreds of tissue samples from a wide range of archival ovarian cancers, for which clinicopathological data are readily available. This method has proven powerful in the past for correlating gene and protein expression patterns.

In the future, miRNA profiles, as described in chapter 4, may ultimately be useful for targeted treatment in cancer. Recent success of miRNA inhibition at the cellular level [496] also enabled miRNA targeted therapy [497]. Most of these clinical applications will depend on accurate assessment of miRNA profiles in human samples.

While individual miRNA biomarkers are important discoveries, the variability among different patients, even with the same type of cancer, makes using just one marker an unreliable method of determining cancer status. However, if a miRNA biomarker fingerprint can be established, a more accurate assessment would be more likely.

While cancer-specific miRNAs are also important for shedding light onto the molecular basis of cancer, being able to identify cancer-specific miRNAs in the blood to be used as biomarkers of cancers could be vital in detecting early-stage cancers. As technologies continue to improve, miRNA profiling will get even easier, faster, and cheaper. In order to show their usefulness for detecting cancers early, it would also be interesting to determine how early these biomarkers become significant; when a cancer is at its earliest stages or perhaps even before a tumor has fully developed? At most, published studies identifying serum biomarkers have only looked at ~150 cancer patients from very limited populations; therefore, further testing on larger populations will be necessary before any such markers can be proven to be useful in a clinical setting. Meanwhile, analyzing miRNA levels in serum is a promising area for

identifying biomarkers of cancer [498]. This emerging field of study has only just begun identifying biomarkers in serum, the first such biomarker being miR-21 in diffuse B-cell lymphoma [499]. The detection of differentially expressed microRNAs from the serum of ovarian cancer patients using a novel real-time PCR platform has been only recently made feasible [500].

miRNAs are very stable in blood plasma and serum: they are well protected from RNases and remain stable after being subjected to harsh conditions [501]. Therefore, their stability makes miRNA levels well suited for being tested in patient samples.

Currently a study is underway with our collaborators to identify early markers in the detection of ovarian cancer. Serum samples are being collected from patients with ovarian cancer and age matched controls and incubated against a protein expression library of 10,000 different (non-redundant) human proteins. This is being extended to correlate the finding with response to chemotherapy and outcome of the patient so additional bloods will be taken following completion of chemotherapy and on presentation of a recurrence. Should novel biomarkers for chemoresistance arise in this study they will be further investigated.

We are now entering a new era where we will be able to combine gene expression data, pathological data and proteomic data (defined as disease traits) with imaging traits obtained from MRI, CT, 3-D Doppler and PET scans in order to construct association maps so that using non invasive techniques we will be able to determine who will really benefit from surgery and individualize chemotherapy so that patients will not relapse (highlighted in Figure 6.1).

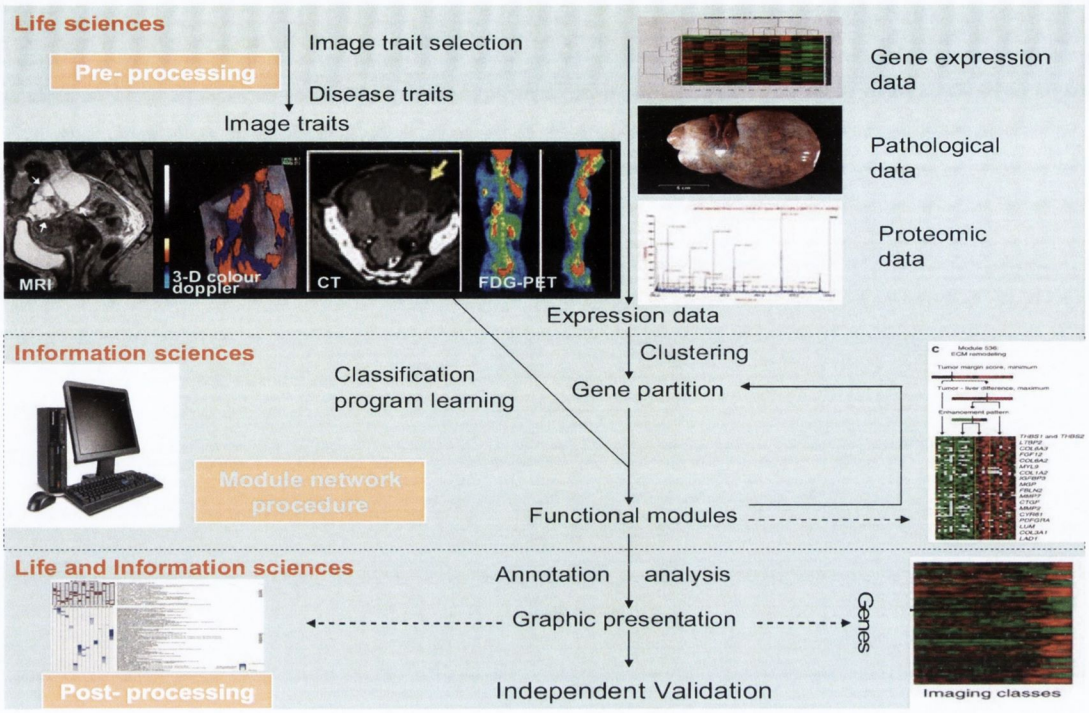

Figure 6.1 Examples of imaging traits in ovarian cancer. Model for constructing association maps between imaging traits, gene expression, proteomic and pathological data. Assessing the biochemical makeup of living tissue through noninvasive imaging will be a key goal of our future project.

It appears that towards this direction, we will need major bioinformatic support in order to be able to deliver our results from "bench to bedside". Much of this falls under the umbrella of systems biology that uses computational models to capture the network dynamics of interacting genes. It is also important in the future to couple genomic and pathway alterations with patient outcomes and responses to chemotherapy. Putting all this together into a network analysis would enable clinicians to ask what all the changes in a given patient add up to.

Our combined transcriptomic approach showed that there are probably many genetic routes to the same end point: perturbation of common cellular pathway(s) leading to relapsed ovarian cancer. If a personalized medicine approach to cancer is the aim in the years to come, then we need to look directly at the protein information for our proposed markers at a functional signalling level.

The advent of HCS or the integration of tools that include automated systems for high content cell analysis, data management and knowledge mining, promises to drive a revolution in cell biology similar to that of DNA sequencing in the pregenomic era. Further studies are needed to define optimal strategies for fluorescent monitoring of relevant cytotoxicity biomarkers. The effectiveness and mechanistic information of the HCS cytotoxicity assay may be enhanced by the replacement of existing dyes with others that could measure glutathione or reactive oxygen species, safety-signal transduction, additional morphological features and cell cycle information. Given the importance of oxidative stress in drug-induced toxicity [502], perhaps, an oxidative stress biomarker could be incorporated and preliminary studies from our group in hypoxia and chemoresistant ovarian cancer are currently underway.

In addition, non-toxic drugs need to be tested to more accurately assess the safety margin to interprete cytotoxicity. As the usefulness of conventional non cancer drugs in the treatment of cancer is currently revisited, knowledge of their potential cytotoxicity can create alternatives with lower toxicity potential.

Based on the results of our study, a prospective clinical trial using a highly selective *MMP-9* inhibitor in combination with current chemotherapeutic agents should be carried out to compare the results of chemotherapy in patients with recurrent ovarian cancer.

Another key unresolved issue is the identity of the *in vivo* substrates of MMPs. In future studies, it will be of great interest to use mouse models to establish the specific mechanisms for activation and inactivation of MMPs, to unfold the full core group of the perturbed pathways and to determine the potential role of these pathways in the pathogenesis of human ovarian cancer.

6.6 Conclusions

In conclusion, this thesis is unique because:

- We identified a distinct gene expression profile between primary and recurrent ovarian cancers and we identified genes that might represent markers of recurrence/chemoresistance.
- We identified a distinct miRNA profile between primary and recurrent ovarian cancers that strongly correlates with our transcriptome profile and we propose a miRNA signature that can predict PFS in ovarian cancer
- We successfully adapted a novel technology, the High Content Screening (HCS) analysis tool to assess cytotoxicity of a commercially available *MMP-9* inhibitor in chemosensitive and chemoresistant ovarian cancer cell lines. We provide strong evidence that a highly selective *MMP-9i* might have a place in the treatment of recurrent/chemoresistant ovarian cancer.

REFERENCES

1. Tachibana KE, Gonzalez MA, Coleman N: **Cell-cycle-dependent regulation of DNA replication and its relevance to cancer pathology.** *The Journal of Pathology* 2005, **205:**123-129.
2. Harper JW, Adams PD: **Cyclin-dependent kinases.** *Chem Rev* 2001, **191:**2511-2526.
3. Renan MJ: **How many mutations are required for tumorigenesis? Implications from human cancer data.** *Mol Carcinog* 1993, **7:**139-146.
4. Cappell MS: **From colonic polyps to colon cancer: pathophysiology, clinical presentation, screening and colonoscopic therapy.** *Minerva Gastroenterol Dietol* 2007, **53:**351-373.
5. Mastracci TL, Boulos FI, Andrulis IL, Lam WL: **Genomics and premalignant breast lesions: clues to the development and progression of lobular breast cancer.** *Breast Cancer Res* 2007, **9:**215-229.
6. Chan GK, Jablonski SA, Sudakin V, Hittle JC, Yen TJ: **Human BUBR1 Is a Mitotic Checkpoint Kinase that Monitors CENP-E Functions at Kinetochores and Binds the Cyclosome/APC.** *J Cell Biol* 1999, **146:**941-954.
7. Malumbres M: **Therapeutic opportunities to control tumor cell cycles.** *Clin Transl Oncol* 2006, **8:**399-408.
8. Hanahan D, Weinberg RA: **The Hallmarks of Cancer.** *Cell* 2000, **100:**57-70.
9. Giancotti FG, Ruoslahti E: **Integrin Signaling.** *Science* 1999, **285:**1028-1033.
10. Weinberg RA: **The retinoblastoma protein and cell cycle control.** *Cell* 1995, **81:**323-330.
11. Harris A, Curtis C: **Commentary: *p53* Tumor suppressor gene: from the basic research laboratory to the clinic--an abridged historical perspective.** *Carcinogenesis* 1996, **17:**1187-1198.
12. Shay JW, Bacchetti S: **A survey of telomerase activity in human cancer.** *European Journal of Cancer* 1997, **33:**787-791.
13. Paweletz N, Knierim M: **Tumor-related angiogenesis.** *Critical Reviews in Oncology/Hematology* 1989, **9:**197-242.
14. Hanahan D, Folkman J: **Patterns and Emerging Mechanisms of the Angiogenic Switch during Tumorigenesis.** *Cell* 1996, **86:**353-364.
15. Norton L, Massague J: **Is cancer a disease of self-seeding?** *Nat Med* 2006, **12:**875-878.
16. Heppner GH: **Tumor Heterogeneity.** *Cancer Res* 1984, **44:**2259-2265.
17. Wang V, Li C, Lin M, Welch W, Bell D, Wong YF, Berkowitz R, Mok SC, Bandera CA: **Ovarian cancer is a heterogeneous disease.** *Cancer Genet Cytogenet* 2005, **161:**170-173.
18. Hoskins WJ: **Prospective on ovarian cancer: why prevent?** *J Cell Biochem* Suppl 1995; **23**:189-99.
19. Parkin DM, Bray F, Ferlay J, Pisani P: **Global cancer statistics, 2002.** *CA Cancer J Clin* 2005, **55:**74-108.
20. Kliewer EV, Smith KR: **Ovarian cancer mortality among immigrants in Australia and Canada.** *Cancer Epidemiol Biomarkers Prev* 1995, **4:**453-458.
21. Aebi S, Castiglione M: **Epithelial ovarian carcinoma: ESMO Clinical Recommendations for diagnosis, treatment and follow-up.** *Ann Oncol* 2008, **19:**ii14-16.
22. Krag KJ, Canellos GP, Griffiths CT, Knapp RC, Parker LM, Welch WR, Klatt M, Andersen J: **Predictive factors for long-term survival in patients with advanced ovarian cancer.** *Gynecol Oncol* 1989, **34:**88-93.

23. Goldberg JM, Piver MS, Jishi MF, Blumenson L: **Age at Onset of Ovarian Cancer in Women with a Strong Family History of Ovarian Cancer.** *Gynecologic Oncology* 1997, **66:**3-9.
24. Piver MS: **Rates and risks of ovarian cancer in subgroups of white women in the United States.** *Obstet Gynecol* 1995, **85:**320.
25. Ferlay J, Bray F, Sankila R, Parkin DM. **EUCAN Cancer Incidence, mortality and prevalence in the European Union (1998 Estimates),Version 5.0. IARC CancerBase No. 4. Lyon, France: IARC Press, 1999.** *Available at: http://www-depiarcfr/eucan/eucanhtm* Accessed March 2005.
26. Bray F, Loos AH, Tognazzo S, La Vecchia C: **Ovarian cancer in Europe: Cross-sectional trends in incidence and mortality in 28 countries, 1953-2000.** *International Journal of Cancer* 2005, **113:**977-990.
27. O'Lorcain P, Comber H: **Mortality predictions for Ireland, 2001-2015: cancers of the breast, ovary, and cervix and corpus uteri.** *International Journal of Gynecological Cancer* 2006, **16:**1-10.
28. Fathalla MF: **Incessant ovulation--a factor in ovarian neoplasia?** *Lancet* 1971, **2:**163.
29. Cramer DW, Welch WR: **Determinants of ovarian cancer risk. II. Inferences regarding pathogenesis.** *J Natl Cancer Inst* 1983, **Oct:**717-721.
30. Riman T, Persson I, Nilsson S: **Hormonal aspects of epithelial ovarian cancer: review of epidemiological evidence.** *Clinical Endocrinology* 1998, **49:**695-707.
31. Aravindakshan J, Chen X, Sairam MR: **Differential Expression of Claudin Family Proteins in Mouse Ovarian Serous Papillary Epithelial Adenoma in Aging FSH ReceptorDeficient Mutants.** *Neoplasia* 2006, **8:**984-994.
32. Godwin AK, Testa JR, Handel LM, Liu Z, Vanderveer LA, Tracey PA, Hamilton TC: **Spontaneous Transformation of Rat Ovarian Surface Epithelial Cells: Association With Cytogenetic Changes and Implications of Repeated Ovulation in the Etiology of Ovarian Cancer.** *J Natl Cancer Inst* 1992, **84:**592-601.
33. Ozols RF, Bookman MA, Connolly DC, Daly MB, Godwin AK, Schilder RJ, Xu X, Hamilton TC: **Focus on epithelial ovarian cancer.** *Cancer Cell* 2004, **5:**19-24.
34. Feeley KM, Wells M: **Precursor lesions of ovarian epithelial malignancy.** *Histopathology* 2001, **38:**87-95.
35. Ness RB, Cottreau C: **Possible Role of Ovarian Epithelial Inflammation in Ovarian Cancer.** *J Natl Cancer Inst* 1999, **91:**1459-1467.
36. Ames BN, Gold LS, Willett WC: **The Causes and Prevention of Cancer.** *Proceedings of the National Academy of Sciences* 1995, **92:**5258-5265.
37. Adami HO, Lambe M, Persson I, Ekbom A, Adami HO, Hsieh CC, Trichopoulos D, Ekbom A, Lambe M, Leon D, Janson PO: **Parity, age at first childbirth, and risk of ovarian cancer.** *The Lancet* 1994, **344:**1250-1254.
38. Risch HA, Marrett LD, Howe GR: **Parity, Contraception, Infertility, and the Risk of Epithelial Ovarian Cancer.** *Am J Epidemiol* 1994, **140:**585-597.
39. Franco EL, Duarte-Franco E: **Ovarian cancer and oral contraceptives.** *The Lancet*, **371:**277-278.
40. Rosenberg L, Palmer JR, Zauber AG, Warshauer ME, Lewis JL, Strom BL, Harlap S, Shapiro S: **A Case-Control Study of Oral Contraceptive Use and Invasive Epithelial Ovarian Cancer.** *Am J Epidemiol* 1994, **139:**654-661.

41. Risch HA: **Estrogen Replacement Therapy and Risk of Epithelial Ovarian Cancer.** *Gynecologic Oncology* 1996, **63:**254-257.
42. Vessey MP, Painter R: **Endometrial and ovarian cancer and oral contraceptives--findings in a large cohort study.** *Br J Cancer* 1995, **71:**1340-1342.
43. Whittemore AS, Harris R, ltnyre J, the Collaborative Ovarian Cancer Group: **Characteristics Relating to ovarian Cancer Risk: Collaborative Analysis of 12 US case-Control Studies: IV. The Pathogenesis of Epithelial Ovarian Cancer.** *Am J Epidemiol* 1992, **136:**1212-1220.
44. Rossing MA, Daling JR, Weiss NS, Moore DE, Self SG: **Ovarian Tumors in a Cohort of Infertile Women.** *N Engl J Med* 1994, **331:**771-776.
45. Hankinson SE, Hunter DJ, Colditz GA, Willett WC, Stampfer MJ, Rosner B, Hennekens CH, Speizer FE: **Tubal ligation, hysterectomy, and risk of ovarian cancer. A prospective study.** *JAMA* 1993, **15:**2813-2818.
46. Schouten LJ, Rivera C, Hunter DJ, Spiegelman D, Adami HO, Arslan A, Beeson WL, van den Brandt PA, Buring JE, Folsom AR, Fraser GE, Freudenheim JL, Goldbohm RA, Hankinson SE, Lacey JV Jr, Leitzmann M, Lukanova A, Marshall JR, Miller AB, Patel AV, Rodriguez C, Rohan TE, Ross JA, Wolk A, Zhang SM, Smith-Warner SA: **Height, Body Mass Index, and Ovarian Cancer: A Pooled Analysis of 12 Cohort Studies.** *Cancer Epidemiol Biomarkers Prev* 2008, **17:**902-912.
47. Harlow BL, Cramer DW, Baron JA, Titus-Ernstoff L, Greenberg ER: **Psychotropic medication use and risk of epithelial ovarian cancer.** *Cancer Epidemiol Biomarkers Prev* 1998, **7:**697-702.
48. Koralek DO, Bertone-Johnson ER, Leitzmann MF, Sturgeon SR, Lacey JV Jr, Schairer C, Schatzkin A: **Relationship between calcium, lactose, vitamin D, and dairy products and ovarian cancer.** *Nutr Cancer* 2006, **56:**22-30.
49. Tworoger SS, Gertig DM, Gates MA, Hecht JL, Hankinson SE: **Caffeine, alcohol, smoking, and the risk of incident epithelial ovarian cancer.** *Cancer* 2008, **112:**1169-77.
50. Risch HA, Howe GR: **Pelvic inflammatory disease and the risk of epithelial ovarian cancer.** *Cancer Epidemiol Biomarkers Prev* 1995, **4:**447-451.
51. Schildkraut JM, Schwingl PJ, Bastos E, Evanoff A, Hughes C: **Epithelial ovarian cancer risk among women with polycystic ovary syndrome.** *Obstet Gynecol* 1996, **88:**554-559.
52. Brinton LA, Gridley G, Persson I, Baron J, Bergqvist A: **Cancer risk after a hospital discharge diagnosis of endometriosis.** *American Journal of Obstetrics and Gynecology* 1997, **176:**572-579.
53. Ligtenberg MJ, Hogervorst FB, Willems HW, Arts PJ, Brink G, Hageman S, Bosgoed EA, Van der Looij E, Rookus MA, Devilee P, Vos EM, Wigbout G, Struycken PM, Menko FH, Rutgers EJ, Hoefsloot EH, Mariman EC, Brunner HG, Van 't Veer LJ.: **Characteristics of small breast and/or ovarian cancer families with germline mutations in BRCA1 and BRCA2.** *Br J Cancer* 1999, **79:**1475-1478.
54. Venkitaraman AR, Ashok R: **Cancer Susceptibility and the Functions of BRCA1 and BRCA2.** *Cell* 2002, **108:**171-182.
55. Frank TS, Manley SA, Olopade OI, Cummings S, Garber JE, Bernhardt B, Antman K, Russo D, Wood ME, Mullineau L, Isaacs C, Peshkin B, Buys S, Venne V, Rowley PT, Loader S, Offit K, Robson M, Hampel H, Brener D, Winer EP, Clark S, Weber B, Strong LC, Thomas A: **Sequence analysis of**

BRCA1 and BRCA2: correlation of mutations with family history and ovarian cancer risk. *J Clin Oncol* 1998, **16:**2417-2425.

56. Pal T, Permuth-Wey J, Betts JA, Krischer JP, Fiorica J, Arango H, LaPolla J, Hoffman M, Martino MA, Wakeley K, Wilbanks G, Nicosia S, Cantor A, Sutphen R: **BRCA1 and BRCA2 mutations account for a large proportion of ovarian carcinoma cases.** *Cancer* 2005, **104:**2807-2816.
57. Merajver SD, Pham TM, Caduff RF, Chen M, Poy EL, Cooney KA, Weber BL, Collins FS, Johnston C, Frank TS: **Somatic mutations in the BRCA1 gene in sporadic ovarian tumours.** *Nat Genet* 1995, **9:**439-443.
58. Cass I, Baldwin RL, Varkey T, Moslehi R, Narod SA, Karlan BY: **Improved survival in women with BRCA-associated ovarian carcinoma.** *Cancer* 2003, **97:**2187-2195.
59. Lynch HT, Lemon SJ, Karr B, Franklin B, Lynch JF, Watson P, Tinley S, Lerman C, Carter C: **Etiology, natural history, management and molecular genetics of hereditary nonpolyposis colorectal cancer (Lynch syndromes): genetic counseling implications.** *Cancer Epidemiol Biomarkers Prev* 1997, **6:**987-991.
60. Serov SF, Scully RE, Sobin LH: **Histological typing of ovarian tumours.** *International Histological Classification of Tumours No 9 World Health Organisation* 1973.
61. Scully RE: **Classification of human ovarian tumors.** *Environ Health Perspect* 1987,73:15-24.
62. Bell DA: **Origins and molecular pathology of ovarian cancer.** *Mod Pathol* 2005, **18:**S19-S32.
63. Gilks CB, Ionescu DN, Kalloger SE, Köbel M, Irving J, Clarke B, Santos J, Le N, Moravan V, Swenerton K: **Tumor cell type can be reproducibly diagnosed and is of independent prognostic significance in patients with maximally debulked ovarian carcinoma.** *Human Pathology* 2008, **39:**1239-1251.
64. Zanagnolo V, Sartori E, Trussardi E, Pasinetti B, Maggino T: **Preservation of ovarian function, reproductive ability and emotional attitudes in patients with malignant ovarian tumors.** *European Journal of Obstetrics & Gynecology and Reproductive Biology* 2005, **123:**235-243.
65. Köbel M, Huntsman D, Gilks CB.: **Critical molecular abnormalities in high-grade serous carcinoma of the ovary** *Expert Rev Mol Med* 2008, **10**.
66. Auersperg N, Wong AST, Choi K-C, Kang SK, Leung PC: **Ovarian Surface Epithelium: Biology, Endocrinology, and Pathology.** *Endocr Rev* 2001, **22:**255-288.
67. Crum CP, Drapkin R, Kindelberger D, Medeiros F, Miron A, Lee Y: **Lessons from BRCA: The Tubal Fimbria Emerges as an Origin for Pelvic Serous Cancer.** *Clinical Medicine & Research* 2007, **5:**35-44.
68. Jarboe EA, Folkins AK, Drapkin R, Ince TA, Agoston ES, Crum CP: **Tubal and ovarian pathways to pelvic epithelial cancer: a pathological perspective.** *Histopathology 2008*, **53**:127-138.
69. Hutson R, Ramsdale J, Wells M: ***p53*** **protein expression in putative precursor lesions of epithelial ovarian cancer.** *Histopathology* 1995, **27:**367-371.
70. Werness BA, Parvatiyar P, Ramus SJ, Whittemore AS, Garlinghouse-Jones K, Oakley-Girvan I, DiCioccio RA, Wiest J, Tsukada Y, Ponder BAJ, Piver MS: **Ovarian Carcinoma In Situ With Germline BRCA1 Mutation and Loss of**

Heterozygosity at BRCA1 and T*P53*. *J Natl Cancer Inst* 2000, **92:**1088-1091.

71. Fraumeni JF, Grundi GW, Creagan ET, Everson RB: **Six families prone to ovarian cancer.** *Cancer* 1975, **36:**364-369.
72. Salazar H, Godwin AK, Daly MB, Laub PB, Hogan WM, Rosenblum N, Boente MP, Lynch HT, Hamilton TC: **Microscopic Benign and Invasive Malignant Neoplasms and a Cancer-Prone Phenotype in Prophylactic Oophorectomies.** *J Natl Cancer Inst* 1996, **88:**1810-1820.
73. Colgan T: **Challenges in the early diagnosis and staging of Fallopian-tube carcinomas associated with BRCA mutations.** *Int J Gynecol Pathol* 2003, **22:**109-120.
74. Piek JM, Dorsman JC, Zweemer RP, Verheijen RH, van Diest PJ, Colgan TJ: **Women harboring BRCA1/2 germline mutations are at risk for breast and female adnexal carcinoma.** *Int J Gynecol Pathol* 2003, **22:**315-316.
75. Jarboe E, Folkins A, Nucci MR, Kindelberger D, Drapkin R, Miron A, Lee Y, Crum CP: **Serous carcinogenesis in the fallopian tube: a descriptive classification.** *Int J Gynecol Pathol* 2008, **27:**1-9.
76. Finch A, Beiner M, Lubinski J, Lynch HT, Moller P, Rosen B, Murphy J, Ghadirian P, Friedman E, Foulkes WD, Kim-Sing C, Wagner T, Tung N, Couch F, Stoppa-Lyonnet D, Ainsworth P, Daly M, Pasini B, Gershoni-Baruch R, Eng C, Olopade OI, McLennan J, Karlan B, Weitzel J, Sun P, Narod SA; Hereditary Ovarian Cancer Clinical Study Group: **Salpingo-oophorectomy and the Risk of Ovarian, Fallopian Tube, and Peritoneal Cancers in Women With a BRCA1 or BRCA2 Mutation.** *JAMA* 2006, **296:**185-192.
77. Cho KR, Shih IM: **Ovarian Cancer.** *Annual Review of Pathology: Mechanisms of Disease* 2009, **4**.
78. Davidson B: **Anatomic Site-Related Expression of Cancer-Associated Molecules in Ovarian Carcinoma.** *Current Cancer Drug Targets* 2007, **7:**109-120.
79. Levine AJ: ***p53*, the Cellular Gatekeeper for Growth and Division.** *Cell* 1997, **88:**323-331.
80. Agarwal ML, Taylor WR, Chernov MV, Chernova OB, Stark GR: **The *p53* Network.** *J Biol Chem* 1998, **273:**1-4.
81. Tyner SD, Venkatachalam S, Choi J, Jones S, Ghebranious N, Igelmann H, Lu X, Soron G, Cooper B, Brayton C, Hee Park S, Thompson T, Karsenty G, Bradley A, Donehower LA: ***p53* mutant mice that display early ageing-associated phenotypes.** *Nature* 2002, **415:**45-53.
82. Jimenez GS, Khan SH, Stommel JM, Wahl GM: ***p53* regulation by post-translational modification and nuclear retention in response to diverse stresses.** *Oncogene* 1999, **18:**7656-7665.
83. Salani R, Kurman RJ, Giuntoli R, Gardner G, Bristow R, Wang TL, Shih IM: **Assessment of T*P53* mutation using purified tissue samples of ovarian serous carcinomas reveals a higher mutation rate than previously reported and does not correlate with drug resistance.** *International Journal of Gynecological Cancer* 2008, **18:**487-491.
84. Nnene IO, Nieto JJ, Crow JC, Sundaresan M, MacLean AB, Perrett CW, Hardiman P: **Cell cycle and apoptotic proteins in relation to ovarian epithelial morphology.** *Gynecologic Oncology* 2004, **92:**247-251.

85. Teneriello MG, Ebina M, Linnoila RI, Henry M, Nash JD, Park RC, Birrer MJ: ***p53* and Ki-ras Gene Mutations in Epithelial Ovarian Neoplasms.** *Cancer Res* 1993, **53:**3103-3108.
86. Hilton JL, Geisler JP, Rathe JA, Hattermann-Zogg MA, DeYoung B, Buller RE: **Inactivation of BRCA1 and BRCA2 in Ovarian Cancer.** *J Natl Cancer Inst* 2002, **94:**1396-1406.
87. Pothuri B, Leitao M, Barakat R: **Genetic analysis of ovarian carcinoma histogenesis. Abstracts Presented for the Thirty-Second Annual Meeting of the Society of Gynecologic Oncologists: The Opryland Hotel, Nashville, Tennessee, March 3-7, 2001.** *Gynecologic Oncology* 2001, **80:**275-330.
88. Shridhar V, Lee J, Pandita A, Iturria S, Avula R, Staub J, Morrissey M, Calhoun E, Sen A, Kalli K, Keeney G, Roche P, Cliby W, Lu K, Schmandt R, Mills GB, Bast RC Jr, James CD, Couch FJ, Hartmann LC, Lillie J, Smith DI: **Genetic Analysis of Early-versus Late-Stage Ovarian Tumors.** *Cancer Res* 2001, **61:**5895-5904.
89. Singer G, Oldt R, Cohen Y, Wang BG, Sidransky D, Kurman RJ, Shih IM: **Mutations in BRAF and KRAS characterize the development of low-grade ovarian serous carcinoma.** *J Natl Cancer Inst* 2003, **95:**484-486.
90. Gershenson DM, Sun CC, Lu KH, Coleman RL, Sood AK, Malpica A, Deavers MT, Silva EG, Bodurka DC: **Clinical Behavior of Stage II-IV Low-Grade Serous Carcinoma of the Ovary.** *Obstet Gynecol* 2006, **108:**361-368.
91. Bonome T, Lee J-Y, Park D-C, Radonovich M, Pise-Masison C, Brady J, Gardner GJ, Hao K, Wong WH, Barrett JC, Lu KH, Sood AK, Gershenson DM, Mok SC, Birrer MJ: **Expression Profiling of Serous Low Malignant Potential, Low-Grade, and High-Grade Tumors of the Ovary.** *Cancer Res* 2005, **65:**10602-10612.
92. Nikitin AY, Connolly DC, Hamilton TC: **Pathology of Ovarian Neoplasms in Genetically Modified Mice.** *Comp Med* 2004, **54:**26-26.
93. Connolly DC, Bao R, Nikitin AY, Stephens KC, Poole TW, Hua X, Harris SS, Vanderhyden BC, Hamilton TC: **Female Mice Chimeric for Expression of the Simian Virus 40 TAg under Control of the MISIIR Promoter Develop Epithelial Ovarian Cancer.** *Cancer Res* 2003, **63:**1389-1397.
94. Goff BA, Mandel LS, Drescher CW, Urban N, Gough S, Schurman KM, Patras J, Mahony BS, Andersen MR: **Development of an ovarian cancer symptom index.** *Cancer* 2007, **109:**221-227.
95. Rodriguez AO, Wun T, Chew H, Zhou H, Harvey D, White RH: **Venous thromboembolism in ovarian cancer.** *Gynecologic Oncology* 2007, **105:**784-790.
96. Mangan CE, Rubin SC, Rabin DS, Mikuta JJ: **Lymph node nomenclature in gynecologic oncology.** *Gynecol Oncol* 1986, **23:**222-226.
97. Hoskins WJ, Bundy BN, Thigpen JT, Omura GA: **The influence of cytoreductive surgery on recurrence-free interval and survival in small-volume Stage III epithelial ovarian cancer: A gynecologic oncology group study.** *Gynecologic Oncology* 1992, **47:**159-166.
98. Ng LW, Rubin SC, Hoskins WJ, Jones WB, Hakes TB, Markman M, Reichman B, Almadrones L, Lewis JL: **Aggressive chemosurgical debulking in patients with advanced ovarian cancer.** *Gynecologic Oncology* 1990, **38:**358-363.
99. Earle CC, Schrag D, Neville BA, Yabroff KR, Topor M, Fahey A, Trimble EL, Bodurka DC, Bristow RE, Carney M, Warren JL: **Effect of Surgeon**

Specialty on Processes of Care and Outcomes for Ovarian Cancer Patients. *J Natl Cancer Inst* 2006, **98:**172-180.

100. Winter WE, Maxwell GL, Tian C, Carlson JW, Ozols RF, Rose PG, Markman M, Armstrong DK, Muggia F, McGuire WP: **Prognostic Factors for Stage III Epithelial Ovarian Cancer: A Gynecologic Oncology Group Study.** *J Clin Oncol* 2007, **25:**3621-3627.
101. Fox H: **Ploidy in gynaecological cancers.** *Histopathology* 2005, **46:**121-129.
102. Duska LR, Chang YC, Flynn CE, Chen AH, Goodman A, Fuller AF, Nikrui N: **Epithelial ovarian carcinoma in the reproductive age group.** *Cancer* 1999, **85:**2623-2629.
103. Lloyd KO, Yin BW, Kudryasov V: **Isolation and characterization of ovarian cancer antigen CA 125 using a new monoclonal antibody (VK-8): identification as a mucin-type molecule.** *International Journal of Cancer* 1997, **71:**842-850.
104. Bast RC Jr, Klug TL, St John E, Jenison E, Niloff JM, Lazarus H, Berkowitz RS, Leavitt T, Griffiths CT, Parker L, Zurawski VR Jr, Knapp RC: **A radioimmunoassay using a monoclonal antibody to monitor the course of epithelial ovarian cancer.** *N Engl J Med* 1983, **309:**883-887.
105. Markman M: **The CA125 antigen level as a prognostic versus a predictive test in epithelial ovarian cancer.** *Nat Clin Pract Oncol* 2007, **4:**628-629.
106. Rustin GJ, Nelstrop AE, McClean P, Brady MF, McGuire WP, Hoskins WJ, Mitchell H, Lambert HE: **Defining response of ovarian carcinoma to initial chemotherapy according to serum CA 125.** *J Clin Oncol* 1996, **14:**1545-1551.
107. Santillan A, Garg R, Zahurak ML, Gardner GJ, Giuntoli RL, Armstrong DK, Bristow RE: **Risk of Epithelial Ovarian Cancer Recurrence in Patients With Rising Serum CA-125 Levels Within the Normal Range.** *J Clin Oncol* 2005, **23:**9338-9343.
108. Juretzka MM, Barakat RR, Chi DS, Iasonos A, Dupont J, Abu-Rustum NR, Poynor EA, Aghajanian C, Spriggs D, Hensley ML, Sabbatini P: **CA125 level as a predictor of progression-free survival and overall survival in ovarian cancer patients with surgically defined disease status prior to the initiation of intraperitoneal consolidation therapy.** *Gynecologic Oncology* 2007, **104:**176-180.
109. Malkasian GD Jr, Knapp RC, Lavin PT, Zurawski VR Jr, Podratz KC, Stanhope CR, Mortel R, Berek JS, Bast RC Jr, Ritts RE: **Preoperative evaluation of serum CA 125 levels in premenopausal and postmenopausal patients with pelvic masses: discrimination of benign from malignant disease.** *Am J Obstet Gynecol* 1988, **159:**341-346.
110. Whitehouse C, Solomon E: **Current Status of the Molecular Characterization of the Ovarian Cancer Antigen CA125 and Implications for Its Use in Clinical Screening.** *Gynecologic Oncology* 2003, **88:**S152-S157.
111. Jacobs I, Oram D, Fairbanks J, Turner J, Frost C, Grudzinskas JG: **A risk of malignancy index incorporating CA 125, ultrasound and menopausal status for the accurate preoperative diagnosis of ovarian cancer.** *Br J Obstet Gynaecol* 1990, **97:**922-929.
112. Hunter VJ, Daly L, Helms M, Soper JT, Berchuck A, Clarke-Pearson DL, Bast RC Jr: **The prognostic significance of CA 125 half-life in patients with**

ovarian cancer who have received primary chemotherapy after surgical cytoreduction. *Am J Obstet Gynecol* 1990, **163:**1164-1167.

113. Xu Y, Shen Z, Wiper DW, Wu M, Morton RE, Elson P, Kennedy AW, Belinson J, Markman M, Casey G: **Lysophosphatidic Acid as a Potential Biomarker for Ovarian and Other Gynecologic Cancers.** *JAMA* 1998, **280:**719-723.
114. Scholler N, Fu N, Yang Y, Ye Z, Goodman GE, Hellstrom KE, Hellstrom I: **Soluble member(s) of the mesothelin/megakaryocyte potentiating factor family are detectable in sera from patients with ovarian carcinoma.** *Proceedings of the National Academy of Sciences* 1999, **96:**11531-11536.
115. Moore RG, Brown AK, Miller MC, Skates S, Allard WJ, Verch T, Steinhoff M, Messerlian G, DiSilvestro P, Granai CO, Bast Jr RC: **The use of multiple novel tumor biomarkers for the detection of ovarian carcinoma in patients with a pelvic mass.** *Gynecologic Oncology* 2008, **108:**402-408.
116. Secord AA, Darcy KM, Hutson A, Lee PS, Havrilesky LJ, Grace LA, Berchuck A: **Co-expression of angiogenic markers and associations with prognosis in advanced epithelial ovarian cancer: A Gynecologic Oncology Group study.** *Gynecologic Oncology* 2007, **106:**221-232.
117. Psyrri A, Kountourakis P, Scorilas A, Markakis S, Camp R, Kowalski D, Diamandis EP, Dimopoulos MA: **Human tissue kallikrein 7, a novel biomarker for advanced ovarian carcinoma using a novel in situ quantitative method of protein expression.** *Ann Oncol* 2008, **19:** 1201-7.
118. Zheng Y, Katsaros D, Shan SJC, de la Longrais IR, Porpiglia M, Scorilas A, Kim NW, Wolfert RL, Simon I, Li L, Feng Z, Diamandis EP: **A Multiparametric Panel for Ovarian Cancer Diagnosis, Prognosis, and Response to Chemotherapy.** *Clin Cancer Res* 2007, **13:**6984-6992.
119. Lu KH, Patterson AP, Wang L, Marquez RT, Atkinson EN, Baggerly KA, Ramoth LR, Rosen DG, Liu J, Hellstrom I, Smith D, Hartmann L, Fishman D, Berchuck A, Schmandt R, Whitaker R, Gershenson DM, Mills GB, Bast RC Jr: **Selection of Potential Markers for Epithelial Ovarian Cancer with Gene Expression Arrays and Recursive Descent Partition Analysis.** *Clin Cancer Res* 2004, **10:**3291-3300.
120. Kawamoto S, Urban BA, Fishman EK: **CT of epithelial ovarian tumors.** *Radiographics* 1999, **S85-102:**S263-264.
121. Yamamoto Y, Oguri H, Yamada R, Maeda N, Kohsaki S, Fukaya T: **Preoperative evaluation of pelvic masses with combined 18F-fluorodeoxyglucose positron emission tomography and computed tomography.** *International Journal of Gynecology & Obstetrics* 2008, **102**:124-127.
122. Grab D, Flock F, Stöhr I, Nüssle K, Rieber A, Fenchel S, Brambs HJ, Reske SN, Kreienberg R: **Classification of Asymptomatic Adnexal Masses by Ultrasound, Magnetic Resonance Imaging, and Positron Emission Tomography.** *Gynecologic Oncology* 2000, **77:**454-459.
123. Austoker J: **Cancer Prevention in Primary Care: Screening for ovarian, prostatic, and testicular cancers.** *BMJ* 1994, **309:**315-320.
124. Skates SJ, Menon U, MacDonald N, Rosenthal AN, Oram DH, Knapp RC, Jacobs IJ: **Calculation of the Risk of Ovarian Cancer From Serial CA-125 Values for Preclinical Detection in Postmenopausal Women.** *J Clin Oncol* 2003, **21:**206-210.

125. Van Nagell JR, DePriest PD, Reedy MB, Gallion HH, Ueland FR, Pavlik EJ, Kryscio RJ: **The Efficacy of Transvaginal Sonographic Screening in Asymptomatic Women at Risk for Ovarian Cancer.** *Gynecologic Oncology* 2000, **77:**350-356.
126. Rosenthal AN, Menon U, Jacobs IJ: **Screening for ovarian cancer.** *Clin Obstet Gynecol* 2006, **49:**433-447.
127. Jacobs IJ, Skates SJ, MacDonald N, Menon U, Rosenthal AN, Davies AP, Woolas R, Jeyarajah AR, Sibley K, Lowe DG, Oram DH: **Screening for ovarian cancer: a pilot randomised controlled trial.** *The Lancet* 1999, **353:**1207-1210.
128. Chatterjee M, Mohapatra S, Ionan A, Bawa G, Ali-Fehmi R, Wang X, Nowak J, Ye B, Nahhas FA, Lu K, Witkin SS, Fishman D, Munkarah A, Morris R, Levin NK, Shirley NN, Tromp G, Abrams J, Draghici S, Tainsky MA: **Diagnostic Markers of Ovarian Cancer by High-Throughput Antigen Cloning and Detection on Arrays.** *Cancer Res* 2006, **66:**1181-1190.
129. McGuire WP, Hoskins WJ, Brady MF, Kucera PR, Partridge EE, Look KY, Clarke-Pearson DL, Davidson M: **Cyclophosphamide and Cisplatin Compared with Paclitaxel and Cisplatin in Patients with Stage III and Stage IV Ovarian Cancer.** *N Engl J Med* 1996, **334:**1-6.
130. Young RC, Decker DG, Wharton JT, Piver MS, Sindelar WF, Edwards BK, Smith JP: **Staging laparotomy in early ovarian cancer.** *JAMA* 1983, **250:**3072-3076.
131. Trimbos JB, Vergote I, Bolis G, Vermorken JB, Mangioni C, Madronal C, Franchi M, Tateo S, Zanetta G, Scarfone G, Giurgea L, Timmers P, Coens C, Pecorelli S: **Impact of Adjuvant Chemotherapy and Surgical Staging in Early-Stage Ovarian Carcinoma: European Organisation for Research and Treatment of Cancer-Adjuvant ChemoTherapy in Ovarian Neoplasm Trial.** *J Natl Cancer Inst* 2003, **95:**113-125.
132. Bristow RE, Tomacruz RS, Armstrong DK, Trimble EL, Montz FJ: **Survival Effect of Maximal Cytoreductive Surgery for Advanced Ovarian Carcinoma During the Platinum Era: A Meta-Analysis.** *J Clin Oncol* 2002, **20:**1248-1259.
133. Mc Gowan L: **Patterns of care in carcinoma of the ovary.** *Cancer* 1993, **71:**628-633.
134. Crawford SC, Vasey PA, Paul J, Hay A, Davis JA, Kaye SB: **Does Aggressive Surgery Only Benefit Patients With Less Advanced Ovarian Cancer? Results From an International Comparison Within the SCOTROC-1 Trial.** *J Clin Oncol* 2005, **23:**8802-8811.
135. Onda T, Kamura T, Ishizuka N, Katsumata N, Fukuda H, Yoshikawa H: **Feasibility Study of Neoadjuvant Chemotherapy Followed by Interval Cytoreductive Surgery for Stage III/IV Ovarian, Tubal and Peritoneal Cancers: Japan Clinical Oncology Group Study JCOG0206.** *Jpn J Clin Oncol* 2004, **34:**43-45.
136. Ray-Coquard I, Saba C, Bachelot T, Méeus P, Mignotte H, Blondet R, Treilleux I, Peix M, Guastalla JP: **Neoadjuvant chemotherapy and ovarian cancer.** *Bull Cancer* 2006, **93:**669-676.
137. Rose PG, Nerenstone S, Brady MF, Clarke-Pearson D, Olt G, Rubin SC, Moore DH, Small JM, the Gynecologic Oncology Group: **Secondary Surgical Cytoreduction for Advanced Ovarian Carcinoma.** *N Engl J Med* 2004, **351:**2489-2497.

138. Qayyum A, Coakley FV, Westphalen AC, Hricak H, Okuno WT, Powell B: **Role of CT and MR imaging in predicting optimal cytoreduction of newly diagnosed primary epithelial ovarian cancer.** *Gynecologic Oncology* 2005, **96:**301-306.
139. Memarzadeh S, Lee SB, Berek JS, Farias-Eisner R: **CA125 levels are a weak predictor of optimal cytoreductive surgery in patients with advanced epithelial ovarian cancer.** *International Journal of Gynecological Cancer* 2003, **13:**120-124.
140. Berchuck A, Iversen ES, Lancaster JM, Dressman HK, West M, Nevins JR, Marks JR: **Prediction of optimal versus suboptimal cytoreduction of advanced-stage serous ovarian cancer with the use of microarrays.** *American Journal of Obstetrics and Gynecology* 2004, **190:**910-923.
141. Creasman MD, William T: **Second-Look Laparotomy in Ovarian Cancer.** *Gynecologic Oncology* 1994, **55:**S122-S127.
142. Escobar PF, Michener CM, Rose PG: **Second-look operation improves survival in suboptimal, debulked, stage III ovarian cancer.** *International Journal of Gynecological Cancer* 2005, **15:**1258-1258.
143. Onda T, Yoshikawa H, Yasugi T, Yamada M, Matsumoto K, Taketani Y: **Secondary cytoreductive surgery for recurrent epithelial ovarian carcinoma: proposal for patients selection.** *Br J Cancer* 2005, **92:**1026-1032.
144. Fioretti P, Gadducci A, Ferdeghini M, Prontera C, Malagnino G, Facchini V, Mariani G, Bianchi R: **The concomitant determination of different serum tumor markers in epithelial ovarian cancer: Relevance for monitoring the response to chemotherapy and follow-up of patients.** *Gynecologic Oncology* 1992, **44:**155-160.
145. Schilder JM, Thompson AM, DePriest PD, Ueland FR, Cibull ML, Kryscio RJ, Modesitt SC, Lu KH, Geisler JP, Higgins RV, Magtibay PM, Cohn DE, Powell MA, Chu C, Stehman FB, van Nagell J: **Outcome of Reproductive Age Women with Stage IA or IC Invasive Epithelial Ovarian Cancer Treated with Fertility-Sparing Therapy.** *Gynecologic Oncology* 2002, **87:**1-7.
146. Ledermann JA, Dembo AJ, Sturgeon JF, Fine S, Bush RS, Fyles AW: **Outcome of patients with unfavorable optimally cytoreduced ovarian cancer treated with chemotherapy and whole abdominal radiation.** *Gynecol Oncol* 1991, **41:**30 - 35.
147. du Bois A, Luck H-J, Meier W, Adams H-P, Mobus V, Costa S, Bauknecht T, Richter B, Warm M, Schroder W, Olbricht S, Nitz U, Jackisch C, Emons G, Wagner U, Kuhn W, Pfisterer J: **A Randomized Clinical Trial of Cisplatin/Paclitaxel Versus Carboplatin/Paclitaxel as First-Line Treatment of Ovarian Cancer.** *J Natl Cancer Inst* 2003, **95:**1320-1329.
148. Takano M, Kikushi Y, Yaegashi N, Kuzuya K, Ueki M, Tsuda H, Suzuki M, Kigawa J, Takeuchi S, Tsuda H, Moriya T, Sugiyama T: **Clear cell carcinoma of the ovary: a retrospective multicentre experience of 254 patients with complete surgical staging.** *Br J Cancer* 2006, **94:**1369-1374.
149. Bookman MA: **Standard treatment in advanced ovarian cancer in 2005: the state of the art.** *International Journal of Gynecological Cancer* 2005, **15:**212-220.
150. McGuire WP: **Is It Time for Some New Approaches for Treating Advanced Ovarian Cancer?** *J Natl Cancer Inst* 2006, **98:**1024-1026.

151. Holzer AK, Manorek GH, Howell SB: **Contribution of the Major Copper Influx Transporter CTR1 to the Cellular Accumulation of Cisplatin, Carboplatin, and Oxaliplatin.** *Mol Pharmacol* 2006, **70:**1390-1394.
152. Fink D, Nebel S, Aebi S, Zheng H, Cenni B, Nehme A, Christen RD, Howell SB: **The role of DNA mismatch repair in platinum drug resistance.** *Cancer Res* 1996, **56:**4881 - 4886.
153. Young RC, Canellos GP, Chabner BA, Schein PS, Hubbard SP, DeVita VT Jr.: **Chemotherapy of advanced ovarian carcinoma: a prospective randomized comparison of phenylalanine mustard and high dose cyclophosphamide.** *Gynecol Oncol* 1974, **2:**489-497.
154. Young RC, Chabner BA, Hubbard SP, Fisher RI, Bender RA, Anderson T, Simon RM, Canellos GP, DeVita VT Jr: **Advanced ovarian adenocarcinoma. A prospective clinical trial of melphalan (L-PAM) versus combination chemotherapy.** *N Engl J Med* 1978, **299:**1261-1266.
155. Decker DG, Fleming TR, Malkasian GD Jr, Webb MJ, Jeffries JA, Edmonson JH.: **Cyclophosphamide plus cis-platinum in combination: treatment program for stage III or IV ovarian carcinoma.** *Obstet Gynecol* 1982, **60:**481-487.
156. Omura G, Blessing JA, Ehrlich CE, Miller A, Yordan E, Creasman WT, Homesley HD: **A randomized trial of cyclophosphamide and doxorubicin with or without cisplatin in advanced ovarian carcinoma. A Gynecologic Oncology Group Study.** *Cancer* 1986, **57:**1725-1730.
157. Neijt JP, van der Burg ME, van Oosterom AT, Vriesendorp R, Kooyman CD, van Lindert AC, Hamerlynck JV, van Lent M, van Houwelingen JC: **Randomised trial comparing two combination chemotherapy regimens (Hexa-CAF vs CHAP-5) in advanced ovarian carcinoma.** *Lancet* 1984, **2:**594-600.
158. McGuire WP, Rowinsky EK, Rosenshein NB, Grumbine FC, Ettinger DS, Armstrong DK, Donehower RC: **Taxol: a unique antineoplastic agent with significant activity in advanced ovarian epithelial neoplasms.** *Ann Intern Med* 1989, **111:**273-279.
159. Piccart MJ, Bertelsen K, James K, Cassidy J, Mangioni C, Simonsen E, Stuart G, Kaye S, Vergote I, Blom R, Grimshaw R, Atkinson RJ, Swenerton KD, Trope C, Nardi M, Kaern J, Tumolo S, Timmers P, Roy JA, Lhoas F, Lindvall B, Bacon M, Birt A, Andersen JE, Zee B, Paul J, Baron B, Pecorelli S: **Randomized Intergroup Trial of Cisplatin-Paclitaxel Versus Cisplatin-Cyclophosphamide in Women With Advanced Epithelial Ovarian Cancer: Three-Year Results.** *J Natl Cancer Inst* 2000, **92:**699-708.
160. Ozols R: **Paclitaxel plus carboplatin in the treatment of ovarian cancer.** *Semin Oncol* 1999, **26:**84-89.
161. Ozols RF, Bundy BN, Greer BE, Fowler JM, Clarke-Pearson D, Burger RA, Mannel RS, DeGeest K, Hartenbach EM, Baergen R: **Phase III Trial of Carboplatin and Paclitaxel Compared With Cisplatin and Paclitaxel in Patients With Optimally Resected Stage III Ovarian Cancer: A Gynecologic Oncology Group Study.** *J Clin Oncol* 2003, **21:**3194-3200.
162. Bookman M: **GOG0182-ICON5: 5-arm phase III randomized trial of paclitaxel (P) and carboplatin (C) vs combination with gemcitabine (G), PEGliposomal doxorubicin (D), or topotecan (T) in patients (pts) with advanced-stage epithelial ovarian (EOC) or primary peritoneal (PPC) carcinoma** *J Clin Oncol* 2006, **24:**5002.

163. Alberts DS, Liu PY, Hannigan EV, O'Toole R, Williams SD, Young JA, Franklin EW, Clarke-Pearson DL, Malviya VK, DuBeshter B: **Intraperitoneal Cisplatin plus Intravenous Cyclophosphamide versus Intravenous Cisplatin plus Intravenous Cyclophosphamide for Stage III Ovarian Cancer.** *N Engl J Med* 1996, **335:**1950-1955.
164. Markman M, Liu PY, Wilczynski S, Monk B, Copeland LJ, Alvarez RD, Jiang C, Alberts D: **Phase III Randomized Trial of 12 Versus 3 Months of Maintenance Paclitaxel in Patients With Advanced Ovarian Cancer After Complete Response to Platinum and Paclitaxel-Based Chemotherapy: A Southwest Oncology Group and Gynecologic Oncology Group Trial.** *J Clin Oncol* 2003, **21:**2460-2465.
165. Armstrong DK, Bundy B, Wenzel L, Huang HQ, Baergen R, Lele S, Copeland LJ, Walker JL, Burger RA: **Intraperitoneal cisplatin and paclitaxel in ovarian cancer.** *N Engl J Med* 2006, **354:**34-43.
166. **www.nlm.nih.gov/databases/alerts/ovarian_ip_chemo.html.**
167. Alberts DS, Markman M, Muggia F, Ozols RF, Eldermire E, Bookman MA, Chen T, Curtin J, Hess LM, Liebes L, Young RC, Trimble E: **Proceedings of a GOG workshop on intraperitoneal therapy for ovarian cancer.** *Gynecologic Oncology* 2006, **103:**783-792.
168. De Placido S, Scambia G, Di Vagno G, Naglieri E, Lombardi AV, Biamonte R, Marinaccio M, Carteni G, Manzione L, Febbraro A, De Matteis A, Gasparini G, Valerio MR, Danese S, Perrone F, Lauria R, De Laurentiis M, Greggi S, Gallo C, Pignata S: **Topotecan Compared With No Therapy After Response to Surgery and Carboplatin/Paclitaxel in Patients With Ovarian Cancer: Multicenter Italian Trials in Ovarian Cancer (MITO-1) Randomized Study.** *J Clin Oncol* 2004, **22:**2635-2642.
169. Hall GD, Brown JM, Coleman RE, Stead M, Metcalf KS, Peel KR, Poole C, Crawford M, Hancock B, Selby PJ, Perren TJ: **Maintenance treatment with interferon for advanced ovarian cancer: results of the Northern and Yorkshire gynaecology group randomised phase III study.** *Br J Cancer* 2004, **91:**621-626.
170. Berek JS, Taylor PT, Gordon A, Cunningham MJ, Finkler N, Orr J, Jr., Rivkin S, Schultes BC, Whiteside TL, Nicodemus CF: **Randomized, Placebo-Controlled Study of Oregovomab for Consolidation of Clinical Remission in Patients With Advanced Ovarian Cancer.** *J Clin Oncol* 2004, **22:**3507-3516.
171. Sorbe B: **Consolidation treatment of advanced ovarian carcinoma with radiotherapy after induction chemotherapy.** *Int J Gynecol Cancer* 2003, **13:**192-195.
172. Cure H, Guastalla JP: **Phase III randomized trial of high-dose chemotherapy and peripheral blood stem cell support as consolidation in patients with advanced ovarian cancer: 5-year follow-up of GINECO/FNCLCC/SFGM-TC study [abstract.** *Proc Am Soc Clin Oncol* 2004, **23:**Abstract 5006.
173. Varia MA, Stehman FB, Bundy BN, Benda JA, Clarke-Pearson DL, Alvarez RD, Long HJ: **Intraperitoneal Radioactive Phosphorus (32P) Versus Observation After Negative Second-Look Laparotomy for Stage III Ovarian Carcinoma: A Randomized Trial of the Gynecologic Oncology Group.** *J Clin Oncol* 2003, **21:**2849-2855.

174. Vergote I, van Gorp T, Amant F, Neven P, Berteloot P: **Neoadjuvant chemotherapy for ovarian cancer.** *Oncology (Williston Park)* 2005, **19:**1615-1622.
175. Bhoola S, Hoskins WJ: **Diagnosis and Management of Epithelial Ovarian Cancer.** *Obstet Gynecol* 2006, **107:**1399-1410.
176. Ozols RF: **Treatment goals in ovarian cancer.** *International Journal of Gynecological Cancer* 2005, **15:**3-11.
177. Ozols RF: **Recurrent Ovarian Cancer: Evidence-Based Treatment.** *J Clin Oncol* 2002, **20:**1161-1163.
178. Gore ME, Fryatt I, Wiltshaw E, Dawson T: **Treatment of relapsed carcinoma of the ovary with cisplatin or carboplatin following initial treatment with these compounds.** *Gynecol Oncol* 1990, **36:**207-211.
179. Eisenhauer EA, ten Bokkel Huinink WW, Swenerton KD, Gianni L, Myles J, van der Burg ME, Kerr I, Vermorken JB, Buser K, Colombo N: **European-Canadian randomized trial of paclitaxel in relapsed ovarian cancer: high-dose versus low-dose and long versus short infusion.** *J Clin Oncol* 1994, **12:**2654-2666.
180. Eisenhauer EA, Vermorken JB, van Glabbeke M: **Predictors of response to subsequent chemotherapy in platinum pretreated ovarian cancer: A multivariate analysis of 704 patients.** *Ann Oncol* 1997, **8:**963-968.
181. Hoskins P, Eisenhauer E, Beare S, Roy M, Drouin P, Stuart G, Bryson P, Grimshaw R, Capstick V, Zee B: **Randomized phase II study of two schedules of topotecan in previously treated patients with ovarian cancer: a National Cancer Institute of Canada Clinical Trials Group study.** *J Clin Oncol* 1998, **16:**2233-2237.
182. Gordon AN, Fleagle JT, Guthrie D, Parkin DE, Gore ME, Lacave AJ: **Recurrent Epithelial Ovarian Carcinoma: A Randomized Phase III Study of Pegylated Liposomal Doxorubicin Versus Topotecan.** *J Clin Oncol* 2001, **19:**3312-3322.
183. Rose PG, Blessing JA, Ball HG, Hoffman J, Warshal D, DeGeest K, Moore DH: **A phase II study of docetaxel in paclitaxel-resistant ovarian and peritoneal carcinoma: a gynecologic oncology group study.** *Gynecologic Oncology* 2003, **88:**130-135.
184. Petru E, Angleitner-Boubenizek L, Reinthaller A, Deibl M, Zeimet AG, Volgger B, Stempfl A, Marth C: **Combined PEG liposomal doxorubicin and gemcitabine are active and have acceptable toxicity in patients with platinum-refractory and -resistant ovarian cancer after previous platinum-taxane therapy: A phase II Austrian AGO study.** *Gynecologic Oncology* 2006, **102:**226-229.
185. Rose PG, Blessing JA, Soper JT, Barter JF: **Prolonged Oral Etoposide in Recurrent or Advanced Leiomyosarcoma of the Uterus: A Gynecologic Oncology Group Study.** *Gynecologic Oncology* 1998, **70:**267-271.
186. Keldsen N, Havsteen H, Vergote I, Bertelsen K, Jakobsen A: **Altretamine (hexamethylmelamine) in the treatment of platinum-resistant ovarian cancer: a phase II study.** *Gynecologic Oncology* 2003, **88:**118-122.
187. Markman M, Kennedy A, Sutton G, Hurteau J, Webster K, Peterson G, Kulp B, Belinson J: **Phase 2 Trial of Single Agent Ifosfamide/Mesna in Patients with Platinum/Paclitaxel Refractory Ovarian Cancer Who Have Not Previously Been Treated with an Alkylating Agent.** *Gynecologic Oncology* 1998, **70:**272-274.

188. Schrag D, Garewal HS, Burstein HJ, Samson DJ, Von Hoff DD, Somerfield MR: **American Society of Clinical Oncology Technology Assessment: Chemotherapy Sensitivity and Resistance Assays.** *J Clin Oncol* 2004, **22:**3631-3638.
189. Hess V, A'Hern R, Nasiri N, King DM, Blake PR, Barton DPJ, Shepherd JH, Ind T, Bridges J, Harrington K, Kaye SB, Gore ME: **Mucinous Epithelial Ovarian Cancer: A Separate Entity Requiring Specific Treatment.** *J Clin Oncol* 2004, **22:**1040-1044.
190. Knight LA, Conroy M, Fernando A, Polak M, Kurbacher CM, Cree IA: **Pilot studies of the effect of zoledronic acid (Zometa) on tumor-derived cells ex vivo in the ATP-based tumor chemosensitivity assay.** *Anticancer Drugs* 2005, **16:**969-976.
191. Sargent DJ, Conley BA, Allegra C, Collette L: **Clinical Trial Designs for Predictive Marker Validation in Cancer Treatment Trials.** *J Clin Oncol* 2005, **23:**2020-2027.
192. Hartmann LC, Lu KH, Linette GP, Cliby WA, Kalli KR, Gershenson D, Bast RC, Stec J, Iartchouk N, Smith DI, Ross JS, Hoersch S, Shridhar V, Lillie J, Kaufmann SH, Clark EA, Damokosh AI: **Gene Expression Profiles Predict Early Relapse in Ovarian Cancer after Platinum-Paclitaxel Chemotherapy.** *Clin Cancer Res* 2005, **11:**2149-2155.
193. Bollag DM, McQueney PA, Zhu J, Hensens O, Koupal L, Liesch J, Goetz M, Lazarides E, Woods CM: **Epothilones, a New Class of Microtubule-stabilizing Agents with a Taxol-like Mechanism of Action.** *Cancer Res* 1995, **55:**2325-2333.
194. Chou T-C, Zhang X-G, Harris CR, Kuduk SD, Balog A, Savin KA, Bertino JR, Danishefsky SJ: **Desoxyepothilone B is curative against human tumor xenografts that are refractory to paclitaxel.** *Proceedings of the National Academy of Sciences* 1998, **95:**15798-15802.
195. Minuzzo M, Marchini S, Broggini M, Faircloth G, D'Incalci M, Mantovani R: **Interference of transcriptional activation by the antineoplastic drug ecteinascidin-743.** *Proceedings of the National Academy of Sciences* 2000, **97:**6780-6784.
196. Sessa C, DeBtaud F, Perotti A, Bauer J, Curigliano G, Noberasco C, Zanaboni F, Gianni L, Marsoni S, Jimeno J, D'Incalci M, Dallo E, Colombo N.: **Trabectedin for women with ovarian carcinoma after treatment with platinum and taxanes fails.** *J Clin Oncol* 2005, **23:**1867-1874.
197. Townsend DM, Findlay VL, Tew KD, Sies H, Packer L: **Glutathione STransferases as Regulators of Kinase Pathways and Anticancer Drug Targets.** In *Methods in Enzymology. Volume* Volume 401: Academic Press; 2005: 287-307
198. Darcy KM, Schilder RJ: **Relevant molecular markers and targets.** *Gynecologic Oncology* 2006, **103:**6-13.
199. Gordon AN, Finkler N, Edwards RP, Garcia AA, Crozier M, Irwin DH, Barrett E: **Efficacy and safety of erlotinib HCl, an epidermal growth factor receptor (HER1/EGFR) tyrosine kinase inhibitor, in patients with advanced ovarian carcinoma: results from a phase II multicenter study.** *International Journal of Gynecological Cancer* 2005, **15:**785-792.
200. Martin L, Schilder R: **Novel Approaches in Advancing the Treatment of Epithelial Ovarian Cancer: The Role of Angiogenesis Inhibition.** *J Clin Oncol* 2007, **25:**2894-2901.

201. O'Toole SA, Sheppard BL, Laios A, O'Leary JJ, McGuinness EPJ, D'Arcy T, Bonnar J: **Potential predictors of chemotherapy response in ovarian cancer--How do we define chemosensitivity?** *Gynecologic Oncology* 2007, **104:**345-351.
202. Burger RA, Sill MW, Monk BJ, Greer BE, Sorosky JI: **Phase II Trial of Bevacizumab in Persistent or Recurrent Epithelial Ovarian Cancer or Primary Peritoneal Cancer: A Gynecologic Oncology Group Study.** *J Clin Oncol* 2007, **25:**5165-5171.
203. Han ES, Monk BJ: **Bevacizumab in the treatment of ovarian cancer.** *Expert Review of Anticancer Therapy* 2007, **7:**1339-1345.
204. Herzog TJ: **The current treatment of recurrent ovarian cancer.** *Curr Oncol Rep* 2006, **8:**448-454.
205. Peng K-W, TenEyck CJ, Galanis E, Kalli KR, Hartmann LC, Russell SJ: **Intraperitoneal Therapy of Ovarian Cancer Using an Engineered Measles Virus.** *Cancer Res* 2002, **62:**4656-4662.
206. Altomare DA, Wang HQ, Skele KL, Rienzo AD, Klein-Szanto AJ, Godwin AK, Testa JR: **AKT and mTOR phosphorylation is frequently detected in ovarian cancer and can be targeted to disrupt ovarian tumor cell growth.** *Oncogene* 2004, **23:**5853-5857.
207. Kamat AA, Fletcher M, Gruman LM, Mueller P, Lopez A, Landen CN, Jr., Han L, Gershenson DM, Sood AK: **The Clinical Relevance of Stromal Matrix Metalloproteinase Expression in Ovarian Cancer.** *Clin Cancer Res* 2006, **12:**1707-1714.
208. Chu CS, Kim SH, June CH, Coukos G: **Immunotherapy opportunities in ovarian cancer.** *Expert Review of Anticancer Therapy* 2008, **8:**243-257.
209. Azad NS, Annunziata CM, Steinberg SM, Minasian L, Premkumar A, Chow C, Kotz HL, kohn EC: **Lack of reliability of CA125 response criteria with anti-VEGF molecularly targeted therapy.** *Cancer* 2008, **9999:**NA.
210. Tew KD, O'Brien M, Laing NM, Shen H: **Coordinate changes in expression of protective genes in drug-resistant cells.** *Chem Biol Interact* 1998, **111-112:199-211**.
211. Persidis A: **Cancer multidrug resistance.** *Nat Biotech* 1999, **17:**94-95.
212. Cloven NG, Kyshtoobayeva A, Burger RA, Yu I-R, Fruehauf JP: **In vitro chemoresistance and biomarker profiles are unique for histologic subtypes of epithelial ovarian cancer.** *Gynecologic Oncology* 2004, **92:**160-166.
213. Shimizu Y, Kamoi S, Amada S, Hasumi K, Akiyama F, Silverberg SG: **Toward the Development of a Universal Grading System for Ovarian Epithelial Carcinoma: I. Prognostic Significance of Histopathologic Features--Problems Involved in the Architectural Grading System.** *Gynecologic Oncology* 1998, **70:**2-12.
214. Armstrong DK, Bundy B, Wenzel L, Huang HQ, Baergen R, Lele S, Copeland LJ, Walker JL, Burger RA, the Gynecologic Oncology Group: **Intraperitoneal Cisplatin and Paclitaxel in Ovarian Cancer.** *N Engl J Med* 2006, **354:**34-43.
215. Jemal A, Siegel R, Ward E, Murray T, Xu J, Smigal C, Thun MJ: **Cancer Statistics, 2006.** *CA Cancer J Clin* 2006, **56:**106-130.
216. Sabbatini P, Spriggs DR: **Consolidation for Ovarian Cancer in Remission.** *J Clin Oncol* 2006, **24:**537-539.

217. Zhang K, Mack P, Wong KP: **Glutathione-related mechanisms in cellular resistance to anticancer drugs.** *Int J Oncol* 1998, **12:**871-882.
218. Cole SP, Bhardwaj G, Gerlach JH, Mackie JE, Grant CE, Almquist KC, Stewart AJ, Kurz EU, Duncan AM, Deeley RG: **Overexpression of a transporter gene in a multidrug-resistant human lung cancer cell line.** *Science* 1992, **258:**1650-1654.
219. Yasui K, Mihara S, Zhao C, Okamoto H, Saito-Ohara F, Tomida A, Funato T, Yokomizo A, Naito S, Imoto I, Tsuruo T, Inazawa J: **Alteration in Copy Numbers of Genes as a Mechanism for Acquired Drug Resistance.** *Cancer Res* 2004, **64:**1403-1410.
220. Szakacs G, Paterson JK, Ludwig JA, Booth-Genthe C, Gottesman MM: **Targeting multidrug resistance in cancer.** *Nat Rev Drug Discov* 2006, **5:**219-234.
221. Kelland L: **The resurgence of platinum-based cancer chemotherapy.** *Nat Rev Cancer* 2007, **7:**573-584.
222. Vakifahmetoglu H, Olsson M, Tamm C, Heidari N, Orrenius S, Zhivotovsky B: **DNA damage induces two distinct modes of cell death in ovarian carcinomas.** *Cell Death Differ* 2007, **15:**555-566.
223. Knox RJ, Friedlos F, Lydall DA, Roberts JJ: **Mechanism of Cytotoxicity of Anticancer Platinum Drugs: Evidence That cis-Diamminedichloroplatinum(II) and cis-Diammine-(1,1-cyclobutanedicarboxylato)platinum(II) Differ Only in the Kinetics of their Interaction with DNA.** *Cancer Res* 1986, **46:**1972-1979.
224. Wheate NJ, Collins JG: **Multi-Nuclear Platinum Drugs: A New Paradigm in Chemotherapy.** *Current Medicinal Chemistry - Anti-Cancer Agents* 2005, **5:**267-279.
225. Gately DP, Howell SB: **Cellular accumulation of the anticancer agent cisplatin: a review.** *Br J Cancer* 1993, **67:**1171-1176.
226. Katano K, Kondo A, Safaei R, Holzer A, Samimi G, Mishima M, Kuo Y-M, Rochdi M, Howell SB: **Acquisition of Resistance to Cisplatin Is Accompanied by Changes in the Cellular Pharmacology of Copper.** *Cancer Res* 2002, **62:**6559-6565.
227. Holzer AK, Howell SB: **The Internalization and Degradation of Human Copper Transporter 1 following Cisplatin Exposure.** *Cancer Res* 2006, **66:**10944-10952.
228. Safaei R, Holzer AK, Katano K, Samimi G, Howell SB: **The role of copper transporters in the development of resistance to Pt drugs.** *Journal of Inorganic Biochemistry* 2004, **98:**1607-1613.
229. Samimi G, Safaei R, Katano K, Holzer AK, Rochdi M, Tomioka M, Goodman M, Howell SB: **Increased Expression of the Copper Efflux Transporter ATP7A Mediates Resistance to Cisplatin, Carboplatin, and Oxaliplatin in Ovarian Cancer Cells.** *Clin Cancer Res* 2004, **10:**4661-4669.
230. Germain I, Tetu B, Brisson J, Mondor M, Cherian MG: **Markers of chemoresistance in ovarian carcinomas: an immunohistochemical study of 86 cases.** *Int J Gynecol Pathol* 1996, **15:**54-62.
231. Ikeda K, Sakai K, Yamamoto R, Hareyama H, Tsumura N, Watari H, Shimizu M, Minakami H, Sakuragi N: **Multivariate analysis for prognostic significance of histologic subtype, GST-pi, MDR-1, and *p53* in stages II-IV ovarian cancer.** *International Journal of Gynecological Cancer* 2003, **13:**776-784.

232. Mistry P, Kelland LR, Abel G, Sidhar S, Harrap KR: **The relationships between glutathione, glutathione-S-transferase and cytotoxicity of platinum drugs and melphalan in eight human ovarian carcinoma cell lines.** *Br J Cancer* 1991, **64:**215-220.
233. Ishikawa T: **The ATP-dependent glutathione S-conjugate export pump.** *Trends in Biochemical Sciences* 1992, **17:**463-468.
234. Lewis AD, Hayes JD, Wolf CR: **Glutathione and glutathione-dependent enzymes in ovarian adenocarcinoma cell lines derived from a patient before and after the onset of drug resistance: intrinsic differences and cell cycle effects.** *Carcinogenesis* 1988, **9:**1283-1287.
235. Yang P, Ebbert JO, Sun Z, Weinshilboum RM: **Role of the Glutathione Metabolic Pathway in Lung Cancer Treatment and Prognosis: A Review.** *J Clin Oncol* 2006, **24:**1761-1769.
236. Holford J, Beale PJ, Boxall FE, Sharp SY, Kelland LR: **Mechanisms of drug resistance to the platinum complex ZD0473 in ovarian cancer cell lines.** *European Journal of Cancer* 2000, **36:**1984-1990.
237. Kelland LR, Mistry P, Abel G, Freidlos F, Loh SY, Roberts JJ, Harrap KR: **Establishment and Characterization of an in Vitro Model of Acquired Resistance to Cisplatin in a Human Testicular Nonseminomatous Germ Cell Line.** *Cancer Res* 1992, **52:**1710-1716.
238. Johnson SW, Swiggard PA, Handel LM, Brennan JM, Godwin AK, Ozols RF, Hamilton TC: **Relationship between Platinum-DNA Adduct Formation and Removal and Cisplatin Cytotoxicity in Cisplatin-sensitive and -resistant Human Ovarian Cancer Cells.** *Cancer Res* 1994, **54:**5911-5916.
239. Ferry KV, Hamilton TC, Johnson SW: **Increased nucleotide excision repair in cisplatin-resistant ovarian cancer cells: Role of ercc1-xpf.** *Biochemical Pharmacology* 2000, **60:**1305-1313.
240. Dabholkar M, Bostick-Bruton F, Weber C, Bohr VA, Egwuagu C, Reed E: **ERCC1 and ERCC2 Expression in Malignant Tissues From Ovarian Cancer Patients.** *J Natl Cancer Inst* 1992, **84:**1512-1517.
241. Fink D, Nebel S, Aebi S, Zheng H, Cenni B, Nehme A, Christen RD, Howell SB: **The Role of DNA Mismatch Repair in Platinum Drug Resistance.** *Cancer Res* 1996, **56:**4881-4886.
242. Gifford G, Paul J, Vasey PA, Kaye SB, Brown R: **The Acquisition of hMLH1 Methylation in Plasma DNA after Chemotherapy Predicts Poor Survival for Ovarian Cancer Patients.** *Clin Cancer Res* 2004, **10:**4420-4426.
243. Helleman J, van Staveren I, Dinjens W, van Kuijk P, Ritstier K, Ewing P, van der Burg M, Stoter G, Berns E: **Mismatch repair and treatment resistance in ovarian cancer.** *BMC Cancer* 2006, **6:**201.
244. Albertella MR, Green CM, Lehmann AR, O'Connor MJ: **A Role for Polymerase {eta} in the Cellular Tolerance to Cisplatin-Induced Damage.** *Cancer Res* 2005, **65:**9799-9806.
245. Gadducci A, Cosio S, Muraca S, Genazzani AR: **Molecular mechanisms of apoptosis and chemosensitivity to platinum and paclitaxel in ovarian cancer: biological data and clinical implications.** *Eur J Gynaecol Oncol* 2002, **23:**390-396.
246. Gordon AN, Tonda M, Sun S, Rackoff W: **Long-term survival advantage for women treated with pegylated liposomal doxorubicin compared with**

topotecan in a phase 3 randomized study of recurrent and refractory epithelial ovarian cancer. *Gynecologic Oncology* 2004, **95:**1-8.

247. Gradishar WJ, Tjulandin S, Davidson N, Shaw H, Desai N, Bhar P, Hawkins M, O'Shaughnessy J: **Phase III Trial of Nanoparticle Albumin-Bound Paclitaxel Compared With Polyethylated Castor Oil-Based Paclitaxel in Women With Breast Cancer.** *J Clin Oncol* 2005, **23:**7794-7803.
248. White SC, Lorigan P, Margison GP, Margison JM, Martin F, Thatcher N, Anderson H, Ranson M: **Phase II study of SPI-77 (sterically stabilised liposomal cisplatin) in advanced non-small-cell lung cancer.** *Br J Cancer* 2006, **95:**822-828.
249. Rademaker-Lakhai JM, Terret C, Howell SB, Baud CM, de Boer RF, Pluim D, Beijnen JH, Schellens JHM, Droz J-P: **A Phase I and Pharmacological Study of the Platinum Polymer AP5280 Given as an Intravenous Infusion Once Every 3 Weeks in Patients with Solid Tumors.** *Clin Cancer Res* 2004, **10:**3386-3395.
250. Rice JR, Gerberich JL, Nowotnik DP, Howell SB: **Preclinical Efficacy and Pharmacokinetics of A*P5346*, A Novel Diaminocyclohexane-Platinum Tumor-Targeting Drug Delivery System.** *Clin Cancer Res* 2006, **12:**2248-2254.
251. Lewandowicz GM, Britt P, Elgie AW, Williamson CJ, Coley HM, Hall AG, Sargent JM: **Cellular Glutathione Content, in Vitro Chemoresponse, and the Effect of BSO Modulation in Samples Derived from Patients with Advanced Ovarian Cancer.** *Gynecologic Oncology* 2002, **85:**298-304.
252. Plumb JA, Strathdee G, Sludden J, Kaye SB, Brown R: **Reversal of Drug Resistance in Human Tumor Xenografts by 2'-Deoxy-5-azacytidine-induced Demethylation of the hMLH1 Gene Promoter.** *Cancer Res* 2000, **60:**6039-6044.
253. Scatena CD, Stewart ZA, Mays D, Tang LJ, Keefer CJ, Leach SD, Pietenpol JA: **Mitotic Phosphorylation of Bcl-2 during Normal Cell Cycle Progression and Taxol-induced Growth Arrest.** *J Biol Chem* 1998, **273:**30777-30784.
254. Gundersen GG, Kalnoski MH, Bulinski JC: **Distinct populations of microtubules: Tyrosinated and nontyrosinated alpha tubulin are distributed differently in vivo.** *Cell* 1984, **38:**779-789.
255. Schiff PB, Fant J, Horwitz SB.: **Promotion of microtubule assembly in vitro by taxol.** *Nature* 1979, **Feb 22:**665-667.
256. Hari M, Loganzo F, Annable T, Tan X, Musto S, Morilla DB, Nettles JH, Snyder JP, Greenberger LM: **Paclitaxel-resistant cells have a mutation in the paclitaxel-binding region of {beta}-tubulin (Asp26Glu) and less stable microtubules.** *Mol Cancer Ther* 2006, **5:**270-278.
257. Peer D, Dekel Y, Melikhov D, Margalit R: **Fluoxetine Inhibits Multidrug Resistance Extrusion Pumps and Enhances Responses to Chemotherapy in Syngeneic and in Human Xenograft Mouse Tumor Models.** *Cancer Res* 2004, **64:**7562-7569.
258. Tan M, Jing T, Lan K-H, Neal CL, Li P, Lee S, Fang D, Nagata Y, Liu J, Arlinghaus R, Hung MC, Yu D: **Phosphorylation on Tyrosine-15 of p34Cdc2 by ErbB2 Inhibits p34Cdc2 Activation and Is Involved in Resistance to Taxol-Induced Apoptosis.** *Molecular Cell* 2002, **9:**993-1004.

259. Anand S, Penrhyn-Lowe S, Venkitaraman AR: **AURORA-A amplification overrides the mitotic spindle assembly checkpoint, inducing resistance to Taxol.** *Cancer Cell* 2003, **3:**51-62.
260. Huang Y, Swapan R, Reed JC, Ibrado AM, Tang C, Nawabi A, Bhalla K: **Estrogen increases intracellular p26Bcl-2 to p21Bax ratios and inhibits taxol-inducd apoptosis of human breast cancer MCF-7 cells.** *Breast Cancer Research and Treatment* 1997, **42:**73-81.
261. Giannakakou P, Sackett DL, Kang Y-K, Zhan Z, Buters JTM, Fojo T, Poruchynsky MS: **Paclitaxel-resistant Human Ovarian Cancer Cells Have Mutant beta -Tubulins That Exhibit Impaired Paclitaxel-driven Polymerization.** *J Biol Chem* 1997, **272:**17118-17125.
262. Alli E, Bash-Babula J, Yang J-M, Hait WN: **Effect of Stathmin on the Sensitivity to Antimicrotubule Drugs in Human Breast Cancer.** *Cancer Res* 2002, **62:**6864-6869.
263. Goncalves A, Braguer D, Kamath K, Martello L, Briand C, Horwitz S, Wilson L, Jordan MA: **Resistance to Taxol in lung cancer cells associated with increased microtubule dynamics.** *Proceedings of the National Academy of Sciences* 2001, **98:**11737-11742.
264. Ahmed AA, Mills AD, Ibrahim AEK, Temple J, Blenkiron C, Vias M, Massie CE, Iyer NG, McGeoch A, Crawford R, Nicke B, Downward J, Swanton C, Bell SD, Earl HM, Laskey RA, Caldas C, Brenton JD: **The Extracellular Matrix Protein TGFBI Induces Microtubule Stabilization and Sensitizes Ovarian Cancers to Paclitaxel.** *Cancer Cell* 2007, **12:**514-527.
265. Palazzo AF, Eng CH, Schlaepfer DD, Marcantonio EE, Gundersen GG: **Localized Stabilization of Microtubules by Integrin- and FAK-Facilitated Rho Signaling.** *Science* 2004, **303:**836-839.
266. Lowe SW, Ruley HE, Jacks T, Housman DE: ***p53*-dependent apoptosis modulates the cytotoxicity of anticancer agents.** *Cell* 1993, **74:**957-967.
267. Zhang CC, Yang J-M, Bash-Babula J, White E, Murphy M, Levine AJ, Hait WN: **DNA Damage Increases Sensitivity to Vinca Alkaloids and Decreases Sensitivity to Taxanes through *p53*-dependent Repression of Microtubule-associated Protein 4.** *Cancer Res* 1999, **59:**3663-3670.
268. Seiler N, Schneider Y, Gossé F, Schleiffer R, Raul F: **Polyploidisation of metastatic colon carcinoma cells by microtubule and tubulin interacting drugs: effect on proteolytic activity and invasiveness.** *Int J Oncol 2004 Oct;25(4):1039-48* 2004.
269. Ludwig JA, Weinstein JN: **Biomarkers in Cancer Staging, Prognosis and Treatment Selection.** *Nat Rev Cancer* 2005, **5:**845-856.
270. Potti A, Dressman HK, Bild A, Riedel RF, Chan G, Sayer R, Cragun J, Cottrill H, Kelley MJ, Petersen R, Harpole D, Marks J, Berchunk A, Ginsburg GS, Febbo P, Lancaster J, Nevins JR: **Genomic signatures to guide the use of chemotherapeutics.** *Nat Med* 2006, **12:**1294-1300.
271. Geschwind DH: **DNA microarrays: translation of the genome from laboratory to clinic.** *The Lancet Neurology* 2003, **2:**275-282.
272. Heller MJ: **DNA Microarray Technology: Devices, Systems, and Applications.** *Annual Review of Biomedical Engineering* 2002, **4:**129-153.
273. Crijns AP, Dulker EW, de Jong S, Willemse PH, van der Zee AG, de Vries EG: **Molecular prognostic markers in ovarian cancer: toward patient-tailored therapy.** *International Journal of Gynecological Cancer* 2006, **16:**152-165.

274. Marks JR, Davidoff AM, Kerns BJ, Humphrey PA, Pence JC, Dodge RK, Clarke-Pearson DL, Iglehart JD, Bast RC, Jr., Berchuck A: **Overexpression and Mutation of *p53* in Epithelial Ovarian Cancer.** *Cancer Res* 1991, **51:**2979-2984.
275. Havrilesky L, Darcy KM, Hamdan H, Priore RL, Leon J, Bell J, Berchuck A: **Prognostic Significance of *p53* Mutation and *p53* Overexpression in Advanced Epithelial Ovarian Cancer: A Gynecologic Oncology Group Study.** *J Clin Oncol* 2003, **21:**3814-3825.
276. Carr KM, Rosenblat K, Petricoin EF, Liotta LA: **Genomic and proteomic approaches for studying human cancer: prospects for true patient-tailored therapy.** *Hum Genomics* 2004, **1:**134-140.
277. Zorn KK, Jazaeri AA, Awtrey CS, Gardner GJ, Mok SC, Boyd J, Birrer MJ: **Choice of Normal Ovarian Control Influences Determination of Differentially Expressed Genes in Ovarian Cancer Expression Profiling Studies.** *Clin Cancer Res* 2003, **9:**4811-4818.
278. Crijns A, Gerbens F, Plantinga AE, Meersma GJ, de Jong S, Hofstra R, de Vries E, van der Zee A, de Bock G, te Meerman G: **A biological question and a balanced (orthogonal) design: the ingredients to efficiently analyze two-color microarrays with Confirmatory Factor Analysis.** *BMC Genomics* 2006, **7:**232.
279. Lamendola DE, Duan Z, Yusuf RZ, Seiden MV: **Molecular Description of Evolving Paclitaxel Resistance in the SKOV-3 Human Ovarian Carcinoma Cell Line.** *Cancer Res* 2003, **63:**2200-2205.
280. Farley J, Ozbun LL, Birrer MJ: **Genomic analysis of epithelial ovarian cancer.** *Cell Res* 2008.
281. Gilks CB, Vanderhyden BC, Zhu S, van de Rijn M, Longacre TA: **Distinction between serous tumors of low malignant potential and serous carcinomas based on global mRNA expression profiling.** *Gynecologic Oncology* 2005, **96:**684-694.
282. Zorn KK, Bonome T, Gangi L, Chandramouli GVR, Awtrey CS, Gardner GJ, Barrett JC, Boyd J, Birrer MJ: **Gene Expression Profiles of Serous, Endometrioid, and Clear Cell Subtypes of Ovarian and Endometrial Cancer.** *Clin Cancer Res* 2005, **11:**6422-6430.
283. Schwartz DR, Kardia SL, Shedden KA, Kuick R, Michailidis G, Taylor JM, Misek DE, Wu R, Zhai Y, Darrah DM, Reed H, Ellenson LH, Giordano TJ, Fearon ER, Hanash SM, Cho KR: **Gene expression in ovarian cancer reflects both morphology and biological behavior, distinguishing clear cell from other poor-prognosis ovarian carcinomas.** *Cancer Res* 2002, **62:**4722 - 4729.
284. Spentzos D, Levine DA, Ramoni MF, Joseph M, Gu X, Boyd J, Libermann TA, Cannistra SA: **Gene expression signature with independent prognostic significance in epithelial ovarian cancer.** *J Clin Oncol* 2004, **22:**4700-4710.
285. Helleman J, Jansen MP, Berns EM: **Gene expression profiling of treatment resistance: hype or hope for therapeutic target identification.** *International Journal of Gynecological Cancer* 2006, **16:**538-542.
286. Spentzos D, Levine DA, Kolia S, Otu H, Boyd J, Libermann TA, Cannistra SA: **Unique Gene Expression Profile Based on Pathologic Response in Epithelial Ovarian Cancer.** *J Clin Oncol* 2005, **23:**7911-7918.
287. Dressman HK, Berchuck A, Chan G, Zhai J, Bild A, Sayer R, Cragun J, Clarke J, Whitaker RS, Li L, Gray J, Marks J, Ginsburg GS, Potti A, West M,

Nevins JR, Lancaster JM: **An Integrated Genomic-Based Approach to Individualized Treatment of Patients With Advanced-Stage Ovarian Cancer.** *J Clin Oncol* 2007, **25:**517-525.

288. Helleman J: **Molecular profiling of platinum resistant ovarian cancer.** *International Journal of Cancer* 2006, **118:**1963-1971.
289. Berchuck A, Iversen ES, Lancaster JM, Pittman J, Luo J, Lee P, Murphy S, Dressman HK, Febbo PG, West M, Nevins JR, Marks JR: **Patterns of gene expression that characterize long-term survival in advanced stage serous ovarian cancers.** *Clin Cancer Res* 2005, **11:**3686 - 3696.
290. Spentzos D, Levine DA, Kolia S, Otu H, Boyd J, Libermann TA, Cannistra SA: **Unique gene expression profile based on pathologic response in epithelial ovarian cancer.** *J Clin Oncol* 2005, **23:**7911 - 7918.
291. Helleman J, Jansen MP, Span PN, van Staveren IL, Massuger LF, Meijer-van Gelder ME, Sweep FC, Ewing PC, van der Burg ME, Stoter G, Nooter K, Berns EM: **Molecular profiling of platinum resistant ovarian cancer.** *Int J Cancer* 2006, **118:**1963 - 1971.
292. Bild AH, Potti A, Nevins JR: **Linking oncogenic pathways with therapeutic opportunities.** *Nat Rev Cancer* 2006, **6:**735-741.
293. Yamamoto K, Okamoto A, Isonishi S, Ochiai K, Ohtake Y: **Heat shock protein 27 was up-regulated in cisplatin resistant human ovarian tumor cell line and associated with the cisplatin resistance.** *Cancer Letters* 2001, **168:**173-181.
294. Thant AA, Nawa A, Kikkawa F, Ichigotani Y, Zhang Y, Sein TT, Amin AR, Hamaguchi M: **Fibronectin activates matrix metalloproteinase-9 secretion via the MEK1-MAPK and the PI3K-Akt pathways in ovarian cancer cells.** *Clin Exp Metastasis* 2000, **18:**423-428.
295. Tai YT, Lee S, Niloff E, Weisman C, Strobel T, Cannistra SA: **BAX protein expression and clinical outcome in epithelial ovarian cancer [published erratum appears in J Clin Oncol 1998 Sep;16(9):3211].** *J Clin Oncol* 1998, **16:**2583-2590.
296. Shawver LK, Schwartz DP, Mann E, Chen H, Tsai J, Chu L, Taylorson L, Longhi M, Meredith S, Germain L, Jacobs JS, Tang C, Ullrich A, Berens ME, Hersh E, McMahon G, Hirth KP, Powell TJ: **Inhibition of platelet-derived growth factor-mediated signal transduction and tumor growth by N-[4-(trifluoromethyl)-phenyl]5-methylisoxazole-4-carboxamide.** *Clin Cancer Res* 1997, **3:**1167-1177.
297. Hayes DF, Bast RC, Desch CE, Fritsche H, Jr., Kemeny NE, Jessup JM, Locker GY, Macdonald JS, Mennel RG, Norton L, Ravdin P, Taube S, Winn RJ: **Tumor Marker Utility Grading System: a Framework to Evaluate Clinical Utility of Tumor Markers.** *J Natl Cancer Inst* 1996, **88:**1456-1466.
298. Ransohoff D: **Rules of evidence for cancer molecular-marker discovery and validation.** *Nat Rev Cancer* 2004, **4:**309-314.
299. Draghici S, Khatri P, Eklund AC, Szallasi Z: **Reliability and reproducibility issues in DNA microarray measurements.** *Trends in Genetics* 2006, **22:**101-109.
300. De Smet F, Pochet NL, De Moor BL, Van Gorp T, Timmerman D, Vergote IB, Hartmann LC, Damokosh AI, Hoersch S: **Independent Test Set Performance in the Prediction of Early Relapse in Ovarian Cancer with Gene Expression Profiles.** *Clin Cancer Res* 2005, **11:**7958-7959.

301. Dupuy A, Simon RM: **Critical Review of Published Microarray Studies for Cancer Outcome and Guidelines on Statistical Analysis and Reporting.** *J Natl Cancer Inst* 2007, **99:**147-157.
302. Gevaert O, De Smet F, Van Gorp T, Pochet N, Engelen K, Amant F, De Moor B, Timmerman D, Vergote I: **Expression profiling to predict the clinical behaviour of ovarian cancer fails independent evaluation.** *BMC Cancer* 2008, **8:**18.
303. Gava N, L Clarke C, Bye C, Byth K, deFazio A: **Global gene expression profiles of ovarian surface epithelial cells in vivo.** *J Mol Endocrinol* 2008, **40:**281-296.
304. Krützfeldt J, Rajewsky N, Braich R, Rajeev KG, Tuschl T, Manoharan M, Stoffel M.: **Silencing of microRNAs in vivo with 'antagomirs'.** *Nature* 2005, **438:**685-689.
305. Kim VN, Nam J-W: **Genomics of microRNA.** *Trends in Genetics* 2006, **22:**165-173.
306. Meltzer PS: **Cancer genomics: Small RNAs with big impacts.** *Nature* 2005, **435:**745-746.
307. Kloosterman WP, Plasterk RHA: **The Diverse Functions of MicroRNAs in Animal Development and Disease.** *Developmental Cell* 2006, **11:**441-450.
308. Ambros V, Bartel B, Bartel DP, Burge CB, Carrington JC, Chen X, Dreyfuss G, Eddy SR, Griffiths-Jones SAM, Marshall M, Matzke M, Ruvkun G, Tuschl T: **A uniform system for microRNA annotation.** *RNA* 2003, **9:**277-279.
309. Griffiths-Jones S, Grocock RJ, van Dongen S, Bateman A, Enright AJ: **miRBase: microRNA sequences, targets and gene nomenclature.** *Nucl Acids Res* 2006, **34:**D140-144.
310. Lee RC, Feinbaum RL, Ambros V: **The C. elegans heterochronic gene lin-4 encodes small RNAs with antisense complementarity to lin-14.** *Cell* 1993, **75:**843-854.
311. Calin GA, Croce CM: **MicroRNA signatures in human cancers.** *Nat Rev Cancer* 2006, **6:**857-866.
312. Chendrimada TP, Finn KJ, Ji X, Baillat D, Gregory RI, Liebhaber SA, Pasquinelli AE, Shiekhattar R: **MicroRNA silencing through RISC recruitment of eIF6.** *Nature* 2007, **447:**823-828.
313. Barad O, Meiri E, Avniel A, Aharonov R, Barzilai A, Bentwich I, Einav U, Gilad S, Hurban P, Karov Y, Lobenhofer EK, Sharon E, Shiboleth YM, Shtutman M, Bentwich Z, Einat P: **MicroRNA expression detected by oligonucleotide microarrays: System establishment and expression profiling in human tissues.** *Genome Res* 2004, **14:**2486-2494.
314. Johnson SM, Grosshans H, Shingara J, Byrom M, Jarvis R, Cheng A, Labourier E, Reinert KL, Brown D, Slack FJ: **RAS is regulated by the let-7 microRNA family.** *Cell* 2005, **120:**635-647.
315. Calin GA, Dumitru CD, Shimizu M, Bichi R, Zupo S, Noch E, Aldler H, Rattan S, Keating M, Rai K, Rassenti L, Kipps T, Negrini M, Bullrich F, Croce CM: **Frequent deletions and down-regulation of micro- RNA genes miR15 and miR16 at 13q14 in chronic lymphocytic leukemia.** *Proceedings of the National Academy of Sciences of the United States of America* 2002, **99:**15524-15529.
316. Calin GA, Sevignani C, Dumitru CD, Hyslop T, Noch E, Yendamuri S, Shimizu M, Rattan S, Bullrich F, Negrini M, Croce CM: **Human microRNA genes are frequently located at fragile sites and genomic regions involved**

in cancers. *Proceedings of the National Academy of Sciences of the United States of America* 2004, **101:**2999-3004.

317. Volinia S, Calin GA, Liu C-G, Ambs S, Cimmino A, Petrocca F, Visone R, Iorio M, Roldo C, Ferracin M, Prueitt RL, Yanaihara N, Lanza G, Scarpa A, Vecchione A, Negrini M, Harris CC, Croce CM: **A microRNA expression signature of human solid tumors defines cancer gene targets.** *PNAS* 2006, **103:**2257-2261.
318. Meng F, Henson R, Wehbe-Janek H, Ghoshal K, Jacob ST, Patel T: **MicroRNA-21 Regulates Expression of the PTEN Tumor Suppressor Gene in Human Hepatocellular Cancer.** *Gastroenterology* 2007, **133:**647-658.
319. Cimmino A, Calin GA, Fabbri M, Iorio MV, Ferracin M, Shimizu M, Wojcik SE, Aqeilan RI, Zupo S, Dono M, Rassenti L, Alder H, Volinia S, Liu CG, Kipps TJ, Negrini M, Croce CM: **miR-15 and miR-16 induce apoptosis by targeting BCL2.** *Proceedings of the National Academy of Sciences of the United States of America* 2005, **102:**13944-13949.
320. Szafranska AE, Davison TS, John J, Cannon T, Sipos B, Maghnouj A, Labourier E, Hahn SA: **MicroRNA expression alterations are linked to tumorigenesis and non-neoplastic processes in pancreatic ductal adenocarcinoma.** *Oncogene* 2007, **26:**4442-4452.
321. Bandres E, Cubedo E, Agirre X, Malumbres R, Zarate R, Ramirez N, Abajo A, Navarro A, Moreno I, Monzo M, Garcia-Foncillas J: **Identification by Real-time PCR of 13 mature microRNAs differentially expressed in colorectal cancer and non-tumoral tissues.** *Molecular Cancer* 2006, **5:**29.
322. Iorio MV, Ferracin M, Liu CG, Veronese A, Spizzo R, Sabbioni S, Magri E, Pedriali M, Fabbri M, Campiglio M, Ménard S, Palazzo JP, Rosenberg A, Musiani P, Volinia S, Nenci I, Calin GA, Querzoli P, Negrini M, Croce CM: **MicroRNA Gene Expression Deregulation in Human Breast Cancer.** *Cancer Res* 2005, **65:**7065 - 7070.
323. Iorio MV, Visone R, Di Leva G, Donati V, Petrocca F, Casalini P, Taccioli C, Volinia S, Liu CG, Alder H, Calin GA, Ménard S, Croce CM: **MicroRNA Signatures in Human Ovarian Cancer.** *Cancer Res* 2007, **67:**8699-8707.
324. Takamizawa J, Konishi H, Yanagisawa K, Tomida S, Osada H, Endoh H, Harano T, Yatabe Y, Nagino M, Nimura Y, Mitsudomi T, Takahashi T: **Reduced Expression of the let-7 MicroRNAs in Human Lung Cancers in Association with Shortened Postoperative Survival.** *Cancer Res* 2004, **64:**3753 - 3756.
325. Mi S, Lu J, Sun M, Li Z, Zhang H, Neilly MB, Wang Y, Qian Z, Jin J, Zhang Y, Bohlander SK, Le Beau MM, Larson RA, Golub TR, Rowley JD, Chen J: **MicroRNA expression signatures accurately discriminate acute lymphoblastic leukemia from acute myeloid leukemia.** *Proceedings of the National Academy of Sciences* 2007, **104:**19971-19976.
326. Ramaswamy S, Tamayo P, Rifkin R, Mukherjee S, Yeang C-H, Angelo M, Ladd C, Reich M, Latulippe E, Mesirov JP, Poggio T, Gerald W, Loda M, Lander ES, Golub TR: **Multiclass cancer diagnosis using tumor gene expression signatures.** *Proceedings of the National Academy of Sciences of the United States of America* 2001, **98:**15149-15154.
327. Yanaihara N, Caplen N, Bowman E, Seike M, Kumamoto K, Yi M, Stephens RM, Okamoto A, Yokota J, Tanaka T, Calin GA, Liu CG, Croce CM, Harris

CC: **Unique microRNA molecular profiles in lung cancer diagnosis and prognosis.** *Cancer Cell* 2006, **9:**189 - 198.

328. Xi Y, Formentini A, Chien M, Weir DB, Russo JJ, Ju J, Kornmann M, Ju J.: **Prognostic Values of microRNAs in Colorectal Cancer.** *Biomark Insights* 2006, **2:**113-121.
329. Nelson PT, Baldwin DA, Scearce LM, Oberholtzer JC, Tobias JW, Mourelatos Z: **Microarray-based, high-throughput gene expression profiling of microRNAs.** *Nat Meth* 2004, **1:**155 - 161.
330. Li J, Smyth P, Flavin R, Cahill S, Denning K, Aherne S, Guenther S, O'Leary J, Sheils O: **Comparison of miRNA expression patterns using total RNA extracted from matched samples of formalin-fixed paraffin-embedded (FFPE) cells and snap frozen cells.** *BMC Biotechnology* 2007, **7:**36.
331. Si ML, Zhu S, Wu H, Lu Z, Wu F, Mo YY: **miR-21-mediated tumor growth.** *Oncogene* 2006, **26:**2799-2803.
332. Scott GK, Goga A, Bhaumik D, Berger CE, Sullivan CS, Benz CC: **Coordinate Suppression of ERBB2 and ERBB3 by Enforced Expression of Micro-RNA miR-125a or miR-125b.** *J Biol Chem* 2007, **282:**1479-1486.
333. Chen C, Ridzon DA, Broomer AJ, Zhou Z, Lee DH, Nguyen JT, Barbisin M, Xu NL, Mahuvakar VR, Andersen MR, Lao KQ, Livak KJ, Guegler KJ: **Real-time quantification of microRNAs by stem-loop RT-PCR.** *Nucl Acids Res* 2005, **33:**179.
334. Cai X, Hagedorn CH, Cullen BR: **Human microRNAs are processed from capped, polyadenylated transcripts that can also function as mRNAs.** *RNA* 2004, **10:**1957-1966.
335. Lee EJ, Baek M, Gusev Y, Brackett DJ, Nuovo GJ, Schmittgen TD: **Systematic evaluation of microRNA processing patterns in tissues, cell lines, and tumors.** *RNA* 2008**:14:**35-42.
336. Abraham VC, Taylor DL, Haskins JR: **High content screening applied to large-scale cell biology.** *Trends in Biotechnology* 2004, **22:**15-22.
337. Giuliano KA, Haskins JR, Taylor DL.: **Advances in high content screening for drug discovery.** *Assay Drug Dev Technol* 2003, **1:**565-577.
338. Vogt A, Kalb EN, Lazo JS: **A scalable high-content cytotoxicity assay insensitive to changes in mitochondrial metabolic activity.** *Oncol Res* 2004, **14:**305-314.
339. Rutledge RG: **Sigmoidal curve-fitting redefines quantitative real-time PCR with the prospective of developing automated high-throughput applications.** *Nucl Acids Res* 2004, **32:**e178-.
340. Livak KJ, Schmittgen TD: **Analysis of Relative Gene Expression Data Using Real-Time Quantitative PCR and the 2-[Delta][Delta]CT Method.** *Methods* 2001, **25:**402-408.
341. Schmittgen TD, Jiang J, Liu Q, Yang L: **A high-throughput method to monitor the expression of microRNA precursors.** *Nucl Acids Res* 2004, **32:**e43.
342. www.bioconductor.org.
343. Benjamini Y, Hochberg Y: **Controlling the false discovery rate: a practical and powerful approach to multiple testing.** *Journal of the Royal Statistical Society Series B* 1995, **57:**289 - 300.
344. Thomas PD, Kejariwal A, Campbell MJ, Mi H, Diemer K, Guo N, Ladunga I, Ulitsky-Lazareva B, Muruganujan A, Rabkin S, Vandergriff JA, Doremieux O: **PANTHER: a browsable database of gene products organized by**

biological function, using curated protein family and subfamily classification. *Nucl Acids Res* 2003, **31:**334-341.

345. www.ingenuity.com.
346. Bolstad BM, Irizarry RA, Astrand M, Speed TP: **A comparison of normalization methods for high density oligonucleotide array data based on variance and bias.** *Bioinformatics* 2003, **19:**185-193.
347. Skipper HE: **Kinetics of mammary tumor cell growth and implications for therapy.** *Cancer* 1971, **28:**1479-1499.
348. Di Nicolantonio F, Mercer S, Knight L, Gabriel F, Whitehouse P, Sharma S, Fernando A, Glaysher S, Di Palma S, Johnson P, Somers SS, Toh S, Higgins B, Lamont A, Gulliford T, Hurren J, Yiangou C, Cree IA: **Cancer cell adaptation to chemotherapy.** *BMC Cancer* 2005, **5:**78.
349. Nguyen DX, Massague J: **Genetic determinants of cancer metastasis.** *Nat Rev Genet* 2007, **8:**341-352.
350. Ching YP, Wong CM, Chan SF, Leung TY, Ng DCH, Jin DY, Ng I: **Deleted in Liver Cancer (DLC) 2 Encodes a RhoGAP Protein with Growth Suppressor Function and Is Underexpressed in Hepatocellular Carcinoma.** *J Biol Chem* 2003, **278:**10824-10830.
351. Olayioye MA, Vehring S, Muller P, Herrmann A, Schiller J, Thiele C, Lindeman GJ, Visvader JE, Pomorski T: **StarD10, a START Domain Protein Overexpressed in Breast Cancer, Functions as a Phospholipid Transfer Protein.** *J Biol Chem* 2005, **280:**27436-27442.
352. Lin J, Yang Q, Yan Z, Markowitz J, Wilder PT, Carrier F, Weber DJ: **Inhibiting S100B Restores *p53* Levels in Primary Malignant Melanoma Cancer Cells.** *J Biol Chem* 2004, **279:**34071-34077.
353. Baudier J, Delphin C, Grunwald D, Khochbin S, Lawrence JJ: **Characterization of the Tumor Suppressor Protein *p53* as a Protein Kinase C Substrate and a S100b-Binding Protein.** *PNAS* 1992, **89:**11627-11631.
354. Stewart JJ, White JT, Yan X, Collins S, Drescher CW, Urban ND, Hood L, Lin B: **Proteins associated with Cisplatin resistance in ovarian cancer cells identified by quantitative proteomic technology and integrated with mRNA expression levels.** *Mol Cell Proteomics* 2006, **5:**433-443.
355. Sorci G, Agneletti AL, Donato R: **Effects of S100A1 and S100B on microtubule stability. An in vitro study using triton-cytoskeletons from astrocyte and myoblast cell lines.** *Neuroscience* 2000, **99:**773-783.
356. Shen D-W, Liang X-J, Gawinowicz MA, Gottesman MM: **Identification of Cytoskeletal [14C]Carboplatin-Binding Proteins Reveals Reduced Expression and Disorganization of Actin and Filamin in Cisplatin-Resistant Cell Lines.** *Mol Pharmacol* 2004, **66:**789-793.
357. Sherman-Baust CA, Weeraratna AT, Rangel LBA, Pizer ES, Cho KR, Schwartz DR, Shock T, Morin PJ: **Remodeling of the extracellular matrix through overexpression of collagen VI contributes to cisplatin resistance in ovarian cancer cells.** *Cancer Cell* 2003, **3:**377-386.
358. Agarwal R, D'Souza T, Morin PJ: **Claudin-3 and Claudin-4 Expression in Ovarian Epithelial Cells Enhances Invasion and Is Associated with Increased Matrix Metalloproteinase-2 Activity.** *Cancer Res* 2005, **65:**7378-7385.
359. Hough CD, Sherman-Baust CA, Pizer ES, Montz FJ, Im DD, Rosenshein NB, Cho KR, Riggins GJ, Morin PJ: **Large-Scale Serial Analysis of Gene**

Expression Reveals Genes Differentially Expressed in Ovarian Cancer. *Cancer Research* 2000, **60:**6281 - 6287.

360. Sonoda N, Furuse M, Sasaki H, Yonemura S, Katahira J, Horiguchi Y, Tsukita S: **Clostridium perfringens enterotoxin fragment removes specific claudins from tight junction strands: Evidence for direct involvement of claudins in tight junction barrier.** *J Cell Biol* 1999, **147:**195-204.
361. Tassi RA, Bignotti E, Falchetti M, Ravanini M, Calza S, Ravaggi A, Bandiera E, Facchetti F, Pecorelli S, Santin AD: **Claudin-7 expression in human epithelial ovarian cancer.** *International Journal of Gynecological Cancer*, 2008,**18**:1262-71.
362. Cheung ST, Leung KL, Ip YC, Chen X, Fong DY, Ng IO, Fan ST, So S: **Claudin-10 expression level is associated with recurrence of primary hepatocellular carcinoma.** *Clin Cancer Res* 2005, **11:**551-556.
363. Gonzalez-Mariscal L, Betanzos A, Avila-Flores A: **MAGUK proteins: structure and role in the tight junction.** *Seminars in Cell & Developmental Biology* 2000, **11:**315-324.
364. Frisch SM, Francis H: **Disruption of epithelial cell-matrix interactions induces apoptosis.** *J Cell Biol* 1994, **124:**619-626.
365. Morin PJ: **Drug resistance and the microenvironment: nature and nurture.** *Drug Resistance Updates* 2003, **6:**169-172.
366. Wilson J, Balkwill F: **The role of cytokines in the epithelial cancer microenvironment.** *Seminars in Cancer Biology* 2002, **12:**113-120.
367. Wang Y, Yang J, Gao Y, Du Y, Bao L, Niu W, Yao Z: **Regulatory effect of e2, IL-6 and IL-8 on the growth of epithelial ovarian cancer cells.** *Cell Mol Immunol* 2005, **2:**365-372.
368. Apte SM, Vadhan-Raj S, Cohen L, Bassett RL, Gordon IO, Levenback CF, Ramirez PT, Gallardo ST, Patenia RS, Garcia ME, Iyer RB, Freedman RS: **Cytokines, GM-CSF and IFNgamma administered by priming and post-chemotherapy cycling in recurrent ovarian cancer patients receiving carboplatin.** *J Transl Med* 2006, **4:**16-27.
369. Vitkovic L, Bockaert J, Jacque C: **"Inflammatory" Cytokines. Neuromodulators in Normal Brain?** *Journal of Neurochemistry* 2000, **74:**457-471.
370. Voronov E, Shouval DS, Krelin Y, Cagnano E, Benharroch D, Iwakura Y, Dinarello CA, Apte RN: **IL-1 is required for tumor invasiveness and angiogenesis.** *PNAS* 2003, **100:**2645-2650.
371. Shao J, Sheng H: **Prostaglandin E2 Induces the Expression of IL-1{alpha} in Colon Cancer Cells.** *J Immunol* 2007, **178:**4097-4103.
372. Tanner MM, Grenman S, Koul A, Johannsson O, Meltzer P, Pejovic T, Borg A, Isola JJ: **Frequent Amplification of Chromosomal Region 20q12-q13 in Ovarian Cancer.** *Clin Cancer Res* 2000, **6:**1833-1839.
373. Quinlan KGR, Verger A, Yaswen P, Crossley M: **Amplification of zinc finger gene 217 (ZNF217) and cancer: When good fingers go bad.** *Biochimica et Biophysica Acta (BBA) - Reviews on Cancer* 2007, **1775:**333-340.
374. Collins C, Rommens JM, Kowbel D, Godfrey T, Tanner M, Hwang S-i, Polikoff D, Nonet G, Cochran J, Myambo K, Jay KE, Froula J, Cloutier T, Kuo WL, Yaswen P, Dairkee S, Giovanola J, Hutchinson GB, Isola J, Kallioniemi OP, Palazzolo M, Martin C, Ericsson C, Pinkel D, Albertson D, Li WB, Gray JW: **Positional cloning of ZNF217 and NABC1: Genes**

amplified at 20q13.2 and overexpressed in breast carcinoma. *Proceedings of the National Academy of Sciences* 1998, **95:**8703-8708.

375. Schlessinger J: **Common and Distinct Elements in Cellular Signaling via EGF and FGF Receptors.** *Science* 2004, **306:**1506-1507.
376. Normanno N, Bianco C, De Luca A, Maiello MR, Salomon DS: **Target-based agents against ErbB receptors and their ligands: a novel approach to cancer treatment.** *Endocr Relat Cancer* 2003, **10:**1-21.
377. Scambia G, Benedetti Panici P, Battaglia F, Ferrandina G, Baiocchi G, Greggi S, De Vincenzo R, Mancuso S: **Significance of epidermal growth factor receptor in advanced ovarian cancer.** *J Clin Oncol* 1992, **10:**529-535.
378. Ebert AD, Wechselberger C, Martinez-Lacaci I, Bianco C, Weitzel HK, Salomon DS: **Expression and function of EGF-related peptides and their receptors in gynecological cancer--from basic science to therapy.** *J Recept Signal Transduct Res* 2000, **20:**1 - 46.
379. **Posters: 6. Epidemiology/Pathology.** *Ann Oncol* 2002, **13:**65-68.
380. Fischer OM, Hart S, Gschwind A, Ullrich A: **EGFR signal transactivation in cancer cells.** *Biochem Soc Trans* 2003, **31:**1203-1208.
381. O- Charoenrat P, Wongkajornsilp A, Rhys-Evans PH, Eccles SA: **Signaling pathways required for matrix metalloproteinase-9 induction by betacellulin in head-and-neck squamous carcinoma cells.** *Int J Cancer* 2004, **111:**174-183.
382. Prenzel N, Zwick E, Daub H, Leserer M, Abraham R, Wallasch C, Ullrich A: **EGF receptor transactivation by G-protein-coupled receptors requires metalloproteinase cleavage of proHB-EGF.** *Nature* 1999, **402:**884-888.
383. Pommier Y, Sordet O, Antony S, Hayward RL, Kohn KW: **Apoptosis defects and chemotherapy resistance: molecular interaction maps and networks.** *Oncogene* 2004, **23:**2934-2949.
384. Cowden Dahl KD, Zeineldin R, Hudson LG: **PEA3 Is Necessary for Optimal Epidermal Growth Factor Receptor-Stimulated Matrix Metalloproteinase Expression and Invasion of Ovarian Tumor Cells.** *Mol Cancer Res* 2007, **5:**413-421.
385. Rintoul RC, Sethi T: **The role of extracellular matrix in small-cell lung cancer.** *The Lancet Oncology* 2001, **2:**437-442.
386. Pellikainen JM, Ropponen KM, Kataja VV, Kellokoski JK, Eskelinen MJ, Kosma VM: **Expression of Matrix Metalloproteinase (MMP)-2 and *MMP-9* in Breast Cancer with a Special Reference to Activator Protein-2, HER2, and Prognosis.** *Clin Cancer Res* 2004, **10:**7621-7628.
387. Birnie R, Bryce SD, Roome C, Dussupt V, Droop A, Lang SH, Berry PA, Hyde CF, Lewis JL, Stower MJ, Maitland NJ, Collins AT: **Gene expression profiling of human prostate cancer stem cells reveals a pro-inflammatory phenotype and the importance of extracellular matrix interactions.** *Genome Biol* 2008, **20:**R83.
388. Gupta GP, Nguyen DX, Chiang AC, Bos PD, Kim JY, Nadal C, Gomis RR, Manova-Todorova K, Massague J: **Mediators of vascular remodelling co-opted for sequential steps in lung metastasis.** *Nature* 2007, **446:**765-770.
389. Miyake H, Yoshimura K, Hara I, Eto H, Arakawa S, Kamidono S: **Basic Fibroblast Growth Factor Regulates Matrix Metalloproteinases Production and In Vitro Invasiveness in Human Bladder Cancer Cell Lines.** *The Journal of Urology* 1997, **157:**2351-2355.

390. Yu Q, Stamenkovic I: **Cell surface-localized matrix metalloproteinase-9 proteolytically activates TGF-beta and promotes tumor invasion and angiogenesis.** *Genes Dev* 2000, **14:**163-176.
391. Chaffer CL, Dopheide B, Savagner P, Thompson EW, Williams ED: **Aberrant fibroblast growth factor receptor signaling in bladder and other cancers.** *Differentiation* 2007, **75:**831-842.
392. Yoshiji H, Kuriyama S, Yoshii J, Ikenaka Y, Noguchi R, Nakatani T, Tsujinoue H, Yanase K, Namisaki T, Imazu H, Fukui H: **Synergistic effect of basic fibroblast growth factor and vascular endothelial growth factor in murine hepatocellular carcinoma.** *Hepatology* 2002, **35:**834-842.
393. Pardo OE, Arcaro A, Salerno G, Raguz S, Downward J, Seckl MJ: **Fibroblast Growth Factor-2 Induces Translational Regulation of Bcl-XL and Bcl-2 via a MEK-dependent Pathway. Correlation with resistance to etoposide-induced apoptosis.** *J Biol Chem* 2002, **277:**12040-12046.
394. Greenman C, Stephens P, Smith R, Dalgliesh GL, Hunter C, Bignell G, Davies H, Teague J, Butler A, Stevens C, Edkins S, O'Meara S, Vastrik I, Schmidt EE, Avis T, Barthorpe S, Bhamra G, Buck G, Choudhury B, Clements J, Cole J, Dicks E, Forbes S, Gray K, Halliday K, Harrison R, Hills K, Hinton J, Jenkinson A, Jones D, Menzies A, Mironenko T, Perry J, Raine K, Richardson D, Shepherd R, Small A, Tofts C, Varian J, Webb T, West S, Widaa S, Yates A, Cahill DP, Louis DN, Goldstraw P, Nicholson AG, Brasseur F, Looijenga L, Weber BL, Chiew YE, DeFazio A, Greaves MF, Green AR, Campbell P, Birney E, Easton DF, Chenevix-Trench G, Tan MH, Khoo SK, Teh BT, Yuen ST, Leung SY, Wooster R, Futreal PA, Stratton MR: **Patterns of somatic mutation in human cancer genomes.** *Nature* 2007, **446:**153-158.
395. Chaffer CL, Brennan JP, Slavin JL, Blick T, Thompson EW, Williams ED: **Mesenchymal-to-Epithelial Transition Facilitates Bladder Cancer Metastasis: Role of Fibroblast Growth Factor Receptor-2.** *Cancer Res* 2006, **66:**11271-11278.
396. Di Leva G, Calin GA, Croce CM: **MicroRNAs: Fundamental facts and involvement in human diseases.** *Birth Defects Research Part C: Embryo Today: Reviews* 2006, **78:**180-189.
397. Lewis BP, Burge CB, Bartel DP: **Conserved Seed Pairing, Often Flanked by Adenosines, Indicates that Thousands of Human Genes are MicroRNA Targets.** *Cell* 2005, **120:**15-20.
398. Laios A, O'Toole S, Martin C, Ring M, Gleeson N, D'Arcy T, McGuinness E, Sheils O, Sheppard B, O'Leary JJ: **Molecular profiling of primary verus recurrent serous papillary adenocarcinomas.** *Laboratory Investigation* 2006, **86:**185A.
399. Laios A, O'Toole S, Flavin R, Martin C, Ring M, Gleeson N, D'Arcy T, McGuinness E, Sheils O, Sheppard B, O' Leary JJ: **An integrative model for recurrence in ovarian cancer.** *Molecular Cancer* 2008, **7:**8.
400. www.spotfire.com.
401. Cho RJ, Campbell MJ: **Transcription, genomes, function.** *Trends in Genetics* 2000, **16:**409 - 415.
402. Tibshirani R, Hastie T, Narasimhan B, Chu G: **Diagnosis of multiple cancer types by shrunken centroids of gene expression.** *Proceedings of the National Academy of Sciences* 2002, **99:**6567-6572.

403. Rai D, Karanti S, Jung I, Dahia PLM, Aguiar RCT: **Coordinated expression of microRNA-155 and predicted target genes in diffuse large B-cell lymphoma.** *Cancer Genetics and Cytogenetics* 2008, **181:**8 - 15.
404. Pallante P, Visone R, Ferracin M, Ferraro A, Berlingieri MT, Troncone G, Chiappetta G, Liu CG, Santoro M, Negrini M, Croce CM, Fusco A: **MicroRNA deregulation in human thyroid papillary carcinomas.** *Endocr Relat Cancer* 2006, **13:**497 - 508.
405. Calin GA, Croce CM: **MicroRNAs and chromosomal abnormalities in cancer cells.** *Oncogene* 2006, **25:**6202-6210.
406. Lu J, Getz G, Miska EA, Alvarez-Saavedra E, Lamb J, Peck D, Sweet-Cordero A, Ebert BL, Mak RH, Ferrando AA, Downing JR, Jacks T, Horvitz HR, Golub TR: **MicroRNA expression profiles classify human cancers.** *Nature* 2005, **435:**834-838.
407. Corney DC, Flesken-Nikitin A, Godwin AK, Wang W, Nikitin AY: **MicroRNA-34b and MicroRNA-34c Are Targets of *p53* and Cooperate in Control of Cell Proliferation and Adhesion-Independent Growth.** *Cancer Res* 2007, **67:**8433-8438.
408. Yang H, Kong W, He L, Zhao J-J, O'Donnell JD, Wang J, Wenham RM, Coppola D, Kruk PA, Nicosia SV, Cheng JQ: **MicroRNA Expression Profiling in Human Ovarian Cancer: miR-214 Induces Cell Survival and Cisplatin Resistance by Targeting PTEN.** *Cancer Res* 2008, **68:**425-433.
409. DeRisi J, Penaland L, Brown PO, Bittner ML, Meltzer PS, Ray M, Chen Y, Su YA, Trent JM: **Use of a cDNA microarray to analyse gene expression patterns in human cancer.** *Nat Genet* 1996, **14:**457-460.
410. Calin GA, Croce CM: **MicroRNA-cancer connection: the beginning of a new tale.** *Cancer Res* 2006, **66:**7390-7394.
411. Kluiver J, Poppema S, de Jong D, Blokzijl T, Harms G, Jacobs S, Kroesen BJ, van den Berg A: **BIC and miR-155 are highly expressed in Hodgkin, primary mediastinal and diffuse large B cell lymphomas.** *The Journal of Pathology* 2005, **207:**243-249.
412. Espina V, Heiby M, Pierobon M, Liotta LA: **Laser capture microdissection technology.** *Expert Review of Molecular Diagnostics* 2007, **7:**647-657.
413. Eis PS, Tam W, Sun L, Chadburn A, Li Z, Gomez MF, Lund E, Dahlberg JE: **Accumulation of miR-155 and BIC RNA in human B cell lymphomas.** *PNAS* 2005, **102:**3627-3632.
414. Smith JA, Gaikwad A, Yu J, Wolf JK, Brown J, Ramondetta LM, Stewart CF: **In vitro evaluation of the effects of gefitinib on the modulation of cytotoxic activity of selected anticancer agents in a panel of human ovarian cancer cell lines.** *Cancer Chemother Pharmacol* 2008, **62:**51-58.
415. Yang H, Kong W, He L, Zhao JJ, O'Donnell JD, Wang J, Wenham RM, Coppola D, Kruk PA, Nicosia SV, Cheng JQ: **MicroRNA Expression Profiling in Human Ovarian Cancer: miR-214 Induces Cell Survival and Cisplatin Resistance by Targeting PTEN.** *Cancer Res* 2008, **68:**425-433.
416. Silver DL, Naora H, Liu J, Cheng W, Montell DJ: **Activated Signal Transducer and Activator of Transcription (STAT) 3: Localization in Focal Adhesions and Function in Ovarian Cancer Cell Motility.** *Cancer Res* 2004, **64:**3550-3558.
417. Ramkissoon SH, Mainwaring LA, Ogasawara Y, Keyvanfar K, Philip McCoy JJ, Sloand EM, Kajigaya S, Young NS: **Hematopoietic-specific microRNA expression in human cells.** *Leukemia Research* 2006, **30:**643-647.

418. Fazi F, Rosa A, Fatica A, Gelmetti V, De Marchis ML, Nervi C, Bozzoni I: **A Minicircuitry Comprised of MicroRNA-223 and Transcription Factors NFI-A and C/EBP[alpha] Regulates Human Granulopoiesis.** *Cell* 2005, **123:**819-831.
419. Fukao T, Fukuda Y, Kiga K, Sharif J, Hino K, Enomoto Y, Kawamura A, Nakamura K, Takeuchi T, Tanabe M: **An Evolutionarily Conserved Mechanism for MicroRNA-223 Expression Revealed by MicroRNA Gene Profiling.** *Cell* 2007, **129:**617-631.
420. Wong QWL, Lung RWM, Law PTY, Lai PBS, Chan KYY, To K-F, Wong N: **MicroRNA-223 Is Commonly Repressed in Hepatocellular Carcinoma and Potentiates Expression of Stathmin1.** *Gastroenterology* 2008, **135:**257-269.
421. Krichevsky AM, Sonntag KC, Isacson O, Kosik KS: **Specific MicroRNAs Modulate Embryonic Stem Cell-Derived Neurogenesis.** *Stem Cells* 2006, **24:**857-864.
422. Lehmann U, Hasemeier B, Rommerman D, Muller M, Langer F, Kreipe H: **Epigenetic inactivation of microRNA gene hsa-mir-9-1 in human breast cancer.** *The Journal of Pathology* 2008, **214:**17-24.
423. Lehmann U, Hasemeier B: **Epigenetic inactivation of microRNA gene hsa-mir-9-1 in human breast cancer.** *J Pathol* 2008, **214:**17-24.
424. Sorrentino A, Liu CG, Addario A, Peschle C, Scambia G, Ferlini C: **Role of microRNAs in drug-resistant ovarian cancer cells.** *Gynecologic Oncology* 2008, **111**:478-86.
425. Megraw M, Sethupathy P, Corda B, Hatzigeorgiou AG: **miRGen: a database for the study of animal microRNA genomic organization and function.** *Nucl Acids Res* 2007, **35:**D149 - 155.
426. Laios A O'Toole S, Sheppard BL, Gleeson NC, D'Arcy, Mc Guinness EPJ, Ring M, Sheils O, O'Leary JJ: **Molecular profiling of primary verus recurrent serous papillary adenocarcinomas.** *Laboratory Investigation* 2006, **86:**185A.
427. Lanza G, Ferracin M, Gafa R, Veronese A, Spizzo R, Pichiorri F, Liu C-g, Calin G, Croce C, Negrini M: **mRNA/microRNA gene expression profile in microsatellite unstable colorectal cancer.** *Molecular Cancer* 2007, **6:**54.
428. Cahill S, Smyth P, Denning K, Flavin R, Li J, Potratz A, Guenther S, Henfrey R, O'Leary J, Sheils O: **Effect of BRAFV600E mutation on transcription and post-transcriptional regulation in a papillary thyroid carcinoma model.** *Molecular Cancer* 2007, **6:**21.
429. Gaggioli C, Hooper S, Hidalgo-Carcedo C, Grosse R, Marshall JF, Harrington K, Sahai E: **Fibroblast-led collective invasion of carcinoma cells with differing roles for RhoGTPases in leading and following cells.** *Nat Cell Biol* 2007, **9:**1392 - 1400.
430. Sweetman D, Rathjen T, Jefferson M, Wheeler G, Smith TG, Wheeler GN, Munsterberg A, Dalmay T: **FGF-4 signaling is involved in mir-206 expression in developing somites of chicken embryos.** *Developmental Dynamics* 2006, **235:**2185-2191.
431. Obernosterer G, Leuschner PJF, Alenius M, Martinez J: **Post-transcriptional regulation of microRNA expression.** *RNA* 2006, **12:**1161-1167.
432. Chiosea S, Jelezcova E, Chandran U, Luo J, Mantha G, Sobol RW, Dacic S: **Overexpression of Dicer in Precursor Lesions of Lung Adenocarcinoma.** *Cancer Res* 2007, **67:**2345 - 2350.

433. Thomson JM, Newman M, Parker JS, Morin-Kensicki EM, Wright T, Hammond SM: **Extensive post-transcriptional regulation of microRNAs and its implications for cancer.** *Genes Dev* 2006, **20:**2202-2207.
434. Zhang L, Huang J, Yang N, Greshock J, Megraw MS, Giannakakis A, Liang S, Naylor TL, Barchetti A, Ward MR, Yao G, Medina A, O'Brien-Jenkins A, Katsaros D, Hatzigeorgiou A, Gimotty PA, Weber BL, Coukos G: **microRNAs exhibit high frequency genomic alterations in human cancer.** *Proceedings of the National Academy of Sciences* 2006, **103:**9136-9141.
435. Vasey PA: **Resistance to chemotherapy in advanced ovarian cancer: mechanisms and current strategies.** *Br J Cancer* 2003, **89:**S23-S28.
436. Fu X, Parks WC, Heinecke JW: **Retracted: Activation and silencing of matrix metalloproteinases.** *Seminars in Cell & Developmental Biology* 2008, **19:**2-13.
437. Stetler-Stevenson WG, Yu AE: **Proteases in invasion:matrix metalloproteinases.** *Semin Cancer Biol* 2001, **11:**143-152.
438. Egeblad M, Werb Z: **New functions for the matrix metalloproteinases in cancer progression.** *Nat Rev Cancer* 2002, **2:**161-174.
439. Kondraganti S, Mohanam S, Chintala SK, Kin Y, Jasti SL, Nirmala C, Lakka SS, Adachi Y, Kyritsis AP, Ali-Osman F, Sawaya R, Fuller GN, Rao JS: **Selective Suppression of Matrix Metalloproteinase-9 in Human Glioblastoma Cells by Antisense Gene Transfer Impairs Glioblastoma Cell Invasion.** *Cancer Res* 2000, **60:**6851-6855.
440. Silletti S, Kessler T, Goldberg J, Boger DL, Cheresh DA: **Disruption of matrix metalloproteinase 2 binding to integrin alpha vbeta3 by an organic molecule inhibits angiogenesis and tumor growth in vivo.** *Proceedings of the National Academy of Sciences of the United States of America* 2001, **98:**119-124.
441. Liu S, Netzel-Arnett S, Birkedal-Hansen H, Leppla SH: **Tumor Cell-selective Cytotoxicity of Matrix Metalloproteinase-activated Anthrax Toxin.** *Cancer Res* 2000, **60:**6061-6067.
442. Celiker MY, Wang M, Atsidaftos E, Liu X, Liu YE, Jiang Y, Valderrama E, Goldberg ID, Shi YE: **Inhibition of Wilms' tumor growth by intramuscular administration of tissue inhibitor of metalloproteinases-4 plasmid DNA.** *Oncogene* 2001, **20:**4337-4343.
443. Jiang Y, Wang M, Celiker MY, Liu YE, Amy Sang QX, Goldberg ID, Shi YE: **Stimulation of Mammary Tumorigenesis by Systemic Tissue Inhibitor of Matrix Metalloproteinase 4 Gene Delivery.** *Cancer Res* 2001, **61:**2365-2370.
444. Oh J, Takahashi R, Kondo S, Mizoguchi A, Adachi E, Sasahara RM, Nishimura S, Imamura Y, Kitayama H, Alexander DB, Ide C, Horan TP, Arakawa T, Yoshida H, Nishikawa S, Itoh Y, Seiki M, Itohara S, Takahashi C, Noda M.: **The Membrane-Anchored MMP Inhibitor RECK Is a Key Regulator of Extracellular Matrix Integrity and Angiogenesis.** *Cell* 2001, **107:**789-800.
445. Davies B, Brown PD, East N, Crimmin MJ, Balkwill FR: **A Synthetic Matrix Metalloproteinase Inhibitor Decreases Tumor Burden and Prolongs Survival of Mice Bearing Human Ovarian Carcinoma Xenografts.** *Cancer Res* 1993, **53:**2087-2091.

446. Garbisa S, Biggin S, Cavallarin N, Sartor L, Benelli R, Albini A: **Tumor invasion: molecular shears blunted by green tea.** *Nat Med* 1999, **5:**1216-1216.
447. Levin JI, Chen J, Du M, Hogan M, Kincaid S, Nelson FC, Venkatesan AM, Wehr T, Zask A, DiJoseph J, Killar LM, Skala S, Sung A, Sharr MA, Roth CE, Jin G, Cowling R, Di L, Sherman M, Xu ZB, March CJ, Mohler KM, Black RA, Skotnicki JS: **The discovery of anthranilic acid-Based MMP inhibitors. Part 2: SAR of the 5-position and P11 groups.** *Bioorganic & Medicinal Chemistry Letters* 2001, **11:**2189-2192.
448. Nyormoi O, Mills L, Bar-Eli M: **An MMP-2//MMP-9 inhibitor, 5a, enhances apoptosis induced by ligands of the TNF receptor superfamily in cancer cells.** *Cell Death Differ* 2003, **10:**558-569.
449. Giavazzi R, Garofalo A, Ferri C, Lucchini V, Bone EA, Chiari S, Brown PD, Nicoletti MI, Taraboletti G: **Batimastat, a synthetic inhibitor of matrix metalloproteinases, potentiates the antitumor activity of cisplatin in ovarian carcinoma xenografts.** *Clin Cancer Res* 1998, **4:**985-992.
450. Hoffman RM: **In vitro assays for chemotherapy sensitivity.** *Critical Reviews in Oncology/Hematology* 1993, **15:**99-111.
451. Brown E, Markman M: **Tumor chemosensitivity and chemoresistance assays.** *Cancer* 1996, **77:**1020-1025.
452. O'Toole SA, Sheppard BL, McGuinness EPJ, Gleeson NC, Yoneda M, Bonnar J: **The MTS assay as an indicator of chemosensitivity/resistance in malignant gynaecological tumours.** *Cancer Detection and Prevention* 2003, **27:**47-54.
453. O'Toole SA, Sheppard BL, McGuinness E, Gleeson NC, Bonnar J: **Serous papillary adenocarcinomas of the ovary display heterogeneity in their response to chemotherapy.** *International Journal of Gynecological Cancer* 2001, **11:**365-371.
454. Tamura Y, Watanabe F, Nakatani T, Yasui K, Fuji M, Komurasaki T, Tsuzuki H, Maekawa R, Yoshioka T, Kawada K, Sugita K, Ohtani M: **Highly selective and orally active inhibitors of type IV collagenase (MMP-9 and MMP-2): N-sulfonylamino acid derivatives.** *J Med Chem* 1998, **41:**640-649.
455. Agarwal R, Kaye SB: **Ovarian cancer: strategies for overcoming resistance to chemotherapy.** *Nat Rev Cancer* 2003, **3:**502-516.
456. Andreotti PE, Linder D, Hartmann DM, Cree IA, Pazzagli M, Bruckner HW: **TCA-100 tumour chemosensitivity assay: differences in sensitivity between cultured tumour cell lines and clinical studies.** *J Biolumin Chemilumin* 1994, **9:**373-378.
457. Giaccone G: **Clinical perspectives on platinum resistance.** *Drugs* 2000, **59:**9-17; discussion 37-18.
458. Ormerod MG, O'Neil C, Robertson D, Kelland LR, Harrap KR: **cis-Diamminedichloroplatinum(II)-induced cell death through apoptosis in sensitive and resistant human ovarian carcinoma cell lines.** *Cancer Chemother Pharmacol* 1996, **37:**463-471.
459. Boulikas T, Vougiouka M: **Cisplatin and platinum drugs at the molecular level.** *Oncol Rep* 2003, **10:**1663-1682.
460. Schilder RJ, Ozols RF: **New therapies for ovarian cancer.** *Cancer Invest* 1992, **10:**307-315.
461. Hagopian GS, Mills GB, Khokhar AR, Bast RC, Jr., Siddik ZH: **Expression of *p53* in Cisplatin-resistant Ovarian Cancer Cell Lines: Modulation with**

the Novel Platinum Analogue (1R, 2R-Diaminocyclohexane)(trans-diacetato)(dichloro)-platinum(IV). *Clin Cancer Res* 1999, **5:**655-663.

462. Perego P, Beretta GL, Gatti L: **Identification of determinants of sensitivity to antitumour drugs.** *Handbook of Proteomic Methods, Humana Press Inc, Totowa, NJ, USA,* 2003**:**319-331.
463. Li J, Wood WH, III, Becker KG, Weeraratna AT, Morin PJ: **Gene expression response to cisplatin treatment in drug-sensitive and drug-resistant ovarian cancer cells.** *Oncogene* 2006, **26:**2860-2872.
464. Sternlicht MD, Werb Z: **How matrix metalloproteinases regulate cell behavior.** *Annual Review of Cell and Developmental Biology* 2001, **17:**463-516.
465. Zucker S, Lysik RM, Zarrabi MH, Moll U: **Mr 92,000 Type IV Collagenase Is Increased in Plasma of Patients with Colon Cancer and Breast Cancer.** *Cancer Res* 1993, **53:**140-146.
466. Iizasa T, Fujisawa T, Suzuki M, Motohashi S-i, Yasufuku K, Yasukawa T, Baba M, Shiba M: **Elevated Levels of Circulating Plasma Matrix Metalloproteinase 9 in Non-Small Cell Lung Cancer Patients.** *Clin Cancer Res* 1999, **5:**149-153.
467. Bond M, Murphy G, Bennett MR, Amour A, Knauper V, Newby AC, Baker AH: **Localization of the Death Domain of Tissue Inhibitor of Metalloproteinase-3 to the N Terminus. Metalloproteinase inhibition is associated with proapoptotic activity.** *J Biol Chem* 2000, **275:**41358-41363.
468. Bendeck MP, Irvin C, Reidy MA: **Inhibition of Matrix Metalloproteinase Activity Inhibits Smooth Muscle Cell Migration but Not Neointimal Thickening After Arterial Injury.** *Circ Res* 1996, **78:**38-43.
469. Southgate KM, Davies M, Booth RF, Newby AC: **Involvement of extracellular-matrix-degrading metalloproteinases in rabbit aortic smooth-muscle cell proliferation.** *Biochem J* 1992, **288:**93-99.
470. Kathleen J. Heppner Goss: **Differing effects of endogenous and synthetic inhibitors of metalloproteinases on intestinal tumorigenesis.** *International Journal of Cancer* 1998, **78:**629-635.
471. Dunn M, Sinha P, Campbell R, Blackburn E, Levinson N, Rampaul R, Bates T, Humphreys S, Gullick WJ : **Co-expression of neuregulins 1, 2, 3 and 4 in human breast cancer.** *The Journal of Pathology* 2004, **203:**672-680.
472. Gilmour LMR, Macleod KG, McCaig A, Sewell JM, Gullick WJ, Smyth JF, Langdon SP: **Neuregulin Expression, Function, and Signaling in Human Ovarian Cancer Cells.** *Clin Cancer Res* 2002, **8:**3933-3942.
473. Normanno N, De Luca A, Bianco C, Strizzi L, Mancino M, Maiello MR, Carotenuto A, De Feo G, Caponigro F, Salomon DS: **Epidermal growth factor receptor (EGFR) signaling in cancer.** *Gene* 2006, **366:**2-16.
474. Grant S, Jarvis WD: **Modulation of drug-induced apoptosis by interruption of the protein kinase C signal transduction pathway: a new therapeutic strategy.** *Clin Cancer Res* 1996, **2:**1915-1920.
475. Davidson B: **Ovarian carcinoma and serous effusions. Changing views regarding tumor progression and review of current literature.** *Anal Cell Pathol* 2002, **23:**107-128.
476. Moser TL, Young TN, Rodriguez GC, Pizzo SV, Bast RC Jr, Stack MS: **Secretion of extracellular matrix-degrading proteinases is increased in epithelial ovarian carcinoma.** *Int J Cancer* 1994, **15:**552-559.

477. Cowden Dahl KD, Symowicz J, Ning Y, Gutierrez E, Fishman DA, Adley BP, Stack MS, Hudson LG: **Matrix Metalloproteinase 9 Is a Mediator of Epidermal Growth Factor-Dependent E-Cadherin Loss in Ovarian Carcinoma Cells.** *Cancer Res* 2008, **68:**4606-4613.
478. Ikeda M, Maekawa R, Tanaka H, Matsumoto M, Takeda Y, Tamura Y, Nemori R, Yoshioka T: **Inhibition of Gelatinolytic Activity in Tumor Tissues by Synthetic Matrix Metalloproteinase Inhibitor: Application of Film in Situ Zymography.** *Clin Cancer Res* 2000, **6:**3290-3296.
479. Olson H, Betton G, Robinson D, Thomas K, Monro A, Kolaja G, Lilly P, Sanders J, Sipes G, Bracken W, Dorato M, Van Deun K, Smith P, Berger B, Heller A: **Concordance of the Toxicity of Pharmaceuticals in Humans and in Animals.** *Regulatory Toxicology and Pharmacology* 2000, **32:**56-67.
480. Raguz S, Yague E: **Resistance to chemotherapy: new treatments and novel insights into an old problem.** *Br J Cancer* 2008, **99:**387-391.
481. Boehm JS, Hahn WC: **Understanding transformation: progress and gaps.** *Current Opinion in Genetics & Development* 2005, **15:**13-17.
482. Nemunaitis J, Poole C, Primrose J, Rosemurgy A, Malfetano J, Brown P, Berrington A, Cornish A, Lynch K, Rasmussen H, Kerr D, Cox D, Millar A: **Combined analysis of studies of the effects of the matrix metalloproteinase inhibitor marimastat on serum tumor markers in advanced cancer: selection of a biologically active and tolerable dose for longer-term studies.** *Clin Cancer Res* 1998, **4:**1101-1109.
483. Hirte H, Vergote IB, Jeffrey JR, Grimshaw RN, Coppieters S, Schwartz B, Tu D, Sadura A, Brundage M, Seymour L: **A phase III randomized trial of BAY 12-9566 (tanomastat) as maintenance therapy in patients with advanced ovarian cancer responsive to primary surgery and paclitaxel/platinum containing chemotherapy: A National Cancer Institute of Canada Clinical Trials Group Study.** *Gynecologic Oncology* 2006, **102:**300-308.
484. Kaye SB, Eisenhauer EA, Hamilton TC: **New non-cytotoxic approaches to ovarian cancer.** *Ann Oncol* 1999, **10 Suppl 1:**65-68.
485. Rowinsky EK, Humphrey R, Hammond LA, Aylesworth C, Smetzer L, Hidalgo M, Morrow M, Smith L, Garner A, Sorensen JM, Von Hoff DD, Eckhardt SG: **Phase I and Pharmacologic Study of the Specific Matrix Metalloproteinase Inhibitor BAY 12-9566 on a Protracted Oral Daily Dosing Schedule in Patients With Solid Malignancies.** *J Clin Oncol* 2000, **18:**178.
486. Kilian M, Gregor JI, Heukamp I, Hanel M, Ahlgrimm M, Schimke I, Kristiansen G, Ommer A, Walz MK, Jacobi CA, Wenger FA: **Matrix metalloproteinase inhibitor RO 28-2653 decreases liver metastasis by reduction of MMP-2 and MMP-9 concentration in BOP-induced ductal pancreatic cancer in Syrian Hamsters: Inhibition of matrix metalloproteinases in pancreatic cancer.** *Prostaglandins, Leukotrienes and Essential Fatty Acids* 2006, **75:**429-434.
487. Nuti E, Tuccinardi T, Rossello A.: **Matrix metalloproteinase inhibitors: new challenges in the era of post broad-spectrum inhibitors.** *Curr Pharm Des* 2007, **13:**2087-2100.
488. Selvanayagam ZE, Cheung TH, Wei N, Vittal R, Kit Lo KW, Yeo W, Kita T, Ravatn R, Hung Chung TK, Wong YF, Chin K-V: **Prediction of**

chemotherapeutic response in ovarian cancer with DNA microarray expression profiling. *Cancer Genetics and Cytogenetics* 2004, **154:**63-66.

489. Hough CD, Cho KR, Zonderman AB, Schwartz DR, Morin PJ: **Coordinately up-regulated genes in ovarian cancer.** *Cancer Res* 2001, **61:**3869 - 3876.
490. Skobe M, Fusenig NE: **Tumorigenic conversion of immortal human keratinocytes through stromal cell activation.** *Proceedings of the National Academy of Sciences* 1998, **95:**1050-1055.
491. Swann JB, Vesely MD, Silva A, Sharkey J, Akira S, Schreiber RD, Smyth MJ: **Demonstration of inflammation-induced cancer and cancer immunoediting during primary tumorigenesis.** *Proceedings of the National Academy of Sciences* 2008, **105:**652-656.
492. Lee LY WC, Wang CC, Yu JS, Liang Y, Huang KH, Lo CH, Hwang TL: **Expression of matrix metalloproteinases MMP-2 and MMP-9 in gastric cancer and their relation to claudin-4 expression.** *Histol and Histopathol* 2008, **23:**515-521.
493. Ambros V: **The functions of animal microRNAs.** *Nature* 2004, **431:**350 - 355.
494. Lujambio A, Calin GA, Villanueva A, Ropero S, Sanchez-Caspedes M, Blanco D, Montuenga LM, Rossi S, Nicoloso MS, Faller WJ, Gallagher WM, Eccles SA, Croce CM, Esteller M: **A microRNA DNA methylation signature for human cancer metastasis.** *Proceedings of the National Academy of Sciences* 2008, **105:**13556-13561.
495. Pushparaj PN, Melendez AJ: **Short interfering RNA (siRNA) as a novel therapeutic.** *Clinical and Experimental Pharmacology and Physiology* 2006, **33:**504-510.
496. Hutvágner G, Simard MJ, Mello CC, Zamore PD: **Sequence-specific inhibition of small RNA function.** *PLoS Biol* 2004, **2:**E98.
497. Saito Y, Liang G, Egger G, Friedman JM, Chuang JC, Coetzee GA, Jones PA: **Specific activation of microRNA-127 with downregulation of the proto-oncogene BCL6 by chromatin-modifying drugs in human cancer cells.** *Cancer Cell* 2006, **9:**435-443.
498. Chin LJ, Slack FJ: **A truth serum for cancer; microRNAs have major potential as cancer biomarkers.** *Cell Res*, **18:**983-984.
499. Lawrie CH, Gal S, Dunlop HM, Pushkaran B, Liggins AP, Pulford K, Banham AH, Pezzella F, Boultwood J, Wainscoat JS, Hatton CS, Harris AL: **Detection of elevated levels of tumour-associated microRNAs in serum of patients with diffuse large B-cell lymphoma.** *British Journal of Haematology* 2008, **141:**672-675.
500. Resnick KE, Alder H, Hagan JP, Richardson DL, Croce CM, Cohn DE: **The detection of differentially expressed microRNAs from the serum of ovarian cancer patients using a novel real-time PCR platform.** *Gynecologic Oncology*, **In Press, Corrected Proof**.
501. Mitchell PS, Parkin RK, Kroh EM, Fritz BR, Wyman SK, Pogosova-Agadjanyan EL, Peterson A, Noteboom J, O'Briant KC, Allen A, Lin DW, Urban N, Drescher CW, Knudsen BS, Stirewalt DL, Gentleman R, Vessella RL, Nelson PS, Martin DB, Tewari M: **Circulating microRNAs as stable blood-based markers for cancer detection.** *Proceedings of the National Academy of Sciences* 2008, **105:**10513-10518.

502. Xu JJ, Diaz D, O'Brien PJ: **Applications of cytotoxicity assays and pre-lethal mechanistic assays for assessment of human hepatotoxicity potential.** *Chemico-Biological Interactions* 2004, **150:**115-128.